2007

Four essays on environmental policy under uncertainty with applications to water quality and carbon sequestration

Sergey S. Rabotyagov
Iowa State University

Four essays on environmental policy under uncertainty with applications to water quality and carbon sequestration

by

Sergey S. Rabotyagov

A dissertation submitted to the graduate faculty

in partial fulfillment of the requirements for the degree of

DOCTOR OF PHILOSOPHY

Major: Economics

Program of Study Committee:
Catherine L. Kling, Major Professor
Joseph Herriges
Maureen Kilkenny
Jean Opsomer
Jinhua Zhao

Iowa State University

Ames, Iowa

2007

TABLE OF CONTENTS

To Stacey and my family

CHAPTER 1. GENERAL INTRODUCTION

In this thesis, I present four essays that deal with several pressing, and diverse, issues in environmental economics. While all four essays are relevant to the problems of the environment that arise in the course of agricultural production, one essay also provides a contribution to the more general methodology of environmental economics. The issues dealt with by each essay are diverse, ranging from soil carbon sequestration, to a design of a pollution permit trading program, to proposing watershed-scale solutions to water quality problems, both on state and regional scale. However, a common thread connects all the essays: they all attempt to find a systematic way of dealing with ex ante uncertainty that is endemic in environmental policy. The term ex ante in this context does not refer to the timing of resolution of uncertainty, as that would be tautological, but rather to the timing of policy decisions relative to the possible resolution of uncertainty. It is helpful to categorize uncertainty that is present in policy decisions into two types: epistemic uncertainty, that is, uncertainty stemming from a lack of knowledge about the problem (e.g., scientific uncertainty); and aleatory uncertainty, associated with a truly random process. Each of the four essays provides an attempt to deal with one, or both types of uncertainty in making policy decisions.

The first essay, titled “Environmental policy under benefit and cost uncertainty: application to soil carbon offsets,” deals with both types of uncertainty. In this essay, I address some aspects of uncertainty in soil carbon sequestration. Such uncertainty has been a widely stated reason for not including soil carbon sequestration in the portfolio of greenhouse gases reduction measures. On the benefit side, I use a biophysical simulation model to deal

with weather uncertainty (aleatory) and draw from farm surveys to deal with the uncertainty in the way farmers may undertake conservation tillage (epistemic). On the cost side, I use an econometric model of conservation tillage adoption to reduce the epistemic uncertainty regarding the potential costs of carbon sequestration. The second essay, titled "Optimal design of permit markets with an ex ante pollution target," explores how a regulator should choose the parameters of a pollution permit trading market in the case that a pollution goal is expressed as a policymaker's expectation and the abatement costs of firms are uncertain. Aleatory uncertainty in costs provides the motivation to the analysis presented in the paper. The case when the firms' environmental impacts are differentiated, but the relative impact is uncertain, is also investigated.

The third essay and fourth essays, titled, respectively, "Efficient reductions in local and state-level nonpoint source nutrient pollution: an application to the state of Iowa," and "Searching for efficiency: least cost nonpoint source pollution control with multiple pollutants, practices, and targets," deals with a kind of epistemic uncertainty a regulator faces when charged with finding a cost-efficient allocation of water pollution abatement activities in a watershed. This uncertainty stems from a complex, combinatorial nature of the optimization problem, even when the costs and water quality benefits of conservation practices are known. Without employing an optimization technique appropriate for such problems a regulator can be virtually sure that whatever allocation is chosen, it will not be cost-efficient.

Next, I describe the essays present some of the findings. Subsequent chapters of the thesis contain the full essays.

The first chapter contains the essay titled “Environmental policy under benefit and cost uncertainty: application to soil carbon offsets”. In this work I aim to characterize an optimal spatial allocation of land parcels to specific environmental practices explicitly dealing with uncertainty in both the benefits and program costs. The empirical application focuses on a heavily agricultural Iowa watershed, and atmospheric carbon sequestered by agricultural soils is used as a measure of environmental benefit. Biophysical simulation models are used to evaluate the performance of parcel-level alternatives, as well as to generate a distribution of resulting environmental benefits. An econometric model of conservation practice adoption is used to generate a distribution of costs. The results provide a magnitude of uncertainty discount for soil carbon offsets and the margin of safety necessary in the budget to ensure at the planning stage that the program’s costs will not exceed the planned expenditures. The optimal mix between land retirement and conservation tillage depends on the size of the budget available. Overall, the magnitudes of the uncertainty discount for soil carbon suggest that soil carbon sequestration may be a viable option both for a regulator concerned with reducing greenhouse gas emissions and for an aggregator who considers consolidating land enrollment and selling carbon credits.

The second chapter presents the essay “Optimal design of permit markets with an ex ante pollution target”. In this essay, the design of permit trading programs when the objective is to minimize the cost of achieving an *ex ante* pollution target; that is, one that is defined in expectation rather than an *ex pos*t deterministic value, is examined. I demonstrate that to minimize expected abatement costs regulators must use information on the joint distribution of firms’ abatement costs, as well as the pollution delivery coefficients. As a result, the

optimal trading ratio is a function of the delivery coefficient, as well as the moments of abatement costs, and the total permit allocation deviates from the pollution goal. These findings differ from a typical permit market design, where no cost information is needed to achieve cost-efficiency, the trading ratio is set to the ratio of pollution delivery coefficients, and the permit allocation exactly equals the pollution goal.

The model is motivated by both positive and normative concerns. Real-world examples of pollution goals being set in terms of averages, or expectations, provide the motivation on the positive side. When pollution goals are set in this fashion, traditional permit market theory no longer can be relied upon to make claims of *ex ante* cost-efficiency.

On the normative side, there may be pollutants, where the shape of the damage function makes meeting pollution goals on the average an appropriate policy focus. In those cases, the model builds flexibility in the permit market mechanism and allows for higher pollution when abatement costs are unexpectedly high, while tightening the pollution constraint when abatement costs turn out to be lower than expected.
Information on firms' abatement costs is important for the regulator to induce the optimal alignment between pollution level and abatement costs.

The third and the fourth chapters of the thesis build a simulation-optimization modeling framework for the analysis of efficient nonpoint source pollution reduction strategies. These essays integrate modern multi-objective optimization tools with a realistic water quality model to provide decision-makers with sets of cost-efficient pollution reduction solutions.

In the first application, in an essay titled "Efficient reductions in local and state-level nonpoint source nutrient pollution: an application to the state of Iowa," I incorporate a water

quality model, SWAT, in conjunction with detailed information on conservation practices, into an evolutionary search algorithm to find allocations of conservation practices that minimize the costs of achieving given water quality targets for all the major watersheds in the state of Iowa, a state greatly affected by nonpoint source pollution. The set of conservation practices considered includes contour farming, terraces, conservation tillage, nitrogen fertilizer reductions, and land retirement. The resulting set of tradeoffs is used to generate watershed-level nonpoint source pollution abatement curve. Availability of nonpoint source pollution abatement cost curves makes solving for a cost-minimizing way of reducing state-level nutrient loadings straightforward. In particular, watershed-level loading reduction allocations for a variety of state-level nutrient reduction goals are found. I also explore how the cost-minimizing solution changes as a result of imposing local water quality constraints.

Furthermore, watershed-level nutrient pollution reductions which minimize state-wide costs are translated into a specific mix and distribution of conservation practices which achieve these water quality goals. For the range of nutrient loading reductions considered, grassed waterways (often implemented jointly with no-till and nitrogen fertilizer reductions) was the conservation practice selected most often. Terraces and targeted land retirement were also found to be a part of cost-minimizing solutions.

Given that the version of the model used in the third essay is free to change the land use and a set of conservation practices on Iowa's cropland (without being constrained by baseline land use and conservation practices), the results can be used to gauge the degree of inefficiency of the current set of water quality protection efforts. Indeed, the results do suggest that significant inefficiencies (and, therefore, a great potential for improvement) exist.

The final essay, titled “Searching for efficiency: least cost nonpoint source pollution control with multiple pollutants, practices, and targets,” also utilizes the integrated simulation-optimization modeling framework based on a multiobjective evolutionary optimization algorithm and a hydrologic model. In this chapter, I examine the policy implications for efficient control of nonpoint source pollution using a spatially explicit model of a large and critically important agricultural region: the Upper Mississippi River Basin in the central U.S. I derive the conservation production possibility frontier that explicitly incorporates the tradeoffs between pollution control costs and water quality benefits, between different pollutants, or between different control targets. To empirically estimate these tradeoffs, a modeling framework that (a) realistically incorporates the key attributes of NPS pollution and (b) is able to approximate the efficient solutions by optimally choosing the set of conservation practices for each spatial unit in the Basin was developed. The regional scale of the modeling framework facilitates the investigation of relevant policy analyses related to the growing “dead zone” in the Gulf of Mexico and the tradeoff between regional and local pollution reduction targets.

CHAPTER 2. ENVIRONMENTAL POLICY UNDER BENEFIT AND COST UNCERTAINTY: AN APPLICATION TO SOIL CARBON OFFSETS

2.1. Introduction

Intensively managed ecosystems present a challenging set of problems for policymakers, environmental scientists, and environmental economists. They also provide opportunities for providing the public with environmental benefits such as improved water quality, recreational services, and mitigation of greenhouse gas emissions. Often, the goal is to procure a particular level of such environmental benefits at least cost to society. An important complication is that both the benefits and costs are often uncertain. Furthermore, there are usually several competing options for providing environmental benefits. For example, each land parcel currently in agricultural production can be either retired from production altogether, or an environmentally-friendly production practice can be utilized. Under such conditions, an optimal policy of providing environmental benefits from intensively managed ecosystems must jointly consider both the multiple conservation options and the uncertain nature of benefits and costs.

In this work I aim to characterize an optimal spatial allocation of land parcels to specific environmental practices explicitly dealing with uncertainty in both the benefits and program costs. Such a framework may be applicable to policy questions that extend beyond the problems of the environment (e.g., health, education, job training programs). For example, it may be applicable to a problem in education policy, where a regulator may need to find the maximum academic achievement level, so that, given the distribution of benefits and costs of alternative programs, 95 percent of all school districts achieve at least to that

level. Or, a jobs training program may have to be structured in such a way that, at the end of training, an employment target is achieved a high percentage of the time.

The empirical application focuses on a heavily agricultural Iowa watershed, and atmospheric carbon sequestered by agricultural soils is used as a measure of environmental benefit. Biophysical simulation models are used to evaluate the performance of parcel-level alternatives, as well as to generate a distribution of resulting environmental benefits. An econometric model of conservation practice adoption is used to generate a distribution of costs[1].

2.2. Methodology and Related Literature

Uncertain quantities are often present in both the objective function and in the constraints in many optimization problems. Among the multitude of ways of dealing with uncertainty in a formal way, one approach has found extensive use in engineering, operations research, agricultural, health, and environmental economics. This is the chance-constrained programming approach first introduced by Charnes and Cooper (1959). As the name suggests, this method is applicable to cases when an uncertain quantity can be dealt with by imposing a probabilistic constraint of the form:

(2.1) $$\Pr(X \le a) \ge \eta,$$

where X is a random variable, a specifies the threshold for X, and $\eta \in [0,1]$ specifies the reliability, or confidence, level with which X remains in the acceptable range. The crux of the chance-constrained programming (CCP) approach is to convert probabilistic constraints

[1] Use of simulation and an econometric model allows us to assign probabilities to different environmental and cost outcomes, thereby converting a situation of true Knightian uncertainty where probabilities of different outcomes are not known, into a situation involving "risk". While the term "uncertainty" is used throughout the paper, from this point on, I refer to quantifiable uncertainty.

into their deterministic equivalents. Given that X has mean EX and variance $Var(X)$, the above probability statement is rewritten as

(2.2) $$\Pr\left(\frac{X-EX}{\sqrt{Var(X)}} \le \frac{a-EX}{\sqrt{Var(X)}}\right) \ge \eta,$$

which in turn yields

(2.3) $$EX \le a - \theta^{-1}(\eta)\sqrt{Var(X)},$$

a deterministic equivalent of the chance constraint expressed in terms of the mean, variance, and the standardized cumulative distribution of X, $\theta(x)$ [2]. The deterministic equivalent of the chance constraint can then be used as an object in the optimization program, and can usually be handled with standard optimization techniques.

The CCP method has found numerous applications in various fields of study over the years. Examples of its use in operations research include studies in capital budgeting by Keown and Taylor (1980) and by De, Acharya, and Sahu (1982). Keown and Taylor use chance constraints to allocate expenses between production lines to ensure that the probability of excess capacity in production of each of several products is low. De et al. extend this project selection problem to allow for random technological coefficients and for integer (that is, 0 or 1) project selection. Gurgur and Luxhoj (2003) analyze a budget rationing problem where, every year, the manager has to stay within budget with high probability, and the costs are not symmetrically distributed. In accounting, Hagigi, Kluger, and Shields (1990) consider a problem of a budget manager who gets penalized for both

[2] In the case where the standardized distribution allows for computation of critical values, such values are used in the deterministic equivalents of probabilistic constraints. In cases where the distribution does not assume a convenient form, results such as Chebyschev's inequality can be used to produce such statements, or an empirical distribution can be used.

over- and under-spending, and thus uses chance constraints to control the spending. In engineering, Kibzun and Kan (1996) consider a problem of minimizing the cost of building an aircraft landing strip subject to the constraint that a high share of all attempted landings is successful.

Various branches of economics literature have also utilized the CCP approach. In health economics, and in many problems dealt with by environmental economists, the task often is to find the maximum level of a non-monetized benefit subject to a budget constraint, or to find a cost-efficient way of reaching a particular target. In an influential paper on controlling environmental health risks, Lichtenberg and Zilberman (1988) analyze the problem of minimizing the total cost of meeting a health risk standard, subject to the condition that the frequency of the standard violation is low. The authors analyze a special case of a health agency minimizing the cost of regulating health risk, subject to the probabilistic constraint on the health risk determined by exposure, contamination level, and dose-response parameter (modeled to be outside of regulator's control). The regulator has two options for controlling health risk, 1) regulating exposure to health hazards, or 2) regulating the contamination level. The authors derive the comparative statics results, providing the effects of stringency of health regulation and uncontrollable risk on minimum cost, as well as on optimal allocation of expenditure between the two options.

One recent application in health economics, by Al, Feenstra, and van Hout (2005), considers first the problem where a task is to reach a maximum benefit subject to a probabilistic budget constraint (reflecting uncertainty about the costs of some health care options), and then the task of minimizing cost subject to achieving a health benefit a high percentage of times (reflecting uncertainty in health benefits). While the second problem is

essentially the problem considered by Lichtenberg and Zilberman, the authors do not utilize the previously obtained results. Further, the authors do not consider the possibility that benefits and costs may be simultaneously uncertain and this may have implications for the optimal solution. While an empirical example is provided, no real data is used; instead, fictitious health care programs are analyzed.

A relevant work in the agricultural economics literature is by Paris and Easter (1985), who consider a model of Australian agriculture where producers face two primary sources of risk: production risk due to rainfall variability and price risk from international commodity markets. Producers are modeled as risk-averse toward price uncertainty, and the production risk is modeled through constructing a set of probabilistic input availability constraints, which subsequently are converted to their deterministic equivalents.

Chance-constrained programming has found extensive use in the field of environmental economics, with most applications focusing on non-point-source pollution control. In one of the earlier studies, McSweeny and Shortle (1990) consider a risk-neutral farmer who faces a stochastic constraint on the amount of pollutant reduction. Three target reductions in nitrogen runoff were considered, (20, 40, and 60 percent), along with confidence (reliability) levels of achieving these reductions (50, 75, and 95 percent). Consistent with Lichtenberg and Zilberman's analysis, increases in the reliability of stochastic runoff control increased the minimum costs of compliance. The magnitude of this effect in this study was enormous: increasing reliability level from 50 to 95 percent increased the cost of achieving a 40 percent runoff reduction sevenfold! Similar, if not quite so dramatic, results are obtained by Byström, Andersson, and Gren (2000), who also focus on nitrogen pollution reductions, and find that achieving a 30 percent reduction in nitrogen

levels is almost twice as costly when the target is to be reached with 90 percent certainty as opposed to 50 percent. Given that the distribution of the stochastic pollution quantity is symmetric, a 50 percent confidence required corresponds to the case when the deterministic equivalent of a chance constraint reduces to a deterministic constraint involving only the expected value.

Eloffson (2003) also finds that when a 95 percent confidence in pollution reduction is required, the costs of compliance are 1.8 times higher than in the 50 percent confidence case. In this study, however, two pollutants are considered, nitrogen and phosphorus, and multiple abatement options are considered simultaneously. Kampas and White (2004) again focus on nitrogen as the only stochastic pollutant to be controlled. The regulator's objective is to minimize the social costs of compliance with a pollution reduction standard expressed in probabilistic terms. The authors consider several options for reaching the standard, and explicitly model the administrative costs of each option. Unlike Eloffson, who considered multiple options simultaneously, Kampas and White consider the options one by one and rank them according to their relative efficiency in terms of achieving the probabilistically specified environmental goal at least cost. The confidence (reliability) level with which a standard is achieved is found to be important in ranking the policy options. Again, as expected, the minimum costs of compliance rise with the confidence level.

Notably absent from the literature are models that explicitly consider uncertainty in both the costs of policy options that yield some socially desirable benefit, and in the benefits themselves. All the studies above (with the exception of Al et al., who consider uncertainty in costs) focus on uncertainty in benefits, however they happen to be defined, and no study as of

yet analyzes both. A need for this type of analysis, along with explicit consideration of multiple options for achievement of desired results, provides the motivation for this paper.

2.3. The Problem Considered

In this chapter, I consider an optimal allocation of agricultural land parcels between two mutually exclusive environmentally friendly alternatives to achieve a maximum claimable environmental benefit, subject to a probabilistic budget constraint. The term *claimable benefit* refers to the benefit level that is achieved (or exceeded) by actual benefits resulting from a land allocation with a given probability.

The costs of one of the alternatives are modeled as ex ante stochastic, while contributions of *both* alternatives to the benefit are also stochastic. The first alternative is retiring land from production altogether, and the second one is implementing an environmentally friendly production practice. Conservation Reserve Program (CRP) provides a real-world example of land retirement, while conservation tillage serves as an established example of working land conservation. The costs of land retirement are taken to be deterministic, while the costs of implementing conservation tillage are taken to be stochastic.

Carbon sequestered in soil is the environmental benefit being considered. As agricultural soil carbon sequestration is believed to have potential to at least delay the global warming problem (Rosenberg and Izzauralde, 2001), it is likely that agricultural carbon offsets should be utilized in some way as part of the solution. However, uncertainty is inherent in the process of carbon sequestration in agricultural soils, and its presence has been one of the obstacles for including agricultural carbon sinks in international agreements on climate change, such as the Kyoto Protocol (see, e.g. Marland, McCarl, and Schneider, 2001;

Butt and McCarl, 2003)), or in the recent greenhouse gas reduction initiative adopted by the State of California. Policymakers insist on greater "certainty" for soil carbon offsets. For example, in 1998, the government of Canada proposed that agricultural carbon can be used for carbon credits only if there is a 95 percent certainty in the amount sequestered. Such preferences can be modeled using chance-constrained formulations.

In a recent paper, Kurkalova (2005) investigates discounting of carbon offsets to account for benefit uncertainty. The author models an aggregator, or broker, who purchases carbon offsets from farmers in the form of offering payment for retiring land from production. The aggregator then uses the acquired carbon offsets to generate claimable carbon credits that can be traded in an open carbon market. In order to make the offsets claimable, some extra carbon offsets have to be purchased to create a "safety margin". With claimability constraints, total expected carbon sequestered from a watershed in Iowa must be discounted 2.5 percent to 4.7 percent. Also, from 3.4 percent to 6.9 percent of the aggregator's expenditure on purchasing carbon offsets goes to create a "safety margin" and pays for ensuring the claimability of purchased offsets. These findings are consistent with earlier results, where uncertainty in benefits increased the minimum cost of achieving benefit targets.

Feng, Kurkalova, Kling, and Gassman (2006) analyze the two options for providing carbon benefits, land retirement, and working land conservation in a fully deterministic setting. The authors compare the benefit-to-cost ratio for each land parcel, and pick the option with the highest ratio. Although this "critical ratios" approach is both historically popular (Weinstein and Zeckhauser, 1973; Babcock, Lakshminarayan, Wu, and Zilberman, 1996, 1997), and easy to implement in practice, when more than one option is available at a

parcel level, it is second-best. While the authors recognize this fact, they, based on this algorithm, recommend that a high share of land in Iowa be allocated to working land conservation. The results of Feng et al. provide a useful benchmark for comparison purposes, as well as a "sanity check".

The next section develops the analytical framework for analyzing the problem at hand.

2.4. The Conceptual Model

2.4.1. Statement of the Problem

In circumstances where the benefits are uncertain and a given level of performance has to be achieved in probabilistic terms, it is convenient to specify the objective function implicitly. In particular, I model a decision-maker (regulator, or an aggregator, in sense of Kurkalova (2005)), who seeks to maximize B, a claimable level of benefit obtainable from a region, defined by a probabilistic constraint:

$$\Pr\left(\sum_{i=1}^{N}(b_i^{wl}\delta_i^{wl}+\delta_i^{lr}b_i^{lr})\geq B\right)=\eta \tag{2.4}$$

subject to the budget constraint

$$\Pr\left(\sum_{i=1}^{N}(\delta_i^{wl}c_i^{wl}+\delta_i^{lr}c_i^{lr})\leq M\right)\geq\alpha \tag{2.5}$$

where $i = 1,\ldots,N$ indexes the decision-making unit in the region (a land parcel), δ_i^{wl} is a share of parcel i allocated to the working land conservation option, δ_i^{lr} is a share allocated to land retirement option, b_i^j refers to the per-parcel benefit from option j, $j=lr,wl$, and $\eta \in [0,1]$ specifies the confidence level with which an a particular benefit level is deemed claimable. For example, if Canada's 1998 recommendation of accepting carbon credits only if there is a 95 percent chance that the claimed level would actually be sequestered were adopted, η would be set to 0.95. Similar provisions, if institutionalized through international agreements or as a part of a design of a carbon offsets trading program may give rise to the formulation adopted here.

On the cost side, $\mathbf{c}^{\mathbf{wl}} \sim \mathbf{f}(\boldsymbol{\mu}^{\mathbf{wl}}, \boldsymbol{\Omega}_{\mathbf{wl}})$ is a $N \times 1$ random vector of per-parcel costs of working land conservation with mean $\boldsymbol{\mu}^{\mathbf{wl}}$ and variance-covariance $\boldsymbol{\Omega}_{\mathbf{wl}}$, $\mathbf{c}^{\mathbf{lr}}$ is a $N \times 1$ vector of non-stochastic per-parcel costs of land retirement, M is the available conservation budget, and $\alpha \in [0,1]$ is the minimum acceptable probability of the entire program staying within the available budget. I model the costs of working land conservation as random because ex ante, in the design stage of the program, the decision-maker is uncertain what the actual adoption subsidies will turn out to be. On the other hand, it is more realistic to expect that costs of land retirement are known with a greater degree of certainty.

There are several reasons why a decision-maker may be concerned with staying within the allotted budget. If one thinks of an aggregator, she will profit from a sale of claimable carbon offsets from agricultural land if the revenues exceed the costs. While modeling the aggregator's beliefs about the distribution of a carbon offset price is outside the scope of this paper, an aggregator may wish to control the distribution of costs ex ante. There

may also be reasons for this kind of behavior on the part of a regulator. Some of these reasons may be administrative in nature, as when penalties exist for budget violations. The regulator may then want to solve this kind of problem in order to be reasonably sure that the maximum amount of environmental benefit is obtained from a particular area and that the program is going to stay within its budget. One can also imagine a situation where the regulator, perhaps motivated by environmental concerns, wishes to preserve a particular land allocation for a lengthy period into the future (as one expects the case to be for carbon sequestration). However, the regulator may be allotted a budget only yearly and can only draw up annual contracts, and the program itself may be in jeopardy should the budget be exceeded. Under these circumstances it is warranted for the regulator to treat the costs as draws from a distribution in order to find a land allocation that could be sustained in the future.

In general, the probabilistic constraint on the program cost can be interpreted as describing scenarios where conservation contracts have to be drawn up ex ante, while the program payments are made ex post, once the true costs of adoption become known.

2.4.2. Reformulation of the Problem

The next step is to reformulate the problem from one involving probability statements to one employing deterministic equivalents, in which case the problem becomes amenable to standard techniques of mathematical programming.

First, rewrite the claimable benefit constraint to obtain its deterministic equivalent. It is convenient at this point to switch to vector and matrix notation in benefits as well. Denote a $2N \times 1$ vector $\boldsymbol{\delta}$ to be the allocation vector: $\boldsymbol{\delta} = \begin{bmatrix} \boldsymbol{\delta}^{\mathbf{lr}} \\ \boldsymbol{\delta}^{\mathbf{wl}} \end{bmatrix}$. Stack the per-parcel benefits from

land retirement and working land options into a $2N \times 1$ vector of random variables $\mathbf{b}$, where $\mathbf{b} = \begin{bmatrix} \mathbf{b}^{\mathbf{lr}} \\ \mathbf{b}^{\mathbf{wl}} \end{bmatrix}$. Let $\mathbf{b}$ follow a multivariate distribution F_b with mean vector $\boldsymbol{\beta}$ and variance-covariance matrix $\boldsymbol{\Sigma}$. The $2N \times 2N$ matrix $\boldsymbol{\Sigma}$ describes all the inter-parcel and inter-option covariances.

Using above notation, one can rewrite the probabilistic benefit constraint as a deterministic function of the mean, variance, and the standardized distribution of benefits, $\hat{F}_b$:

$$\begin{aligned} \Pr\left(\boldsymbol{\delta}'\mathbf{b} \geq B\right) &= \Pr\left(\frac{\boldsymbol{\delta}'\mathbf{b} - \boldsymbol{\delta}'\boldsymbol{\beta}}{\left(\boldsymbol{\delta}'\boldsymbol{\Sigma}\boldsymbol{\delta}\right)^{1/2}} \geq \frac{B - \boldsymbol{\delta}'\boldsymbol{\beta}}{\left(\boldsymbol{\delta}'\boldsymbol{\Sigma}\boldsymbol{\delta}\right)^{1/2}}\right) \\ &= \Pr\left(z \geq \frac{B - \boldsymbol{\delta}'\boldsymbol{\beta}}{\left(\boldsymbol{\delta}'\boldsymbol{\Sigma}\boldsymbol{\delta}\right)^{1/2}}\right) = 1 - \hat{F}_b\left(\frac{B - \boldsymbol{\delta}'\boldsymbol{\beta}}{\left(\boldsymbol{\delta}'\boldsymbol{\Sigma}\boldsymbol{\delta}\right)^{1/2}}\right) \geq \eta \end{aligned} \tag{2.6}$$

Which further implies that the maximum claimable benefit, B, can be written as:

$$B = \boldsymbol{\delta}'\boldsymbol{\beta} + \hat{F}_b^{-1}(1-\eta)\left(\boldsymbol{\delta}'\boldsymbol{\Sigma}\boldsymbol{\delta}\right)^{1/2} \tag{2.7}$$

The maximum claimable benefit is therefore a function of the mean obtainable benefit, its standard deviation, and the confidence level required to make the benefit claimable.

If I further assume that the vector of benefits follows a multivariate normal distribution: $\mathbf{b} \sim MVN(\boldsymbol{\beta}, \boldsymbol{\Sigma})$, the expression above can be simpliefied, making use of the symmetry of the standard normal probability density function. The expression for maximum claimable benefit becomes:

$$B = \boldsymbol{\delta}'\boldsymbol{\beta} - \Phi^{-1}(\eta) \cdot \left(\boldsymbol{\delta}'\boldsymbol{\Sigma}\boldsymbol{\delta}\right)^{1/2} \tag{2.8}$$

where $\Phi(\bullet)$ is the cumulative density function of a standard normal random variable. Letting $z_\eta = \Phi^{-1}(\eta)$, one can interpret this scalar as a weight placed on risk associated with a particular parcel allocation $\boldsymbol{\delta}$, where the standard deviation of the resulting benefit serves as a measure of risk. Furthermore, the higher the η, the higher the z_η, and, for a given level of *expected* benefit, $\boldsymbol{\delta}'\boldsymbol{\beta}$, the smaller the *claimable* benefit *B*.

Next I turn to the budget constraint. Given that the total cost of working land conservation, $\boldsymbol{\delta}^{\mathrm{wl}\prime}\mathbf{c}^{\mathrm{wl}}$, has mean $\boldsymbol{\delta}^{\mathrm{wl}\prime}\boldsymbol{\mu}^{\mathrm{wl}}$ and variance $\boldsymbol{\delta}^{\mathrm{wl}\prime}\boldsymbol{\Omega}_{\mathrm{wl}}\boldsymbol{\delta}^{\mathrm{wl}}$, one can rewrite the probabilistic cost constraint the following way:

$$\begin{aligned}\Pr\left(\boldsymbol{\delta}^{\mathrm{wl}\prime}\mathbf{c}^{\mathrm{wl}} \le M - \boldsymbol{\delta}^{\mathrm{lr}\prime}\mathbf{c}^{\mathrm{lr}}\right) &= \Pr\left(\frac{\boldsymbol{\delta}^{\mathrm{wl}\prime}\mathbf{c}^{\mathrm{wl}} - \boldsymbol{\delta}^{\mathrm{wl}\prime}\boldsymbol{\mu}^{\mathrm{wl}}}{\left(\boldsymbol{\delta}^{\mathrm{wl}\prime}\boldsymbol{\Omega}_{\mathrm{wl}}\boldsymbol{\delta}^{\mathrm{wl}}\right)^{1/2}} \le \frac{M - \boldsymbol{\delta}^{\mathrm{lr}\prime}\mathbf{c}^{\mathrm{lr}} - \boldsymbol{\delta}^{\mathrm{wl}\prime}\boldsymbol{\mu}^{\mathrm{wl}}}{\left(\boldsymbol{\delta}^{\mathrm{wl}\prime}\boldsymbol{\Omega}_{\mathrm{wl}}\boldsymbol{\delta}^{\mathrm{wl}}\right)^{1/2}}\right) \\ &= \theta\left(\frac{M - \boldsymbol{\delta}^{\mathrm{lr}\prime}\mathbf{c}^{\mathrm{lr}} - \boldsymbol{\delta}^{\mathrm{wl}\prime}\boldsymbol{\mu}^{\mathrm{wl}}}{\left(\boldsymbol{\delta}^{\mathrm{wl}\prime}\boldsymbol{\Omega}_{\mathrm{wl}}\boldsymbol{\delta}^{\mathrm{wl}}\right)^{1/2}}\right) \ge \alpha\end{aligned} \tag{2.9}$$

where $\theta(\bullet)$ is the standardized distribution of total working land conservation costs. The deterministic equivalent of the probabilistic budget constraint becomes:

$$\boldsymbol{\delta}^{\mathrm{wl}\prime}\boldsymbol{\mu}^{\mathrm{wl}} + \boldsymbol{\delta}^{\mathrm{lr}\prime}\mathbf{c}^{\mathrm{lr}} + \theta^{-1}(\alpha)\left(\boldsymbol{\delta}^{\mathrm{wl}\prime}\boldsymbol{\Omega}_{\mathrm{wl}}\boldsymbol{\delta}^{\mathrm{wl}}\right)^{1/2} \le M\ . \tag{2.10}$$

Given that $\boldsymbol{\delta}^{\mathrm{wl}\prime}\boldsymbol{\Omega}_{\mathrm{wl}}\boldsymbol{\delta}^{\mathrm{wl}} \ge 0$ and α is high enough so that $\theta^{-1}(\alpha) \ge 0$, uncertainty in costs acts to decrease the effective size of the conservation budget. In other words, conservation funds have to be allocated so as to create a "margin of safety" in an attempt to prevent budget constraint violations.

The conversion of probabilistic, or chance, constraints into their deterministic equivalents allows a formulation of the problem in terms of maximizing a deterministic function subject to a deterministic constraint, and subsequent derivation of the necessary first order conditions and characterizing the properties of the optimal solution. Two issues may complicate the matters. The first issue to address is the concavity of the objective function. The second is the convexity of the constraint. Beavis and Walker (1983) analyze a case where the feasible set defined by the deterministic equivalents of chance constraints is non-convex. In this case, the appropriate Kuhn-Tucker necessary conditions are not also sufficient, and the global maximizers may lie elsewhere. Thus, before proceeding to characterize the optimal solution, curvature issues need to be addressed.

First, to show that the objective function is concave, one only needs to show that $\left(\boldsymbol{\delta}'\boldsymbol{\Sigma}\boldsymbol{\delta}\right)^{1/2}$ is convex. As a variance-covariance matrix, $\boldsymbol{\Sigma}$ is positive semi-definite. Following Paris and Easter (1985), in this case one can show that $\left(\boldsymbol{\delta}'\boldsymbol{\Sigma}\boldsymbol{\delta}\right)^{1/2}$ is convex. Since this result is an important one in the analysis of the problem, it is replicated in the Appendix to this chapter.

Proposition 1 (Paris and Easter, 1985). *If* $\boldsymbol{\Omega}$ *is a positive semi-definite matrix, the function* $\left(\mathbf{x}'\boldsymbol{\Omega}\mathbf{x}\right)^{1/2}$ *is convex.*

Proof. (in the Appendix). The objective function being maximized therefore possesses the desired curvature property of being concave.

Second, if one can show that the deterministic equivalent of the budget constraint is convex, then it is assured that the Kuhn-Tucker necessary conditions are sufficient to define the unique global maximizer (Takayama, 1993).

Proposition 2. The left-hand side of the deterministic equivalent of a budget constraint, $\boldsymbol{\delta}^{\mathbf{wl}\prime}\boldsymbol{\mu}^{\mathbf{wl}} + \boldsymbol{\delta}^{\mathbf{lr}\prime}\mathbf{c}^{\mathbf{lr}} + \theta^{-1}(\alpha)\left(\boldsymbol{\delta}^{\mathbf{wl}\prime}\boldsymbol{\Omega}_{\mathbf{wl}}\boldsymbol{\delta}^{\mathbf{wl}}\right)^{1/2} \leq M$ *, is a convex function.*

Proof. The linear terms drop out, and assuming that α is set high enough so that $\theta^{-1}(\alpha) > 0$, what remains to be demonstrated is that $\left(\boldsymbol{\delta}^{\mathbf{wl}\prime}\boldsymbol{\Omega}_{\mathbf{wl}}\boldsymbol{\delta}^{\mathbf{wl}}\right)^{1/2}$ is a convex function, which was demonstrated above.

The problem can now be restated in terms of the associated Lagrangean function and the Kuhn-Tucker conditions, which, under the curvature conditions outlined above, are necessary and sufficient for a unique optimal land parcel allocation vector, can now be presented. The Lagrangean is:

$$\begin{aligned} L &= \boldsymbol{\delta}'\boldsymbol{\beta} - z_{\eta}\left(\boldsymbol{\delta}'\boldsymbol{\Sigma}\boldsymbol{\delta}\right)^{1/2} \\ &+\lambda[M - z_{\alpha}\left(\boldsymbol{\delta}^{\mathbf{wl}\prime}\boldsymbol{\Omega}_{\mathbf{wl}}\boldsymbol{\delta}^{\mathbf{wl}}\right)^{1/2} - \boldsymbol{\delta}^{\mathbf{wl}\prime}\boldsymbol{\mu}^{\mathbf{wl}} - \boldsymbol{\delta}^{\mathbf{lr}\prime}\mathbf{c}^{\mathbf{lr}}] + \boldsymbol{\upsilon}'[\mathbf{1} - \boldsymbol{\delta}^{\mathbf{lr}} - \boldsymbol{\delta}^{\mathbf{wl}}] \end{aligned} \tag{2.11}$$

Here, $z_{\eta} = \Phi^{-1}(\eta) \geq 0$ and $z_{\alpha} = \theta^{-1}(\alpha) \geq 0$, and $\boldsymbol{\upsilon}$ is a $N \times 1$ vector of constraints representing the fact that the sum of shares of each land parcel allocated either to a working land or a land retirement option cannot exceed one. The structure of the problem lends itself to a discounting interpretation (Kurkalova, 2005): the total benefit in the objective function is discounted by $z_{\eta}\left(\boldsymbol{\delta}'\boldsymbol{\Sigma}\boldsymbol{\delta}\right)^{1/2} \geq 0$, and the magnitude of this discount rises with the stringency level η, as well as the total variance of the resulting carbon sequestration benefit, $\boldsymbol{\delta}'\boldsymbol{\Sigma}\boldsymbol{\delta}$.

It is perhaps useful to note here that the present formulation of the problem does not allow the decision-maker any recourse in case either the benefit or the budget constraint is violated. Stochastic programming with recourse is one methodology that has been developed to deal with situations where recourse is possible. However, in the present setting, making an

assumption of no recourse seems to be justified as a decision-maker is unlikely to have an option of direct and prompt intervention for adjusting the optimal conservation option shares at a potentially very large set of land parcels. Further, the above specification is appropriate for analyzing large-scale policy decisions (Paris and Easter, 1985).

The following Kuhn-Tucker conditions are necessary and sufficient for the optimal solution to the policymaker's problem. All the decision variables are taken at their optimal level, and not distinguished from their generic counterparts to reduce notational clutter.

The marginal condition with respect to the working land shares vector:

$$(2.12)\quad \frac{\partial L}{\partial \boldsymbol{\delta}^{\mathbf{wl}}} = \boldsymbol{\beta}^{\mathbf{wl}} - z_{\eta}\frac{\partial\left(\boldsymbol{\delta}'\boldsymbol{\Sigma}\boldsymbol{\delta}\right)^{1/2}}{\partial \boldsymbol{\delta}^{\mathbf{wl}}} - \lambda[z_{\alpha}\boldsymbol{\Omega}_{\mathbf{wl}}\boldsymbol{\delta}^{\mathbf{wl}}(\boldsymbol{\delta}^{\mathbf{wl}\prime}\boldsymbol{\Omega}_{\mathbf{wl}}\boldsymbol{\delta}^{\mathbf{wl}})^{1/2} + \boldsymbol{\mu}^{\mathbf{wl}}] - \boldsymbol{\upsilon} \le \mathbf{0}\,,\ \boldsymbol{\delta}^{\mathbf{wl}} \ge \mathbf{0}$$

along with its complementary slackness condition:

$$(2.13)\qquad \boldsymbol{\delta}^{\mathbf{wl}}\left[\boldsymbol{\beta}^{\mathbf{wl}} - z_{\eta}\frac{\partial\left(\boldsymbol{\delta}'\boldsymbol{\Sigma}\boldsymbol{\delta}\right)^{1/2}}{\partial \boldsymbol{\delta}^{\mathbf{wl}}} - \lambda[z_{\alpha}\boldsymbol{\Omega}_{\mathbf{wl}}\boldsymbol{\delta}^{\mathbf{wl}}(\boldsymbol{\delta}^{\mathbf{wl}\prime}\boldsymbol{\Omega}_{\mathbf{wl}}\boldsymbol{\delta}^{\mathbf{wl}})^{1/2} + \boldsymbol{\mu}^{\mathbf{wl}}] - \boldsymbol{\upsilon}\right] = \mathbf{0}\,.$$

The marginal condition with respect to the land retirement shares vector is:

$$(2.14)\qquad \frac{\partial L}{\partial \boldsymbol{\delta}^{\mathbf{lr}}} = \boldsymbol{\beta}^{\mathbf{lr}} - z_{\eta}\frac{\partial\left(\boldsymbol{\delta}'\boldsymbol{\Sigma}\boldsymbol{\delta}\right)^{1/2}}{\partial \boldsymbol{\delta}^{\mathbf{lr}}} - \lambda\mathbf{c}^{\mathbf{lr}} - \boldsymbol{\upsilon} \le \mathbf{0}\,,\ \boldsymbol{\delta}^{\mathbf{lr}} \ge \mathbf{0}\,,$$

along with the associated complementary slackness condition:

$$(2.15)\qquad \boldsymbol{\delta}^{\mathbf{lr}}\left[\boldsymbol{\beta}^{\mathbf{lr}} - z_{\eta}\frac{\partial\left(\boldsymbol{\delta}'\boldsymbol{\Sigma}\boldsymbol{\delta}\right)^{1/2}}{\partial \boldsymbol{\delta}^{\mathbf{lr}}} - \lambda\mathbf{c}^{\mathbf{lr}} - \boldsymbol{\upsilon}\right] = \mathbf{0}$$

The marginal conditions state that, if a parcel is to be allocated to a particular conservation option, the marginal benefit of this decision, when adjusted for uncertainty in benefits, must

be at least as large as the marginal cost of that decision, adjusted for the uncertainty in costs. Otherwise, using the complementary slackness condition, the option should not be used. It is interesting to note that while the total benefit obtained from a region is discounted by a non-negative quantity $z_\eta \left(\boldsymbol{\delta}'\boldsymbol{\Sigma}\boldsymbol{\delta}\right)^{1/2} \geq 0$, per-parcel marginal benefit is adjusted by $z_\eta \frac{\partial \left(\boldsymbol{\delta}'\boldsymbol{\Sigma}\boldsymbol{\delta}\right)^{1/2}}{\partial \boldsymbol{\delta}^{\mathbf{j}}}, \mathbf{j} = \mathbf{wl}, \mathbf{lr}$, which can be either positive or negative, depending on variances and covariances of per-parcel benefits in the entire region.

The marginal condition with respect to the dual variables, and their associated complementary slackness conditions are:

$$\frac{\partial L}{\partial \lambda} = M - z_\alpha(\boldsymbol{\delta}^{\mathbf{wl}\prime}\boldsymbol{\Omega}_{\mathbf{wl}}\boldsymbol{\delta}^{\mathbf{wl}})^{1/2} - \boldsymbol{\delta}^{\mathbf{wl}\prime}\boldsymbol{\mu}^{\mathbf{wl}} - \boldsymbol{\delta}^{\mathbf{lr}\prime}\mathbf{c}^{\mathbf{lr}} \geq 0\,,\ \lambda \geq 0 \tag{2.16}$$

$$\lambda\left[M - z_\alpha(\boldsymbol{\delta}^{\mathbf{wl}\prime}\boldsymbol{\Omega}_{\mathbf{wl}}\boldsymbol{\delta}^{\mathbf{wl}})^{1/2} - \boldsymbol{\delta}^{\mathbf{wl}\prime}\boldsymbol{\mu}^{\mathbf{wl}} - \boldsymbol{\delta}^{\mathbf{lr}\prime}\mathbf{c}^{\mathbf{lr}}\right] = 0\,, \text{ and} \tag{2.17}$$

$$\frac{\partial L}{\partial \boldsymbol{\upsilon}} = \mathbf{1} - \boldsymbol{\delta}^{\mathbf{lr}} - \boldsymbol{\delta}^{\mathbf{wl}} \geq \mathbf{0}\,,\ \boldsymbol{\upsilon} \geq \mathbf{0} \tag{2.18}$$

$$\boldsymbol{\upsilon}\left[\mathbf{1} - \boldsymbol{\delta}^{\mathbf{lr}} - \boldsymbol{\delta}^{\mathbf{wl}}\right] = \mathbf{0}\,. \tag{2.19}$$

Examining the first order conditions, it becomes clear that the optimal allocation involves comparing *modified* benefit-to-cost ratios. In general, the rule becomes: at the optimum, one needs to compare the ratios of uncertainty-adjusted benefits to uncertainty-adjusted costs. However, the magnitude of the uncertainty adjustment is a function of the optimal solution. It then is clear that once uncertainty in benefits and costs is explicitly

considered, no simple heuristic algorithm exists for allocating land parcels to conservation options, and the optimal parcel share is a function of all the parameters that characterize the distribution of benefits and costs in the entire policy region.

It is thus difficult to make comparative static prediction for a general case of N parcels. However, a consideration of a special $N = 2$ case may illuminate the effects of uncertainty on the optimal allocation, as well as provide additional intuition on the properties of the solution.[3]

2.4.3. Special Case and Comparative Statics

For simplicity, assume that both parcels are used completely for working land conservation and land retirement, that is, $\delta_i = \delta_i^{wl} = 1 - \delta_i^{lr}$, *i=1,2.* This, of course, presupposes that the budget is sufficient to convert both parcels to environmentally friendly practices. While in general this will not be the case, the simplification allows us to focus on the relevant parameters describing uncertainty instead of on the effect of the marginal benefit of available budget, or of the scarcity of land. Using the same notation as in the general case, the Lagrangean function becomes:

$$L = \delta_1\beta_1^{wl} + (1-\delta_1)\beta_1^{lr} + \delta_2\beta_2^{wl} + (1-\delta_2)\beta_2^{lr} - z_\eta\sigma(\delta_1,\delta_2) + \lambda\left[M - \delta_1\mu_1^{wl} - \delta_2\mu_2^{wl} - (1-\delta_1)c_1^{lr} - (1-\delta_2)c_2^{lr} - z_\alpha\omega(\delta_1,\delta_2)\right] \tag{2.20}$$

The Kuhn-Tucker conditions are:

[3] Results below only apply to the complete conversion of all land, i.e., each parcel is fully in LR and WL. Furthermore, land constraints are no longer needed as they become degenerate. This is done in order to keep the comparative statics analysis tractable by focusing on 3 variables.

$$(2.21)\quad \frac{\partial L}{\partial \delta_1} = \beta_1^{wl} - \beta_1^{lr} - z_\eta \frac{\partial \sigma(\delta_1, \delta_2)}{\partial \delta_1} - \lambda \left[\mu_1^{wl} - c_1^{lr} + z_\alpha \frac{\partial \omega(\delta_1, \delta_2)}{\partial \delta_1} \right] \leq 0,\ \delta_1 \geq 0,$$

plus the corresponding complementary slackness condition, and

$$(2.22)\quad \frac{\partial L}{\partial \delta_2} = \beta_2^{wl} - \beta_2^{lr} - z_\eta \frac{\partial \sigma(\delta_1, \delta_2)}{\partial \delta_2} - \lambda \left[\mu_2^{wl} - c_2^{lr} + z_\alpha \frac{\partial \omega(\delta_1, \delta_2)}{\partial \delta_2} \right] \leq 0, \delta_2 \geq 0,$$

plus the corresponding complementary slackness condition, and

$$(2.23)\quad \frac{\partial L}{\partial \lambda} \geq 0,\ \lambda \geq 0,\ \lambda \frac{\partial L}{\partial \lambda} = 0$$

First thing to note is that, for an interior solution to be optimal at both parcels, the following needs to hold:

$$(2.24)\quad \frac{\beta_1^{wl} - \beta_1^{lr} - z_\eta \frac{\partial \sigma(\delta_1, \delta_2)}{\partial \delta_1}}{\mu_1^{wl} - c_1^{lr} + z_\alpha \frac{\partial \omega(\delta_1, \delta_2)}{\partial \delta_1}} = \frac{\beta_2^{wl} - \beta_2^{lr} - z_\eta \frac{\partial \sigma(\delta_1, \delta_2)}{\partial \delta_2}}{\mu_2^{wl} - c_2^{lr} + z_\alpha \frac{\partial \omega(\delta_1, \delta_2)}{\partial \delta_2}},$$

which states that the ratio of marginal benefit to marginal cost of working land conservation, adjusted for benefit uncertainty and cost uncertainty, is equalized across the two parcels.

The second observation that can be made is that, when more than one conservation option is present, and the land is to be allocated between the two alternatives, the rule of per-parcel decision-making that recommends picking the option with the highest benefit-to-cost ratio (Babcock et al., 1996, Feng et al., 2006) is no longer optimal, as the optimal decision is made based on ratios of *extra* benefits to *extra* costs.

The next step in analyzing the properties of the solution is to derive a series of comparative statics results that also may extend to the general case. In particular, the effects

of parameters that describe the uncertainty in benefits and costs are of interest. In this most simple case, these parameters are:

1. $\sigma^2_{1,wl}$ -- variance of working land option benefit at parcel 1.
2. $\sigma^2_{2,wl}$ -- variance of working land option benefit at parcel 2.
3. $\sigma^2_{1,lr}$ -- variance of land retirement option benefit at parcel 1.
4. $\sigma^2_{2,lr}$ -- variance of land retirement option benefit at parcel 2.
5. $\text{cov}\left(b_1^{wl}, b_1^{lr}\right)$ -- within-parcel, across-option covariance at parcel 1.
6. $\text{cov}\left(b_1^{wl}, b_2^{wl}\right)$ -- across-parcel, within-option covariance in working land benefits.
7. $\text{cov}\left(b_1^{wl}, b_2^{lr}\right)$ -- across-parcel, across-option covariance in benefits.
8. $\text{cov}\left(b_1^{lr}, b_2^{wl}\right)$ -- across-parcel, across-option covariance in benefits.
9. $\text{cov}\left(b_1^{lr}, b_2^{lr}\right)$ -- across-parcel, within-option covariance in land retirement benefits.
10. ω_1^2 -- variance of working land option cost at parcel 1.
11. ω_2^2 -- variance of working land option cost at parcel 2.
12. $\text{cov}\left(c_1^{wl}, c_2^{wl}\right)$ -- covariance of working land option costs at parcels 1 and 2.

For simplicity, the effects of the above parameters will be assessed according to their influence on δ_1 -- the optimal share of parcel 1 allocated to a working land option.

Assuming an interior solution, the Kuhn-Tucker conditions above can be represented by:

(2.25) $$f^1(\delta_1^*, \delta_2^*, \lambda^*, \alpha_1, \ldots, \alpha_m) = 0$$

(2.26) $$f^2(\delta_1^*, \delta_2^*, \lambda^*, \alpha_1, \ldots, \alpha_m) = 0$$

(2.27) $$f^3(\delta_1^*, \delta_2^*, \lambda^*, \alpha_1, \ldots, \alpha_m) = 0,$$

where f^j, $j = 1,2,3$ represent the first derivatives of the Lagrangean function with respect to $\delta_1, \delta_2, \lambda$, respectively, evaluated at the interior optimum, and α_k, $k = 1,\ldots,12$ represent the parameters governing uncertainty as outlined above. Then, differentiating with respect to any α_j, and presuming that differentiable functions $\delta_1 = \delta_1(\alpha_1,...,\alpha_m)$, $\delta_2 = \delta_2(\alpha_1,...,\alpha_m)$, and $\lambda = \lambda(\alpha_1,...,\alpha_m)$ exist, obtain:

(2.28) $$\begin{bmatrix} f_1^1 & f_2^1 & f_3^1 \\ f_1^2 & f_2^2 & f_3^2 \\ f_1^3 & f_2^3 & f_3^3 \end{bmatrix} \begin{bmatrix} \partial\delta_1/\partial\alpha_j \\ \partial\delta_2/\partial\alpha_j \\ \partial\lambda/\partial\alpha_j \end{bmatrix} = \begin{bmatrix} -f_{\alpha_j}^1 \\ -f_{\alpha_j}^2 \\ -f_{\alpha_j}^3 \end{bmatrix}$$

where

(2.29)

$$F = \begin{bmatrix} -z_\eta \dfrac{\partial^2\sigma}{\partial\delta_1^2} - \lambda z_\alpha \dfrac{\partial^2\omega}{\partial\delta_1^2} & -z_\eta \dfrac{\partial^2\sigma}{\partial\delta_1\partial\delta_2} - \lambda z_\alpha \dfrac{\partial^2\omega}{\partial\delta_1\partial\delta_2} & c_1^{lr} - \mu_1^{wl} - z_\alpha \dfrac{\partial\omega}{\partial\delta_1} \\ -z_\eta \dfrac{\partial^2\sigma}{\partial\delta_1\partial\delta_2} - \lambda z_\alpha \dfrac{\partial^2\omega}{\partial\delta_1\partial\delta_2} & -z_\eta \dfrac{\partial^2\sigma}{\partial\delta_2^2} - \lambda z_\alpha \dfrac{\partial^2\omega}{\partial\delta_2^2} & c_2^{lr} - \mu_2^{wl} - z_\alpha \dfrac{\partial\omega}{\partial\delta_2} \\ c_1^{lr} - \mu_1^{wl} - z_\alpha \dfrac{\partial\omega}{\partial\delta_1} & c_2^{lr} - \mu_2^{wl} - z_\alpha \dfrac{\partial\omega}{\partial\delta_2} & 0 \end{bmatrix} = \begin{bmatrix} f_1^1 & f_2^1 & f_3^1 \\ f_2^1 & f_2^2 & f_3^2 \\ f_3^1 & f_3^2 & 0 \end{bmatrix}$$

is the Hessian matrix, and by the second-order conditions for the maximum, $|F| > 0$.

Furthermore, $f_3^1, f_3^2 > 0$ as long as the effective cost of working land option, $\mu_i^{wl} + z_\alpha \dfrac{\partial\omega}{\partial\delta_i}$, is less than the effective cost of the land retirement option, c_i^{lr}.[4]

Evaluation of individual comparative statics effects is done using Cramer's rule:

[4] A weaker assumption, namely, $\text{sgn}[f_3^1] = \text{sgn}[f_3^2]$, is sufficient for the subsequent comparative statics results to hold. In the absence of such an assumption, comparative static results (1), (3), and (7) still hold.

(2.30) $$\frac{\partial \delta_1}{\partial \alpha_j} = \frac{|F_{1j}|}{|F|},$$

where $|F_{1j}|$ is obtained by replacing the first column of F with $\begin{bmatrix} -f^1_{\alpha_j} \\ -f^2_{\alpha_j} \\ -f^3_{\alpha_j} \end{bmatrix}$. Since the determinant of the Hessian matrix is positive, $\operatorname{sgn}\left[\frac{\partial \delta_1}{\partial \alpha_j}\right] = \operatorname{sgn}|F_{1j}|$.

The following comparative statics results emerge:

1. $\frac{\partial \delta_1}{\partial \sigma^2_{1,wl}} < 0$. *An increase in the variance of working land benefit at parcel 1 acts to decrease the optimal share of parcel 1 allocated to the working land option.* Indeed, evaluating the derivatives of the first-order conditions with respect to $\sigma^2_{1,wl}$, obtain $-f^1_\alpha = z_\eta \frac{\partial^2 \sigma}{\partial \delta_1 \partial \sigma^2_{1,wl}} = \frac{\delta_1}{\sigma} > 0$, $-f^2_\alpha = 0$, $-f^3_\alpha = 0$, and $|F_{11}| = \frac{\delta_1}{\sigma}\left(0 - (f^2_3)^2\right) < 0$. This is intuitive and is also likely to hold for a general case. Then, at a parcel level, if working land conservation practice yields carbon benefits with greater degree of uncertainty, the share of land allocated to that option should decline.

2. $\frac{\partial \delta_1}{\partial \sigma^2_{2,wl}} > 0$. *An increase in the variance of working land benefit at parcel 2 acts to increase the optimal share of parcel 1 allocated to the working land option.* $-f^1_\alpha = 0$, $-f^2_\alpha = z_\eta \frac{\partial^2 \sigma}{\partial \delta_2 \partial \sigma^2_{2,wl}} = \frac{\delta_2}{\sigma} > 0$, $-f^3_\alpha = 0$, and $|F_{12}| = -\frac{\delta_1}{\sigma}\left(0 - f^1_3 f^2_3\right) > 0$. Again, this is intuitive, and is likely to hold in the general case, as one would expect the policymaker to

switch from parcel with high variability of working land benefits to ones that have a relatively lower working land benefit variability.

3. $\frac{\partial \delta_1}{\partial \sigma^2_{1,lr}} > 0$. *An increase in the variability of land retirement option benefit in parcel 1 acts to increase the optimal share of parcel 1 allocated to the working land option.* $-f^1_\alpha = \frac{-(1-\delta_1)}{\sigma}$, $-f^2_\alpha = 0$, $-f^3_\alpha = 0$, and $|F_{13}| = -\frac{(1-\delta_1)}{\sigma}\left(0-(f^2_3)^2\right) > 0$. As one would expect, when within a parcel, one particular option becomes "more risky", it is optimal to shift to the alternative.

4. $\frac{\partial \delta_1}{\partial \sigma^2_{2,lr}} < 0$. *An increase in the variability of land retirement option benefit in parcel 2 acts to decrease the optimal share of parcel 1 allocated to the working land option.* $-f^1_\alpha = 0$, $-f^2_\alpha = z_\eta \frac{\partial^2 \sigma}{\partial \delta_2 \partial \sigma^2_{2,lr}} = \frac{-(1-\delta_2)}{\sigma} < 0$, $-f^3_\alpha = 0$, and $|F_{14}| = \frac{(1-\delta_2)}{\sigma}\left(0 - f^1_3 f^2_3\right) < 0$. This is intuitive: as these results presume complete conversion of a land parcel either to land retirement or the working land option, this result implies that the share of parcel 1 allocated to land retirement will rise. This can be viewed as a substitution effect, as land retirement in parcel 2 becomes more risky.

5. *The effects of within-parcel (*$\mathrm{cov}\left(b^{wl}_1, b^{lr}_1\right)$*) and within-option (*$\mathrm{cov}\left(b^{wl}_1, b^{wl}_2\right)$, $\mathrm{cov}\left(b^{lr}_1, b^{lr}_2\right)$*) covariances are ambiguous.* The comparative statics results indicate that the sign of the effect depends on the initial optimal allocation share.

6. $\frac{\partial \delta_1}{\partial \,\mathrm{cov}(b^{wl}_1, b^{lr}_2)} < 0$. *An increase in across-parcel, across-option covariance of parcel 1 working land benefits with parcel 2 land retirement benefits results in a decrease in the*

optimal share of parcel 1 devoted to the working land option. $-f_\alpha^1 = \frac{1-\delta_2}{\sigma} > 0$,

$-f_\alpha^2 = \frac{-\delta_1}{\sigma} < 0$, $-f_\alpha^3 = 0$, and $|F_{15}| = -f_3^2\left(\frac{(1-\delta_2)}{\sigma} f_3^2 + \frac{\delta_1}{\sigma} f_3^1\right) < 0$.

7. $\frac{\partial \delta_1}{\partial \operatorname{cov}(b_1^{lr}, b_2^{wl})} > 0$. *An increase in across-parcel, across-option covariance of parcel 1 land retirement benefits with parcel 2 working land benefits results in an increase in the optimal share of parcel 1 devoted to the working land option.* $-f_\alpha^1 = \frac{-\delta_2}{\sigma} < 0$,

$-f_\alpha^2 = \frac{1-\delta_1}{\sigma} > 0$, $-f_\alpha^3 = 0$, and $|F_{16}| = -f_3^2\left(\frac{-\delta_2}{\sigma} f_3^2 - \frac{1-\delta_1}{\sigma} f_3^1\right) > 0$.

The following interpretation may be given for results 6 and 7. At this point it is helpful to establish that $\frac{\partial \delta_2}{\partial \operatorname{cov}(b_1^{wl}, b_2^{lr})} > 0$ and $\frac{\partial \delta_2}{\partial \operatorname{cov}(b_1^{lr}, b_2^{wl})} < 0$. While it is difficult to provide an intuitive explanation for individual effects in (6) and (7), they appear more logical when considered jointly with the simultaneous adjustment of working land share occurring at parcel 2. In particular, the effects of the covariances have opposite directions: whenever more is spent on working land conservation at parcel 1, less is spent at parcel 2. Given that working land costs are positively correlated across parcels, this behavior is consistent with the policymaker's desire to not increase the probability of budget constraint violation as the "portfolio" of land parcels is adjusted.

8. Finally, the somewhat surprising result is that the effects of ω_1^2, ω_2^2, and $\operatorname{cov}\left(c_1^{wl}, c_2^{wl}\right)$ are all ambiguous.[5]

[5] For example, the sign of the effect of ω_1^2 is:

In particular, this suggests that one cannot outright claim that the increase in the variance of working land conservation costs at parcel 1 is necessarily going to decrease the share of parcel 1 allotted to working land option. The relative magnitudes of benefit and cost variances and covariances determine the direction of this effect.

2.4.4. Safety First

The probabilistic approach to benefits and program costs adopted in this paper is motivated by some evidence that policymakers actually attempt to make environmental and budget decisions in a similar way. A natural counterpart to such behavior as it relates to investments in risky assets is called "safety first". The "safety first" models focus on investors who specify their criteria for portfolio returns in probabilistic terms. Elton, Gruber, Brown, and Goetzmann (2003) specify three types of safety first criteria and denote them as: (1) Roy's (1952) criterion, (2) Kataoka's (1963) criterion, and (3) Telser's (1955) criterion. The first two types of the safety first criteria are directly related to the behavior of a decision-maker analyzed in this paper. Investors following Roy's criterion minimize the probability that the portfolio return falls below some pre-specified critical level. The investors using Kataoka's criterion maximize the lowest level of portfolio return subject to the constraint that

---

$$\operatorname{sgn}\begin{vmatrix} 2\lambda z_\alpha \delta_1 & -z_\eta \frac{\partial^2\sigma}{\partial\delta_1\partial\delta_2} - \lambda z_\alpha \frac{\partial^2\omega}{\partial\delta_1\partial\delta_2} & c_1^{lr} - \mu_1^{wl} - z_\alpha \frac{\partial\omega}{\partial\delta_1} \\ 0 & -z_\eta \frac{\partial^2\sigma}{\partial\delta_2^2} - \lambda z_\alpha \frac{\partial^2\omega}{\partial\delta_2^2} & c_2^{lr} - \mu_2^{wl} - z_\alpha \frac{\partial\omega}{\partial\delta_2} \\ z_\alpha \delta_1 & c_2^{lr} - \mu_2^{wl} - z_\alpha \frac{\partial\omega}{\partial\delta_2} & 0 \end{vmatrix}$$

Thus, one needs: $f_2^1 f_3^2 - f_2^2 f_3^1 < 0$ for the variance of working land cost to have a negative effect.

the probability of actual portfolio return falling below this level is not greater than some predetermined value.

Viewed in the light of safety first terminology, the decision-maker maximizing the claimable benefit subject to a given level of probability of staying within an allotted budget is utilizing Kataoka's criterion with respect to environmental benefits, and is facing a Roy's-type budget constraint.

2.4.5. Efficiency of Solutions

In addition, realizing the connection that exists between our model and the portfolio choice theory, one can show that the allocations chosen by the decision-maker analyzed in this paper are efficient in the sense of Markowitz, that is, the allocations belong to the efficient mean-variance frontier. Then, the following propositions hold:

Proposition 3: For every stringency level in claimability of benefits, η, the optimal allocation $\boldsymbol{\delta}$ which solves (2.11) lies on the efficient frontier in the mean-standard deviation space of environmental benefits. That is, one cannot find alternative allocations that either provide a higher mean benefit for the same level of benefit variance, or lead to lower benefit variance for the same level of mean benefit, or do both.

Proof. By definition, the optimal allocation maximizes $B = \boldsymbol{\delta}'\boldsymbol{\beta} - z_{\eta} \cdot \left(\boldsymbol{\delta}'\boldsymbol{\Sigma}\boldsymbol{\delta}\right)^{1/2}$. Clearly, no feasible alternative solution can increase the mean without increasing the variance, decrease the variance without decreasing the mean, or do both, as that would contradict the optimality of $\boldsymbol{\delta}$. A similar proposition holds on the cost side:

Proposition 4. For every budget level which results in a binding budget constraint and for every pre-specified probability of staying within the budget α, the optimal allocation

$\boldsymbol{\delta}$ which solves (2.11) lies on the efficient frontier in the mean-standard deviation space of costs. That is, one cannot find alternative allocations that either provide a lower mean cost for the same level of cost variance, or lead to lower cost variance for the same level of mean costs, or do both.

Proof. Since the budget constraint is binding, it can be rewritten in the following form: $\boldsymbol{\delta}^{\mathbf{wl}\prime}\boldsymbol{\mu}^{\mathbf{wl}} + \boldsymbol{\delta}^{\mathbf{lr}\prime}\mathbf{c}^{\mathbf{lr}} = M - \theta^{-1}(\alpha)\left(\boldsymbol{\delta}^{\mathbf{wl}\prime}\boldsymbol{\Omega}_{\mathbf{wl}}\boldsymbol{\delta}^{\mathbf{wl}}\right)^{1/2}$. Clearly, given this relationship, it is impossible to decrease the left-hand side of the equality (mean costs) without decreasing the right-hand side through an increase in variance of costs. Conversely, decreasing the variance of costs is only possible via an increase in mean costs.

2.4.6. Risk Aversion and the Confidencel Level for Claimability of Benefits

The previous section establishes that for any given level of probabilities in the claimable benefit and the budget constraint expressions, one can be assured that the optimal solution is mean-variance efficient. Decision-makers, who value benefits, dislike costs, and exhibit aversion to risk both in regards to benefits and to costs will find their optimal allocations on the mean-variance frontier. However, is there a more precise way to relate aversion to risk and the probabilities that the decision-maker uses in finding optimal allocations? This section attempts to clarify this connection.

As can be noted from the statement of the general problem, the higher the η, the probability with which a particular benefit level has to be achieved in order to be considered claimable, the higher the weight the decision-maker puts on uncertainty regarding the benefits. One way to connect risk aversion and the confidence level in claimability of

benefits is to think about the decision-maker who has preferences over the quantity of benefits that can be described in terms of a constant absolute risk-aversion (CARA) utility function. An agent having such preferences would be placing the greater weight on the variance of benefits, the greater the coefficient of absolute risk-aversion, just like the decision-maker considered here places a greater weight on the standard deviation of obtained benefits, the greater the confidence level with which the benefits are claimable, η. Paris (1979) derived an explicit relationship between the coefficient of absolute risk aversion and the stringency, or confidence, level expressed by an agricultural firm regarding having sufficient quantity of inputs to produce the output. However, his analysis, pertaining to a limited class of so-called linear complementarity problems, is not directly applicable in the present case. Lichtenberg and Zilberman (1988) make an informal connection between the confidence level and the degree of risk aversion, but do not derive the formal relationship between the two.

Here, the formal connection between risk aversion on decision-maker's part regarding benefits and the confidence level for claimability of benefits is made. Consider again the general, N -parcel problem and return to vector notation. If the per-parcel benefits are jointly normal $\left(\mathbf{b} \sim MVN\left(\boldsymbol{\beta}, \boldsymbol{\Sigma}\right)\right)$, the benefits obtained follow a normal distribution: $\boldsymbol{\delta}'\mathbf{b} \sim N(\boldsymbol{\delta}'\boldsymbol{\beta}, \boldsymbol{\delta}'\boldsymbol{\Sigma}\boldsymbol{\delta})$. In our present formulation, the claimable benefits can then be denoted as $B = \boldsymbol{\delta}'\boldsymbol{\beta} - z_{\eta} \cdot \left(\boldsymbol{\delta}'\boldsymbol{\Sigma}\boldsymbol{\delta}\right)^{1/2}$. If, on the other hand, the decision-maker was risk-averse over obtained benefit level, he, following the famous mean-variance (E-V) rule, would seek to maximize $\max_{\boldsymbol{\delta}} \boldsymbol{\delta}'\boldsymbol{\beta} - \frac{r}{2}\boldsymbol{\delta}'\boldsymbol{\Sigma}\boldsymbol{\delta}$, where r is the coefficient of absolute risk aversion. Provided

that the maximization takes place under the same probabilistic cost constraint outlined above, the two approaches are equivalent if and only if $r = \frac{z_\eta}{(\boldsymbol{\delta}'\boldsymbol{\Sigma}\boldsymbol{\delta})^{1/2}}$.

Proof. Consider a regulator who values environmental benefits, $\boldsymbol{\delta}'\mathbf{b}$. In particular, this regulator's preferences can be described by a von Neumann-Morgenstern utility function of the form: $U(\boldsymbol{\delta}'\mathbf{b}) = -e^{-r(\boldsymbol{\delta}'\mathbf{b})}$. Faced with an uncertain prospect, the regulator maximizes expected utility, $EU(\boldsymbol{\delta}'\mathbf{b})$. Given that the benefits follow a normal distribution, and that the moment-generating function of a normal variate X with mean μ and standard deviation σ is: $M(t) = Ee^{tX} = e^{\mu t + \frac{\sigma^2 t^t}{2}}$, one can write the regulator's expected utility as:

$EU(\boldsymbol{\delta}'\mathbf{b}) = E\left(-e^{-r(\boldsymbol{\delta}'\mathbf{b})}\right) = -M(-r) = -e^{-r(\boldsymbol{\delta}'\boldsymbol{\beta}) + \frac{r^2(\boldsymbol{\delta}'\boldsymbol{\Sigma}\boldsymbol{\delta})}{2}}$. Hence, maximizing expected utility is equivalent to maximizing the negative of the exponent, $r(\boldsymbol{\delta}'\boldsymbol{\beta}) - \frac{r^2(\boldsymbol{\delta}'\boldsymbol{\Sigma}\boldsymbol{\delta})}{2}$. Factoring out r, one is left with maximizing the quantity, $\boldsymbol{\delta}'\boldsymbol{\beta} - \frac{r(\boldsymbol{\delta}'\boldsymbol{\Sigma}\boldsymbol{\delta})}{2}$, which is the mean-variance (E-V) rule. Rewriting the problem in terms of the standard deviation, the resulting first-order condition for maximization is: $\boldsymbol{\beta} - r(\boldsymbol{\delta}'\boldsymbol{\Sigma}\boldsymbol{\delta})^{1/2} \frac{\partial(\boldsymbol{\delta}'\boldsymbol{\Sigma}\boldsymbol{\delta})^{1/2}}{\partial\boldsymbol{\delta}} \overset{set}{=} \mathbf{0}$. Denote the solution to this problem as $\hat{\boldsymbol{\delta}}$. If the regulator maximizes claimable benefits, the first-order condition is: $\boldsymbol{\beta} - z_\eta \frac{\partial(\boldsymbol{\delta}'\boldsymbol{\Sigma}\boldsymbol{\delta})^{1/2}}{\partial\boldsymbol{\delta}} \overset{set}{=} \mathbf{0}$. Denote the solution to this problem as $\boldsymbol{\delta}^*$. The two approaches are equivalent if they result in the same decision vector $\boldsymbol{\delta}$. Clearly, this obtains if $r \equiv \frac{z_\eta}{(\boldsymbol{\delta}^{*\prime}\boldsymbol{\Sigma}\boldsymbol{\delta}^*)^{1/2}}$, which can be seen by substituting the resulting value of r into the E-V first-order condition

and proposing $\boldsymbol{\delta}^*$ as a solution. Conversely, if set $z_\eta \equiv r(\hat{\boldsymbol{\delta}}'\boldsymbol{\Sigma}\hat{\boldsymbol{\delta}})^{1/2}$ and substitute this expression into the first-order condition for the claimable benefit maximization, one also gets $\boldsymbol{\delta}^* = \hat{\boldsymbol{\delta}}$. This establishes equivalence between the two approaches.

Thus, a link between the two approaches in their treatment of benefits is obtained. For example, if the general N-parcel problem is solved under the conditions that carbon offsets are only claimable if there is 95 percent certainty in obtained reductions, the implied social coefficient of risk aversion regarding carbon emissions may be computed. The connection between the coefficient of absolute risk aversion, r, and the confidence level requirement, η, is highly nonlinear and depends both on the structure of the data given by covariance in benefits (Σ), as well as on the optimal solution, x.

Conversely, if the regulator instead of solving the problem of maximizing claimable benefits maximizes CARA expected utility, the solution will imply the confidence level for claimability of uncertain benefits.

Furthermore, since the regulator in this setup maximizes claimable benefits subject to the probabilistic cost constraint of the same form, one can make a similar connection to the regulator's risk preferences over budget violations. In this light, the regulator's problem can be described as maximizing utility over benefits subject to the constraint on expected disutility of costs[6].

It should be noted, however, that the above analysis does not claim that the decision-maker necessarily possesses CARA utility over benefits. In principle, there are many utility

[6] Since the distribution of total WL costs is not normal, the above analysis does not follow through exactly. However, a very similar analysis can be performed if one assumes a quadratic disutility function on costs. In this case, the assumption of normality is not required, however, and one can no longer interpret the weight placed on variance of costs in terms of the coefficient of absolute risk aversion. The quadratic utility function can be viewed as an approximation to the true utility function of a more complex form. Naturally, one could also assume a quadratic utility function in benefits and carry out a similar analysis.

functions that could give rise to the type of problem that is being solved in this paper. In particular, there is an infinity of expected utility functions that can rationalize a solution obtained using probabilistic constraints (Pyle and Turnovsky, 1970). All I am claiming is that if the decision-maker happened to have such utility function, he would arrive at the same solution, and, conversely, if one is willing to assume a certain type of a utility function, one can back out the preference parameter.

It is also not necessary to assume that the decision-maker has well-defined utility functions over environmental benefits and over program costs. However, it may be useful to think about decision-maker's preferences for the following reason. Suppose a decision-maker is proposing (or implementing) a program that affects, directly or indirectly, the environmental benefit in question. While this hypothetical new program may not have the probabilistic constraints explicitly outlined in it, one may be able to check the consistency of the decision-maker's choices by assuming certain preferences. For example, programs for agricultural carbon sequestration may be structured in a way that imply that the regulator is extremely risk-averse with respect to the benefits of greenhouse gas reductions, and at the same time, the regulatory behavior regarding, for example, power generators, may imply risk neutrality. The type of utility-based analysis used above may aid in identifying and analyzing such potentially troubling situations.

2.5. An Empirical Application

2.5.1. Data and Study Area

An application of the above method is made to a heavily farmed region of Iowa, the North Skunk River Watershed, represented by the US Geological Survey 8-digit Hydrologic

Cataloging Unit 7080106. The watershed runs in a south-eastern direction roughly from the geographical center of the state in the direction of the Mississippi River in Iowa's south-eastern corner (Figure 1). The watershed's cropland area is devoted primarily to cropland (57 percent, Iowa DNR, 2006).

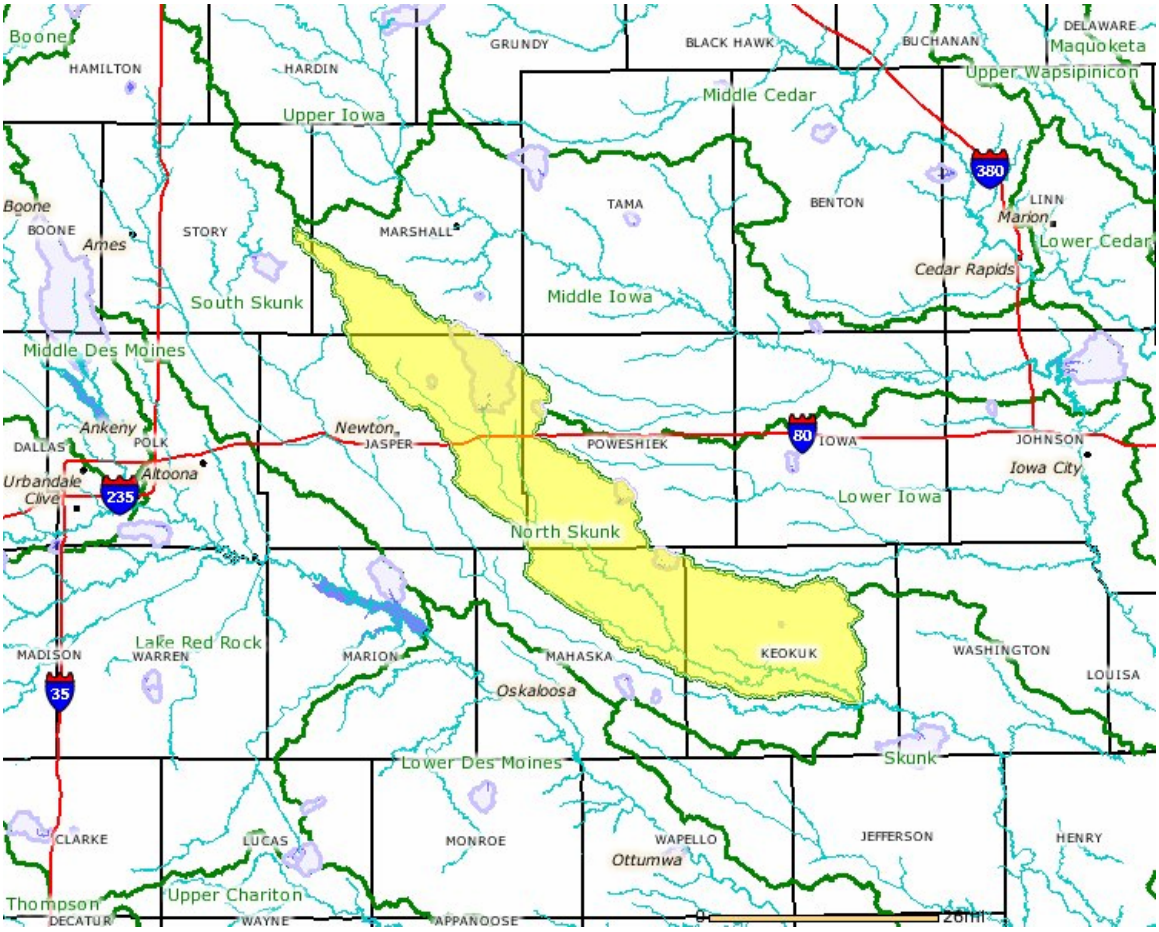

Figure 1. The North Skunk River Watershed, Iowa

Two independent sources of uncertainty are considered in evaluating the carbon sequestration benefits obtainable from the watershed. The first source is uncertainty associated with climate and weather conditions, such as precipitation, average minimum and

maximum temperatures, etc. The weather factors have been identified as important determinants of the potential of agricultural soils to sequester carbon (see, e.g., Bruce, Frome, Haites, Janzen, Lal, and Paustian, 1999).

The second source of uncertainty lies with the way working land conservation is implemented. Conservation tillage is taken to be the working land option as one of the most widely recommended options in this particular part of the country. However, exactly how the conservation tillage is done and what implements are used, and when, is not known with certainty. Instead, one can draw from the surveys of farms from this part of the state to obtain a range of ways conservation tillage may actually be implemented. To this end, I draw from the 1995 Cropping Practices Survey, the most recent set of publicly available farmer surveys available at this level.

The primary source of data on soil characteristics determining the potential carbon sequestration benefit is the 1997 National Resource Inventory (NRI) (Nusser and Goebel, 1997). The expansion factors for each of the sample NRI points represent the area associated with that point, and the sum of the expansion factors (4,524) is used as the cropland area of the watershed. For each of the 216 NRI points in the watershed, 50 draws from the historical weather record are made for each of the 3 options available: conventional tillage, conservation tillage, and land retirement. Also, 50 draws from the farm surveys are made for the conservation tillage option. The data is then used as an input in Erosion Productivity Impact Calculator (EPIC) Version 3060 model simulations to produce the estimates of carbon sequestered. The benefit from conservation tillage is the difference between the annual parcel carbon level yielded by conservation tillage and the baseline conventional tillage scenario. Table 1 presents the summary statistics for simulated soil carbon. The

average quantity of mean per acre carbon is 0.1725 tons C per acre per year for conservation tillage and 0.3256 tons C per acre per year for land retirement. This translates into 0.6326 tons CO_2 per acre per year for conservation tillage and 1.1939 tons CO_2 per acre per year for land retirement. These are consistent with some estimates reported in the literature (West and Post, 2002). While land retirement alternative produces higher mean carbon sequestration levels, it also appears to have lower sample per-acre variance. The mean variance of simulated per-acre carbon benefit from land retirement is higher than the mean variance of simulated per-acre carbon benefit from conservation tillage.[7] While in the optimal choice of alternatives under safety first-type constraints depends on the full variance-covariance structure, the sample data indicates that, on average, land retirement is an alternative associated with less predicted soil carbon variability. This is to be expected, as the carbon benefits from conservation tillage include, in addition to weather, farm implement uncertainty.

The data on costs of the two options, land retirement and conservation tillage, is obtained in the following way. Costs of land retirement are taken to be equal to the cash rental rates of farmland, computed by Kurkalova, Burkart, and Secchi (2004) for every NRI point in the area. The underlying assumption is that the rental rate represents the true opportunity cost of land.

The costs of inducing landowners to switch to conservation tillage are obtained using the conservation tillage adoption model developed by Kurkalova and Rabotyagov (2006). The model is capable of estimating the determinants of NRI-point-level adoption behavior using 1997 NRI data (most recent available), even though individual tillage choices are not observable, and instead one only observes county-level data.

[7] The null hypothesis of equal means is rejected at 1 percent level of significance.

The basic behavioral assumption of the model is the same as in Kurkalova, Kling, and Zhao (2006), namely, the farmer adopts conservation tillage if the net returns from adoption, plus the adoption premium required by farmer, exceed the net returns from conventional tillage. If a farmer chose not to adopt conservation tillage, there exists a payment that can be made to the farmer to induce adoption. This payment, or adoption subsidy, represents a

Table 1. Data summaries

Variable	Sample min	Sample average	Sample max
Mean carbon sequestered from land retirement, metric tons C per acre per year	-0.19	0.33	1.12
Variance of carbon sequestered from land retirement, metric tons C squared per acre squared	1.03×10^{-3}	8.02×10^{-3}	75.13×10^{-3}
Mean carbon sequestered from conservation tillage, metric tons C per acre per year	0.03	0.17	0.49
Variance of carbon sequestered from conservation tillage, metric tons C squared per acre squared	1.07×10^{-3}	11.11×10^{-3}	79.02×10^{-3}
Cost of land retirement, $ per acre per year	78.86	127.30	176.95
Cost of conservation tillage, $ per acre per year	0.0	23.48	86.75
NRI expansion factor, acres	1	20.94	41

natural measure of parcel-level working land conservation cost, and is computed as: $\hat{c}_i^{wl} = \hat{P}_i + (\pi_{oi} - \hat{\pi}_{1i})$, where $\hat{P}_i$ is the estimated adoption premium (due to risk aversion or existence of real options), and π_{oi} and $\hat{\pi}_{1i}$ are net returns from conventional and conservation tillage. Both the adoption premium and the net returns from conservation tillage are linear functions of the underlying model parameter estimates. Thus, the practical way of

constructing the distribution of working land costs at each parcel i is to obtain the conservation tillage adoption model parameter estimates and the corresponding variance-covariance matrix, draw from the estimated parameters distribution, compute the adoption subsidy, and keep the computed value only if the adoption subsidy is positive. At each parcel, the process is repeated 50 times, as each parcel received 50 weather and implement draws. The sample mean value of approximately $23.5 dollars per acre subsidy to induce conservation tillage is consistent with estimates reported elsewhere (Kling et al., 2005).

At this point it is worthwhile to consider a complication in establishing what is the appropriate distribution, and the subsequent critical value, $\theta^{-1}(\alpha)$, to be used in the deterministic equivalent of the probabilistic budget constraint? Clearly, the answer hinges on characterizing the distribution of the working land costs that follow the choice of allocation to parcels to working land, that is, on the distribution of $\sum_{i=1}^{N} \delta_i^* c_i^{wl} = \delta^{*\prime} c^{wl}$, where a star $*$ denotes the optimal solution. In particular, $\theta^{-1}(\alpha)$ cannot be a function of δ, and needs to be a scalar instead. If the vector of per-parcel working land costs, c^{wl}, follow a multivariate normal distribution, the distribution of the linear combination of costs would be normal and could be standardized easily. However, even if the *predicted* adoption subsidy, $\hat{c}^{wl}$, is multivariate normal, due to the fact that only positive adoption subsidies are considered, the distribution of working land costs is going to be censored[8].

[8] The predicted subsidies are linear combinations of maximum-likelihood estimated parameters of the conservation tillage adoption model, which are asymptotically normal. Analyzing histograms of predicted total subsidies required, I am unable to reject the null hypothesis of normality.

I proceed by constructing a series of approximations for the critical value of the distribution of the total working land costs based on standardized empirical distributions[9]. That is, I solve the problem of maximizing expected benefits subject to staying within budget in expectation for different budget levels and use the resulting allocation vectors to construct the total working land costs. Then, based on 50 draws from the working land cost at each parcel, the 50 different total working land costs are obtained. By generating histograms of the standardized total working land cost distribution, critical values can be produced. Table 2 gives the critical values for the range of budgets and probabilities of staying within the budget:

Table 2. Critical values for the standardized total working land cost distribution

		Probability of staying within budget			
		0.75	**0.9**	**0.95**	**0.99**
Budget level, thousands	**100**	0.216	1.333	2.215	3.993
	200	0.275	1.330	2.174	3.904
	300	0.305	1.312	2.110	3.857
	400	0.342	1.358	2.120	3.705

The resulting critical values are quite close to each other for different budget levels, especially for the 90 percent and 95 percent probabilities of staying within the budget. This provides some limited assurance that whatever differences in the allocation vector are introduced by changing the size of the budget, they do not fundamentally change the nature of the standardized distribution. Carbon benefits obtainable from land retirement and conservation tillage were assumed to follow a multivariate normal distribution. This could turn out to be an untenable assumption. However, the normality assumption is not rejected by

[9] A theoretically legitimate way to proceed would be to appeal to Chebyschev's Inequality. As expected, the resulting critical values are rather large. I instead opt for an approximation based on the distribution information available.

the normality tests performed on parcel-level carbon benefits. Therefore, the normality assumption is maintained.

2.5.2. Results

Using the data described above, I solve the constrained optimization problem which allows me to quantify the size of the uncertainty discount for soil carbon offsets, the necessary margin of safety for budget planning, and the optimal allocation of the enrolled land in the watershed to the two mutually exclusive carbon sequestration options. I solve the problem for 4 different annual budget levels: $100,000, $200,000, $300,000, and $400,000. Given that the cost of total enrollment of the watershed to maximize expected carbon benefits is found to be $416,805, these budget levels represent the levels of funding that may enroll progressively larger share of the watershed into the carbon sequestration program, all the way up to almost full cropland enrollment.

First, the size of soil carbon discount in percentage terms, which equals the absolute discount, $z_{\eta}\left(\boldsymbol{\delta}'\boldsymbol{\Sigma}\boldsymbol{\delta}\right)^{1/2} \geq 0$, divided by the mean carbon benefit, is analyzed. Similar to Kurkalova's (2005) findings, I find that the total uncertainty discount for soil carbon ranges from 2.4 percent to 9.4 percent, depending on the required confidence level in benefits, the size of the budget available and on the specified probability of staying within a budget. The following tables provide the magnitudes of the uncertainty discount for the scenarios analyzed. As expected, the size of uncertainty discount grows with the confidence level for claimability of benefits. Also, the uncertainty discount is non-decreasing in the probability of staying within a particular budget. While the first effect is clear to interpret (the weight placed on uncertainty in benefits grows, increasing the magnitude of the discount), the

second effect is indirect: as the decision-maker requires higher level of assurance of program costs, ex ante mean program expenditures fall (Figure 2), resulting, in turn, in lower mean benefits obtainable.

The reduction in the absolute discount due to smaller effective budget does not outweigh the reduction in mean program benefits, so their ratio either rises (budget levels of $100,000, $200,000, and $300,000), or stays unchanged (for the budget of $400,000). Another clear pattern emerges: the higher the budget level, the lower the uncertainty discount for every confidence level/probability of staying within budget combination. This is mostly due to to the change in the mix of the land retirement and conservation tillage on the total

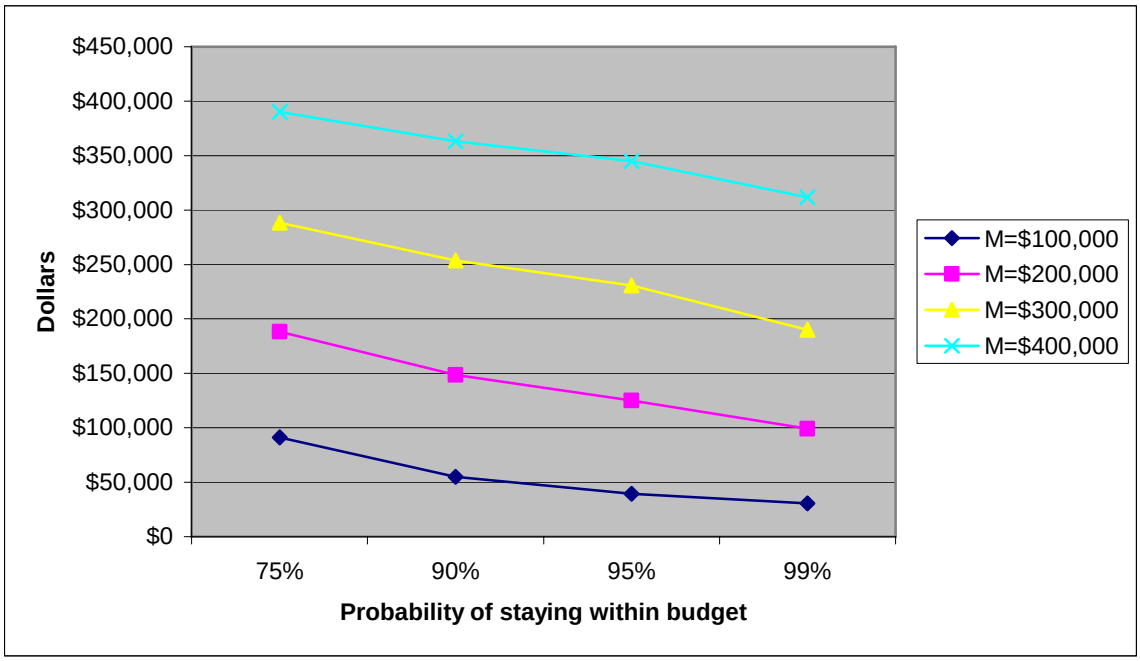

Figure 2. Ex ante mean program costs and the probability of staying within the budget, 95 percent confidence in benefits

land enrolled. In particular, the optimal mix of land retirement and working land practices changes as the size of available budget changes. Figure 3 demonstrates the composition of the land retirement and the working land option in the total land enrolled for different budget

levels for 95 percent confidence level in benefits and 90 percent probability of staying within the budget[10].

Tables 3. Carbon uncertainty discount, $100,000 budget, percent

		Probability of staying within budget			
		75%	**90%**	**95%**	**99%**
Confidence level in benefits	**90%**	4.0	4.5	4.9	5.2
	95%	5.1	5.8	6.4	6.7
	99%	7.2	8.0	8.9	9.4

Tables 4. Carbon uncertainty discount, $200,000 budget, percent

		Probability of staying within budget			
		75%	**90%**	**95%**	**99%**
Confidence level in benefits	**90%**	3.2	3.4	3.5	3.6
	95%	4.1	4.4	4.5	4.7
	99%	5.8	6.2	6.4	6.5

Tables 5. Carbon uncertainty discount, $300,000 budget, percent

		Probability of staying within budget			
		75%	**90%**	**95%**	**99%**
Confidence level in benefits	**90%**	2.7	2.7	2.8	2.8
	95%	3.4	3.5	3.6	3.7
	99%	4.8	5.0	5.1	5.1

Tables 6. Carbon uncertainty discount, $400,000 budget, percent

		Probability of staying within budget			
		75%	**90%**	**95%**	**99%**
Confidence level in benefits	**90%**	2.4	2.4	2.4	2.4
	95%	3.0	3.0	3.1	3.1
	99%	4.2	4.3	4.3	4.3

As the budget size grows to approach the cost of complete conversion of a watershed to carbon sequestration activity, the mix of the two options changes in favor of land

[10] The results for the other probabilistic constraints are similar.

retirement. For example, in the Figure above, the percentage of land enrolled in conservation tillage decreases from 89.9 percent for the $100,000 budget to 37.7 percent for the $400,000 budget. However, in the cases when the size of a budget is fairly small relative to the costs of conversion of the entire watershed, the working land option dominates the mix. Interestingly, the conclusions of Feng et al. (2006) hold up in general even with the introduction of uncertainty into the problem.

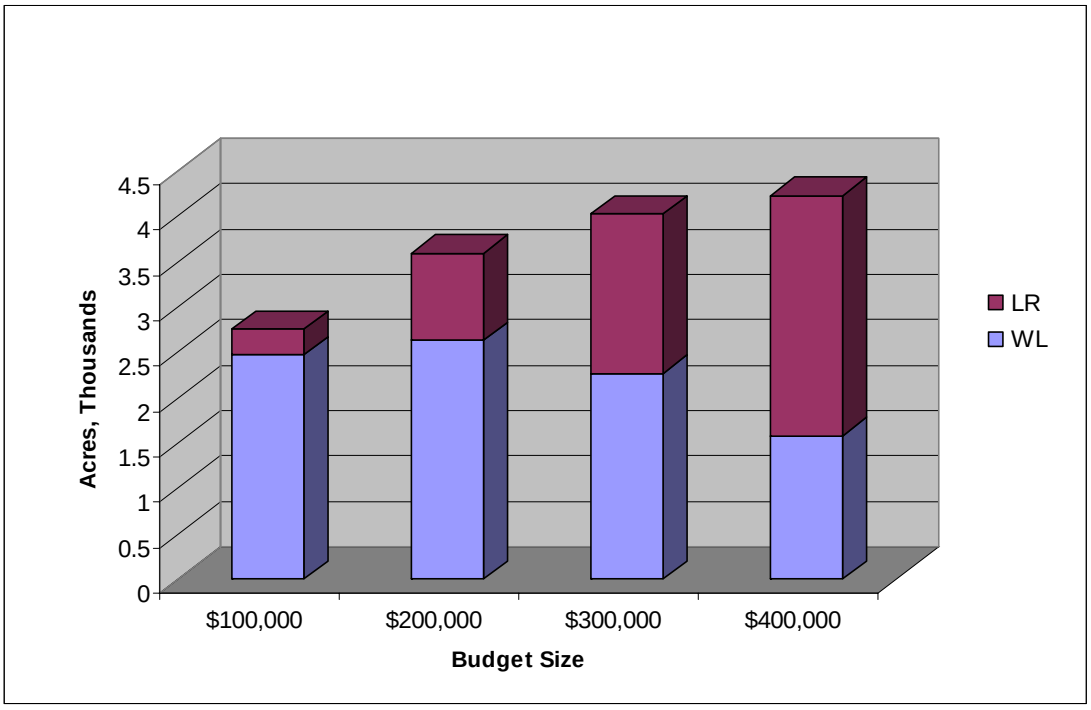

Figure 3. Optimal mix of alternatives in enrolled land

As discussed above, if one assumes certain risk preferences on the part of the decision-maker, one may be able to say something about the coefficient of risk aversion based on the probabilities that the decision-maker specifies go into the safety first constraints. In particular, given the assumed normality of benefits, it was shown that the coefficient of absolute risk aversion can be expressed as the function of the confidence level required and

the standard deviation of total benefits: $r = \frac{z_\eta}{(\boldsymbol{\delta}'\boldsymbol{\Sigma}\boldsymbol{\delta})^{1/2}}$. Thus, given a particular solution, an implied coefficient of risk aversion can be computed. However, it is perhaps more interesting to look at the relative changes in the risk aversion coefficient as the confidence level changes. Suppose one decision-maker requires a η_0 level of confidence in benefits, while the other demands $\eta_1 > \eta_0$. Then, the ratio of their risk aversion coefficients becomes:

$\frac{r_1}{r_0} = \frac{z_{\eta_1}}{z_{\eta_0}} \frac{(\boldsymbol{\delta}_0'\boldsymbol{\Sigma}\boldsymbol{\delta}_0)^{1/2}}{(\boldsymbol{\delta}_1'\boldsymbol{\Sigma}\boldsymbol{\delta}_1)^{1/2}}$, which is the product of a ratio of critical values of standard normal distribution and the ratio of program benefit standard deviations. If the computed standard deviations of program benefits do not differ by much, the coefficient of risk aversion of the second hypothetical decision-maker is directly proportional to their stated required confidence levels: $r_1 \cong \frac{z_{\eta_1}}{z_{\eta_0}} r_0$.

Based on the optimization results, the ratios of standard deviations indeed approximately equal to one. Then, for example, if two decision-makers are observed, and the first one is comfortable with 90 percent level of confidence in benefits, while the other one insists on 99 percent, then one can claim that the second decision-maker's coefficient of absolute risk aversion is $\frac{z_{0.99}}{z_{0.9}} = \frac{2.32}{1.28} = 1.81$ times higher than that of the first decision-maker.

The model used in this paper is motivated by the problem faced by a regulator or an aggregator who wishes to plan for enrolling land into carbon sequestration and does not presume that there is a well-functioning carbon market. However, based on these results, one can compute a "break-even" price per ton of CO_2. For example, if the carbon offsets are claimable with 95 percent confidence in carbon benefits and the decision-maker wishes to

control the program costs to be less than $100,000 dollars per year with 90 percent probability, a sure price of $44.8 per ton of carbon dioxide will ensure that the program will return a positive profit with 90 percent probability. Interestingly, the break-even prices rise monotonically with the available budget. The reason is that the bigger the budget that is to be spent in this particular watershed, the higher the proportion of the costly land retirement option, which in turn requires a higher carbon dioxide price in order to justify the program expense. Interestingly, unlike in Kurkalova's (2005) study, I do not find that the size of the uncertainty discount in benefits increases with carbon price. In fact, the opposite is true, since as the budget size increases, the lower-variance land retirement option becomes more affordable and the magnitude of the uncertainty discount falls. On the cost side, the uncertainty effect can be explained in terms of budgeting with a margin of safety. The margin of safety is quite moderate for up to 90 percent ex ante probability of staying within the budget, which suggests that planning for agricultural carbon sequestration can be undertaken with reasonable certainty about the ex post program costs. In particular, insisting on 75 percent probability of controlling the costs below the budget level results, depending on the budget level and the level of confidence in benefits, in creation of a margin of safety ranging from 2 to 9 percent of the budget. When 90 percent is specified as the relevant budget planning probability, the margin of safety ranges between 9 and 45 percent of the budget. Should the decision-maker insist on further assurances about the program costs, an even greater share of the budget would have to be set aside to create the necessary margin of safety.

2.6. Concluding Remarks

Ignoring uncertainty in environmental benefits obtained from implementing a program that enrolls agricultural land may be both scientifically unjustifiable and politically infeasible. For example, if an analysis of carbon sequestered by agricultural soils ignores uncertainty, it is unlikely to illuminate the political process seeking a solution for greenhouse gas mitigation if the parties involved care about having some assurance of certainty of reaching sequestration targets (as they do). Second, in many cases, researchers and regulators ex ante have imperfect information about the costs of implementing a particular environmental practice.

While the safety first-type constraints employed in this paper are by far not the only reasonable way of dealing with uncertainty, they do appear to enter, implicitly or explicitly, in many regulatory decisions. For example, the TMDL's for water pollutants must include a "margin of safety" which directly follows from a probabilistic, safety first, constraint. Also, decision-makers may be more likely to give a numeric estimate for the desired probability of achieving a benefit or staying within budget than to explicitly voice, for example, the corresponding coefficients of risk aversion. Therefore, careful analysis of choices framed in such ways is necessary for a more systematic way of coping with uncertainties. It is hoped that this work contributes to such analytic framework.

Results of the application of the analytical method to soil carbon sequestration from an Iowa watershed indicate that, while the concerns due to soil carbon uncertainty are justified, the magnitude of predicted discounts are such that inclusion of soil carbon offsets in a portfolio of greenhouse gas mitigation measures appears feasible. Further, accounting for

ex ante uncertainty in program costs by using models of economic behavior may allow the regulators and/or aggregators to better plan their carbon contracting decisions.

2.7. References

Al, M.J., T.L. Feenstra, and B.A. van Hout. 2005. Optimal allocation of resources over health care programmes: dealing with decreasing marginal utility and uncertainty. *Health Economics* 14: 655-667.

Babcock, B.A., P.G. Lakshminarayan, J. Wu, and D. Zilberman. 1996. The economics of a public fund for environmental amenities: a study of CRP contracts. *American Journal of Agricultural Economics* 78: 961-971.

Babcock, B.A., P.G. Lakshminarayan, J. Wu, and D. Zilberman. 1997. Targeting tools for the purchase of environmental amenities. *Land Economics* 73(3): 325-339.

Beavis, B., and M. Walker. 1983. Achieving environmental standards with stochastic discharges. *Journal of Environmental Economics and Management* 10: 103-111.

Bruce, J.P., M. Frome, E. Haites, H. Janzen, R. Lal, and K. Paustian. 1999. Carbon sequestration in soils. *Journal of Soil and Water Conservation* 54(1): 382-389.

Butt, T.A., and B.A. McCarl. 2003. Can farmers sell all the carbon they sequester? Texas A&M University, *unpublished manuscript.*

Byström, O., H. Andersson, and I.-M. Gren. 2000. Economic criteria for using wetlands as nitrogen sinks under uncertainty. *Ecological Economics* 35: 35-45.

Canada. 1998. Methodological issues, inventories and uncertainties. United Nations Framework Convention on Climate Change, Subsidiary Body for Scientific and Technological Advice. Additional submissions by parties to the Ninth Session at Buenos Aires, 2-13 November, 1998, Item 4 of the provisional agenda. Other Matters, Approaches to resolving methodological issues related to national communications from Annex I Parties. Available online at: http://www.unfccc.de/resource/docs/1998/sbsta/misc06a01.pdf. Accessed April 20, 2005.

Charnes, A., and W.W. Cooper. 1959. Chance constrained programming. *Management Science* 6: 73-79.

De, P.K., D. Acharya, and K.C. Sahu. 1982. A chance-constrained goal programming model for capital budgeting. *The Journal of the Operational Research Society* 33(7): 635-638.

Eloffson, K. 2003. Cost-effective reductions of stochastic agricultural loads to the Baltic Sea. *Ecological Economics* 47: 13-31.

Elton, E.J., M.J. Gruber, S.J. Brown, and W.N. Goetzmann. 2003. Modern portfolio theory and investment analysis. Sixth Edition. John Wiley & Sons.

Feng, H., L.A. Kurkalova, C.L. Kling, and P.W. Gassman. 2006. Environmental conservation in agriculture: Land retirement versus changing practices on working land. *Journal of Environmental Economics and Management* 52(2): 600-614.

Gurgur, C.Z., and J.T. Luxhoj. 2003. Application of chance-constrained programming to capital rationing problems with asymmetrically distributed cash flows and available budget. *The Engineering Economist* 48(3): 241-258.

Hagigi, M., B.D. Kluger, and D. Shields. 1990. Cost uncertainty and budget overspending: a safety-first perspective. *Journal of Accounting and Public Policy* 9: 257-270.

Iowa Department of Natural Resources. 2006. Watershed Initiative. Available at: http://www.igsb.uiowa.edu/nrgislibx/watershed/watersheds.htm. Accessed October 10, 2006.

Kampas, A., and B. White. 2004. Administrative costs and instrument choice for stochastic non-point source pollutants. *Environmental and Resource Economics* 27: 109-133.

Keown, A.J., and B.W. Taylor. 1980. A chance-constrained integer goal programming model for capital budgeting in the production area. *The Journal of the Operational Research Society* 31(7): 579-589.

Kibzun, A., and Y. Kan. 1996. Stochastic programming problems with probability and quantile functions. Chichester: John Wiley & Sons.

Kling, C.L., S. Secchi, M. Jha, L. Kurkalova, H.F. Hennessy, and P.W. Gassman. 2005. Nonpoint source needs assessment for Iowa: The cost of improving Iowa's water quality. Final Report to the Iowa Department of Natural Resources. Center for Agricultural and Rural Development, Iowa State University, Ames, Iowa.

Kurkalova L.A., C.L. Kling and J. Zhao. 2006. Green subsidies in agriculture: estimating the adoption costs of conservation tillage from observed behavior, *Canadian Journal of Agricultural Economics* 54: 247–267.

Kurkalova, L.A., and S.S. Rabotyagov. 2006. Estimation of a binary choice model with grouped choice data. *Economics Letters* 90(2): 170-175.

Kurkalova, L.A. 2005. Carbon sequestration in agricultural soils: discounting for uncertainty. *CARD Working Paper 05-WP 388.*

Kurkalova, L.A., C. Burkart, and S. Secchi. 2004. Cropland cash rental rates in the Upper Mississippi River Basin. *CARD Technical Report 04-TR 47.*

Lichtenberg, E., and D. Zilberman. 1988. Efficient regulation of environmental health risks. *The Quarterly Journal of Economics* 103(1): 167-178.

Marland, G., B.A. McCarl, and U. Schneider. 2001. Soil carbon: policy and economics. *Climatic Change* 51: 101-117.

McSweeny, W.T., and J. S. Shortle. 1990. Probabilistic cost effectiveness in agricultural nonpoint pollution control. *Southern Journal of Agricultural Economics* 22(1): 95-104.

Nusser, S.M., and J.J. Goebel. 1997. The National Resource Inventory: A long-term multi-resource monitoring programme. *Environmental and Ecological Statistics* 4: 181–204.

Paris, Q. 1979. Revenue and cost uncertainty, generalized mean-variance, and the linear complementarity problem. *American Journal of Agricultural Economics* 61: 268-275.

Paris, Q., and C.D. Easter. 1985. A programming model with stochastic technology and prices: the case of Australian agriculture. *American Journal of Agricultural Economics* 67: 120-129.

Pyle, D.H., and S.J. Turnovsky. 1970. Safety-first and expected utility maximization in mean-standard deviation portfolio analysis. *The Review of Economics and Statistics* 52(1): 75-81.

Rosenberg, N.J., and R.C. Izaurralde. 2001. Storing carbon in agricultural soils to help head-off a global warming. Guest editorial. *Climatic Change* 51: 1-10.

Takayama, A. 1993. Analytical methods in economics. University of Michigan Press, Ann Arbor.

United States Department of Agriculture (USDA), 1995. Cropping practices survey, unofficial USDA data files. Available at: http://usda.mannlib.cornell.edu/usda/usda.html. Accessed January 23, 2005.

Weinstein, M., and R. Zeckhauser. 1973. Critical ratios and efficient allocation. *Journal of Public Economics* 2: 147-157.

West, T.O., and W.M. Post. 2002. Soil organic carbon sequestration by tillage and crop rotation: a global data analysis. *Soil Science Society of America Journal* 66: 1930-1946.

CHAPTER 3. OPTIMAL DESIGN OF PERMIT MARKETS WITH AN *EX ANTE* POLLUTION TARGET

3.1. Introduction

A highly celebrated property of emissions trading markets is that decentralized decisions made by firms will achieve a preset emissions target at the least possible cost and no information on the firm's abatement costs is required to achieve this outcome (Baumol and Oates, 1988; Montgomery, 1972).[11] Montgomery (1972) demonstrated that this property extends to the class of non-uniformly mixed pollutants, pollutants whose damages differ based on their location. He showed that if the regulatory authority allows firms to trade emissions according to the ratio of delivery coefficients (the effect that a source's emissions have on resulting pollution loadings) and sets the pollution cap equal to the desired pollution standard, the least cost property is retained.

The basic model underlying these findings assumes that the regulator is interested in minimizing the cost of meeting an *ex post* environmental standard. While *ex ante* uncertainty regarding firm's abatement costs is commonly used to motivate the attractiveness of a permit system, the pollution constraint is typically specified in *ex post* terms – the environmental target is invariant with respect to realizations of any sources of uncertainty. As has long been recognized, characterization of the objective function in this way requires that the pollution control level is independent of the actual realization of costs – no tradeoff between abatement costs and benefits (pollution levels) is permitted. As a result, even though the target would be reached at the least cost, the least (realized) cost may turn out to be very expensive. Roberts

[11] The total permit quantity can be set at the socially efficient level, a legally mandated requirement, or any other level deemed appropriate by the regulator.

and Spence (1976) and Montero (2001) recognized that the rigidity of a quantity mechanism may be socially costly. Roberts and Spence (1976) proposed a penalty for exceeding the pollution cap, while Montero (2001) modeled incomplete enforcement to provide a softening of the quantity constraint.

In this chapter, I study the optimal design of a permit trading system when the regulator is uncertain about the firms' abatement costs or delivery coefficients. In such situations, the regulator can specify her objective function based on minimizing expected costs subject to meeting an expected pollution level. This target is called an *ex ante* target. There are at least two situations in which an *ex ante* target will be important to model: 1) when there is genuine uncertainty in the delivery coefficients an *ex ante* target is the only feasible choice for the regulator to consider and 2) even if the delivery coefficients are known to the regulator, the damage function may be such that it is appropriate to focus on the average (or total) emission level. The large array of nonpoint source emission problems are all excellent examples of the first situation. Indeed, uncertainty in the delivery coefficient is often identified as one of the definitional aspects of a nonpoint source pollutant.[12] In the second situation, the use of an *ex ante* target offers another way to soften the rigidity of a quantity constraint. Additional examples of the situations are provided throughout the paper.

Several noteworthy findings emerge from the model. First, the optimal total permit cap does not necessarily equal the regulators pollution target. One is an *ex ante* concept (the desired pollution level) while the other is an *ex post* construct (the emissions cap). This can be viewed as a two-stage decision where in the first time period the regulator settles on a

[12] While the primary focus of the essay is on expected pollution, the model can be extended to deal with pollution targets which are expressed as statements controlling quantiles of the pollution distribution. For example, if, instead of the expectation, the target was specified as a probability of actual pollution not exceeding the target, chance- constrained formulations could be employed.

desired pollution target and then, based on the firms' expected emissions decisions, sets the number of permits and trading ratio to implement the market.

Second, the optimal trading ratio depends on the moments of the uncertain costs as well as the delivery coefficients. In particular, even when the delivery coefficients are assumed to be known with certainty, it is not optimal to set trading ratios equal to the simple ratio of delivery coefficients – the basic Montgomery (1972) solution. Instead, the regulator can lower expected costs by including some information on the uncertain abatement costs in the formation of the trading ratio. That the optimal trading ratio depends on both the regulators information about costs and the delivery coefficients is consistent with the findings from Horan and Shortle (2005) and Malik et al. (1993). However, the result here is derived in a different policy context. While previous studies continue in the tradition of using complete information on abatement costs to characterize first-best levels of pollution control, the focus of this paper is on meeting a given standard (regardless of its social optimality) which, based on established theory should be achievable without any information on abatement costs. In practice, pollution targets are often set by political processes, for example, the sulfur permit trading program where the SO_2 standards were set in legislation or water quality trading programs (e.g., Horan and Shortle, 2005). Furthermore, the social damage of pollutants is often unknown. Thus, it is also important to consider the design of permit markets in a cost-effectiveness context.

These somewhat surprising findings come directly from the fact that the regulator's objective function is specified in *ex ante* terms: she minimizes expected costs subject to an expected pollution level. This allows the regulator flexibility that is not present when

emission levels must be met with certainty *ex post*.[13] In essence, this allows the regulator to adjust for, at least to some degree, the actual cost realizations of firms: if costs are unexpectedly high (low), the resulting pollution levels will be higher (lower) than they would be without this flexibility. In considering this tradeoff, the regulator recognizes that the ultimate abatement levels chosen by firms will depend upon their cost realization and therefore the ultimate emission levels become stochastic from the regulator's perspective. By choosing the parameters of the trading program to be a function of the moments of the distribution of costs, the regulator can lower total expected abatement costs, while ensuring that the environmental goal is still being met on the average.[14]

Whether the regulator has (or should have) the freedom to design a permit market that allows the aforementioned flexibility is a policy question that will have a case by case answer. However, there are many real world examples where averages over time or space define standards. Examples include nitrogen dioxide (an annual arithmetic mean), lead (quarterly average during the phase-out), and sulfur dioxide (annual means, a 24- hour average and a 2-hour average) (USEPA, 2007a). Examples from water pollution abound as well: values for arsenic, cadmium, cyanide, and selenium emissions in storm water under the National Pollutant Discharge Elimination System (a key regulatory program that regulates point sources of water effluents) trigger need for action only when the annual average exceeds the benchmark (USEPA, 2007b).

Perhaps, the best examples of trading programs with an *ex ante* target can be found in emerging water quality trading programs. The Total Maximum Daily Load (TMDL) process

[13] In this way, the current model and findings are in the spirit of Roberts and Spence (1976) and Montero (2001).

[14] Note that I do not consider the important problem of information extraction from firms, but assume that the regulator has some independent source of cost information. See Montero (2000) or Lewis (1996) for careful discussions of asymmetric information problems.

is being implemented around the country to address the nation's still prevalent problem of water quality degradation. Under a TMDL, the sources of water quality impairment are identified and the loading reduction responsibilities allocated among the various sources. Even though it is called TMDL, many of the loadings are specified in terms of the annual average loadings. In this sense, the TMDL is given as an *ex ante* target. Many watersheds have established water quality trading programs or are exploring trading as a policy instrument to implement the TMDL targets in a cost-effective way (Hoag and Hughes-Popp 1997; USEPA 2004; Woodward et al. 2002). Setting trading ratios and permit caps will be a key component of such programs.

In the next section of the paper, the basic model of firms' behavior under a tradable emissions program and the regulator's problem is presented. Section 3 examines the optimal permit market design under two different assumptions. First, the case when the delivery coefficient is known, is considered. This provides results that contrast with the *ex post* standards studied in Baumol and Oates (1988) and Montgomery (1972), highlighting the implication of using *ex ante* targets and objective functions. Second, an important case when the delivery coefficient is uncertain, is presented. While this latter feature is typically viewed as a characteristic of nonpoint sources, there are likely many point sources where the true impact of emissions from the source are known with less than perfect certainty such as air sheds where dispersion of particulates may depend on stochastic weather conditions (Foster and Hahn, 1995). Final remarks and conclusions complete the paper in section 4.

3.2. The Model

3.2.1. Model Setup

Suppose there are two firms acting as sources of emissions and the environmental impacts of the two firms' emissions are not identical. Specifically, assume that the impact of the first firm on the resulting pollution level is such that one unit of Firm 1's emissions increases the resulting pollution level by one unit. The impact of Firm 2 is described by the delivery coefficient d, that is, one unit of Firm 2's emissions increases the resulting pollution level by d units. The delivery coefficient can be thought of as describing the relative environmental impact of the two firms' emissions. Specifically, the total resulting pollution level is $e_1 + de_2$, where e_i for $i = 1,2$ represents Firm *i*'s emissions. Both the situation in which the delivery coefficient is fixed and known by the regulator, as well as a more realistic case where the delivery coefficient is uncertain, is modeled. In the latter case the regulator, however, knows the distribution of the delivery coefficient: its mean, $E(d) = \mu$, and its variance, $Var(d) = \sigma_d^2$. The model lends itself to multiple interpretations including (1) two firms located spatially apart whose emissions contribute differentially to loadings at the receptor (Baumol and Oates, 1988), (2) two firms whose emissions contribute differentially to loadings for reasons other than spatial location, such as production process or concentration of emissions released, or (3) two firms, one of which is a point source and the other is a nonpoint source with an uncertain delivery coefficient.

The abatement cost function for Firm *i* is $C_i(e_i^0 - e_i; \theta_i)$, where, for $i = 1,2$, e_i^0 represents the initial (unregulated) emissions level for firm *i* and $e_i^0 - e_i$ represents the abatement of Firm *i* after the implementation of a permit trading program. The abatement

cost function is assumed to be increasing and convex in abatement, that is, $C_i' > 0$ and $C_i'' \geq 0$. The parameter (θ_i) in the cost function captures the uncertainty regarding the costs of pollution abatement on the regulator's side. I assume that the regulator has some, albeit incomplete, information on abatement costs. Uncertainty is modeled as stochastic information not revealed at the design stage of the permit market, but revealed at the time permit trading decisions are made. Formally, when making their emissions decisions, firms know θ_1 and θ_2. However, the regulator, when making the decisions on the parameters of the permit market, knows only their distribution: the means (zero), variances (σ_1^2 and σ_2^2), and covariance, ($\text{cov}(\theta_1, \theta_2)$). Furthermore, the regulator is assumed to know the covariances, if any, between the delivery coefficient and the cost parameters: $\text{cov}(d, \theta_1)$ and $\text{cov}(d, \theta_2)$. Such correlations may arise, for example, when weather affects the efficacy and cost of abatement as well as its spatial impacts.

The setup of the model is similar to that in the point and nonpoint source trading literature (e.g., Horan and Shortle 2005; and Malik et al. 1993) with the following notable differences. First, I examine the optimal trading programs in a cost-effectiveness context. That is, the policy objective is to set the parameters of the trading program so that a pollution target will be achieved at the least cost. Thus, the social damage of the pollution does not directly enter the design of the trading policy. Second, the regulator is assumed to be uncertain of firms' abatement costs in this model, while in the previous studies full information is assumed at the policy design stage.

3.2.2. *Ex Ante* and *Ex Post* Pollution Targets; Total Permit Cap, and Actual Pollution Level

Since cost minimizing firms equate marginal abatement costs with permit prices to choose their emission levels, once uncertainty is introduced into the cost functions, there will be uncertainty in emission levels. Given this and the potential uncertainty associated with the delivery coefficients, it is necessary to clearly differentiate between *ex ante* and *ex post* measures of pollution as well as other constraints that relate to the design of an emissions trading system. Only one of the two constraints will be relevant for a particular policy and they can be written as

(3.1)
$$\begin{array}{ll} \text{(Ex ante pollution constraint)} & E[e_1]+E[de_2]\le \bar{P}_{ante}, \\ \text{(Ex post pollution constraint)} & e_1+de_2\le \bar{P}_{post}. \end{array}$$

If the pollution target is specified in an *ex ante* manner, the first equation in (1) describes the constraint and indicates that the expected pollution has to be less than or equal to a pre-fixed target ($\bar{P}_{ante}$). Under this constraint, the *ex post* realization of pollution level can be greater or less than the target. In contrast, if the constraint is specified as *ex post*, the realized *ex post* pollution levels must be less than a pollution target ($\bar{P}_{post}$) in each realization.

A third relevant constraint defines the restriction faced by the permit market,

(3.2) (Permit market constraint) $e_1+te_2\le \bar{P}_{permit}.$

Here, t is the trading ratio for the emissions of the two firms—1 unit of Firm 2's emissions is equivalent to t units of Firm 1's emissions—and $\bar{P}_{permit}$ is the total permit cap, denominated in terms of Firm 1's emissions. Thus, this constraint requires that total emissions (weighted by the trading ratio) be less than or equal to the total permit cap. Note that the firms are only concerned with the permit market constraint while the regulator will care predominately

about the pollution constraint (either the *ex ante* or *ex post* version). Finally, $e_1 + de_2 = P_{actual}$ specifies the actual realization of pollution given firms' emissions decisions and the realization of the delivery coefficient.

With perfect information, there is no distinction between *ex ante* and *ex post* and it is known from Montgomery (1972) that efficiency dictates that $t = d$, resulting in $\bar{P}_{ante} = \bar{P}_{post} = \bar{P}_{permit}$. That is, the three constraints are essentially the same. However, when there is uncertainty, either $\bar{P}_{post}$ or $\bar{P}_{ante}$ may be used as a target in pollution reduction policies resulting, as will be shown, in very different efficient designs for a permit program. If it is legally stipulated, or the damage function dictates, that pollution not exceed a deterministic, prefixed standard, then $\bar{P}_{post}$ is the relevant constraint for cost minimization. This is the commonly analyzed case when total pollution is limited to a prefixed cap, regardless of firms' abatement costs. As discussed in the Introduction, there are many examples when standards are framed in terms of averages suggesting that such an inflexible target may not be appropriate or necessary in many cases.

Given an *ex ante* target, the regulator potentially has the flexibility to issue permits, $\bar{P}_{permit}$, and set the trading ratio, t, to achieve the expected pollution target at least cost. The following chart illustrates the decision process and the occurrence of events:

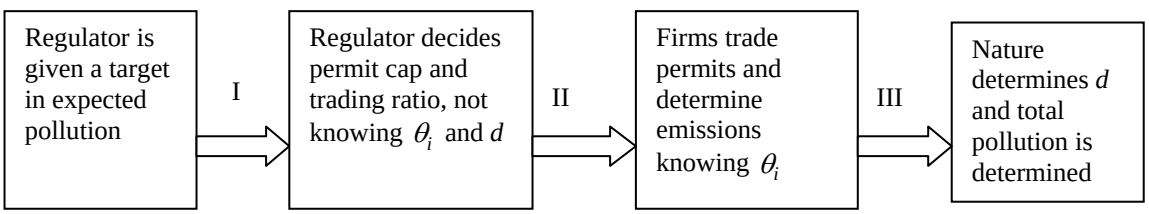

Figure 1. Decision process

This sequential timing process makes clear that the actual pollution, P_{actual}, varies with the realization of firms' abatement costs and/or the delivery coefficient whereas $\bar{P}_{ante}$ (or $\bar{P}_{post}$, or $\bar{P}_{permit}$) must be set before the realization of these uncertainties and will not change when the uncertainties are resolved.

3.2.3. Firms' Emission Decisions in a Permit Trading Market

Should an emissions trading program be introduced, the firms will face the permit market constraint in (3.2). Suppose the initial permit endowments allocated to Firm *i* (and denominated in Firm *i*'s emissions) are $\bar{e}_i$ for $i = 1, 2$; and $\bar{e}_1 + t\bar{e}_2 = \bar{P}_{permit}$. Through trading, both firms can hold the permits denominated in terms of another firm's emissions, and the trading ratio is used to convert between the two types of permits. The trading program requires that each firm's actual emissions do not exceed its holding of permits. Let y_i, denominated in terms of Firm *i*'s emissions, denote the equilibrium quantity of permits traded. Specifically, y_i is the permit quantity sold by Firm *i* and purchased by the other firm. Assuming that each firm takes permit prices as given, then Firm 1's problem would be as follows

$$\min_{e_1, y_1, y_2} C_1(e_1^0 - e_1) - p_1 y_1 + p_2 y_2 \quad \text{subject to} \quad e_1 + y_1 - t y_2 \le \bar{e}_1 \tag{3.3}$$

Firm 2's problem is similar. Solving for the firms' problems, it is well-known that market equilibrium requires that: $MC_i \equiv C_i'(e_i^0 - e_i^*) = p_i$, for $i = 1, 2$; and $p_1 / p_2 = 1/t$. This implies that the ratio of permit prices must be equal to the trading ratio. Otherwise, costless arbitrage opportunities would be available to firms. Then, it must be that

(3.4) $$\frac{MC_2}{MC_1} = t\,.$$

From (3.4) and the permit market constraint in (3.2), one can solve for firms' optimal emissions as a function of t and $\bar{P}_{permit}$, that is, $e_i^*(t, \bar{P}_{permit}; \theta_1, \theta_2)$ for $i = 1, 2.$ When emissions decisions are made in the permit trading market, firms have complete information on their costs, i.e., θ_1 and θ_2 are known with certainty. Equation (3.4) indicates that the results of the permit trading market are such that the ratio of marginal costs equals the trading ratio. However, with complete information on θ_1 and θ_2, it is known from Montgomery (1972) that social efficiency requires $t = d$, resulting in

(3.5) $$\frac{MC_2}{MC_1} = d\,.$$

Any gains in setting t at a level other than d in an *ex ante* targeting program would need to be weighed against the efficiency costs of not attaining the equality in (3.5). This is an issue I will return to in the next section.

3.2.4. The Regulator's Problem

This chapter focuses on the design of permit trading programs where the goal is to reach an environmental target at the lowest cost when the target is set as an *ex ante* pollution level, rather than an *ex post* standard. When damage is linear in pollution, the solution to this problem coincides with the solution to the problem of minimizing the sum of damage and abatement costs. While I believe the conditions of uncertainty modeled are representative of a broad variety of environmental pollutants, water quality provides a strong motivating example. Imagine there are two sources of effluent that enter a river: source 1 is a large

"point" source that is located at the river's edge and source 2 is a "nonpoint" source that is located some distance from the river. Given the proximity of source 1 to the river, its delivery coefficient is known with certainty to be unity whereas the nonpoint nature of source 2 means that the delivery coefficient is uncertain due to weather variability.

For the situation analyzed most in the permit trading literature where the delivery coefficient is known and an *ex post* pollution target is used, the regulator must set the trading ratio equal to d and $\bar{P}_{permit} = \bar{P}_{post}$ if she does not have complete information on firms' abatement costs. Otherwise, there is no guarantee that the target will be met. This is because from (3.1), one knows that

(3.6) $$\bar{P}_{permit} - \bar{P}_{post} = (t - d)e_2 .$$

If $t = d$, then $\bar{P}_{post} = \bar{P}_{permit}$, regardless of the value of e_2. However, if the regulator is to set $t \neq d$, then she needs to adjust $\bar{P}_{permit}$ as well so that the *ex post* pollution target will be met. However, any adjustment will depend on the magnitude of e_2, which is assumed unknown to the regulator when designing the permit market (due to uncertain abatement costs).

Interestingly, as mentioned in the Introduction, it is not even feasible to use an *ex post* pollution constraint if the delivery coefficient is uncertain. This is because, for any given $(t, \bar{P}_{permit})$, the value of $\bar{P}_{post}$ will vary with d and e_2. While the realization of d is affected by weather conditions, the decision regarding e_2 depends on $(t, \bar{P}_{permit})$ and the parameters of the abatement cost function. Thus, there may be different realizations of d for the same value of e_2. It is then obvious that (3.6) will not hold for all possible values of d and e_2 in a permit trading program. In this case, an *ex ante* constraint is the only meaningful policy option.

When an *ex ante* pollution target is used, the realization of total pollution can be higher or lower than the target. Even though the regulator cannot directly control the realization of total pollution, she can set the parameters of the permit system (t and $\bar{P}_{permit}$) in conjunction with her (incomplete) knowledge of the firms' abatement costs. The optimal parameters would generate higher than average emission levels when firms' abatement costs turn out to be high and vice versa. Formally, the regulator's problem is as follows,

$$(3.7) \qquad \min_{t,\bar{P}_{permit}} \quad E[TC] \equiv E\left[C_1(e_1^*(t,\bar{P}_{permit};\theta_1,\theta_2)+C_2(e_2^*(t,\bar{P}_{permit};\theta_1,\theta_2)\right],$$

$$\text{subject to} \qquad \textit{Ex ante pollution constraint in (3.1).}$$

Note that firms emissions decisions, $e_i^*(t,\bar{P}_{permit};\theta_1,\theta_2)$ for $i=1,2$, are incorporated into the regulator's program. Next I explore the optimal trading ratio and total permit cap.

3.3. Characterization of the Optimal Program

3.3.1. Optimal Permit Trading Ratio and Total Permits

For tractability, assume that one firm faces a linear abatement cost function while the other faces an increasing convex abatement cost function, as specified below,

$$(3.8) \qquad C_1(e_1^0-e_1,\theta_1)=(a+\theta_1)(e_1^0-e_1),$$

$$(3.9) \qquad C_2(e_2^0-e_2,\theta_2)=(b+\theta_2)(e_2^0-e_2)+c(e_2^0-e_2)^2.$$

As will be clear later, this linear-quadratic setup is sufficiently rich to generate critical insights while remaining simple enough for intuitive discussion. In (3.8), assume that $a^2-\sigma_1^2>0$, that is, the mean of Firm 1's marginal abatement cost (which represents the deterministic part) dominates the variance (which represents the stochastic part). This

assumption also ensures that the second order condition for the problem in (3.7) is satisfied. With the above cost functions, one can derive firms' optimal emissions from equation (3.4) and the permit market constraint in (3.2),

$$e_1^*(t, \bar{P}_{permit}; \theta_1, \theta_2) = \frac{2c(\bar{P}_{permit} - e_2^0 t) - (b + \theta_2)t + t^2(a + \theta_1)}{2c} \tag{3.10}$$

$$e_2^*(t, \bar{P}_{permit}; \theta_1, \theta_2) = \frac{2ce_2^0 + (b + \theta_2) - t(a + \theta_1)}{2c}. \tag{3.11}$$

With analytical solutions in (3.10) and (3.11) for the firms' choice of emission levels, it is straightforward to solve the *ex ante* optimization problem (3.7) and derive the optimal trading ratio and permit cap. [15] First, I obtain the optimal trading ratio as a function of the regulator's prior information on the covariance structure of abatement cost uncertainties and the delivery coefficient, or specifically,

$$t^* = \mu + \frac{1}{a^2 - \sigma_1^2}\left(\mu\sigma_1^2 + a\,\mathrm{cov}(d, \theta_1) - \mathrm{cov}(\theta_1, \theta_2)\right). \tag{3.12}$$

To derive the optimal permit cap, first note that as long as the program is intended to reduce emissions, both the *ex ante* pollution constraint in (3.1) and the market permit constraint in (3.2) will be binding. Then, one can derive the following,

$$\bar{P}_{permit}^* - \bar{P}_{ante} = E[e_2^*](t^* - \mu) + \frac{Cov(d, \theta_2) - t^* Cov(d, \theta_1)}{2c}. \tag{3.13}$$

The details are provided in the Appendix to the chapter. Equations (3.12) and (3.13) imply that with known values of θ_1, θ_2 and d (with $d = \mu$), the optimal trading ratio would be set equal to the delivery coefficient, i.e., $t^* = d(= \mu)$, and the total permit quantity allocated to firms would equal the pollution target, i.e., $\bar{P}_{permit}^* = \bar{P}_{ante}$. However, in general, $t^* \neq d$ and

[15] The problem is a standard optimization problem with one constraint and so the details on the derivation of the solutions are not presented. To simplify the discussions, interior solutions are assumed throughout the essay.

$\bar{P}^{*}_{permit} \neq \bar{P}_{ante}$. This, of course, differs starkly from most permit trading programs where the trading ratio is the same as the delivery coefficient and the total permit cap is set the same as the pollution target that the regulator sets out to achieve.

3.3.2. The Total Pollution Effect and the Deadweight Loss Effect

To see the effects of setting $t \neq d$ and $\bar{P}_{permit} \neq \bar{P}_{ante}$, consider a benchmark permit trading program where $t = d$ and $\bar{P}_{permit} = \bar{P}_{ante}$. The total abatement costs in the benchmark trading program and in any other permit trading program are denoted as $TC\left(d, \bar{P}_{ante}\right)$ and $TC\left(t, \bar{P}_{permit}\right)$, respectively. The difference between these total costs can be broken down as follows,

$$
\begin{aligned}
& TC\left(d, \bar{P}_{ante}\right) - TC\left(t, \bar{P}_{permit}\right) \\
& = \underbrace{TC\left(d, \bar{P}_{ante}\right) - TC\left(d, \bar{P}_{actual}\right)}_{total\ pollution\ effect} + \underbrace{TC\left(d, \bar{P}_{actual}\right) - TC\left(t, \bar{P}_{permit}\right)}_{deadweight\ loss\ effect},
\end{aligned}
\tag{3.14}
$$

where $\bar{P}_{actual}$ is the actual amount of pollution resulting from a trading program with $\left(t, \bar{P}_{permit}\right)$, that is,

$$
\bar{P}_{actual} = e_1^{*}(t, \bar{P}_{permit}) + de_2^{*}(t, \bar{P}_{permit}) \text{ and } \bar{P}_{permit} = e_1^{*}(t, \bar{P}_{permit}) + te_2^{*}(t, \bar{P}_{permit}). \tag{3.15}
$$

The total cost of each trading program is derived by using firms' emissions decisions under the program, for example, $TC\left(d, \bar{P}_{ante}\right) = C_1(e_1^{*}(d, \bar{P}_{ante})) + C_2(e_2^{*}(d, \bar{P}_{ante}))$.

The *total pollution effect* represents the cost difference that is due to the deviation of total pollution level from the benchmark program. This deviation can arise from a total permit cap that is not equal to that of the benchmark program and/or to the fact that $t \neq d$.

The latter causes a divergence because when t is used in the permit market constraint, instead of d, one unit of permit is no longer necessarily the same as one unit of pollution. The total pollution level will equal the permit cap in the benchmark program. However, this is not necessarily true in a program with trading ratio not equal to *d*.

The *deadweight loss effect* is directly linked to the use of t as the trading ratio, instead of the delivery coefficient d, which leads to a suboptimal allocation of emissions as was pointed out in section II.2. I refer to this effect as the deadweight loss effect since it represents the extra cost incurred by using t to achieve the same amount of total pollution ($\bar{P}_{actual}$). Given an *ex ante* pollution target, the regulator would like to induce a high pollution level when abatement cost turns out to be high and vice versa, that is, to exploit the total pollution effect by setting $t \neq d$ and $\bar{P}_{permit} \neq \bar{P}_{ante}$. However, doing so incurs a cost in the form of a deadweight loss. In designing an optimal program, the regulator will seek to achieve a balance between these two effects in order to minimize abatement costs to achieve the pollution target on average.

3.3.3. A Case of a Known Delivery Coefficient

To isolate the role of uncertainty with regard to the abatement costs, next I examine the optimal trading ratio and permit quantity in the absence of uncertainty in the delivery coefficient. When the delivery coefficient is a known constant, it is known from (3.1) and (3.2) that the gap between the total permits allocated and the pollution target is:

(3.16) $$\bar{P}_{permit} - \bar{P}_{ante} = E[e_2](t - d).$$

Thus, if $t \neq d$, then the total permit quantity will also deviate from the *ex ante* target so that the *ex ante* pollution constraint will be met. Similarly, one can derive

(3.17) $$P_{actual} - \bar{P}_{permit} = -e_2(t - d)$$

That is, if $t > d$, then the actual pollution will be less than the permit allocated. This occurs because 1 unit of Firm 2's emissions contributes d units to total actual pollution, but 1 unit of Firm 2's emissions requires t units of permits in the permit market constraint. Adding up the previous two equations, obtain:

(3.18) $$P_{actual} - \bar{P}_{ante} = (t - d)\left(E[e_2] - e_2\right) = (t - d)\frac{t\theta_1 - \theta_2}{2c}.$$

To derive the second equality in (3.18), equation (3.11) is used. For any given θ_2, the higher θ_1 is, the higher the actual pollution will be if $t > d$.

3.3.3.1. The Tradeoff of the Total Pollution Effect and the Deadweight Loss Effect

With firms' emissions decisions, $e_i^*(d, \bar{P}_{ante})$, $e_i^*(d, \bar{P}_{actual})$ and $e_i^*(t, \bar{P}_{permit})$, onen obtain an expression for the two effects (assuming d is known) as defined in (3.14),

(3.19) $$total\ pollution\ effect = \frac{1}{2c}(t - d)(a + \theta_1)(t\theta_1 - \theta_2),$$

(3.20) $$deadweight\ loss\ effect = -\frac{1}{4c}(a + \theta_1)^2(t - d)^2 .$$

Equation (3.19) indicates that the two effects depend on the parameters in the cost functions and how much the trading ratio differs from *d*. As is expected, (3.20) implies that the deadweight loss effect is never positive. For any given θ_1, the larger the difference between the trading ratio and the delivery coefficient, the larger the deadweight loss effect.

Figure 2 and Figure 3 illustrate the intuition and magnitude of the two effects. For simplicity, the delivery coefficient in the Figures is set to one, which is assumed known by

the regulator. In both figures, the total length of the horizontal axis represents the total permits available and the solid downward sloping line is the marginal abatement cost curve of Firm 2 as emissions are increased (i.e., abatement is decreased).

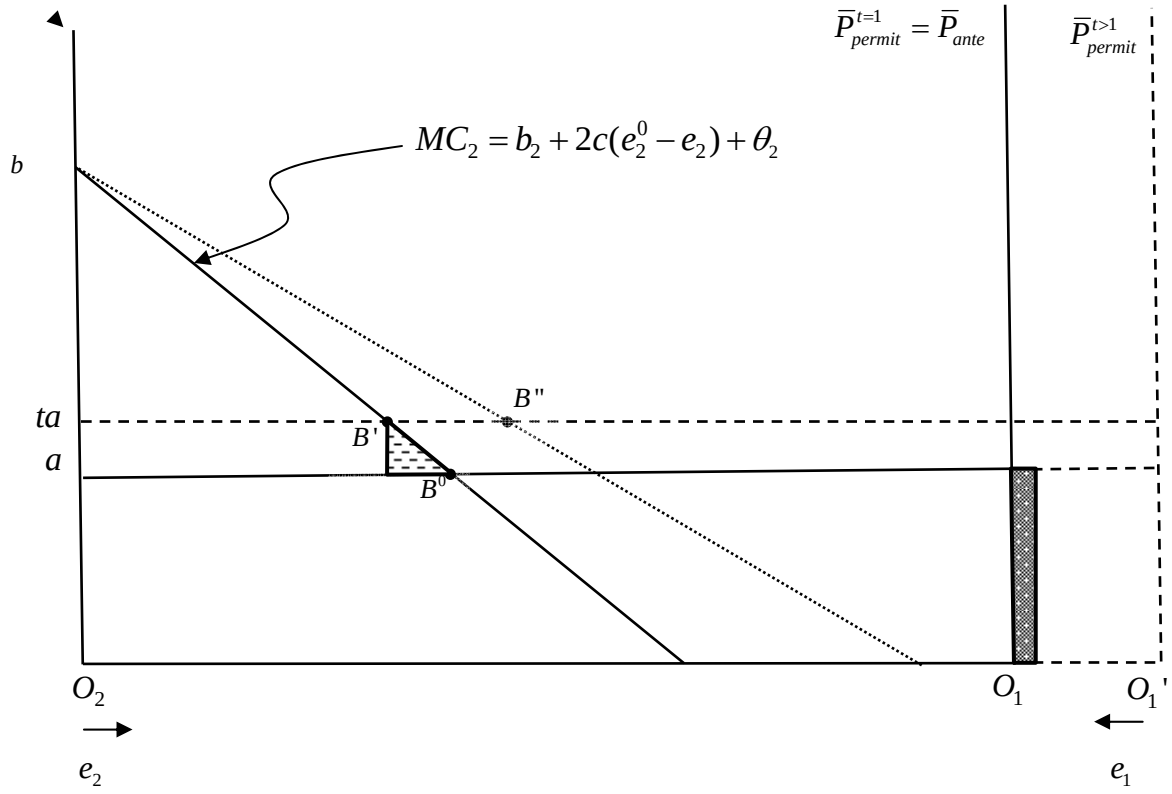

Figure 2. The effects of setting $t^* > d = 1$ under the *ex ante* pollution constraint $e_1 + de_2 = \bar{P}_{ante}$ and the permit market constraint $e_1 + te_2 = \bar{P}_{permit}$ (for $\theta_1 = 0,\ \theta_2 < 0$)

In Figure 2, the marginal abatement cost curve of Firm 1 is represented by the horizontal line that intersects with Firm 2's marginal cost curve at B^0. When $t = d = 1$, $\bar{P}^{t=1}_{permit}$ is set equal to $\bar{P}_{ante}$ by (3.16). Since $MC_1 = MC_2$ at B^0, B^0 represents the permit market equilibrium, indicating the split of the emissions by the two firms with Firm 1's emissions read from the right (O_1) and Firm 2's emissions read from the left (O_2). As (3.5)

is satisfied at B^0, B^0 represents the least cost solution to reach a total pollution level of $\bar{P}_{permit}^{t=1}$ with complete information on θ_1 and θ_2.

When the trading ratio is set greater than the known delivery coefficient several changes occur in Figure 2. First, the optimal total permit cap increases to $\bar{P}_{permit}^{t>1}$ by (3.16), which is reflected by the shifting out of the right boundary of Figure 2 from O_1 to O_1'. Second, the new permit market equilibrium is represented by point B', indicating a reduction in e_2. Third, one can no longer obtain e_1 from right (O_1') to the equilibrium point (B'), since the permit market constraint now requires that the total permits be greater than or equal to the weighted sum of emissions (with the weight on e_2 equal to t), not the simple sum of emissions from the two firms. To reflect the weighting, it would be necessary to adjust the MC curve as in the dotted downward sloping curve to represent $t * e_2$ for every e_2 on MC_2. Then, Firm 1's emissions can be obtained by reading from right (O_1') to B''.

The two effects of setting $t > d$ on the total abatement cost of meeting the *ex ante* pollution target are illustrated by the shaded areas in Figure 2. As to the deadweight loss effect, note that the marginal abatement cost for Firm 1 is still the horizontal line a, not the horizontal line ta. However, firms make their decisions based on the latter, which leads to too few emissions (i.e., too much abatement) by Firm 2, resulting in a deadweight loss represented by the shaded triangle. The area of the triangle is given by (3.20). For the case illustrated in Figure 2 (with $\theta_1 = 0$ and $\theta_2 < 0$), it is clear from (3.18) that the actual total pollution is greater than the *ex ante* pollution target. The savings in abatement cost from this increased pollution are represented by the area of the shaded rectangle and is also given by (3.19).

An optimally designed permit market will try to achieve a balance between the total pollution effect and the deadweight loss effect. To show how the regulator can reduce total *ex ante* expected abatement costs by setting $t > d$, I use the illustration in Figure 3, which is the same as Figure 2 except that it illustrates a case where θ_1 can take on two values ($+\hat{\theta}_1 > 0$ and $-\hat{\theta}_1$) with equal probability. For simplicity, assume $\text{cov}(\theta_1, \theta_2) = 0$. Consistent with (3.20), the figure shows that there is a deadweight loss regardless of whether marginal abatement cost is high or low. The larger (smaller) shaded triangle represents the higher (lower) distortion when the realization of Firm 1's marginal abatement cost is high, i.e., $\theta_1 = +\hat{\theta}_1$ (low, i.e., $\theta_1 = -\hat{\theta}_1$).

The total pollution difference between setting $t > d$ and $t = d$ is given by (3.18) and is represented by the width of the large shaded rectangle for $\theta_1 = +\hat{\theta}_1$ and by the width of the small shaded rectangle for $\theta_1 = -\hat{\theta}_1$. When marginal cost is high (i.e., $\theta_1 = +\hat{\theta}_1$), setting $t > d$ will result in a cost saving from less abatement (or higher than expected pollution level) which is represented by the area of the large shaded rectangle. Similarly, when marginal cost is low (i.e., $\theta_1 = -\hat{\theta}_1$), setting $t > d$ will result in an extra cost from more abatement which is represented by the area of the small shaded rectangle. When the difference between the cost saving and the extra cost is positive, and when the difference is greater than the deadweight loss (the sum of the two shaded triangles), the regulator reduces total abatement cost with $t > d$. As illustrated in Figure 3, the area of the larger rectangle is larger than the sum of the areas of the smaller rectangle and the two shaded triangles, resulting in a welfare gain from setting $t > d$.

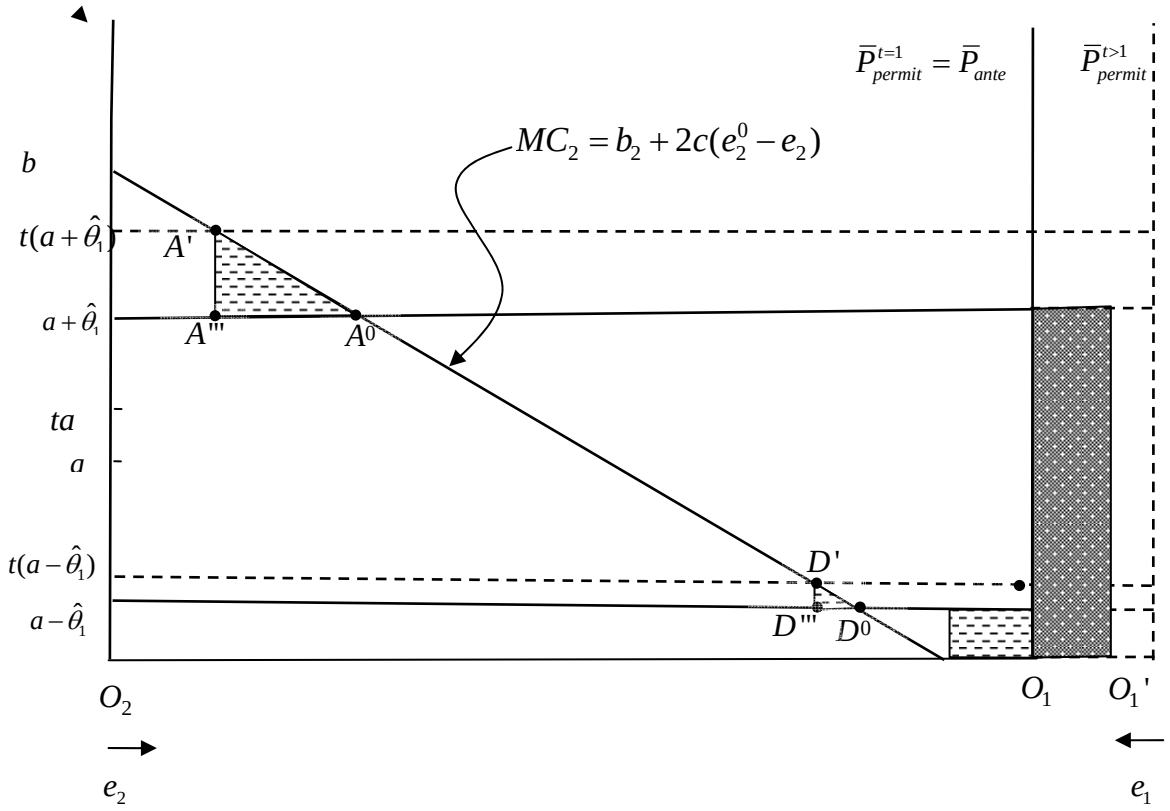

Figure 3. A comparison of the welfare effects when θ_1 is high versus when θ_1 is low for a given value of θ_2 ($\theta_2 = 0$). (In the Figure, θ_1 is assumed to take two values, $+\hat{\theta}_1 > 0$ and $-\hat{\theta}_1$, with equal probability)

3.3.3.2. Effect of the Covariance Structure on the Optimal Permit Trading Program

As noted earlier, if $\sigma_i^2 = 0$ and $\text{cov}(\theta_1, \theta_2) = 0$, then the benchmark program will also be the optimal program. However, as long as $\sigma_1^2 > 0$, in general (3.12) implies that $t^* \neq d$ even when d is known for certain. In this section, the effects of the covariance structure are examined. Since an *ex ante* design minimizes expected abatement costs, begin

by taking the expectation of the total pollution effect and the deadweight loss effect (when d is known),

(3.21) $$E[\textit{total pollution effect}] = \frac{(t-d)}{2c}[t\sigma_1^2 - \text{cov}(\theta_1,\theta_2)], \quad \text{and}$$

(3.22) $$E[\textit{deadweight loss effect}] = -\frac{(t-d)^2}{4c}(a^2+\sigma_1^2).$$

These two expected effects will help one understand how the covariance structure will affect the optimal trading ratio, which will then determine the optimal permit cap through (3.16). By adding up the two expected effects in (3.21) and (3.22), obtain from (3.14)

(3.23) $$E\left[TC\left(d,\bar{P}_{ante}\right) - TC\left(t,\bar{P}_{permit}\right)\right] = \frac{(t-d)}{4c}\left[(t+d)\sigma_1^2 - 2\,\text{cov}(\theta_1,\theta_2) - (t-d)a^2\right]$$

Thus, the larger the variance and the more the cost shocks are negatively correlated, the larger the effects of setting $t > d$ tend to be. Although most of the discussion focuses on the case where $t^* - d > 0$, it is worth noting that it can be optimal for $t^* < d$, which happens if $\text{cov}(\theta_1,\theta_2)$ is very large. More details are provided in the Appendix to the chapter.

3.3.4. Impact of an Uncertain Delivery Coefficient

The delivery coefficient is likely to be known for some pollutants (e.g. carbon dioxide), but there are many pollutants where delivery coefficients will be uncertain. While uncertain delivery coefficients clearly characterize nonpoint source pollution, many point sources can also have uncertain delivery coefficients; for example, wind and weather uncertainty can affect air pollution deposition rates. Many water pollutants exemplify this notion well. The fate and transport of water pollutants is subject to both stochastic elements

related to weather as well as scientific uncertainty concerning the physical diffusion process.[16] This is true for both point and nonpoint water pollution sources.

The impact of uncertain delivery coefficient is reflected in (3.12) by $\text{cov}(d,\theta_1)$ and the use of the expected value of d. The optimal trading ratio moves in the same direction as $\text{cov}(d,\theta_1)$: $\frac{\partial t^*}{\partial \text{cov}(d,\theta_1)} = \frac{a}{a^2-\sigma_1^2} > 0$. Suppose $\text{cov}(d,\theta_1) > 0$, that is, if the delivery coefficient is expected to be high, the marginal cost of abatement by Firm 1 is also expected to be high. For given emissions, a high d means more total pollution in the absence of any abatement. In order to reduce pollution to a fixed target, more abatement has to be undertaken. To ameliorate the pressure for more abatement, combining equations (3.13) and (3.17) implies that the trading ratio should be increased and so more emissions will be allowed when the delivery coefficient is high and the abatement cost is also expected to be high. By the same logic, when the delivery coefficient is low and the abatement cost shock also tends to be low (e.g., negative), a higher trading ratio will restrict the amount of emissions that are allowed. However, the cost savings from extra pollution is higher than the increased cost from more abatement and so total abatement costs are reduced on average. Thus, setting a higher trading ratio pays off.

The optimal permit allocation gap with an uncertain delivery coefficient is given by equation (3.13). Compared to the case with a known delivery coefficient as given in equation (3.16), there are two additional covariance terms, which represent the covariance between

[16] In the nonpoint source pollution literature, where one of the defining features of nonpoint source pollution is its inherent unobservability (Segerson, 1988), the focus has been on the trading in expected, as opposed to actual, emissions from a nonpoint source (e.g., Horan et al, 2001). In this case, basically, another layer of uncertainty would be added to the design of the permit market: both firms and the regulator only know the distribution of emissions given any action taken by the firms. One can show that, like the uncertainty on firms' abatement costs and the delivery coefficient, this uncertainty will also be reflected in the optimal trading ratio and the optimal total number of permits.

e_2 and d (see Appendix B). The terms indicate that if e_2 and d are positively correlated, then the optimal total permit cap should be even higher and vice versa. Thus, with an uncertain delivery coefficient, there is an additional reason that the optimal total permit cap might differ from the *ex ante* pollution target.

3.4. Conclusions

In this chapter, I investigate the optimal design of permit trading programs in a setup that incorporates three key features: (1) the regulator's objective is to minimize the expected abatement costs of meeting an *ex ante* pollution target (i.e., the pollution standard or target is represented as an expectation); (2) the firms' abatement costs are *ex ante* stochastic, the regulator knows their distributions, and uses this information to set the parameters of a permit trading program; and (3) the delivery coefficient of emissions can be uncertain. It is well known that the regulator does not have to have any information on firms' abatement costs for a permit trading program to minimize the cost of achieving an *ex post* pollution target. However, it is found that such information is useful in designing a trading program that meets an *ex ante* target at the lowest abatement costs.

In addition to the result that the optimal total permit cap is in general not equal to the *ex ante* pollution target, it is found that the optimal trading ratio is not equal to the delivery coefficient even if the regulator has complete information on the delivery coefficient *ex ante*. The latter result arises from the dual roles that the trading ratio plays in a permit trading program. First, the trading ratio determines the substitution rate among emissions of different sources. Some studies have examined thoroughly the optimal trading ratio in situations where the regulator, with complete information on firms' abatement costs, seeks to minimize the

sum of abatement costs and damages from pollution (e.g., Kling and Rubin, 1997). Second, and equally importantly, trading ratio affects the actual amount of pollution resulting from a trading program. This is because, when the trading ratio is not equal to the delivery coefficient, the total permit cap is no longer the same as the total pollution that will result from a trading program. When designing a program, the regulator can use the trading ratio to induce the desirable pollution level.

Environmental trading programs have received increasing amount of attention in recent years because of their potential for cost savings relative to other policy instruments. In some of the emerging permit trading programs, for example, water quality trading, environmental targets are commonly set as an *ex ante* standard. The findings in this paper indicate that it is important that the nature of a pollution target be clarified prior to the design of a trading program, given the stark difference between the optimal trading programs with an *ex ante* pollution target and the optimal trading program with an *ex post* target. Under an *ex ante* target, not surprisingly, the actual pollution level as the result of implementing an optimal trading program would fluctuate around the target. When the nature of the pollutant is such that some fluctuation in emissions is acceptable, using the information on the joint distribution of firms' abatement costs and the environmental delivery coefficients allows the regulator to reduce expected pollution abatement costs.

3.5. References

Baumol W, Oates W. *The Theory of Environmental Policy*, Cambridge University Press, second edition: 1988.

Foster V, Hahn R. Designing More Efficient Markets: Lessons from Los Angeles Smog Control. *Journal of Law and Economics* 1995; 38(1);19-48.

Hoag D.L., Hughes-Popp J.S. Theory and Practice of Pollution Credit Trading in Water Quality Management. *Review of Agricultural Economics*, 1997; 19(2); 252-262.

Horan, R.D. "Differences in Social and Public Risk Perceptions and Conflicting Impacts on Point/Nonpoint Trading Ratios." *American Journal of Agricultural Economics* 2001; 83(4):934-41.

Horan R.D., Shortle J.S. When Two Wrongs Make a Right: Second-Best Point-Nonpoint Trading Ratios. *American Journal of Agricultural Economics* 2005; 87(2); 340-352.

Kling C.L., Rubin J. Bankable Permits for the Control of Environmental Pollution. *Journal of Public Economics* 1997; 64; 101-115.

Lewis T.R. Protecting the Environment When Costs and Benefits are Privately Known. *RAND Journal of Economics* 1996; 27(4); 819-847.

Malik A., Letson D, Crutchfield S. Point/Nonpoint Source Trading of Pollution Abatement: Choosing the Right Trading Ratio. *American Journal of Agricultural Economics* 1993; 75(4); 959-967.

Montero J-P. Multipollutant markets. *RAND Journal of Economics* 2001; 32(4); 762-774.

Montero J-P. Optimal Design of a Phase-in Emissions Trading Program. *Journal of Public Economics* 2000; 75; 273-291.

Montgomery W.D. Markets in Licenses and Efficient Pollution Control Programs. *Journal of Economic Theory* 1972; 5; 395-418.

Roberts M.J. Spence A.M. Effluent Charges and Licences Under Uncertainty. *Journal of Public Economics* 1976; 5; 193-208.

Segerson K. Uncertainty and Incentives for Nonpoint Pollution Control. *Journal of Environmental Economics and Management* 1988; 15; 87-98.

U.S. Environmental Protection Agency (USEPA). Water quality trading assessment handbook, EPA-841-B-04-001. 2004.

—National Ambient Air Quality Standards. 2007a. http://www.epa.gov/air/criteria.html. Accessed February 2, 2007.

—Fact Sheet—Proposed Reissuance of National Pollutant Discharge Elimination System (NPDES) Stormwater Multi-Sector General Permit for Industrial Activities. 2007b. http://www.epa.gov/npdes/pubs/msgp2006_factsheet-proposed.pdf. Accessed February 7, 2007.

Woodward R.T., Kaiser R.A., Wicks A.M. The Structure and Practice of Water-Quality Trading Markets. *Journal of the American Water Resources Association* 2002; 38(4); 967-979.

CHAPTER 4. EFFICIENT REDUCTIONS IN LOCAL AND STATE-LEVEL NONPOINT SOURCE NUTRIENT POLLUTION: AN APPLICATION TO THE STATE OF IOWA

4.1. Introduction

Nonpoint source pollution from agriculture continues to be a major policy concern across the country. Historically, U.S. water quality regulation focused on point sources, and, as a result, a large portion of the nation's waters remains too polluted for basic uses (U.S. EPA, 2002). Iowa is a state where nonpoint source pollution from agriculture is one of the most important and pressing environmental issues. Iowa's water quality problems also resonate quite far downstream. Iowa Department of Natural Resources estimates that, despite occupying only 5 percent of land area in the Mississippi River Basin, Iowa contributes almost 25 percent of nitrate loadings delivered by the Mississippi River to the Gulf of Mexico (IA DNR, 2007). Excessive transport of nitrate-nitrogen (and other nutrients like phosphorus and silicate) to the Gulf of Mexico is now believed to be the primary cause for the Gulf of Mexico's annual hypoxic zone, now second largest in the world.

Conservation practices, both involving retirement of land from agricultural production, and those which can be undertaken in conjunction with agricultural production have long been looked to as potential means of reducing negative impacts of agriculture on in-stream water quality. Numerous studies have modeled the effects of conservation practices on nitrate, phosphorus, and sediment loadings (see, e.g., Vache et al., 2002; Hu et. al., 2007; Secchi et al., 2007). Also, beneficial effects of conservation practices have been historically documented in efforts to improve water quality in the Great Lakes (e.g., Richards and Baker, 2002).

A number of federal and state programs exist which provide financial support for implementation of conservation practices on agricultural landscapes. For instance, the 2002 Farm Bill provided up to 1.3 billion dollars in 2007 fiscal year to the Environmental Quality Incentives Program (EQIP), which provides cost-sharing for installation and maintenance of conservation practices. Given that public funds are being invested in the placement of conservation practices which may enhance water quality, discovering efficient ways of allocating conservation practices is of primary importance. Indeed, federal legislators recognize this fact, explicitly specifying that to "optimize environmental benefits" is one of the purposes of EQIP (U.S. Farm Security and Rural Investment Act of 2002, Subtitle D, Section 2301).

However, in nonpoint source water pollution problems, the complex biophysical relationships that connect human actions to eventual environmental outcomes make solving for cost-efficient allocations of abatement activities across space a formidable task. This research integrates modern multi-objective optimization tools, water quality modeling capability, and data on costs of implementing conservation practices to develop a set of cost-efficient nonpoint-source pollution reduction solutions. By combining multi-objective evolutionary algorithm with a hydrologic model, sets of cost-efficient solutions for the watersheds in the state of Iowa are obtained. By interpreting frontiers of cost-efficiency as total pollution cost curves, I am able to solve for least-cost allocations of nutrient loading reductions for problems of reducing state-level nutrient exports.

I discuss the conservation practices selected for the achievement of nutrient loading reductions, both at the watershed and sub-watershed level. The set of practices considered includes contour farming, terraces, no-till, nitrogen fertilizer reductions, and land retirement.

4.2. Efficient Nonpoint Source Pollution Control and the Optimization Algorithm

Studying the least cost solution in the watershed context is fraught with difficulty. The effectiveness of a given conservation practice on a given field depends on the placement of other conservation practices, on cropping systems in the watershed, and the physical characteristics of the watershed location and the watershed itself. In other words, off-site impacts of land use on any parcel in a watershed tend to be endogenous to land use choices on other parcels of the watershed. However, earlier studies on the economics of water pollution control on watershed scale essentially followed Montgomery's (1972) conceptual model of fixed, exogenous, pollution delivery coefficients. Studies by Carpentier, Bosch, and Batie (1998), Kramer, McSweeny, Kerns, and Stravros (1984), and Ribaudo (1986, 1989) assume that off-site impacts can be accurately described as a proportion of on-site pollution generated. Given such assumptions, it is straightforward to solve for cost-efficient allocations of pollution abatement using calculus-based constrained optimization techniques.

Development of realistic, physically-based, spatially distributed hydrologic simulation models highlighted the fact that parcel-level off-site impacts are endogenous and moved the researchers dealing with nonpoint source pollution issues to incorporate some features of these models into their analyses. Until recently, there were essentially two types of studies: studies that attempted spatial optimization (but incorporated only some parts of the hydrologic modeling), and studies that incorporated full hydrologic simulations but relied on comparison of scenarios without explicit optimization.

Of the former type, studies undertaken by Braden, Bouzaher, Johnson and colleagues (Braden, Johnson, Bouzaher, and Miltz, 1989; Bouzaher, Braden, and Johnson, 1990; Bouzaher, Braden, Johnson, and Murley, 1994) in the late 1980's and early 1990's are an

excellent example. Braden et al. (1989) attempt to find cost-efficient sediment control strategies, incorporating management practices of downslope parcels. The authors separate a watershed into hydrologically independent flow paths, and use a hydrologic model to estimate the impact of various management alternatives for the flow paths onto the resulting sediment yield. As a result, a problem of finding cost-efficient sediment reduction solutions becomes a variant of the knapsack model in operations research. By focusing on hydrologically independent flow paths, the authors are able to use dynamic programming to allocate the sediment reductions across flow paths.

A study by Khanna, Yang, Farnsworth, and Onal (2003) provides another good example of the ingenuity that was demonstrated by researchers in attempting to cope with the complexity of water pollution dynamics. In this study, the authors focus on fairly narrow hydrologically independent flow paths that are adjacent to streams, and attempt to fully capture the interdependencies between upslope and downslope parcels by using a hydrologic model. They restrict their attention to three parcels up from a stream, and to two alternatives on each parcel: crop production or land retirement. Even in the stylized model they present, the problem becomes highly nonlinear, and is likely to be non-convex; thus, an empirical simplification is used in order to make the model tractable for calculus-based optimization.

A major drawback to these approaches is that hydrologic models developed for the entire watershed are broken up; hence, one does not get the full benefit of a hydrologic simulation model. Therefore, the studies of the latter type utilize complete hydrologic simulation models and focus on several land use change scenarios that achieve the pollution reduction goals. For example, Secchi, Jha, Kurkalova, Gassman, and Kling (2005) consider

retirement of land in proximity to waterways and with high erodibility and analyze the resulting water quality benefits using a hydrologic simulation model.

Conceptually, if one could analyze all possible (and feasible) scenarios, and evaluate the cost and the pollution outcomes, picking cost-efficient solutions would be trivial. However, for any realistic watershed problem, a brute force approach appears infeasible. Specifically, if there are N conservation practices possible for adoption on each field and there are F fields, this implies a total of N^F possible watershed configurations to compare. In a watershed with hundreds of fields and more than a couple of conservation practices, this comparison quickly becomes unwieldy. The combinatorial nature of the problem was already recognized by Braden et al. (1989), and was one of the reasons for Khanna et al.'s (2003) decision to focus on a narrow band of land around streams.

Recently, however, several researchers have found a tool which appears to be able to deal with the combinatorial nature of a watershed simulation-optimization problem. Evolutionary algorithms provide one systematic way for searching through large search spaces. Evolutionary algorithms aim to mimic the process of biological evolution, which, in the words of Mitchell (1996), "in effect, is a method of searching for solutions among an enormous amount of possibilities". Researchers beginning with Srivastava, Hamlett, Robillard, and Day (2002) and Veith, Wolfe, and Heatwole (2003) have used genetic algorithms (GA) in order to search for single cost-efficient watershed-level pollution reduction solutions. Before I discuss this recent strand of literature, some background on the philosophy and terminology of evolutionary computation is needed. The next section provides some (by no means complete) background on evolutionary computation and genetic

algorithms[17]. The concepts outlined below also provide the foundation behind the approach used in this essay.

4.2.1. Evolutionary Algorithms: Brief Background and Terminology

Beginning in 1950's and 1960's computer scientists came to a realization that the theory of biological evolution can be used as an optimization tool for engineering problems. Since the field of evolutionary computation owes its origins to observations of biological evolution, the terminology used has its analogs in biology, although, typically, the entities used to describe an optimization problem are much simpler than the real biological entities bearing the same name. A *genome* (or a *chromosome*) refers to a complete collection of *genes* and fully describes an *individual* (typically, a candidate solution in an optimization problem). A set of possible values that any gene can take is referred to as an *allele set*, or *alphabet.* Often, a genome representing a candidate solution is a one-dimensional array, or vector. A gene then is an element of this array and encodes a particular element of a candidate solution. A value of a gene comes from its allele set, also a vector. Analogous to haploid organisms in real biology, *offspring* is created from two parent individuals. During sexual reproduction, *recombination* (*crossover*) occurs: the offspring's genome consists of portions of each of the two parents' genomes. As in biological evolution, offspring are subject to *mutation:* a random substitution of a gene's value with a value from its allele set.

In many applications of evolutionary algorithms to spatial optimization (including this one), a genome is a vector of length F, where F is the number of spatial decision-making units (fields). Each element of the vector (gene) represents a field, with its value coming

[17] See, for example, Mitchell (1996), for more history of evolutionary computation.

from the allele set *A*, and encoding a particular land use option. The allele set is typically the same for all genes. Table 1 presents a correspondence of evolutionary computation terms to a typical problem of spatial optimization of a watershed for the purpose of nonpoint source pollution control.

Table 1. Typical correspondence of terms

Evolutionary algorithm term	Interpretation	Corresponding term in a watershed application
Individual (genome)	Candidate solution vector	A particular watershed configuration
Gene	Element of a candidate solution vector	A field; a spatial decision-making unit
Allele set	A set of values that an element of a candidate solution can take	A set of land use/conservation practice options which can be implemented in each field
Allele	A value of an element of a candidate solution; member of the allele set	A particular land use/conservation practice combination which can be assigned to a field
Population	A collection of candidate solutions	A collection of distinct watershed configurations

Finally, as in biological evolution, individuals at every *generation* form *populations*, and are characterized by their *fitness*—a score which measures how well each individual is solving the optimization problem at hand (for example, a value of an objective function). Individuals possessing higher fitness scores are more likely to be selected for reproduction

and therefore are more likely to pass along the characteristics associated with the candidate solutions they represent.

While there are many variations of evolutionary algorithms, most have the following elements in common: populations of individual solutions, selection for reproduction according to fitness levels, crossover to produce new solutions (offspring), and random mutation of new offspring.

There is no strict theoretical guidance as to what are the optimization problems that evolutionary algorithms can attempt to solve, however, most researchers agree that the following characteristics of a problem make it a good candidate for evolutionary-based solution techniques: a) a large search space, which is not smooth or unimodal (or is not well understood), and b) acceptability of sufficiently good approximations (i.e., not needing to find the global solution exactly) (based on Mitchell (1996)) A problem of cost-efficient watershed management appears to fit the criteria outlined. The combinatorial nature of the spatial problem makes for a very large search space, and, given the complexity of the problem, a good approximation to the solution is in itself a worthwhile goal.

One of the earlier applications of genetic algorithms to watershed management is one by Srivastava et al. (2002). The authors use a genetic algorithm to allocate 45 fields to 15 mutually exclusive best management practices (BMPs), combine water pollution and agricultural net returns into the fitness score, and discover a spatial allocation that reduced pollutant loads by 56 percent relative to the baseline of the worst-case scenario, while simultaneously increasing net returns by 109 percent.

Veith, Wolfe, and Heatwole (2003) minimize costs subject to sediment reduction target by proceeding lexicographically – first minimize pollution; then, when pollution target

is reached, minimize costs. Cost minimization is done under an additional constraint of "equitable" distribution of control costs over farms. In a later study, Veith et al. (2004) compare solutions obtained using a genetic algorithm to solutions obtained by targeting land based on slope, and find that optimization reduces costs of sediment reduction from $42 per kg/ha to $36 per kg/ha. Such findings emphasize the fact that for any watershed problem, the returns to using a systematic search technique such as a genetic algorithm are likely to be significant.

4.2.2. Multiobjective Problem and Pareto Optimality

Clearly, efficient solutions must lie on a Pareto-efficient frontier in the pollution-cost space. Multiple pollutants may be of concern; then, for any solution on the Pareto-efficient frontier, it is not possible to identify an alternative solution where either (a) control costs can be lowered without increasing any of the pollutants' loadings; or, (b) any pollutant's loading is lowered without increasing control costs or any other pollutants' loadings. Thus, if one could identify the frontier itself, cost-efficient solutions for given pollution reduction targets could simply be read off the frontier. Given the difficulties outlined above that prevent finding even a single cost-efficient solution for a watershed, how can one hope to find the entire set?[18] Fortunately, one particular class of search algorithms appears to be particularly useful for identifying Pareto-optimal frontiers for competing objectives. Multiobjective optimization evolutionary algorithms (MOEA's) provide a particularly useful way to search for entire sets of cost-efficient nonpoint source pollution reduction strategies.

While most applications of evolutionary algorithms to the problem of watershed

[18] Braden et al. (1989) solve the cost minimization problem for a wide range of sediment reduction targets, and are thus able to provide a full tradeoff curve. Khanna et al (2003) solve for several sediment reduction targets, and can identify several points on the curve.

management have been limited to finding single cost-efficient pollution reduction solutions, recently, some researchers have also utilized multiobjective methods. Muleta and Nicklow (2002) combine an MOEA with a hydrologic model to look for Pareto-optimal frontiers for each spatial decisionmaking unit in the watershed. In the later study, Muleta and Nicklow (2005) subsequently focus more on the watershed scale, and develop an approximation a genetic algorithm to identify the spatial units that would maximize the benefit to cost ratio (where benefits are measured as sediment reductions), subject to an exogenously specified constraint of only 10 percent of land in the watershed being allocated for sediment reduction. Lant, Kraft, Beaulieu, Bennett, Loftus, and Nicklow (2005) model a watershed as a complex adaptive human ecosystem and incorporate an evolutionary algorithm to provide an approximation to the optimal set of tradeoffs between an index of ecosystem services and returns from agricultural production for a small watershed in Illinois by considering land retirement as an option at farm scale. Perhaps the most closely related study is one by Bekele and Nicklow (2005), where the authors applied a multiobjective evolutionary algorithm to search for watershed-level Pareto-optimal solutions in the space defined by nitrogen, phosphorus, sediment, and economic net returns. The authors' focus, however, was mostly on the choice of crop-tillage combinations, and did not consider other conservation practices. Arabi, Govindaraju, and Hantush (2006), on the other hand, considered several structural conservation practices, including terraces and grassed waterways in their application of genetic algorithms to optimizing the placement of conservation practices. The authors, however, aggregate multiple environmental objectives into a single weighted index in order to be able to use single-objective genetic algorithm. The current work offers both methodological and policy contributions.

Methodological contributions to the growing area of watershed-level simulation-optimization literature which relies on evolutionary computation include a) preservation of the population of Pareto-nondominated individuals; b) addition of diversity preservation by weighting individuals based on their location in the objective space, and, c) careful construction of the allele set, designed to capture the non-mutually exclusive nature of some conservation practices. I discuss these in greater detail in the next section which describes the algorithm implementation. Also, previous studies do not make an explicit connection between Pareto-efficient frontiers and total pollution costs. But, a straightforward interpretation of Pareto-efficient frontiers as total pollution cost curves bridges the gap between traditional environmental economics theory which operates with total and marginal abatement cost curves, and problems of nonpoint source pollution.

Policy contributions are also important, however. Previous studies which utilize evolutionary algorithms do so on a much smaller geographic scale. Certainly, none of the studies I am aware of take up the task of a state-wide analysis. This is the kind of scale which is likely to get attention of policymakers and stakeholder groups.

4.3. Application: The Watersheds in the State of Iowa

This section describes the application of an evolutionary algorithm to the hydrologic representation of the state of Iowa. First, I describe the algorithm, the logic of fitness assignment, and the allele set. I then briefly describe the watersheds under study, and turn to the hydrologic model, SWAT. Data needed for the hydrologic model and cost assignment is discussed next. The section concludes with the presentation of the overall flow of simulation-optimization procedure, and the setup of the algorithm run.

4.3.1. Multiobjective evolutionary algorithm

In this application, I consider a three-objective minimization problem: that is, for every watershed under study, I attempt to minimize (1) average annual nitrate-nitrogen (NO_3-N) loadings at the watershed outlet[19]; (2) average annual phosphorus (P) loadings at the watershed outlet, and, (3) the total cost of controlling in-stream nutrient pollution. Environmental objectives represent the two main nutrients (nitrogen and phosphorus) which may be responsible for both local and downstream water quality problems, with nitrates typically being the main source of in-stream nitrogen. Measure of control cost is, of course, necessary to quantify the efficiency of alternative patterns of conservation practices.

The following section describes the logic of a multiobjective optimization problem and a particular MOEA used in this paper. A general multiobjective optimization problem can be described as a vector function f that maps a tuple of m parameters (decision variables) to a tuple of n objectives (Zitzler and Thiele, 1999). Framing the problem as one of minimization (keeping in mind the application to "bads" such as cost or pollution), a typical multiobjective optimization problem is to minimize

(4.1) $$\mathbf{y} = f(\mathbf{x}) = \left(f_1(\mathbf{x}), f_2(\mathbf{x}), \ldots, f_n(\mathbf{x}) \right)$$

subject to

(4.2) $$\mathbf{x} = (x_1, x_2, \ldots, x_m) \in X$$

[19] The term "nitrate-nitrogen" is used to specify the source of nitrogen. In the discussion following, for simplicity, I will use "nitrate", or NO_3. The mass of loadings is expressed, however, as the mass of element N in the nitrate form.

(4.3) $$\mathbf{y} = (y_1, y_2, \ldots, y_m) \in Y,$$

where $\mathbf{x}$ is called the *decision vector*, X is the *parameter space*, $\mathbf{y}$ is the *objective vector*, and Y is the *objective space*. In this application, the objective space is defined by nitrate-P-cost space. The set of solutions to the multiobjective optimization problem consists of all decision vectors that are Pareto-optimal. A decision vector $\mathbf{a}$ is Pareto-optimal if there is no $\tilde{\mathbf{a}} \in X$ such that $f_i(\tilde{\mathbf{a}}) \leq f_i(\mathbf{a})$, $\forall i \in \{1,2,\ldots,n\}$, and $\exists j \in \{1,2,\ldots,n\}: f_j(\tilde{\mathbf{a}}) < f_j(\mathbf{a})$. The decision vectors that are nondominated within the entire search space constitute the Pareto-efficient set, or frontier. Over the last decade, several MOEA's have been suggested (see, e.g., Deb et al., 2000). One advantage of all MOEA's is that they are capable of searching for multiple Pareto-efficient solutions in a single optimization run.

In this paper, I use a modification of the Strength Pareto Evolutionary Algorithm 2 (SPEA2), proposed by Zitzler, Laumanns, and Thiele (2002). As in genetic algorithms (GA), the search process starts with a population of candidate solutions from which a new population is created by the process of selection, crossover, and mutation. Unlike in the GA, the fitness score of each individual $\mathbf{i}$ in the population is now a function of how many other individuals in the population $\mathbf{i}$ dominates (in the sense of Pareto) and by how many individuals is $\mathbf{i}$ dominated by. Furthermore, the algorithm takes into account the degree of "crowding" around $\mathbf{i}$ in order to preserve the diversity in the population and to cover as much as possible with the resulting Pareto-optimal frontier. The following discussion is framed in terms of fitness score minimization, following Zitzler et al. (2002).

To be specific, an individual $\mathbf{i}$ is assigned a strength value $S(\mathbf{i})$ which equals to the number of solutions it dominates:

(4.4) $$S(\mathbf{i}) = \left|\{\mathbf{j} \mid \mathbf{j} \in \mathbf{P}_t \cup \bar{\mathbf{P}}_t \wedge \mathbf{i} \succ \mathbf{j}\}\right|,$$

where $\bar{\mathbf{P}}_t$ is the original population at generation t, $\mathbf{P}_t$ is the temporary population created, $|\cdot|$ denotes the cardinality of a set, and $\succ$ corresponds to the Pareto dominance relation. On the basis of this definition of strength values, the raw fitness for individual $\mathbf{i}$ is calculated:

(4.5) $$R(\mathbf{i}) = \sum_{\mathbf{j} \in \mathbf{P}_t \cup \bar{\mathbf{P}}_t, \mathbf{j} \succ \mathbf{i}} S(\mathbf{j}).$$

Thus, the raw fitness of an individual is determined by the strength of the dominators (individuals that dominate $\mathbf{i}$). Then, the raw fitness value of $R(\mathbf{i}) = 0$ corresponds to a nondominated individual, while a high raw fitness value corresponds to an individual that is dominated by many other individuals (which in turn dominate other individuals). In light of this interpretation, fitness minimization used in the formulation of the algorithm makes intuitive sense. Figure 1 demonstrates the fitness assignment process and highlights the fact that individuals that are located in the "crowded" areas of the objective space get a higher raw fitness value, and therefore are less likely to be selected into a future generation. For instance, point F dominates points B, C, and A, and therefore gets a strength value of 3. Since point F is nondominated, its raw fitness is zero. Point D, on the other hand, dominates only A, and thus gets the strength value of one, but is dominated by point G, which itself dominates 3 points. Thus, point D gets the raw fitness value of 3. Point A is the 'worst' point in the objective space, as it is associated with the highest cost and pollution levels. It itself does not dominate any other points, but is dominated by points F, G (with a strength value of 3), H (with a strength value of 2), D (with a strength value of 1), and E (with a strength value of 1). Therefore, the raw fitness value for point A is 3+3+2+1+1=10. Recalling that in this

algorithm, individuals with the lower fitness scores are considered “more fit”, it is clear that individual A is far less likely to survive into the next generation than, for example, point F.

Such assignment of raw fitness scores also takes into account the relative “isolatedness” of candidate solutions in the objective space. Conceptually, one would like the resulting Pareto-optimal frontier to span a large portion of the objective space. Therefore, candidate solutions on the interior of the frontier are somewhat less preferred than those close to the edges. In the figure, for example, while both points B and C are dominated, point C is dominated by both points F and G by virtue of its “interior” location in the objective space; whereas point B is dominated only by point F and not by point G: its pollution level is lower than that of G. As a result, point B has a raw fitness score of 3 as opposed to the score of 6 for C, and its “genetic makeup” is therefore less likely to be eliminated in the subsequent generations.

Finally, while the raw fitness score assignment outlined above incorporates some information on the location of the solutions in the objective space, additional density information is also incorporated into the calculation of a fitness score. Density estimation technique is used to further differentiate between individuals that are located in the “crowded” areas of the objective space (less preferred) from those located in the relatively sparse areas of the objective space (more preferred). Density estimation is a way to preserve diversity in the Pareto frontier (Deb, 2001). The density estimation technique used in SPEA2 is an adaptation of the k -th nearest neighbor method, where the density at any point is a decreasing function of the distance to the k -th nearest data point. For each individual $\mathbf{i}$, I calculate the distances (in objective space) to all the individuals in the current population,

and store them in a list. After sorting the list in an increasing order, the k -th element yields σ_i^k , the distance.[20]

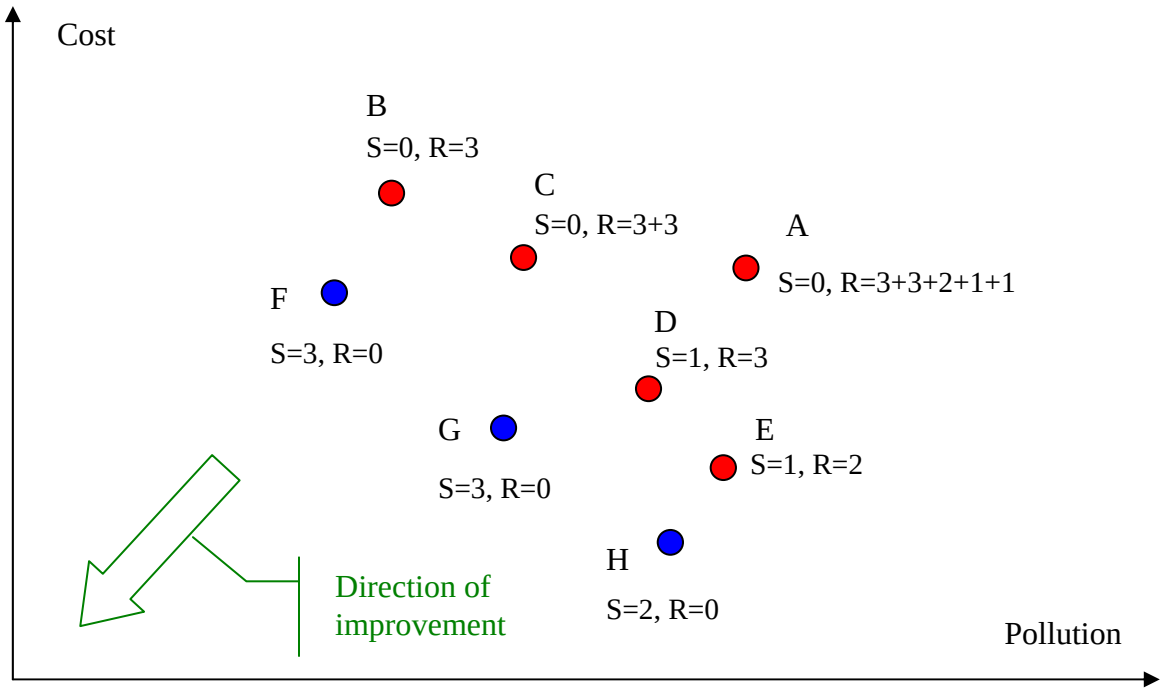

Figure 1. Raw fitness assignment in SPEA2

An additional measure of distance was incorporated into the algorithm in order to preserve diversity in the objective space. In each generation, the distance from a given individual to the center of the cube defined by the endpoints of the frontier was established. The purpose of this calculation is to further reward individuals who are located closer to the edges of the frontier, and thus prevent loss of diversity. This distance is denoted as σ_i^c .

The density is then computed as:

[20] k is chosen to equal to the square root of the sum of the initial population size and the size of the temporary population.

(4.6) $$D(\mathbf{i}) = \frac{1}{\sigma_{\mathbf{i}}^{k} + 0.25\sigma_{\mathbf{i}}^{c} + 2},$$

where 2 is added to the denominator to ensure that the value of the density is greater than zero and less than one.

Given the raw fitness score and the estimated density, the fitness of an individual $\mathbf{i}$ is calculated as:

(4.7) $$F(\mathbf{i}) = R(\mathbf{i}) + D(\mathbf{i}).$$

This is the fitness score used for selecting individuals in the algorithm implemented.[21]

4.3.2. The Hydrologic Model

A process-based hydrologic simulation model, the Soil and Water Assessment Tool (SWAT) (Arnold et al., 1998; Arnold and Forher, 2005; Gassman et al., 2007), is used in this study to estimate changes in water quality due to changes in conservation practices. SWAT is a hydrologic and water quality model developed by the USDA's Agricultural Research Service (ARS). It is a long-term continuous watershed scale simulation model that operates on a daily time step and is designed to assess the impact of different management practices on water, sediment, and nutrient yields. The model is physically based, computationally efficient, and capable of simulating a high level of spatial detail. Major model components include weather, hydrology, soil temperature, crop growth, nutrients, pesticides, and land management. In SWAT, a watershed is divided into multiple subbasins, which are further subdivided into unique soil/land use characteristics called hydrologic response units (HRUs).

[21] In order to preserve the logic of the original GA library which was set up for fitness score maximization, I use K-fitness score as the actual fitness score used by the program, where K=100000.

The water balance of each HRU is represented by four storage volumes: snow, soil profile, shallow aquifer, and deep aquifer. Flow generation, sediment yield, and pollutant loadings are summed across all HRUs in a subbasin, and the resulting loads are then routed through channels, ponds, and/or reservoirs to the watershed outlet. For a more detailed description of the model, see Gassman et al. (2007), or Neitsch et al. (2005).

In terms of the evolutionary algorithm, each HRU is a *gene*, and a particular combination of land use and conservation practices simulated by the SWAT model for each HRU is an *allele.* The next section describes the *allele set* and the means by which each allele is simulated by the hydrologic model.

4.3.3. The Allele Set

The set of mutually exclusive land use options which are to be simulated on each of the hydrologic response units (HRUs) in the watershed comprises the allele set. The allele set is formed by interacting in-field conservation practices with a tillage mode and a presence or a lack of a nitrogen fertilizer reduction. In-field conservation practices considered are contour farming, terraces, grassed waterways, and land retirement. No-till and a 20 percent reduction in the rate of nitrogen fertilizer application are also considered. In reality, many conservation practices can be implemented simultaneously on a given field. For example, terraces could be present on field together with no-till system, or a grassed waterway. I attempt to capture such interactions subject to modeling constraints. For example, SWAT cannot, at the present time, simulate a terrace and a grassed waterway in the same HRU. It can, however, simulate a combination of fertilizer reduction, no-till, and a grassed waterway. Land retirement (modeled as establishment of permanent grass cover) is not interacted with any other

practices. All other practices are modeled in conjunction with a two-year corn-soybean rotation, which is assumed to carry no incremental cost. Costs of conservation practices are discussed below. As a result, 17 mutually exclusive combinations make up the allele set (Table 2).

Table 2. The allele set

Allele number	Allele name	Allele Description
1	*Land retirement*	Retirement of land from production; establishment of permanent grass cover
2	*CT*	Conventional tillage (less than 15% of crop residue remaining)
3	*CT RF*	Conventional tillage, 20% nitrogen fertilizer application reduction
4	*NT*	No-till (more than 30% of crop residue remaining)
5	*NT RF*	No-till, 20% nitrogen fertilizer application reduction
6	*CT Terraced*	Conventional tillage, establishment of parallel terraces
7	*CT Terraced RF*	Conventional tillage, establishment of parallel terraces, 20% nitrogen fertilizer application reduction
8	*NT Terraced*	No-till, establishment of parallel terraces
9	*NT Terraced RF*	No-till, establishment of parallel terraces, 20% nitrogen fertilizer application reduction
10	*CT Contour*	Conventional tillage, contour farming
11	*CT Contour RF*	Conventional tillage, contour farming, 20% nitrogen fertilizer application reduction
12	*NT Contour*	No-till, contour farming
13	*NT Contour RF*	No-till, contour farming, 20% nitrogen fertilizer application reduction
14	*CT GW*	Conventional tillage, establishment of grassed waterways
15	*CT RF GW*	Conventional tillage, establishment of grassed waterways, 20% nitrogen fertilizer application reduction
16	*NT GW*	No-till, establishment of grassed waterways
17	*NT RF GW*	No-till, establishment of grassed waterways, 20% nitrogen fertilizer application reduction

Each of the 17 alleles can be applied to an HRU and simulated by SWAT. SWAT represents in-field and management practices in several different ways. Nitrogen fertilizer reductions are accounted for by reducing the application rate in the management table. In-field conservation practices are simulated by adjustment of SWAT parameters, namely the 'P-factor' and Manning's N coefficients. The effect of all in-field conservation practices is accounted for by adjusting the "support practice (P) factor," which is one of the factors used in the original Universal Soil Loss Equation (USLE) (Wischmeier and Smith, 1978) and also in the Modified USLE (MUSLE) equation that is used in SWAT. The P factors used for contouring and terraces are based on values reported by Wischmeier and Smith (1978) as a function of slope range (Table 3). The choice of a P factor value of 0.4 for grassed waterways is based on the methodology used by Gassman et al. (2006). The effect of grassed waterways was further accounted for in SWAT by adjusting the Manning's N values.[22] No-till is simulated by removing tillage machinery passes in the SWAT management table, as well as by adjusting the Crop Type Factor ("C-factor") in the Modified USLE, where the magnitude of adjustment varies by crop and tillage system.[23]

Table 3. P-factor values for contouring, terraces, and grassed waterways

Slope ranges	Contouring	Terraces	Grassed Waterways
1 to 2	0.6	0.12	0.4
3 to 5	0.5	0.1	0.4
6 to 8	0.5	0.1	0.4
9 to 12	0.6	0.12	0.4
13 to 16	0.7	0.14	0.4
17 to 20	0.8	0.16	0.4
21 to 25	0.9	0.18	0.4

[22] Manning's N value was set to 0.24 for HRUs with grassed waterways.
[23] C-factor is reduced from 0.3 for conventional tillage for both corn and soybeans to 0.04 for no-till for corn and to 0.08 for no-till for soybeans.

Further, the effect of terraces was simulated by adjusting the slope length parameter in accordance with American Society's of Agricultural and Biological Engineers standards (2003).

4.3.4. Iowa Watersheds Under Study

Since the SWAT model is a watershed-based model, the state of Iowa (a political entity) has to be delineated in hydrologic, watershed, terms. To that end, the state is divided into 13 major watersheds, as shown in Figure 1, based on the criterion that the watershed outlet should drain watersheds that either lie entirely or largely within the political boundaries of Iowa. Delineation of each watershed into smaller spatial units required for the SWAT simulations consists of two steps: (1) subdividing each major watershed into smaller units such as U.S. Geological Survey (USGS) 8-digit Hydrologic Cataloging Unit (HCU) watersheds (Seaber et al., 1987) or smaller 10-digit watersheds (as described in

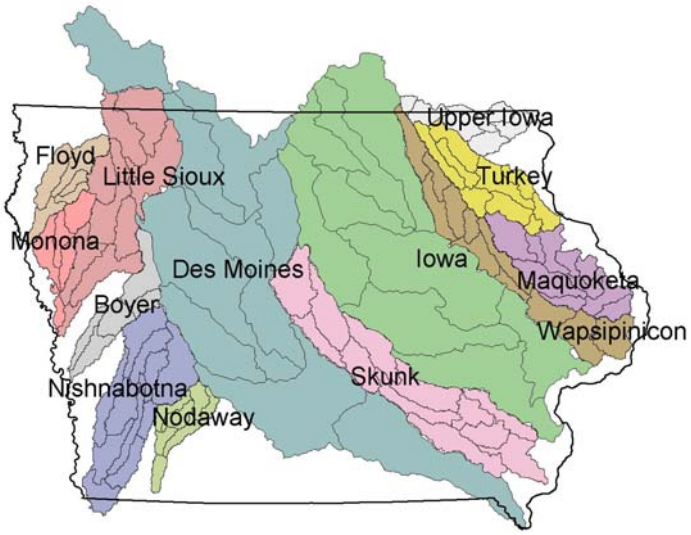

Figure 2. Hydrologic representation of the state of Iowa

http://www.igsb.uiowa.edu/gsbpubs/pdf/WFS-2001-12.pdf), and (2), further subdividing subwatersheds into HRUs.

Larger 8-digit subwatersheds were used for the Des Moines and Iowa River Watersheds (Figure 2), which were the two largest watersheds included in the analysis. The smaller 10-digit subwatersheds were used for those watersheds that consist of 1 to 3 8-digit watersheds (Figure 2), to avoid potential distortions in predicted pollutant indicators when only a small number of subwatersheds are used in a SWAT application, as discussed by Jha et al. (2004).

4.3.5. SWAT Data Inputs

The hydrologic model requires numerous data inputs, including weather, soil, topographic, and land use, and agricultural management data. Historic data on cropping patterns is necessary for model calibration and validation.

Historical precipitation, maximum temperature, and minimum temperature data obtained from Iowa Environmental Mesonet (http://mesonet.agron.iastate.edu/COOP/) were used for the SWAT simulations. The main data source for the land use, soil, and management information is the USDA 1997 NRI database (Nusser and Goebel, 1997; http://www.nrcs.usda.gov/technical/NRI/), which contains soil type, landscape features, cropping histories, conservation practices, and other data for roughly 800,000 U.S. nonfederal land “points” including 23,498 in Iowa. Each point represents an area that is assumed to consist of homogeneous land use, soil, and other characteristics, which generally ranges from a few hundred to several thousand hectares in size. Table 4 provides the characteristics of each watershed.

The NRI clusters serve as HRUs in the SWAT simulations. All of the points within a given category were clustered together within each 8-digit watershed for the Des Moines and

Table 4. Characteristics of the 13 study watersheds

Watershed	# of Delineated Subwatersheds	Number of HRUs	Drainage Area		Key Land Uses (% of watershed)			
			mi^2	km^2	Cropland	Grassland (CRP and Pasture)	Forest	Urban
Boyer	5	425	1,089	2,820	68	26	4	2
Des Moines	9	1,223	14,477	37,496	71	16	6	7
Floyd	5	524	917	2,376	84	13	0	3
Iowa	9	2,055	12,663	32,796	77	12	4	8
Little Sioux	10	1,879	3,553	9,203	86	13	1	0
Maquoketa	10	2,041	1,864	4,827	56	32	10	3
Monona	5	379	947	2,452	78	19	2	1
Nishnabotna	11	2,997	2,980	7,718	84	15	1	0
Nodaway	7	593	792	2,051	52	41	5	3
Skunk	12	3,284	4,342	11,246	69	25	5	1
Turkey	9	1,640	1,699	4,400	56	25	16	3
Upper Iowa	7	664	992	2,569	51	26	19	3
Wapsipinicon	11	3,141	2,542	6,582	77	19	3	1

Iowa River Watershed simulations, except for the cultivated cropland. For the cultivated cropland, the NRI points were first aggregated into different crop rotation land use clusters within each 8-digit watershed, based on the NRI cropping histories. Details on creating HRUs are provided in Kling, Rabotyagov, Jha, Feng, Parcel, Gassman, and Campbell (2007).[24]

To estimate the water quality changes, it is necessary to calibrate SWAT to existing baseline data on the watersheds and to accurately represent the current land use, land management, and weather conditions of the region using data obtained from several sources.

[24] As a result, HRUs can only be identified spatially up to the subbasin level (i.e., 8-digit HUC for Des Moines River and Iowa River Watersheds, and 10-digit HUCs for other watersheds). This limits the spatial resolution of the algorithm results also to the subbasin level.

A calibration and validation exercise was performed with SWAT2005 for all 13 Iowa watersheds. Details on model calibration and validation are provided in Appendix B of Kling et al. (2007). Calibration and validation showed that the SWAT model performed very well, especially for streamflow, because of the abundance of measured data availability. Water quality components were also calibrated but with lower confidence because of a lack of sufficient measured data. However, total simulated state-level nitrate loadings match fairly closely the estimates obtained from measured data (Libra, Schilling, and Wolter, 1999; Libra, Wolter, and Langel, 2004).

4.3.6. Cost Data

Estimates of costs of each of the alleles were collected from several sources. The costs of contour farming were gathered from the report by Kling et al. (2005), while the cost of nitrogen fertilizer reduction was estimated based on agronomic yield response data (Sawyer et al., 2006). The costs of the other practices (terraces, grassed waterways, no-till, land retirement) were calculated from data which Kling et al. (2007) collected from various federal and state conservation program sources. County-level cost estimates were converted into subbasin-level costs by weighting them by the area of a watershed subbasin contained in the county.

Estimates of costs for terraces (per ft) and grassed waterways (per acre) were converted into costs per protected acre and annualized over their useful life using a 5 percent rate of interest. For terraces, a 25-year useful life was assumed, and, based on Kling et al.'s

(2005) results, it was assumed that 166.67 ft of terrace protect one acre or cropland.[25] For grassed waterways, it was assumed (as in Secchi et al. (2007)), that 2 percent of an acre allocated to a grassed waterway protects the entire acre; useful life was assumed to be 20 years.

Table 5 below provides summary statistics for the costs, as well as the source of data. Details on original sources and computation of estimates can be found in Kling et al. (2007), Secchi et al. (2007), and Kling et al. (2005).

Table 5. Summary of the cost data

Practice	Mean, $/acre	Standard Deviation, $/acre	Source
Land Retirement	148.1	21.7	Kling et al. (2007)
Terraces	36.6	15.8	Kling et al. (2007)
Grassed Waterways	5.5	1.3	Kling et al. (2007)
No-till	16.8	8.1	Kling et al. (2007)
Contour farming	6.6	-	Kling et al. (2005)
N fertilizer reduction	3.9	1.7	Sawyer et al. (2006); Libra, Wolter, and Langel (2004)

In estimating the cost of nitrogen fertilizer reductions, I focus on the revenue effect by utilizing the latest available agronomic studies which estimate corn yield response to nitrogen fertilizer under different rotation schemes (Sawyer et al., 2006). Coupled with the best available data on nitrogen fertilization rates for Iowa (Libra et al., 2004), yield response curves (available at http://extension.agron.iastate.edu/soilfertility/nrate.aspx) are used to

[25] In Kling et al. (2005), this conversion factor was a low-cost estimate. Using a high-cost conversion factor would, in many subbasins, resulted in a per acre annualized cost of terracing larger than the estimated cost of retiring land from production altogether.

arrive at the yield effect of reducing fertilizer application by 20 percent in a corn-soybean rotation. Predicted yield reductions are multiplied by the price of corn and divided by two to generate an average cost for corn-soybean crop rotation.[26] An example of yield reduction computation is given in the Appendix to this chapter. To the extent that farmers may over-apply nitrogen fertilizer and not experience appreciable yield effects as a result of fertilizer reductions (e.g., Yadav et al., 1997), yield-based revenue loss may overstate the cost of fertilizer reductions. On the other hand, since such estimate does not account for other costs farmers may incur if they reduce their fertilizer applications, such as the costs of establishing a nutrient management plan (e.g., Secchi et al. (2007)), or costs associated with preferences for risk (e.g., Sheriff, 2005), it may understate the true costs[27].

The cost of land retirement is proxied by the most recently available data on cropland rental rates for Iowa, which represent the opportunity cost of taking land out of production (Edwards and Smith, 2007). County-level land rent estimates were converted into subbasin-level data by weighting county estimates by the share of subbasin area located in a county.

4.4. Algorithm Initialization and Progression

Now that all the components of the simulation-optimization algorithm (a specific evolutionary algorithm, allele set, hydrologic simulation model, input data), optimization runs can be conducted. A publicly available C++ library of genetic algorithms, GALib, originally developed by Wall (1996), was built upon to implement the logic of the

[26] Price of corn is assumed to be $3.54/bushel, which reflects the Chicago Board of Trade May 2007 corn futures price. This time interval was chosen for the measurement of the corn price in order to match the survey period when the information on cash rental rates was collected.

[27] Raw field-trial data that formed the basis of the polynomial yield response function found in http://extension.agron.iastate.edu/soilfertility/nrate.aspx was not available, and precluded testing of various functional forms for yield response (as in Yadav et al., 1997). Polynomial yield response curves may also overstate the yield effect, and thus, the cost estimate.

evolutionary algorithm described above. Implementation of the evolutionary algorithm was coupled with the i_SWAT program (Campbell, 2006), which manages SWAT model inputs and outputs.

The algorithm starts with an initial population of 40 individuals. Unlike previous studies (e.g., Bekele and Nicklow, 2005), I do not create initial population in a purely random fashion. Instead, I "seed" the initial population with 17 individuals which represent a uniform application of each of the 17 alleles on all the cropland in a watershed. Figure 3 presents the population for the initial generation for the Iowa River Watershed. Individuals marked as triangles are Pareto-nondominated, while the ones marked with a cross are dominated.

The remaining 23 individuals in the initial population are created by randomly assigning one of the 17 alleles to an HRU (gene). The effects of seeding are discussed in greater detail below; however, I find that it ensured a very good coverage of the objective space. This has both benefits in terms of the progression of the evolutionary algorithm (ensuring diversity), as well as in terms of interpretation of the results (the allele set spans the entire policy-relevant range of costs: from zero cost with no conservation practices to the highest possible cost of retiring all cropland from production).

It should be noted that since each cropland HRU in a watershed is assigned one of the alleles from the allele set, baseline crop choices and baseline conservation practices are replaced by the selected allele. This represents the algorithm allocating conservation practices on the landscape as if working with a "blank slate". This is true for every baseline conservation practice, with the exception of pasture and CRP land, which is left unchanged. This "blank slate" implementation has its advantages and disadvantages. Given that the baseline set of conservation practices is likely to be placed in an inefficient (relative to the

objectives in this study) fashion, allowing the algorithm to freely place conservation practices to cropland HRUs is advantageous. The disadvantages include missing the effects of

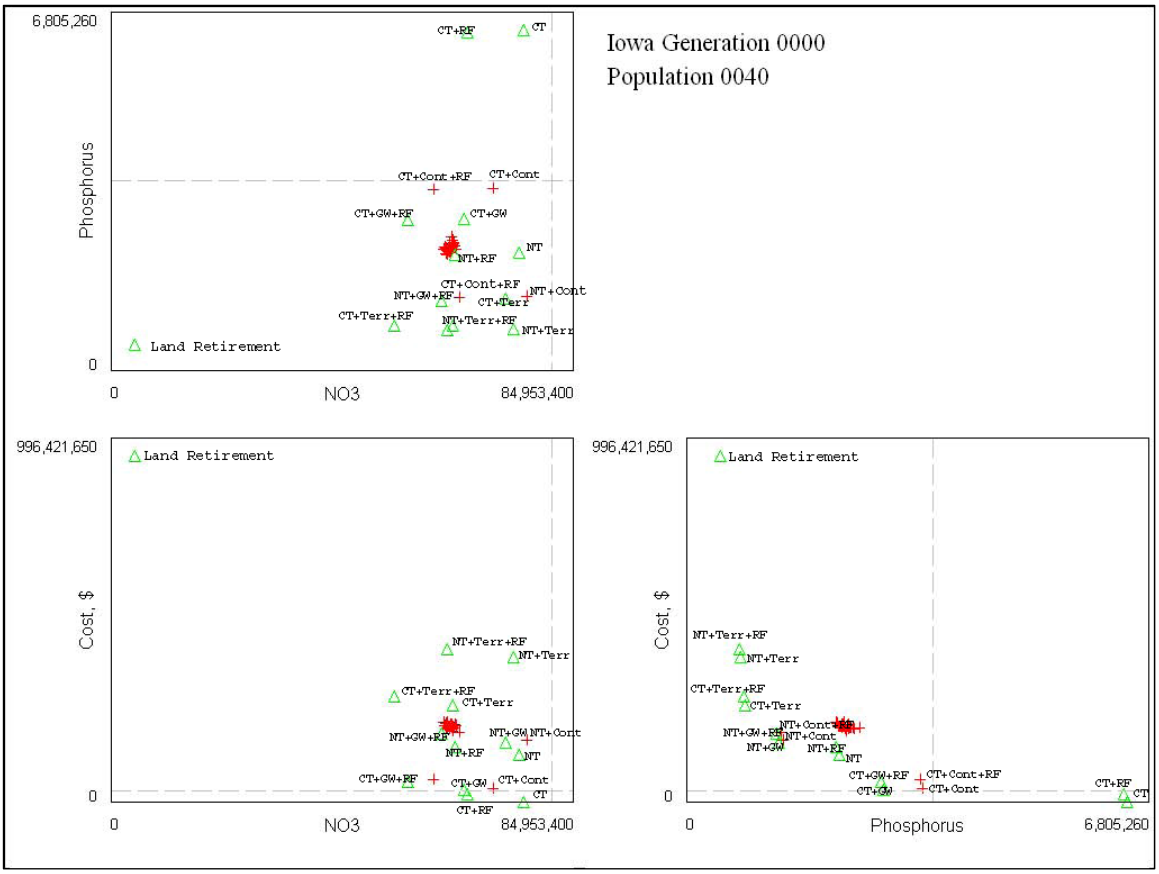

Figure 3. Initial population, Iowa River Watershed

alternative crop rotations present in the baseline data, and a somewhat lessened ability to compare the costs of a solution discovered in the optimization process with the costs of baseline practices.[28,29]

[28] A two-year corn-soybean rotation (staggered randomly as either a corn-soybean or a soybean-corn rotation) provides the basis for 16 of 17 alleles used in this study. This rotation is by far the most common rotation observed in the baseline data, and carries environmental benefits relative to monoculture cropping. Other rotations (most notably, corn-oats-alfalfa rotation) were present in the baseline, but mostly in smaller watersheds. An alternative allele set, including this rotation, was developed. One issue with allowing the

The individuals in the initial population are all evaluated for their nitrate, P, and cost impacts. Fitness scores are then assigned to each individual based on its Pareto-ranking relative to other individuals, as well as based on its location in the objective space. Individuals are then selected for mating using a fitness-proportional selection method[30], and uniform single-point crossover operator is applied to create new individuals. Each of the genes is subject to random mutation (with probability 0.003), whereby any allele value could be chosen for that gene. As a result, 12 new individuals are created. Pareto-ranking and fitness score assignment is done again, and Pareto-dominated individuals are deleted from the population. In the subsequent generation, the newly created population (consisting of Pareto-non-dominated individuals) is used again for the creation of new individuals using operators of selection, crossover, and mutation, and the process continues. The size of the population thus grows dynamically as new non-dominated solutions are created[31]. For the watersheds under study, the target number of generations was set to about 250. This exceeds a typical number of population evaluations conducted in the related literature (e.g., Bekele and Nicklow (2005) used 50, while Arabi et al. (2006) limited optimization runs to 2000 hydrologic model evaluations).

---

algorithm to choose among multiple rotations is producing a good estimate for the cost of a rotation. Extension budgets were used to obtain cost estimates for a corn-oats-alfalfa rotation. Given that this rotation was predicted to carry an incremental cost which was large relative to the cost of most conservation practices, and the fact that this rotation was not observed in most of Iowa, this expanded allele set was not used to generate results presented here.

[29] An alternative, "baseline-aware", implementation, could leave all crop rotations in place, and place conservation practices 'on top of' existing baseline practices. This approach circumvents the necessity to obtain crop rotation cost estimates, and is implemented for the study of the Upper Mississippi River Basin in the next chapter.

[30] Another term is "roulette-wheel selection" where the probability of an individual being selected for reproduction is proportional to the ratio of its fitness score to the sum of the fitness scores of individuals in the current population. Linear scaling of fitness scores (see Wall (1996) for details) was used to correct for effects of fitness score magnitudes.

[31] Thus, the algorithm satisfies the conditions to be of Rudolph and Agapie's (2000) "Base Algorithm VV" type. The authors show that for all evolutionary algorithms of this type, all Pareto-optimal solutions will be members of the population of non-dominated individuals in finite time with probability 1.

Figure 4 below provides a graphic depiction of the basic flow of the algorithm.

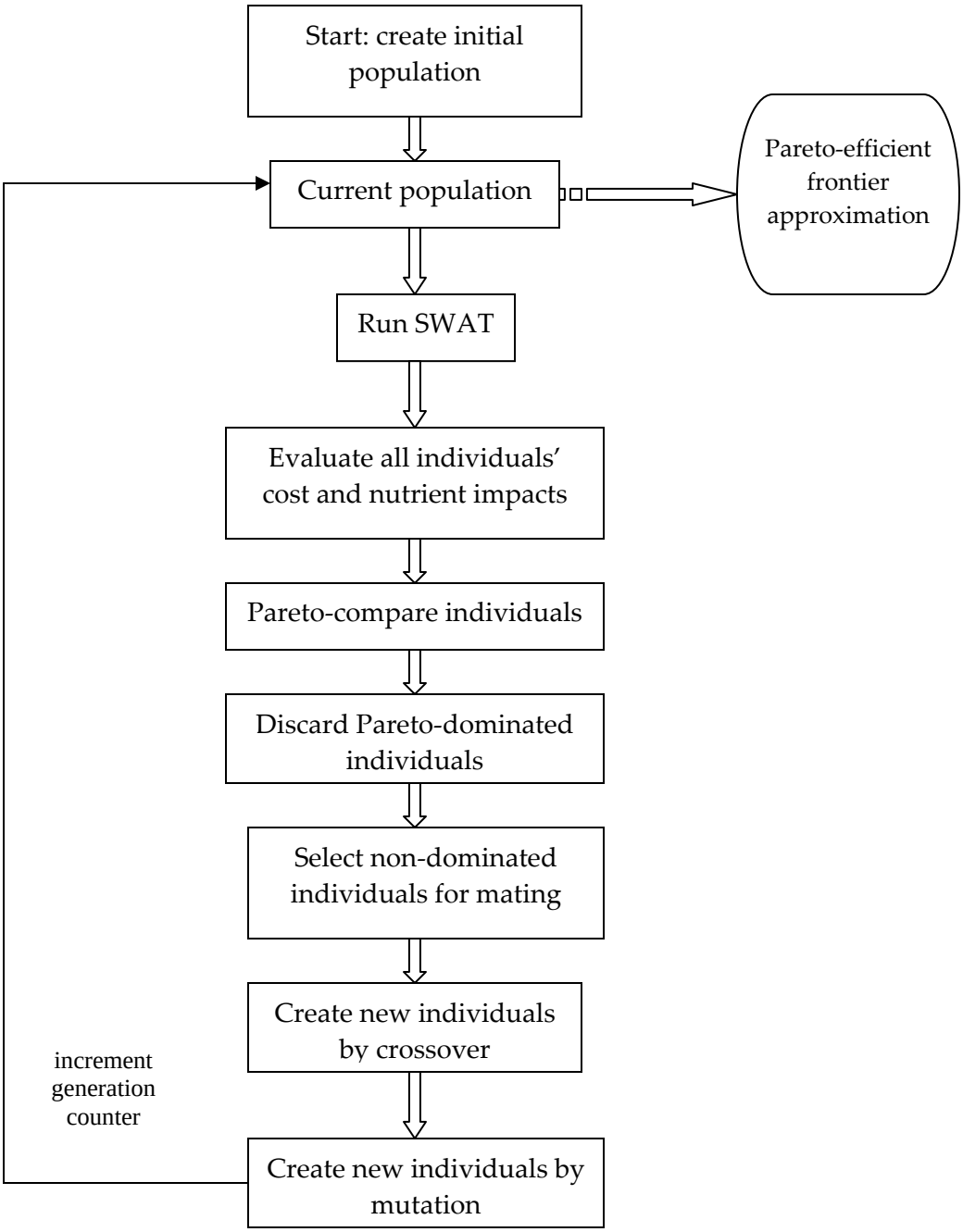

Figure 4. Algorithm flow

4.5. Results and Analysis

The outcome of each simulation run is an approximation to the Pareto-efficient frontier in nitrates-phosphorus-control cost space. Figure 5 presents the final population for the Iowa River Watershed, as two-dimensional, and three-dimensional, projections. The left bottom panel in the two-dimensional image represents a projection of the frontier in nitrates-cost space, and the right bottom panel presents a projection in the phosphorus-cost space, while the top panel presents the nitrate-phosphorus projection. On the watershed level, Pareto-efficient frontier approximations summarize a variety of tradeoffs and can be used to find individuals satisfying particular nutrient reduction goals at least cost or finding efficient (and feasible) nutrient reduction combinations for a given level of control cost.

4.5.1. Pareto-efficient Frontiers as Total Abatement Cost Curves

The empirical approximations of the Pareto-efficient frontiers in nitrates-P-cost space can be thought of as total pollution cost curves, relating pollution (nutrient loadings) to control cost. Thus, looking for efficient nonpoint source pollution reduction strategies using multiobjective evolutionary algorithms produces a set of data which can be easily translated to represent pollution abatement cost curves for each of the watersheds under study.

A final generation from the evolutionary algorithm run results in a data set containing nitrate loadings, P loadings, and estimated control cost. I estimate a relationship between pollution loadings and control cost in order to obtain a convenient mathematical representation of the total pollution cost curve for each of the 13 watersheds in the state.

A semilog approximation to each of the frontiers was developed, resulting in a fitted cost curve $\hat{C}_i(N_i, P_i)$ for each watershed, $i = 1,...,13$, where N is nitrate loading at the outlet,

and P is total phosphorus loading at the watershed outlet. Figure 6 presents an example of the fitted cost surface for the Iowa River Watershed.[32]

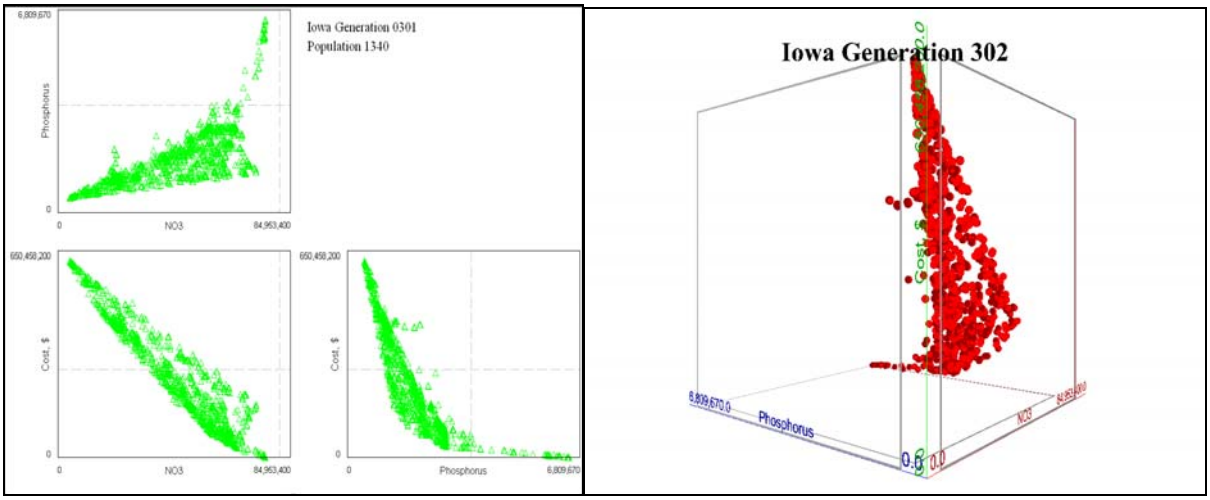

Figure 5. Pareto-efficient frontier approximations, Iowa River Watershed

Cost curves differ across the watersheds (due both to variation in per unit costs of conservation practices and hydrologic and geographic characteristics of each watershed). Thus, if a policy goal is to reduce state-level nutrient exports downstream, then a cost-minimizing solution will likely allocate loading reduction burdens unequally among the watersheds, exploiting differences in marginal abatement costs.

Given that multiple nutrient pollutants are of concern, two sets of problems are solved. One involves reducing state-level nitrate exports, while the other involves reducing state-level phosphorus export. Reducing total nitrate loadings which ultimately make their way to the Gulf of Mexico has long touted as an important step in reducing both the

[32] $C(N,P) = \exp\left(20.49808 - 0.00073216N + 0.0378P + 0.00000112N^2 + 0.00133P^2 - 0.00027571NP\right)$ is the fitted cost curve. R^2=0.82. Nitrate and phosphorus loadings are scaled by dividing by 100,000.

likelihood and the severity of Gulf Hypoxia (CENR, 2000). Policy relevance of reducing statewide nutrient loadings for both nitrates and phosphorus is highlighted by recent research

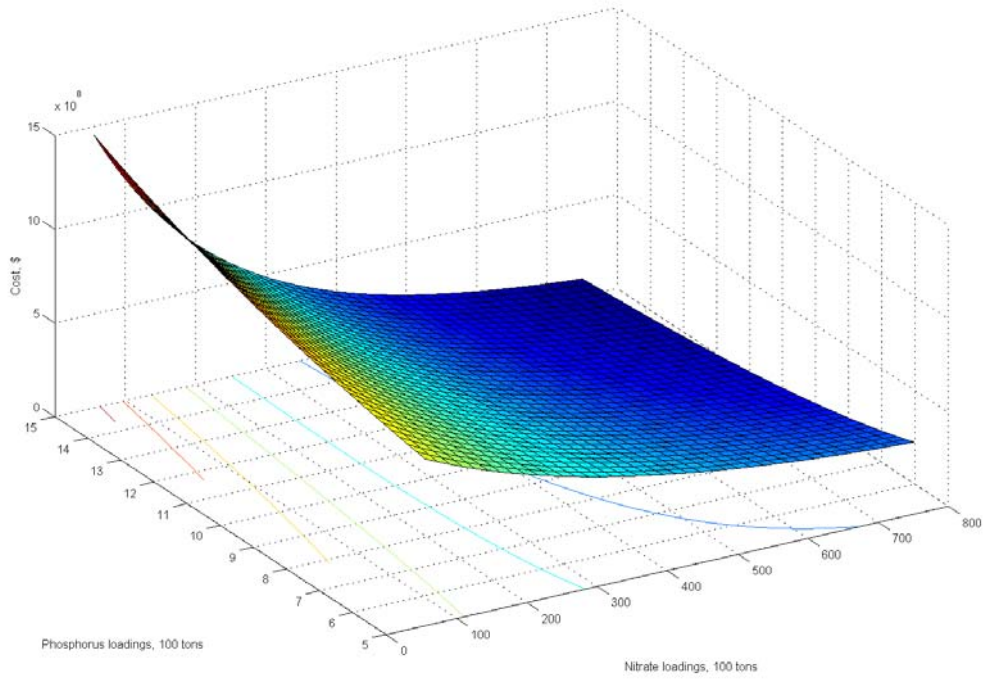

Figure 6. Fitted total pollution cost curve for the Iowa River Watershed

related to the Gulf of Mexico hypoxic zone, which suggests that total phosphorus loadings to the Gulf may also be a contributing factor to the creation of hypoxic conditions (e.g., Lohrentz et al., 1992, 1997, 1999; Ammerman et al., 2004; Sylvan et al., 2006).

4.5.2. State-level Nutrient Abatement Cost Curves

I solve for cost-minimizing allocation of loading reductions to reduce statewide nitrates under two scenarios of treating the other nutrient, phosphorus. In the first scenario, cost of total nitrate loading reductions is minimized subject to the constraint that each

watershed's P loadings remain at or below baseline levels. This represents a case where the state's goal is to meet its downstream environmental obligations of reducing nitrates, and improvements in local (watershed-level) P loadings are not required. The second scenario incorporates local water quality objectives by requiring that each watershed's P loadings be reduced by at least 30 percent relative to baseline.[33] In addition, both sets of problems contain a constraint specifying that nutrient loadings cannot fall below loadings which obtain from uniform land retirement, or above baseline loadings.[34] Formally, both problems solve:

$$\min_{\{N_i,P_i\}} \sum_{i=1}^{13} \hat{C}_i(N_i,P_i), \tag{4.8}$$

subject to

$$\sum_{i=1}^{13} N_i \le TN^{goal} \tag{4.9}$$

and

$$N_i^{landret} \le N_i \le N_i^{baseline}, \tag{4.10}$$

where TN^{goal} is the total state-level nitrates export goal. The first problem uses the following constraints on local P: $P_i \le P_i^{baseline}$, while the second problem tightens the phosphorus constraints: $P_i \le 0.7P_i^{baseline}$. For the sake of convenience, from now on I will refer to the first problem as problem (a), and the second problem as problem (b).

[33] Local water quality goals may exist at a finer geographic level than the watersheds analyzed. That is, subbasin-level targets may be specified. A version of the evolutionary algorithm that searches for solutions which satisfy subbasin-level nutrient constraints has been developed. Results for the Des Moines River Watershed incorporating subbasin-level nitrate reduction goals are presented in the Appendix.

[34] I further impose additional constraints in nitrates-P space in order to limit the domain of the cost-minimization problem to the region where individuals exist in the empirical frontier. Observing 13 empirical frontiers shows that the feasible region, in nitrates-P space, can be constructed by imposing 3 linear constraints and considering the region between these constraints. The 3 constraints in nitrates-P space are defined by: (1) a line between allele #1 (uniform land retirement) and allele #3 (CT+RF); (2) a line between allele #2 (CT) and allele #12 (NT+Contour); and (3) a line between allele #1 and allele #8 (NT+Terr). Further, nitrate loadings in each of the watersheds were not allowed to exceed loadings which obtain from uniform application of allele #2 (CT).

Similarly, the set of problems which allocate loadings in order to minimize statewide export of phosphorus involves two ways of handling local nitrate loadings: first, I require that watershed-level nitrate loadings not exceed baseline levels, and, for the second problem, I impose a 30 percent nitrate reduction constraint in each of the watersheds. Again, the objective function for these two problems is the same:

(4.11) $$\min_{\{N_i,P_i\}} \sum_{i=1}^{13} \hat{C}_i(N_i, P_i),$$

subject to

(4.12) $$\sum_{i=1}^{13} P_i \leq TP^{goal}$$

and

(4.13) $$P_i^{landret} \leq P_i \leq P_i^{baseline}.$$

Similarly, TP^{goal} is the total state-level phosphorus export goal. The first problem (to which I henceforth refer to as problem (c)) imposes the constraint: $N_i \leq N_i^{baseline}$, and the second problem (problem (d)) imposes a tighter local nitrate constraint: $N_i \leq 0.7N_i^{baseline}$.

Figure 7 presents the estimated costs of reducing total statewide nitrates which are obtained by varying the levels of TN^{goal}. The higher of two curves represents solutions to problem (b) and reflects the higher cost of meeting more stringent local P goals.

The two cost curves almost converge after 50 percent nitrate abatement goal, which reflects the fact that, since it is likely that land retirement will be the main option used to arrive at such dramatic nitrate reductions, an addition of watershed-level P constraint adds relatively little to the total abatement cost.

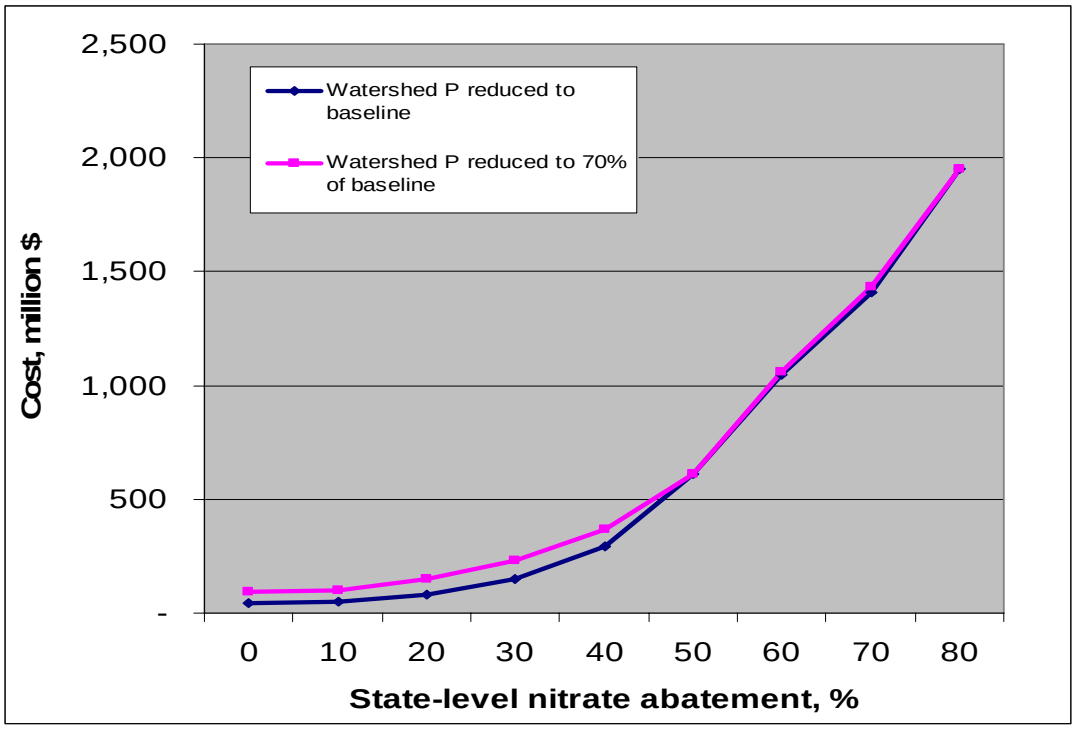

Figure 7. State-level nitrate export reduction cost curves

Figure 8 presents the cost curve for reducing total statewide P loadings, obtained by successively decreasing TP^{goal}.

Both Figures depict cost curves which are increasing and convex. Tightening of constraints on watershed-level nutrient reductions is estimated to increase the cost of total state-level nutrient control. Each of the points on the four cost curves represents a particular nutrient loading allocation across the 13 watersheds. This, in turn, presupposes a particular allocation of conservation practices in each of the watersheds.

Thus, developing the cost curves provides several useful insights into the nature of nonpoint source pollution control at the state level. In addition to summarizing and quantifying the total and marginal abatement costs for nutrients, they, in conjunction with the

watershed-level Pareto-efficient frontiers, may be able to provide practical guidance on how to conduct nutrient reduction policy for a specific nutrient target. In the following section, I

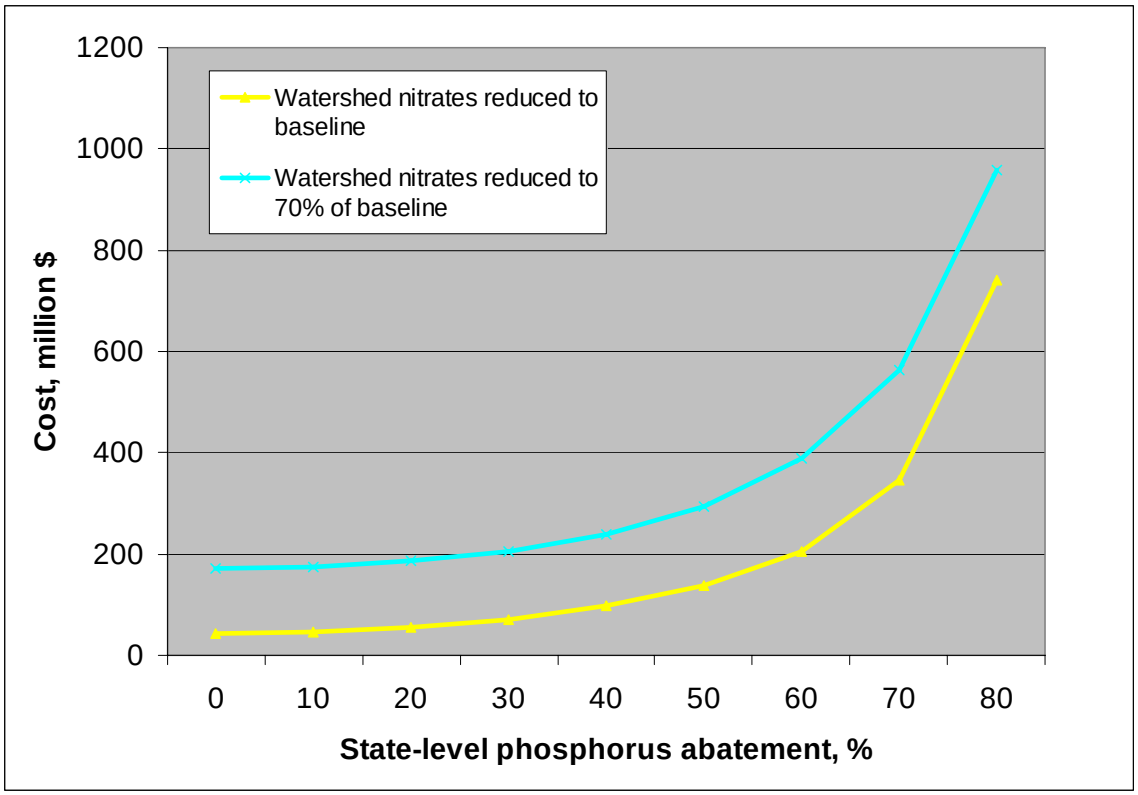

Figure 8. State-level phosphorus export reduction cost curves

illustrate how this might be done using a 30 percent state-level nutrient reduction target as an example.

4.5.3. Ways of Achieving Given State-Level Nutrient Reductions

This section is organized as follows. First, I present the solutions which are obtained from a cost-minimization based on the fitted cost curves. Next, I turn to the watershed-level Pareto-efficient frontiers to identify individuals capable of achieving needed nutrient reductions. Then, I describe the set of conservation practices used to achieve these

reductions. I explain the choice of particular alleles based on the effect which uniform conversion of each watershed to a particular allele has on nutrients. Finally, I discuss the distribution of conservation practices at the subbasin level.

Table 6 below presents the solutions to cost-minimization problems (a) and (b), where total state-level nitrates are to be reduced by 30 percent ($TN^{goal} = 0.7\sum_{i=1}^{13} N_i^{baseline}$). The cost of reducing total state-level nitrates 30 percent and reducing all watershed-level P loadings to the baseline level was estimated to be $149 million, and the addition of the requirement that all watershed-level P loadings be reduced by 30 percent raises the predicted cost to $230 million per year.

Table 6. Solutions to problems (a) and (b), based on fitted cost curves

			Solution to problem (a)				Solution to problem (b)			
Watershed	NO_3 baseline, tons/year	P baseline, tons/year	NO_3, tons/yr	NO_3, % of baseline	P, tons/year	P, % of baseline	NO_3, tons/yr	NO_3, % of baseline	P, tons/year	P, % of baseline
Boyer	2,479	1,087	1,369	100	822	91	1,369	100	630	70
Des Moines	70,250	2,539	49,602	71	2,539	100	49,062	70	1777	70
Floyd	2,420	566	1,117	46	566	100	1,156	48	396	70
Iowa	80,908	3,623	59,262	73	3,623	100	59,167	73	2536	70
Little Sioux	11,513	1,392	6,653	58	1,392	100	6,656	58	975	70
Maquoketa	490	37	271	55	37	100	271	55	26	70
Monona	1,974	332	1,032	52	332	100	1,074	54	232	70
Nishnabotna	9,996	3,075	6,574	66	3,075	100	6,381	64	2153	70
Nodaway	1,968	574	1,458	74	574	100	1,495	76	402	70
Skunk	13,882	2,896	10,276	74	2,896	100	10,594	76	2028	70
Turkey	7,277	1,376	5,326	73	1,376	100	5,515	76	963	70
Upper Iowa	2,761	216	2,304	83	148	69	2,304	83	148	69
Wapsipinicon	16,151	611	9,429	58	611	100	9,627	60	428	70

Table 7 presents the solutions to the cost-minimization problem (d), where total state-level P is targeted for a 30 percent reduction ($TP^{goal} = 0.7\sum_{i=1}^{13} P_i^{baseline}$). Based on estimated watershed cost curves, reducing state-level P by 30 percent while requiring a 30 percent reduction in nitrate loadings in each of the watersheds would cost $206 million.

Table 7. Solution to the problem (d), based on fitted cost curves

Watershed	NO_3 baseline, tons/year	P baseline, tons/year	NO_3, tons/yr	NO_3, % of baseline	P, tons/year	P, % of baseline
Boyer	2,479	1,087	959	70	502	56
Des Moines	70,250	2,539	49,175	70	2,539	100
Floyd	2,420	566	1,694	70	209	37
Iowa	80,908	3,623	56,636	70	3,540	98
Little Sioux	11,513	1,392	8,059	70	564	40
Maquoketa	490	37	343	70	34	93
Monona	1,974	332	1,382	70	196	59
Nishnabotna	9,996	3,075	6,997	70	1,225	40
Nodaway	1,968	574	1,377	70	293	51
Skunk	13,882	2,896	9,718	70	1,939	67
Turkey	7,277	1,376	5,094	70	919	67
Upper Iowa	2,761	216	1,933	70	127	59
Wapsipinicon	16,151	611	11,306	70	611	100

By and large, the exercise of identifying individuals in the empirical Pareto-efficient frontiers, whose nutrient loadings closely mimic the loadings found as a part of cost-minimization solution, was a success. The only solution for which close empirical counterpart could not be identified in a satisfactory manner was the solution to problem (c), which involved P reductions without any nitrate reductions relative to the baseline. Identification of individuals with the kinds of P reductions which were needed to match the solution resulted in finding individuals whose nitrate loadings were oftentimes also reduced. As a result, while the cost predicted from the cost-minimization exercise was estimated to be

around $70 million per year, the empirical counterpart to this solution resulted in an annual cost of over $157 million per year. Thus, presentation of these results is omitted. As to the reasons why this might be happening, I present those below.

The rest of the section is organized as follows. Tables 8, 9, and 10 present the individuals found to be a closest match to the prescriptions of the cost-minimization program.

Tables 8 and 9 below present individuals which match the solutions to problems (a) and (b): problems of minimizing total statewide nitrates subject to holding watershed-level P loading to the baseline levels (problem (a)), or to 70 percent of baseline levels (problem (b)).

Table 8. Individuals identified to correspond to the solution of problem (a)

Watershed	Ind. #	NO_3, tons/yr	$, thousand/year	P, tons/year	NO_3, % of baseline	P, % of baseline
Boyer	2166	1,329	7,405	821	97	91
Des Moines	2049	52,093	50,986	2,661	74	105
Floyd	280	1,085	1,259	620	45	110
Iowa	1733	59,854	47,661	3,974	74	110
Little Sioux	14	6,256	9,712	807	54	58
Maquoketa	732	218	828	26	45	70
Monona	1899	963	1,798	330	49	99
Nishnabotna	2470	6,773	10,719	3,075	68	100
Nodaway	619	1,556	1,539	592	79	103
Skunk	14	9,770	8,374	2,506	70	87
Turkey	113	4,866	6,014	1,338	67	97
Upper Iowa	14	1,971	1,220	203	71	94
Wapsipinicon	1144	9,375	8,104	601	58	98

Individuals in Table 8 carry a combined annual cost of $156 million (relative to $149 million identified from solving problem (a)), and individuals in Table 9 combine for $264 million per year, relative to $230 million estimated as part of the solution to problem (b).

Table 10 presents individuals which were found to result in nutrient reductions consistent with the solution to the problem (d): minimization of total statewide P subject to

reducing nitrates 30 percent in every watershed. The total annual cost of implementing each of the individuals is estimated to be $221 million, which is within 7 percent of cost estimated by the cost-minimization program ($206 million).

Table 9. Individuals identified to correspond to the solution of problem (b)

Watershed	Ind. #	NO_3, tons/yr	$, thousand/year	P, tons/year	NO_3, % of baseline	P, % of baseline
Boyer	2848	1,342	8,603	591	98	66
Des Moines	848	48,698	103,553	1,695	69	67
Floyd	712	1,063	1,955	390	44	69
Iowa	2903	58,408	71,632	2,525	72	70
Little Sioux	14	6,256	9,712	807	54	58
Maquoketa	732	218	828	26	45	70
Monona	14	950	2,793	229	48	69
Nishnabotna	1355	6,129	16,088	2,146	61	70
Nodaway	1270	1,486	3,358	393	76	68
Skunk	962	10,412	16,226	1,960	75	68
Turkey	370	5,097	10,132	937	70	68
Upper Iowa	3402	2,128	3,004	149	77	69
Wapsipinicon	2043	9,624	16,487	406	60	66

Table 10. Individuals identified to correspond to the solution of problem (d)

Watershed	Ind. #	NO_3, tons/yr	$, thousand/year	P, tons/year	NO_3, % of baseline	P, % of baseline
Boyer	1743	944	25,419	230	69	26
Des Moines	2049	52,093	50,986	2,661	74	105
Floyd	1844	1,133	4,353	218	47	39
Iowa	2137	56,356	54,941	3,189	70	88
Little Sioux	2139	6,159	11,187	720	54	52
Maquoketa	732	218	828	26	45	70
Monona	2217	915	3,344	197	46	59
Nishnabotna	100	6,654	22,078	1,169	67	38
Nodaway	2324	1,342	4,556	305	68	53
Skunk	707	9,605	18,676	1,843	69	64
Turkey	370	5,097	10,132	937	70	68
Upper Iowa	5059	1,760	6,186	137	64	63
Wapsipinicon	1144	9,375	8,104	601	58	98

That is, the results suggest that in order to reduce state-level average annual nitrate loadings by 30 percent (and not allow any watershed's P loadings to be greater than the baseline), $156 million per year would have to be spent on appropriately placed conservation practices and targeted additional land retirement. To achieve, in addition to the nitrate reduction goal, a reduction in total P loadings at each of the watershed outlets would cost an additional $108 million per year. Reducing state-level P loadings and simultaneously reducing each watershed's average annual nitrate loadings would cost approximately $221 million per year. It also should be pointed out that the total cost of baseline conservation practices (excluding existing CRP) is estimated to be $150 million per year.[35] Going back to state-level nutrient abatement cost curves, it is clear that reallocating conservation practices in accordance with the algorithm's prescriptions may allow for significantly lower nutrient loadings for the same level of cost. For example, one can almost (falling short by just under $6 million per year) implement solution to the problem (a), and reduce state-level nitrates by 30 percent essentially for the same cost. Another possibility is reducing state-level nitrate exports by 20 percent and reducing watershed-level P by 30 percent at a cost of $147 million. That is, ignoring transaction costs, reallocating conservation practices in accordance to the algorithm's prescriptions results in *lower* state-level nutrient loading, *same or lower* watershed-level nutrient loadings, *and lower* costs. Thus, efficiencies discovered by the algorithm are large.[36]

[35] Existing CRP land is estimated to cost approximately $176 million per year. This cost is presumed to be incurred in all the results presented, since the algorithm assumes that current CRP land does not come back into agricultural production.

[36] One could be concerned that reallocating practices in accordance to the algorithm's prescriptions may hurt other environmental objectives, such as soil erosion protection. This is unlikely to be a concern in the solutions found, given the beneficial soil protection effects of conservation tillage, contouring, terracing, and grassed waterways, and the fact that most of the cropland would be protected by one (or more) of these practices. The only exception perhaps is the Maquoketa River Watershed, where conventional tillage was selected.

Finally, to gauge the efficiency gains from reallocating nutrient loading abatement across watersheds relative to a uniform nutrient reduction case, I compute the costs of uniformly reducing nitrates by 30 percent (and no P reductions), as well as the costs of uniformly reducing nitrates and P by 30 percent in all watersheds. The former scenario results in a control cost of $189 million, while the latter costs involves the annual cost of around $288 million. Thus, the cost savings from reallocating nitrate reductions are $33 million for solution (a) and $24 million for solution (b). The cost savings from reallocating P reductions with a local nitrate constraint (problem (d)) results in efficiency gains of $67 million. While the cost savings are significant for both sets of problems, the results indicate that abatement reallocations for the control of state-level P yields greater cost savings than abatement reallocations for the control of state-level nitrate loadings.

The rest of the section takes a closer look at the alleles used to achieve the needed nutrient reductions. In order to better explain the mix of alleles selected, I describe how each allele, if implemented uniformly on the landscape, would affect nutrient loadings. Tables 11, 12, and 13 below provide a more detailed look at the distribution of the conservation practices within each of these individuals. Figures 8, 9, and 10 further illustrate subbasin-level distribution of the alleles for each of the watersheds.

4.5.4. Watershed-level Analysis

A couple of things need to be mentioned prior to watershed-level analysis of allele utilization. First, cost-minimization problems above were solved to achieve reductions relative to baseline nutrient loading levels. Baseline cropping practices and existing conservation practices all play a role in determining the baseline. Given the nature of the

allele set and the fact that I do not explicitly model the baseline land use and conservation practices, there is no guarantee that the nutrient loadings resulting from, e.g., allele #2 (all conventional tillage), would be greater or lower than the baseline. Two effects may be in play here: first, the allele set I use assumes all cropland is in corn-soybean rotation, which presupposes that every other year nitrogen fertilizer applications are not conducted; and, second, the allele set ignores any conservation practices already in place. To the extent that baseline crop rotations include rotations like continuous corn, or corn-corn-soybeans, the assumption of corn-soybean rotation would serve to reduce nitrate loadings relative to baseline. At the same time, ignoring existing conservation practices serves to increase estimated nutrient loadings stemming from any allele in the current set. Thus, in the discussion below, when I find that a particular allocation of conservation practices acts to reduce nutrient loadings, it is implied that a crop rotation shift is undertaken as well. In practice, analysis of results indicates that, for most watersheds, baseline nitrate loadings either exceed the loadings resulting from allele #2 (zero-cost conventional tillage), or fall just short of it. Thus, achieving baseline loadings for nitrates is often completely costless. On the contrary, baseline P loadings are typically significantly smaller than allele #2's P loadings. Therefore, achieving baseline P loadings typically requires investment in P-reducing alleles. I also believe this to be the reason for not being able to find individuals which replicate nutrient reductions for the solution to problem (c). As the discussion below shows, many P-reducing alleles also reduce nitrates (and are not costless). Thus, it is difficult to find empirical counterparts to solutions involving P reductions but not involving any nitrate reductions relative to the baseline.

Table 11. Allele distribution for individuals matched to the solution to problem (a)

	Boyer	Des Moines	Floyd	Iowa	Little Sioux	Maquoketa	Monona	Nishnabotna	Nodaway	Skunk	Turkey	Upper Iowa	Wapsipinicon
Ind. #	**2166**	**2049**	**280**	**1733**	**14**	**732**	**1899**	**2470**	**619**	**14**	**113**	**14**	**1144**
NO_3/P, % of baseline	97/91	74/105	45/109	74/110	54/58	44/70	49/99	68/100	80/103	70/87	67/97	71/94	58/98
Land retirement	0	0	0	2	0	1	0	0	0	0	1	0	1
CT	2	147	283	0	0	1,967	715	2	0	0	0	0	172
CT RF	0	3,395	1,431	6,583	0	377	84	1	0	0	0	0	377
NT	0	19	0	16	0	0	8	0	25	0	0	0	3
NT RF	0	86	0	11	0	0	9	2	0	0	0	0	1
CT Terraced	0	130	0	0	0	3	0	6	0	0	240	0	2
CT Terraced RF	633	16	0	0	0	1	4	745	0	0	1	0	0
NT Terraced	0	34	0	0	0	2	2	3	0	0	0	0	1
NT Terraced RF	0	13	0	0	0	0	0	0	0	0	1	0	2
CT Contour	2	26	0	10	0	0	0	1	0	0	0	0	1
CT Contour RF	0	82	0	0	0	2	0	1	0	0	0	0	3
NT Contour	0	8	1	18	0	3	9	0	0	0	0	0	2
NT Contour RF	0	0	0	13	0	2	0	10	0	0	3	0	3
CT GW	0	10,213	288	7	6,848	7	877	4,650	1,052	6,648	1	1,289	1,205
CT RF GW	1,299	11,199	2	17,340	0	284	164	0	0	0	2,165	0	2,781
NT GW	0	17	0	5	0	2	4	6	0	0	1	0	6
NT RF GW	0	4	0	2	0	2	4	2	1	0	1	0	0

Table 12. Allele distribution for individuals matched to the solution to problem (b)

	Boyer	Des Moines	Floyd	Iowa	Little Sioux	Maquoketa	Monona	Nishnabotna	Nodaway	Skunk	Turkey	Upper Iowa	Wapsipinicon
Ind. #	**2848**	**848**	**712**	**2903**	**14**	**732**	**14**	**1355**	**1270**	**962**	**370**	**3402**	**2043**
NO_3/P, % of baseline	98/66	69/67	44/69	72/70	54/58	44/70	48/69	61/70	76/68	75/68	70/68	77/69	60/66
Land retirement	4	2,162	0	20	0	1	0	16	0	5	1	0	4
CT	2	0	274	0	0	1,967	0	0	0	20	0	0	1
CT RF	0	14	519	18	0	377	0	0	0	4	17	4	0
NT	1	0	0	8	0	0	0	1	356	0	2	1	816
NT RF	0	20	0	30	0	0	0	1	36	8	0	3	2
CT Terraced	784	0	2	49	0	3	0	2,433	15	113	0	0	0
CT Terraced RF	322	0	0	384	0	1	0	110	135	11	0	0	864
NT Terraced	0	0	2	17	0	2	0	0	0	4	0	1	2
NT Terraced RF	2	20	0	47	0	0	0	8	1	0	2	9	3
CT Contour	2	6	0	21	0	0	0	11	0	7	0	2	2
CT Contour RF	5	55	1	2	0	2	0	5	7	4	1	0	3
NT Contour	5	15	1	10	0	3	0	3	0	2	0	0	8
NT Contour RF	2	0	0	0	0	2	0	1	1	0	5	7	1
CT GW	8	23,058	941	7,785	6,848	7	1,882	2,826	339	4,775	0	719	3
CT RF GW	796	0	253	12,131	0	284	0	6	182	8	771	48	2,847
NT GW	3	17	1	13	0	2	0	0	2	1,677	4	228	1
NT RF GW	1	23	9	3,472	0	2	0	12	3	12	1,611	265	2

Table 13. Allele distribution for individuals matched to the solution to problem (d)

Ind. #	1743	2049	1844	2137	2139	732	2217	100	2324	707	370	5059	1144
NO_3/P, % of baseline	68/26	74/105	47/39	70/88	54/52	44/70	46/59	67/38	68/53	69/64	70/68	64/63	58/98
Land retirement	447	0	0	139	0	1	0	1	1	1	1	7	1
CT	0	147	4	50	1	1,967	4	0	0	2	0	3	172
CT RF	0	3,395	0	3,650	0	377	191	5	0	0	17	3	377
NT	2	19	0	109	0	0	2	1,499	3	1	2	6	3
NT RF	0	86	11	6	0	0	0	0	1	2	0	0	1
CT Terraced	144	130	591	40	0	3	155	2,647	260	18	0	21	2
CT Terraced RF	1,305	16	3	36	498	1	30	1	62	2	0	276	0
NT Terraced	0	34	1	16	0	2	0	2	1	3	0	1	1
NT Terraced RF	26	13	0	26	1	0	0	2	0	3	2	0	2
CT Contour	0	26	3	0	0	0	0	1	1	4	0	1	1
CT Contour RF	4	82	0	0	1	2	0	2	2	24	1	4	3
NT Contour	1	8	0	10	0	3	0	7	1	2	0	0	2
NT Contour RF	0	0	0	72	16	2	8	0	1	2	5	0	3
CT GW	0	10,213	888	3,490	6,321	7	1,230	1	303	733	0	0	1,205
CT RF GW	2	11,199	491	16,337	0	284	250	13	9	3,902	771	812	2,781
NT GW	3	17	7	25	4	2	3	1,244	297	1,946	4	1	6
NT RF GW	2	4	3	2	4	2	8	5	136	2	1,611	152	0

Boyer
Des Moines
Floyd
Iowa
Little Sioux
Maquoketa
Monona
Nishnabotna
Nodaway
Skunk
Turkey
Upper Iowa
Wapsipinicon

4.5.4.1. Effect of Conservation Practices on Nutrient Loadings

As discussed above, for each watershed, the initial population contained 17 individuals which were formed by uniformly applying each of the allele values to all of the cropland HRUs in the watershed. Such seeding can be viewed as utilizing "domain-specific" knowledge, and, as such, is recommended by the practitioners of evolutionary algorithms (Deb, 2001; Reeves and Rowe, 2003). By analyzing the way nitrate and phosphorus loadings in the Iowa watersheds respond to each combination of conservation practices encoded by the allele set one can understand which alleles may be effective at controlling these pollutants. Some practices may be effective across all watersheds, while others may only work for some watersheds. Some understanding of general patterns and also of peculiarities of particular watersheds will also help in explaining why a particular solution was chosen for a specific level of nutrient control.

Tables (in Appendix C) present first 17 individuals in the initial population for all the 13 watersheds. Table 14 below summarizes the effectiveness of each allele in reducing phosphorus and nitrates both in relation to baseline loadings and loadings which would result from a uniform application of allele #2 (corn-soybean rotation, conventional tillage) on all cropland.

Several very interesting patterns emerge. First, I present the patterns observed which relate to conservation practices' estimated effectiveness at reducing phosphorus, and then I present the patterns which relate to nitrate control.

Regarding phosphorus loading reductions, "pure" alleles representing no-till or terraces (alleles #4-5 and #6-7, respectively) perform as expected by reducing phosphorus loadings relative to baseline. Contour farming and grassed waterways interacted with

conventional tillage (alleles #10-11 and #14-15) are not always successful in reducing phosphorus loadings relative to baseline. Uniform application of contour farming actually results in an increase in phosphorus loadings relative to baseline in 8 out of 13 watersheds, and uniform application of grassed waterways with conventional tillage increases P loadings

Table 14. Summary statistics of effectiveness of alleles in nutrient reductions

		P reductions				Nitrate reductions			
		% relative to baseline		% relative to allele #2 (CT)		% relative to baseline		% relative to allele #2 (CT)	
Allele #	Allele Description	Mean	Std. Dev.	Mean	Std. Dev.	Mean	Std. Dev.	Mean	Std. Dev.
1	Land retirement	83	5	91	3	92	3	90	2
2	CT	-79	31	0	0	15	20	0	0
3	CT RF	-65	37	7	18	24	21	11	10
4	NT	24	47	58	18	11	8	-11	30
5	NT RF	37	9	64	6	24	5	5	24
6	CT Terraced	79	6	88	3	35	10	20	18
7	CT Terraced RF	79	6	88	3	48	9	36	14
8	NT Terraced	86	4	92	2	9	8	-15	35
9	NT Terraced RF	87	4	93	2	25	7	5	29
10	CT Contour	0	23	44	6	22	14	6	9
11	CT Contour RF	1	23	45	6	35	14	22	5
12	NT Contour	61	8	78	4	4	7	-20	34
13	NT Contour RF	62	7	79	4	21	6	1	28
14	CT GW	16	19	53	7	33	12	19	9
15	CT RF GW	17	19	54	7	44	12	33	6
16	NT GW	64	7	80	4	14	6	-7	30
17	NT RF GW	65	6	80	4	29	5	11	25

relative to baseline in 4 watersheds. However, in all of the watersheds, contour farming and grassed waterways (with conventional tillage) reduce P loadings relative to allele #2, where all cropland is managed using solely conventional tillage.

Further, interaction of no-till with grassed waterways, and contouring leads to observed “super-additivity” in the effectiveness of such combinations. That is, estimated P

loading reduction which results from a combination of no-till and a an in-field practice is often greater than the sum of the estimated P reductions resulting from uniform application of no-till and reductions resulting from uniform application of an in-field practice. For example, in the Skunk River Watershed, relative to baseline, allele #4 (all no-till) results in a 44 percent P reduction, and allele #14 (all grassed waterways 'on top of' conventional tillage) results in a 13 percent P reduction, while allele #16 (grassed waterways interacted with no-till) results in a 69 percent P reduction. This phenomenon is observed for interactions of no-till and grassed waterways and no-till and contouring in all watersheds, except Floyd and Little Sioux.

A related phenomenon is observed in analyzing nitrate reductions resulting from tillage and conservation practice combinations. Prior to discussing the effect of interactions, the effect of "pure" practices should be presented. Nitrogen fertilizer reductions (allele #3, 20 percent fertilizer reduction) is predicted, on average, to reduce nitrate loadings by 11 percent relative to allele #2 which does not contain any fertilizer reductions. This is consistent with Doering et al. (2001) who found that a 20 percent reduction in nitrogen fertilizer results in an 11 percent (edge-of-field) reduction in nitrogen. Terraces, contouring, and grassed waterways, uniformly applied in combination with conventional tillage all reduce nitrate loadings. No-till, however, increases nitrate loadings relative to conventional tillage in 5 out of 13 watersheds. This can be attributed to the fact that no-till increases infiltration, which, especially in the watersheds utilizing sub-surface tile drainage, can act to increase the export of highly soluble nitrates (P. Gassman, personal communication, August 2007; Dinnes, 2004, p. 51).

This effect of "pure" no-till may be responsible for the observed phenomenon of "sub-additivity" in the interaction of no-till with terraces, grassed waterways, and contouring. Analogous to the effect observed in the interactions of no-till and other practices for P reductions, "sub-additivity" leads to a reduction in nitrate loadings resulting from a combination of no-till and a practice to be smaller than the sum of reductions from a pure no-till and from a conservation practice used in conjunction with conventional tillage. Interacting no-till with grassed waterways (alleles #16-17), terraces (alleles #8-9), and contouring (alleles #12-13) all leads to this phenomenon. In fact, the effect of interacting no-till with contouring is so strong in Floyd, Skunk, and Upper Iowa River Watersheds that, while both no-till and contouring separately result in a decrease in nitrate loadings (relative to baseline), a combination of no-till and contouring actually increases nitrate loadings. The phenomenon of such "sub-additivity" has been observed in relation to the effect of interaction of no-till and contouring on nitrates by, e.g., Gassman, Saleh, Osei, Abraham, and Rodecap (2003), while I have not been able to find descriptions of "super-additivity" in regards to P reductions in the SWAT literature. Of course, one must be cautious in interpreting such model predictions. On the other hand, non-linearities in the effectiveness of conservation practices is definitely something to be expected; moreover, it necessitates the use of hydrologic simulation models, since otherwise, effects of separate practices could just be added up "by hand".

Finally, land retirement, as expected, is very effective in reducing both nitrate and phosphorus loadings, with the average reduction (relative to baseline) of 83 percent in P and 92 percent in nitrates.

Overall, most practices and combinations of practices included in the allele set behave as "conservation" practices – that is, they reduce one or both nutrient loadings. The analysis of the portion of the initial population representing a uniform application of the allele values provides one with a sense of expected direction which the evolutionary algorithm is likely to take.

4.5.4.2. Description of Solutions at the Watershed Level

This section describes the solutions found to best match cost-minimization results for each of the 13 watersheds. Given that the information on how a uniform application of each of the allele values affects the nutrients is available, the makeup of the three different solutions for each of the watersheds can be better understood and explained.

By describing the allele distribution which the evolutionary algorithm selected to achieve a particular level of nutrient reductions for each of the three solutions, and by utilizing watershed-specific information on the effectiveness of particular alleles contained in the initial population, I am able to provide a reasonable explanation for a particular allele distribution. This is yet another advantage of seeding the initial population with each member of the allele set, as opposed to starting the evolutionary algorithm with a population generated completely at random.

Boyer River Watershed. The three individuals selected to match the solutions to problems (a), (b), and (d) are, respectively, #2166, #2848, #1743. As can be seen from the Table 15 above, #1743 is estimated to produce the following nutrient loadings for nitrates/phosphorus, in percent of baseline: 68/26. Similarly, such loadings for #2166 are 97/91, and 98/66 for #2848.

That is, a hypothetical transition from individual #2166 to #2848 involves reducing P without significant changes in nitrate loadings. As can be seen from the distribution of conservation practices, this is achieved by an increased use of alleles containing terraces (alleles #6 and 7). Individual #1743 reduces both nitrates and P, and that is accomplished by extensive use of terraces and land retirement. Given the initial population analysis, such selections are intuitive: alleles containing terraces are quite effective at reducing both nitrates and P, while land retirement is the strongest available option for reducing both nutrient loadings.

Des Moines River Watershed. For this watershed, individual #2049 was selected to match the solutions to problems (a) and (d), and individual #848 was selected to match the solution to problem (b). Nitrate/phosphorus loadings in terms of percentage of baseline are 74/105 for #2049 and 69/67 for #848. While individual #2049 relies primarily on nitrogen fertilizer application reductions alone (allele #3), or in conjunction with grassed waterways (allele #15), individual #848 does not utilize nitrogen fertilizer reductions as part of the solution (although grassed waterways are utilized extensively), and introduced land retirement as an option which can control both nitrates and P.

Floyd River Watershed. The three individuals selected to match the solutions to problems (a), (b), and (d) are, respectively, #280, #712, #1844. Nitrate/phosphorus loadings in terms of percentage of baseline are 45/109, 44/69, and 47/39, respectively. Thus, one can present these individuals basically in terms of successively higher P reductions. While individual #280 uses a small amount of grassed waterways, #712, in order to achieve a 31 percent P reduction, introduces about four times as much grassed waterways-protected area, and, in order to further decrease P, #1844 brings in terraces. Based on the initial population

analysis, it is intuitive as to why the algorithm may do that: while grassed waterways (with conventional tillage) can achieve sizeable P reductions, terraces are capable of reducing P loadings much more effectively, and thus are brought in as a part of the makeup of individual #1844.

Iowa River Watershed. The three individuals selected to match the solutions to problems (a), (b), and (d) are, respectively, #1733, #2903, #2137. Nitrate/phosphorus loadings in terms of percentage of baseline are 74/110, 72/70, and 70/88, respectively. Again, one can look at these solutions in terms of successive P reductions (with minor nitrate changes). Individual #1733 does not reduce P below baseline at all, and all the nitrate reductions are due to nitrogen fertilizer reductions, either alone (allele #3), or with grassed waterways (allele #15). A 12 percent P reduction (individual #2137) is achieved by greater use of grassed waterways, some terraces, and land retirement. In order to reduce P further, by 30 percent, more terraces are needed, as well as grassed waterways combined with no-till. Iowa River Watershed is one of the watersheds where "super-additivity" of no-till and grassed waterways is observed in their combined effect on P reductions, and this effect is exploited.

Little Sioux River Watershed. Two individuals #14, and #2139 are selected to satisfy the requirements for a solution for problems (a)-(b), and (d), respectively. Nitrate/phosphorus loadings in terms of percentage of baseline are 54/58 for #14 and 54/52 for #2139. Interestingly, individual #14 is the member of the initial population, representing uniform application of allele #14 (CT+GW) to all cropland HRUs. While through the iterations of the evolutionary algorithm, many more non-dominated individuals were created, #14 still provided the closest and lowest cost match for nitrate loading reduction required by solutions

to problems (a) and (b). In terms of allele distribution, individual #2139 achieves greater P reductions by utilizing terraces (allele #7).

Maquoketa River Watershed. For this watershed, a single individual #732 was identified as satisfying the requirements for solution for problems (a), (b), and (d). Nitrate/phosphorus loadings as percentage of baseline for this individual are found to be 44/70. Grassed waterways and fertilizer reductions are the primary conservation practices selected for this watershed.

Monona River Watershed. For this watershed, three individuals, approximating cost-minimizing solutions, were found. They (and their loadings descriptions) are: #1899 (49/99), #14 (48/69) for problems (a) and (b), and #2217 (46/59) for problem (d). Again, the successively higher P reductions are achieved by means of higher levels of grassed waterway application, and then by introducing terraces. A uniform application of grassed waterways yields a 31 percent reduction in P, and terraces are needed to achieve further reductions.

Nishnabotna River Watershed. The three individuals selected to match the solutions to problems (a), (b), and (d) are, respectively, #2470, #1355, #100. Nitrate/phosphorus loadings in terms of percentage of baseline are 68/100, 61/70, and 67/38, respectively. Moving from individual #2470 to #1355 involves reducing P loadings by 30 percent and reducing nitrate loadings by additional 7 percentage points. A hypothetical movement to individual #100 involves dramatic reductions in P while somewhat increasing nitrate loadings. Analysis of the uniform application of the alleles in the watershed reveals that grassed waterways are not capable to bring P reductions down even to the level of the baseline. This explains the use of terraces by individual #2470, even though P loadings are exactly at the baseline level. Further P reductions are achieved by utilizing more terraces (in

moving to individual #1355), and by introducing no-till, both as a stand-alone option (allele #4), and in conjunction with grassed waterways (allele #16).

Nodaway River Watershed. Three distinct individuals matching the cost-minimization solutions were found for this watershed. They (and their loadings descriptions) are: #619 (80/103), #1270 (76/68) for problems (a) and (b), and #2324 (68/53) for problem (d). Once again, higher P reductions are achieved by means of increased utilization of terraces and no-till. For individual #2324, no-till is interacted with grassed waterways (given the observed "super-additivity" effect, this is not surprising).

Skunk River Watershed. The three individuals selected to match the solutions to problems (a), (b), and (d) are, respectively, #14, #962, #707. Nitrate/phosphorus loadings in terms of percentage of baseline are 70/87, 75/68, and 69/64, respectively. Individual #14 is a member of the initial population, and represents uniform application of grassed waterways (with conventional tillage) on the cropland. No-till, interacted with grassed waterways provides for higher P loading reductions observed for individuals #962 and #707. Again, the "super-additivity" effect appears to be one reason for these alleles being selected.

Turkey River Watershed. Two individuals are found for this watershed: #113 (69/97), approximating the solution to (a), and #370 (70/68), approximating the solutions to (b) and (d). Both grassed waterways and terraces are part of the makeup of individual #113, owing to relative ineffectiveness of grassed waterways in reducing P in this watershed. Larger P reductions (with a minor increase in nitrate loadings) are achieved by means of allele #17 (NT+GW+RF). Again, the "super-additivity" phenomenon discussed above appears to be playing a role in this selection.

Upper Iowa River Watershed. For this watershed, the three individuals, approximating cost-minimizing solutions to (a), (b), and (d) (and their loadings descriptions) are: #14 (71/94), #3402 (77/69), and #5059 (64/63). As was the case with Little Sioux and Skunk River Watersheds, one of the individuals found is #14, which consists of uniform application of grassed waterways on the cropland. Once again, terraces and no-till (in combination with grassed waterways) are the preferred means of successive P reductions.

Wapsipinicon River Watershed. Two individuals #1144, and #2043 are selected to satisfy the requirements for a solution for problems (a)-(d), and (b), respectively. Nitrate/phosphorus loadings in terms of percentage of baseline are 58/98 for #1144 and 60/66 for #2043. Significant nitrate reductions are allocated to this watershed by the cost-minimization programs. As a result, extensive use of nitrogen fertilizer reductions, alone or in combination with grassed waterways, is part of the makeup of individual #1144. Individual #2043 interacts nitrogen fertilizer reductions with terraces, which maintains most of the nitrate reductions, and further reduces P.

4.5.5. Subbasin-level Distributions of Conservation Practices

Figures below present subbasin-level distributions of the alleles for the 13 watersheds. Given the data limitations, the level of subbasins is the finest spatial resolution for placement of conservation practices on the landscape. However, even at this level of detail, the maps contain a great deal of useful information for policymakers and water quality researchers.

Looking at the solutions to problems (a), (b), and (d) in this sequence, it becomes clear that moving from solution (a) to solution (b) involves reducing P loadings in all

watersheds, and moving from solution (b) to solution (d) involves further reducing P loadings except for 2 watersheds (Des Moines and Wapsipinicon River Watersheds). This is due to solution (d) allowing unequal P abatement across the watersheds, and partially accounts for lower cost of solution (d) relative to the cost of solution (b). Aside from these two watersheds, looking at the 3 solutions in sequence is quite similar to observing the consequences of tightening watershed-level P reduction goals.

The distribution of alleles for the three solutions indicates that, for this range of nutrient reductions, *grassed waterways* is chosen most frequently, while nitrogen fertilizer reductions are chosen frequently as well, either as a stand-alone option (with conventional tillage), or in conjunction with grassed waterways. Successively higher P reductions necessitate the use of terraces and no-till (alone or with grassed waterways). Also, as described above in the description of solutions for each of the watersheds, "super-additive" properties of combining no-till with grassed waterways appear to be utilized in some watersheds for solutions involving large P reductions. Additional land retirement is also needed in some watersheds. Finally, alleles including contour farming are not chosen, despite the fact that contour farming is a relatively inexpensive practice.

Furthermore, as can be seen from Figures 9-11, these alleles are spatially concentrated on the subbasin level. That is, for many watersheds, alleles are chosen in a way that allocates an overwhelming majority of land in any given subbasin to a single allele. Des Moines River Watershed is a dramatic example of such spatial concentration: virtually all of land retirement prescribed by the algorithm (for solution (b)) is allocated to the outlet subbasin.

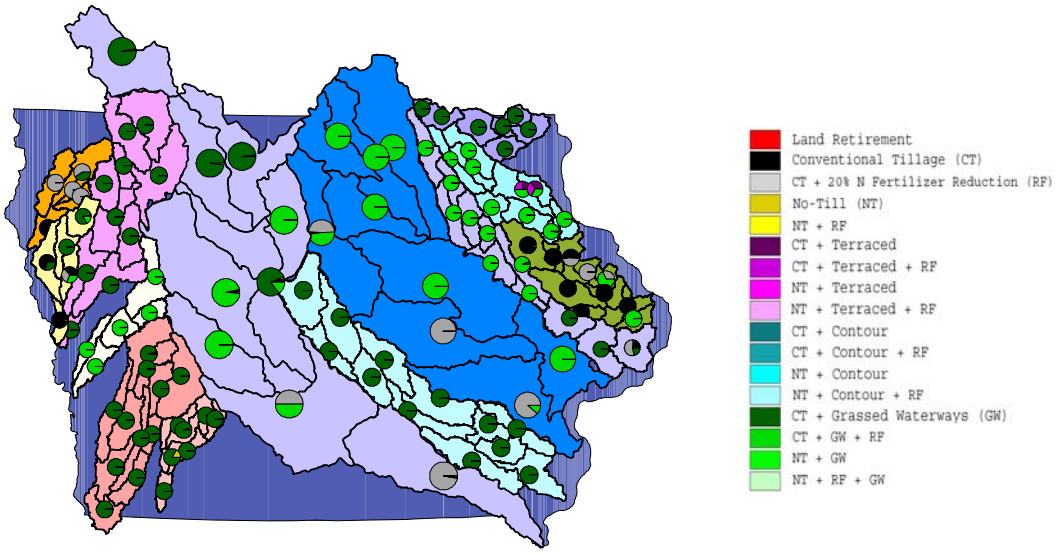

Figure 9. Subbasin distribution of conservation practices for the solution to problem (a): 30 percent state-level reduction in NO_3, holding each watershed's P loadings at or below baseline values

Figures 9 and 10 present subbasin-level distributions of conservation practices for the solutions to problems (a) and (b). Both of these solutions require a 30 percent reduction in total statewide export of nitrates, with problem (a) requiring only that individual watersheds not experience any increases in P loadings as a result, and problem (b) tightening local P constraint and requiring at least a 30 percent reduction in P loadings for every watershed.

Watershed-level analysis of the alleles chosen for these solutions already highlighted the fact that more P-reducing alleles become a part of the solution as one moves from problem (a) to problem (b). This fact is also evident in the subbasin-level maps of allele distributions for the two solutions. In particular, increased use of no-till (combined with grassed waterways) in Nodaway, Iowa and Turkey River Watersheds, as well as more terraces prescribed for Nishnabotna, Boyer, and Nodaway River Watersheds is readily seen

by comparing the two maps. Again, the algorithm's prescriptions imply a fairly homogeneous use of conservation practices at the subbasin level. This alleviates the problem

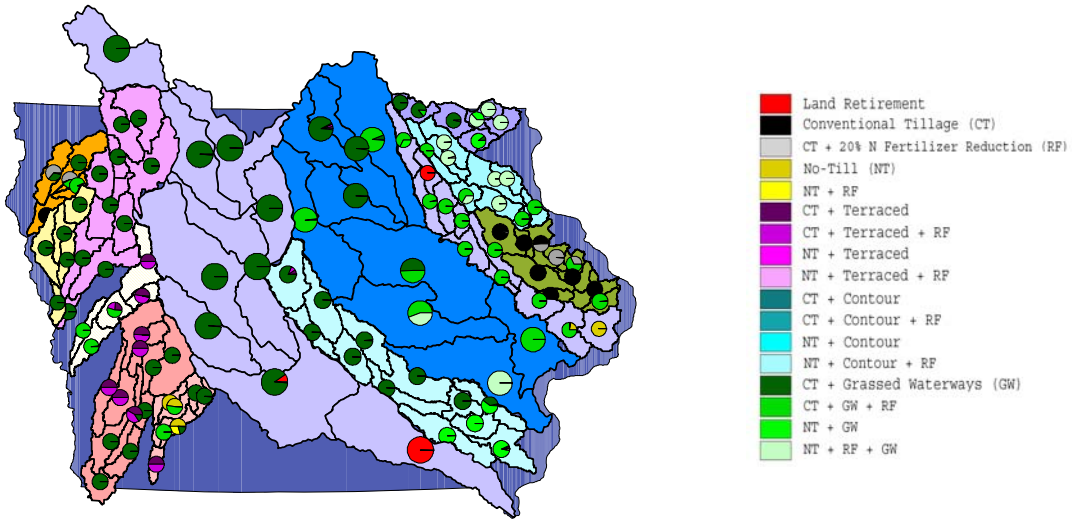

Figure 10. Subbasin distribution of conservation practices for the solution to problem (b): 30 percent state-level reduction in NO_3, while reducing each watershed's P loadings by 30 percent

with the lack of spatial resolution in the data used for the analysis. Still, an analysis based on fully spatially-explicit HRUs would clearly be required to make better policy recommendations.

The last map (Figure 11) presents empirical approximations to the solution of cost-minimization problem (d), where total statewide P loadings are reduced by 30 percent and each of the 13 watersheds also experiences a 30 percent reduction in nitrate loadings. Application of grassed waterways, either in conjunction with conventional tillage (e.g. Des Moines Watershed, Iowa Watershed, Wapsipinicon Watershed) or no-till (e.g., Skunk, Turkey, Nishnabotna River Watersheds) is clearly the most common conservation practice

prescribed for the subbasins in the watersheds. For the solution which achieves reductions in statewide export of P, the greatest reductions are allocated to Boyer, Floyd, Nishnabotna River Watersheds. This can be easily seen on the map, as these watersheds differ from the rest in their extensive use of terraces (Floyd, Nishnabotna River Watersheds), or land retirement (Boyer River Watershed). Again, the spatial concentration of conservation practices is evident in this solution.

The fact that the current analysis is conducted as if starting with a clean slate in terms of ignoring structural conservation practices which were recorded in the available baseline land use data allows one to compare the historical placement of conservation practices and the placement prescribed by the algorithm.

Of course, direct comparisons are difficult here. For example, even if I find that the conservation practices prescribed as being part of a solution to, e.g., problem (a), do not at all match the pattern of conservation practices recorded in the earlier land use data,

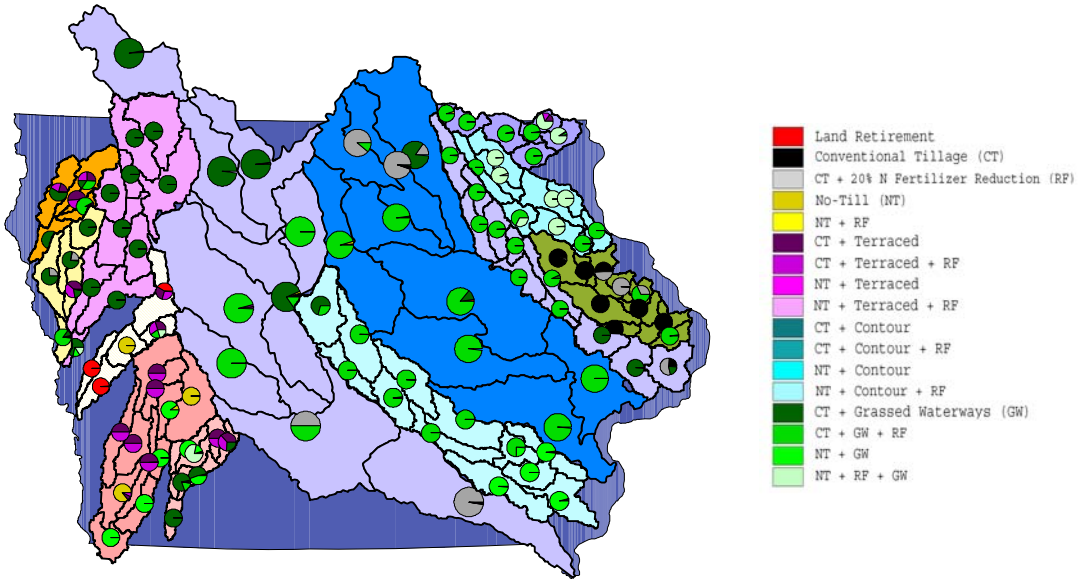

Figure 11. Subbasin distribution of conservation practices for the solution to problem (d): 30 percent state-level reduction in P, while reducing each watershed's NO3 loadings by 30 percent

it does not necessarily mean that baseline conservation practices are inefficient, as the policy context would definitely not match the set-up of problem (a) (minimization of statewide nitrate export subject to "local" P constraint). In fact, it is not clear what (if any) objective function governed the placement of the observed set of conservation practices. One can almost surely state that no watershed-level (or a state-level) objective governed some coordinated effort for the placement of existing conservation practices.

Given these caveats, it is still interesting to make (at least qualitative) comparisons between the observed baseline and the set of conservation practices identified for the present analysis. Secchi et al. (2007) observe that existing terraces in Iowa are located mainly in western part of the state. Interestingly, whenever terraces were selected by the algorithm, they were selected for western Iowa watersheds: Boyer, Floyd, Nishnabotna. That is perhaps the most dramatic similarity. This may also be explained by the soil and geomorphologic characteristics of these watersheds. Boyer and Nishnabotna River Watersheds are located in the Loess Hills region of the state, and Floyd River Watershed is located in the Northwestern Iowa Plains region, both of which are susceptible to soil erosion (Dinnes, 2004, pp. 11-12). Selection of terraces is then reasonable, both in the baseline, and as part of the solution discovered by the algorithm.[37] Another one is that, given the existing distribution of land retirement (presented in Figure 3 of Secchi et al. (2007)), the algorithm allocates land retirement in the Des Moines Watershed to the same subbasin (#9), which is already observed to have the highest amount of CRP land in the state. The results for the distribution of no-till are mixed: baseline conservation tillage is "estimated to be more widespread in the central part of the state" (Secchi et al., 2007). This is consistent with some subbasins of the Skunk Watershed which lie in the central part of the state being allocated to no-till by the

[37] A similar explanation may apply for selection of no-till in the Nishnabotna River Watershed.

algorithm. However, the rest of Central Iowa is not selected for implementation of no-till in the solutions analyzed. Also, while existing grassed waterways are observed to be in south-eastern part of the state, the algorithm allocates grassed waterways to virtually all of Iowa, and not only (or even to the largest extent) to the south-eastern part. Finally, contour farming was observed to be practices mostly in western (and some eastern) parts of the state. The evolutionary algorithm, however, virtually ignored all the alleles involving contouring (#10-13).

4.6. Conclusions and Policy Implications

Application of evolutionary algorithm-based optimization to the problem of finding Pareto-efficient allocations of conservation practices is a flexible and powerful tool for addressing issues in watershed-scale nonpoint-source pollution reduction policy. This approach generates a wealth of information which is of great interest to policymakers, research community, and stakeholders. It is capable of generating watershed-scale Pareto-efficient frontiers which incorporate multiple conflicting environmental and cost objectives. Points on the frontiers can be further analyzed to provide a guide to the mix of conservation practices which the model predicts will generate given water quality improvements. Watershed-level frontiers can be combined within political boundaries to provide guidance to cost-minimizing loading reduction allocations within the political jurisdiction, with the ability to handle local water quality constraints.

I illustrate this by analyzing the frontiers for the 13 watersheds which make up most of the state of Iowa. Several scenarios involving state-level and watershed-level nutrient reduction goals, were analyzed. Cost of achieving these goals varied from $210 to $286

million per year. For the range of nutrient reductions considered, grassed waterways (often interacted with no-till or nitrogen fertilizer reductions), was the most commonly selected type of conservation practice. Terraces and land retirement were also selected, but to a smaller extent.

These kinds of results are definitely linked to the quality of the hydrologic model, its ability to represent conservation practices, as well as the quality of the input (physical and economic) data. Improvements in the hydrologic model and the economic cost estimates can readily be incorporated into the simulation-optimization system. Additional caveats include the possibility that the set of conservation practices misses an important and effective method of reducing nutrient loadings. Wetlands provide one such example. Again, the approach is flexible enough to be able to incorporate additional options through the modifications of the allele set.

With such caveats in mind, the results which specify a particular mix and distribution of conservation practices can provide policymakers with tools for better targeting of conservation policy aimed at water quality improvements. Of course, the specific set of practices targeted will depend on particular (state-level or watershed-level) nonpoint source pollution reduction goals. In particular, it seems that these kinds of simulation-optimization methods ought to be a part of the TMDL process. Armed with the algorithm's prescriptions, policymakers can offer targeted payments (method suggested by Khanna et al. (2003)), or elicit bids and accept or reject them using modeling results as guidance.

On the research side, application of evolutionary algorithms and similar methods to better handle the complexities associated with water quality is likely to grow in scope, accuracy, and realism, reflecting continuing improvements in computational power and

environmental modeling capability. However, unless the current political landscape does not change to make targeting possible in order to improve local and downstream water quality, results presented in this study will likely provide only a lower bound on the costs of water quality improvements.

4.7. References

American Society of Agricultural and Biological Engineers. 2003. Design, layout, construction, and maintenance of terrace systems. *ASAE Standard S268,* St. Joseph, Michigan.

Ammerman, J.W. and Sylvan, J.B. 2004. Phosphorus Limitation of Phytoplankton Growth in the Mississippi River Plume: A Case for Dual Nutrient Control? *Eos Transactions, American Geophysical Union, 85*(47), Fall Meetings Supplement, Abstract OS11B-07.

Arabi, M., R. S. Govindaraju, and M. M. Hantush. 2006. Cost-effective allocation of watershed management practices using a genetic algorithm. *Water Resources Research* (42), W10429.

Arnold, J.G., and Fohrer, N. 2005. Current capabilities and research opportunities in applied watershed modeling. *Hydrological Processes* 19: 563-572.

Arnold, J.G., R. Srinivasan, R.S. Muttiah, and J.R. Williams. 1998. Large area hydrologic modeling and assessment part I: Model development. *Journal of American Water Resources Association* 34(1): 73-89.

Bekele, E.G., and J.W. Nicklow. 2005. Multiobjective management of ecosystem services by integrative watershed modeling and evolutionary algorithms. *Water Resources Research, 41,* W10406, doi:10.1029/2005WR004090.

Bouzaher, A., J.B. Braden, and G.V. Johnson. 1990. A dynamic programming approach to a class of nonpoint source pollution problems. *Management Science* 36: 1-15.

Bouzaher, A., J.B. Braden, G.V. Johnson, and S.E. Murley. 1994. An efficient algorithm for non-point source pollution management problems. *The Journal of the Operational Research Society* 45(1): 39-46.

Braden, J.B., G.V. Johnson, A. Bouzaher, and D. Miltz. 1989. Optimal spatial management of agricultural pollution. *American Journal of Agricultural Economics* 61: 404–13.

Campbell, T. 2006. i_SWAT. Ames, Iowa: Center for Agricultural and Rural Development, Iowa State University. Available at: http://www.public.iastate.edu/~elvis/i_swat_main.html. Accessed May 6, 2006.

Carpentier, C.L., D.J. Bosch, and S.S. Batie. 1998. Using spatial information to reduce costs of controlling agricultural nonpoint source pollution. *American Journal of Agricultural Economics* 61: 404-413.

Corn N-rate calculator. Iowa State University Agronomy Extension. Available at http://extension.agron.iastate.edu/soilfertility/nrate.aspx. Accessed March 13, 2007.

Deb, K, A. Pratap, S. Agarwal, and T. Meyarivan. 2000. A fast and elitist multi-objective genetic algorithm-NSGA-II. KanGAL Report Number 2000001. Available at: http://www.iitk.ac.in/kangal/reports.shtml. Accessed February 10, 2006.

Deb, K. 2001. Multi-objective Optimization Using Evolutionary Algorithms, John Wiley, Hoboken, NJ.

Dinnes, D.L. 2004. Assessments of practices to reduce nitrogen and phosphorus nonpoint source pollution of Iowa's surface waters. USDA-ARS National Soil Tilth Laboratory, Ames, Iowa.

Doering, O.C., M. Ribaudo, F. Diaz-Hermelo, R. Heimlich, F. Hitzhusen, C. Howard, R.F.Kazmierczak, Jr., J. Lee, L. Libby, W. Milon, M. Peters and A. Prato. 2001. Economic Analysis as a Basis for Large-Scale Nitrogen Control Decisions: Reducing Nitrogen Loads to the Gulf of Mexico." *The Scientific World* 1(S2): 968-975.

Edwards, W., and D. Smith. 2007. Cash rental rates for Iowa 2007 survey. Iowa State University Extension, *Ag Decision Maker,* File C2-10.

Gassman, P.W., M. Reyes, C.H. Green, and J.G. Arnold. 2007. The Soil and Water Assessment Tool: Historical development, applications, and future directions. *Transactions of ASABE*. (forthcoming).

Gassman, P.W., S. Secchi, M. Jha, and L. Kurkalova. 2006. Upper Mississippi river basin modeling system part 1: SWAT input data requirements and issues. In: Coastal Hydrology and Processes (ed. V.P. Singh and V.J. Xu). Water Resources Publications, Highlands Ranch, Colorado, pp. 103-116.

Gassman, P.W., Campbell, T., Secchi, S., Jha, M., and Arnold, J.G., 2003. The i_SWAT software package: a tool for supporting SWAT watershed applications. In: SWAT2003: The 2nd International SWAT Conference, 1-4 July, Bari, Italy. Instituto di Ricerca sulle Acque, IRSACNR,Bari, Italy. pp. 66-69.

Gassman, P.W., A. Saleh, E. Osei, J. Abraham, and J. Rodecap. 2003. Environmental and economic impacts of alternative management scenarios for the Mineral Creek Watershed. Proceedings of the Total maximum Daily Load (TMDL) Environmental

Regulations II, 8-12 November, Albuquerque, New Mexico. American Society of Agricultural Engineers, St. Joseph, Michigan. pp. 323-331.

Hu, X., McIssac, G.F., David, M.B., and Louwers, C.A.L., 2007, Modeling riverine nitrate export from an east-central Illinois watershed using SWAT: Journal of Environmental Quality, v. 36, p. 996-1005.

Iowa Department of Natural Resources. Nitrate Nitrogen: Iowa's Unintended Export. Available at: http://www.igsb.uiowa.edu/inforsch/nitraten/nitraten.htm. Accessed July 5, 2007.

Jha M., Arnold J.G., Gassman P.W. 2006. Water Quality Modeling for the Raccoon River Watershed Using SWAT. CARD Working Paper 06-WP 428, Iowa State University, Ames, Iowa.

Jha, M., P.W. Gassman, S. Secchi, R. Gu, and J. Arnold. 2004. Impact of watershed subdivision level on flows, sediment loads, and nutrient losses predicted by SWAT. *Journal of American Water Resources Association* 40(3): 811-825.

Khanna, M.,W. Yang, R. Farnsworth, and H. Onal. 2003. Cost effective targeting of CREP to improve water quality with endogenous sediment deposition coefficients. *American Journal of Agricultural Economics* 85: 538–53.

Kling, C.L., S. Rabotyagov, M. Jha, H. Feng, J. Parcel, P. Gassman, and T. Campbell. 2007. Conservation practices in Iowa: historical investments, water quality and gaps. Draft report. Center for Agricultural and Rural Development, Iowa State University, Ames, Iowa.

Kling, C., S. Secchi, M. Jha, L. Kurkalova, H.F. Hennessy, and P.W. Gassman. 2005. Nonpoint source needs assessment for Iowa: The cost of improving Iowa's water quality. Final Report to the Iowa Department of Natural Resources. Center for Agricultural and Rural Development, Iowa State University, Ames, Iowa.

Kramer, R.A., W.T. McSweeny, W.R. Kerns, and R.W. Stravros. 1984. An evaluation of alternative policies for controlling agricultural nonpoint source pollution. *Water Resources Bulletin* 20: 841–46.

Lant, C.L., S.E. Kraft, J. Beaulieu, D. Bennett, T. Loftus, and J. Nicklow. 2005. Using GIS-based ecological–economic modeling to evaluate policies affecting agricultural watersheds. *Ecological Economics* 55: 467– 484.

Libra, R.D., C.F. Wolter, and R.J. Langel. 2004. Nitrogen and phosphorus budgets for Iowa and Iowa watersheds. Iowa Geological Survey, Technical Information Series 47.

Libra, R.D., K.E. Schilling, and C.F. Wolter. 1999. The relationship of nitrate-N concentrations and loads to row-crop land use in Iowa, 1996-1998. Iowa Geological Survey. 44th Annual Midwest Groundwater Conference, St. Paul, MN.

Lohrenz, S.E., Fahnenstiel, G.L., Redalje, D.G., and Lang, G.A., 1992, Regulation and distribution of primary production in the northern Gulf of Mexico: In Program, N.C.O., Nutrient Enhanced Coastal Ocean Productivity, NECOP Workshop Proceedings, October 1991, Texas Sea Grant Publications, College Station, TX, p.95-104.

Lohrenz, S.E., Fahnenstiel, G.L., Redalje, D.G., Lang, G.A., Chen, X.G., and Dagg, M.J.,1997, Variations in primary production of northern Gulf of Mexico continental shelf waters linked to nutrient inputs from the Mississippi River: Marine Ecology-Progress Series, v. 155, p. 45-54.

Lohrenz, S.E., Fahnenstiel, G.L., Redalje, D.G., Lang, G.A., Dagg, M.J., Whitledge, T.E., and Dortch, Q., 1999b, Nutrients, irradiance, and mixing as factors regulating primary production in coastal waters impacted by the Mississippi River plume: Continental Shelf Research, v. 19, p. 1113-1141.

Lohrenz, S.E., Wiesenburg, D.A., Arnone, R.A., and Chen, X.G., 1999a, What controls primary production in the Gulf of Mexico?: In Sherman, K., et al., (eds.), The Gulf of Mexico Large Marine Ecosystem: Assessment, Sustainability and Management, Blackwell Science, Inc., Malden, MA, p. 151-170.

Mitchell, M. 1996. An introduction to genetic algorithms. Cambridge, Massachusetts: the MIT Press.

Montgomery, W.D. Markets in licenses and efficient pollution control programs. *Journal of Economic Theory* 1972; 5; 395-418.

Muleta, M.K. and Nicklow, J.W. 2005. Decision support for watershed management using evolutionary algorithms. *Journal of Water Resources Planning and Management* 131(1): 35-44.

Muleta, M.K. and Nicklow, J.W. 2002. Evolutionary algorithms for multiobjective evaluation of watershed management decisions. *Journal of Hydroinformatics* 4(2): 83-97.

Neitsch, S.L., J.G. Arnold, J.R. Kiniry, R. Srinivasan, and J.R. Williams. 2005a. *Soil and Water Assessment Tool Theoretical Documentation*, version 2005. Temple, TX: Grassland, Soil and Water Research Laboratory, Agricultural Research Service.

Nusser, S. M., and J.J. Goebel. 1997. The national resources inventory: a long-term multisource monitoring programme. *Environmental and Ecological Statistics*. 4: 181-204.

Reeves, C.R., and J.E. Rowe. 2003. Genetic algorithms—principles and perspectives: a guide to GA theory. Kluwer Academic Publishers

Ribaudo, M.O. 1986. Consideration of off-site impacts in targeting soil conservation programs. *Land Economics* 62: 402–11.

Ribaudo, M.O. 1989. Targeting the conservation reserve program to maximize water quality benefits. *Land Economics* 65: 320–32.

Richards, R.P. and Baker, D.B. 2002. Trends in water quality in LEASEQ rivers and streams (northwestern Ohio), 197501995: Journal of Environmental Quality, v. 31, p. 90-96.

Rudolph, G., and A. Agapie. 2000. Convergence properties of some multi-objective evolutionary algorithms. In *Proceedings of the Congress on Evolutionary Computation (CEC-2000)*, p. 1010-1016.

Sawyer, J., E. Nafziger, G. Randall, L. Bundy, G. Rehm, B. Joern. 2006. Concepts and rational for regional nitrogen rate guidelines for corn. Iowa State University, Ames, Iowa. Available at: http://extension.agron.iastate.edu/soilfertility/nrate.aspx. Accessed April 10, 2006.

Seaber, P.R., F.P. Kapinos, and G.L. Knapp. 1987. Hydrologic Units Maps. U.S. Geological Survey, Water-Supply Paper 2294.

Secchi, S., P.W. Gassman, M. Jha, H.H. Feng, T. Campbell, and C.L. Kling. 2007. The cost of cleaner water: Assessing agricultural pollution reduction at the watershed scale. *Journal of Soil and Water Conservation.* 62(1): 10-21.

Secchi, S., M. Jha, L. A. Kurkalova, H. Feng, P.W. Gassman, C.L. Kling. 2005. The designation of co-benefits and its implication for policy: water quality versus carbon sequestration in agricultural soils. CARD Working Paper 05-WP 389, Iowa State University, Ames, Iowa.

Sheriff, G. 2005. Efficient waste? Why farmers over-apply nutrients and the implications for policy design. *Review of Agricultural Economics* 27(4): 542-557.

Srivastava, P., J.M. Hamlett, P.D. Robillard, and R.L. Day. 2002. Watershed optimization of best management practices using AnnAGNPS and a genetic algorithm. *Water Resources Research* 38(3): 1-14.

Sylvan, J.B., Dortch, Q., Nelson, D.M., Maier Brown, A.F., Morrison, W., and Ammerman, J.W. 2006. Phosphorus limits phytoplankton growth on the Louisiana shelf during the period of hypoxia formation. *Environmental Science and Technology*, 40 (24), 7548 - 7553.

Vache, K.B., Eilers, J.M., and Santelman, M.V. 2002. Water quality modeling of alternative agricultural scenarios in the U.S. corn belt. *Journal of the American Water Resources Association*, 38(2): 773-787

Veith, T.L., M.L. Wolfe, and C.D. Heatwole. 2003. Development of optimization procedure for cost-effective BMP placement. *Journal of the American Water Resources Association* 39(6): 1331-1343

Veith, T.L., M.L. Wolfe, and C.D. Heatwole. 2004. Cost-effective BMP placement: optimization versus targeting. *Transactions of the ASAE* 47(5): 1585-1594.

Wall, M. 1996. GAlib: A C++ Library of Genetic Algorithm Components. Version 2.4.6. Available at: http://lancet.mit.edu/ga/. Accessed January 20, 2006.

Wischmeier, W. H. and D. D. Smith. 1978. Predicting rainfall erosion losses – A guide to conservation planning. USDA Handbook No. 537. Washington, D.C.

Yadav, S., W. Peterson, and K.W. Easter. 1997. Do farmers overuse nitrogen fertilizer to the detriment of the environment? *Environmental and Resource Economics* 9:323-340.

Zitzler, E., and L. Thiele. 1999. Multiobjective evolutionary algorithm: A comparative case study and the Strength Pareto Approach. *IEEE Transactions on Evolutionary Computation* 3(4): 257-271.

Zitzler E., Laumanns M., Thiele L. 2002. SPEA2: Improving the Strength Pareto Evolutionary Algorithm for Multiobjective Optimization. Evolutionary Methods for Design, Optimisation, and Control, CIMNE, Barcelona, Spain, pp. 95-100.

CHAPTER 5. SEARCHING FOR EFFICIENCY: LEAST COST NONPOINT SOURCE POLLUTION CONTROL WITH MULTIPLE POLLUTANTS, PRACTICES, AND TARGETS

5.1. Introduction

Nonpoint source (NPS) pollution from agriculture remains a major source of water degradation in the U.S. despite the devotion of substantial resources to its control over the past two decades. By definition, NPS pollution comes from many sources whose contributions to water pollution are hard to measure. Numerous economic studies have investigated the efficiency of different policy instruments in this context; Shortle and Horan (2001) provided an excellent survey of the literature.

However, some attributes of NPS pollution that can be critical in the design of policies have received little attention. The first is that there are multiple NPS pollutants which may interact with each other, including nitrogen, phosphorous, sediment, pathogens, and pesticides. Conservation practices that are effective at controlling one pollutant are not necessarily equally good at controlling other pollutants. Another characteristic of NPS pollution control is that multiple conservation practices can be implemented simultaneously in the same field and different fields within a watershed can have distinct practices. Some practices achieve more pollution reduction than others on a given field. Moreover, the effectiveness of a given conservation practice on a given field depends on the conservation practices and cropping systems in place elsewhere in the watershed. In other words, off-site impacts of land use on any given field in a watershed are endogenous to land use choices on other fields of the watershed.

In this chapter, I examine the policy implications of these three attributes of NPS pollution using a spatially explicit model of a large and critically important agricultural region: the Upper Mississippi River Basin in the central U.S. Specifically, I study (1) the tradeoffs between the costs of pollution control and the level of water quality; (2), the tradeoffs between meeting the water quality targets of different pollutants. While the fact that higher control costs are necessary to achieve larger water quality improvements is intuitive, the nature of the second tradeoff is less obvious and will depend on the nature of the pollutants and the physical conditions of a watershed. In this paper, I will quantify these tradeoffs and explore the subsequent policy implications.

To empirically estimate these tradeoffs, a modeling framework that (a) realistically incorporates the key attributes of NPS pollution and (b) is able to approximate the efficient solutions by optimally choosing the set of conservation practices for each field, is developed. Neither (a) nor (b) is an easy task, as manifested by the dearth of economic studies that reflect both features. Instead, economists have in general utilized simplified representations of the biophysical process of water pollution so that optimization could be performed with conventional approaches. For example, early studies used a simplified model with fixed, exogenous pollution delivery coefficients (e.g., Montgomery, 1972; Ribaudo, 1986 and 1989). Given such assumptions, it is straightforward to solve for cost-efficient allocations of pollution abatement using calculus-based constrained optimization techniques.

Development in the past two decades of realistic, physically-based, spatially distributed hydrologic simulation models highlighted the fact that field-level off-site impacts are endogenous and led several economists to incorporate some features of these models into their analyses via one of two approaches: full spatial optimization using a simplified version

of the hydrologic process or incorporation of the hydrologic process but comparing the efficiency of a few select scenarios without explicit optimization.

One example of the first type is Braden et al. (1989), who separated a watershed into hydrologically independent flow paths and use a hydrologic model to estimate the impact of various management alternatives for the flow paths on the resulting sediment yield. As a result, a problem of finding cost-efficient sediment reduction solutions becomes a variant of the knapsack model in operations research. A study by Khanna et al. (2003) provides another good example of the ingenuity demonstrated by researchers to cope with the problem's complexity. The authors capture the interdependencies between upslope and downslope parcels by using coefficients derived from a hydrologic model. They restrict their attention to three parcels up from a stream, and to two alternatives on each parcel: crop production and land retirement.

A drawback to these approaches is that hydrologic models developed for the entire watershed are broken up; hence, one does not get the full benefit of a hydrologic simulation model. By contrast, studies that incorporate the complete hydrologic simulation models typically have not attempted optimization of land use choices. Instead, alternative land use change scenarios that achieve the pollution reduction goals are evaluated (e.g., Secchi et al. (2005)).

Agricultural engineers have recently examined the cost of NPS control with integrated modeling systems that incorporate the full water quality models into optimization routines that are capable of finding the optimal or near optimal solutions to a problem otherwise intractable with conventional optimization methods. Arabi et al. (2006), Srivastava et al. (2002), and Bekele and Nicklow (2005) are outstanding examples. However, these

studies are done at a small scale (smaller than 133 km^2 in Bekele and Nicklow (2005) versus 492,000 km^2 in the region studied here). In addition, none of these studies examined explicitly the tradeoffs between different NPS pollutants and the tradeoffs between meeting targets at different spatial scales both of which are important policy issues in the control of NPS pollution.

In this essay, a modeling framework that closely integrates an optimization methodology with a biophysical model, is developed. The full biophysical model, not simplified proxies, is employed. Second, the modeling framework is built at a regional scale to facilitate the investigation of relevant policy analyses related to the growing "dead zone" in the Gulf of Mexico and the tradeoff between regional and local pollution reduction targets. Third, I derive the conservation production possibility frontier that explicitly incorporates the tradeoffs between pollution control costs and water quality benefits, between different pollutants, or between different control targets. Although the empirical results of this essay may be specific to the region and pollutants considered in this study, the modeling framework and the issues raised in the paper have wide applications in the NPS control of any watershed or area.

The rest of the chapter is organized as follows. The next section sets up a conceptual framework for water pollution control in a watershed. Next, I introduce an empirical modeling framework that integrates a water quality model and an optimization algorithm. After that, the study region, the pollutants, and the implementation of the optimization algorithm are described. Results are presented in section 6 with regard to the three tradeoffs discussed above. The final section provides concluding remarks.

5.2. Theoretical Framework

Suppose there is a watershed with J subwatersheds. In each subwatershed j, there are K_j fields each of which has its own unique land characteristics and land management practices. A set of conservation actions, $\boldsymbol{x}_{jk}$, can be taken for field k of subwatershed j in order to improve the environmental conditions of the watershed. The vector $\boldsymbol{x}_{jk}$ has I elements, which indicate the adoption of a set of I distinct conservation practices. That is, if conservation practice, i, is taken, then $x_{jk}^{i}=1$; otherwise, $x_{jk}^{i}=0$ for all $i=1,2,.....I$. Note that more than one conservation practice can be adopted on a field so multiple elements of this vector can be non-zero. For ease of reference, I will denote the conservation actions in all fields of the whole watershed as X, i.e., $X=(\boldsymbol{x}_{11},\boldsymbol{x}_{12},.....\boldsymbol{x}_{1K_1};\boldsymbol{x}_{21},\boldsymbol{x}_{22},...\boldsymbol{x}_{2K_2};.....\boldsymbol{x}_{J1},\boldsymbol{x}_{J2},...\boldsymbol{x}_{JK_J})$. In other words, X is a collection of conservation actions planned for the watershed. The impacts of any $\boldsymbol{x}_{jk}$ are likely to be affected by conservation actions on other fields of the watershed. Thus, for convenience, I will refer to a set of conservation actions planned for the entire watershed, X, as a single plan.

The environmental impact of X is denoted as Y where Y is a vector with N elements, i.e., $Y=(y^1,y^2,.....y^N)$. Each element represents one environmental indicator; for example, y^n can be any pollutant (nitrogen, phosphorus, etc) loading at the watershed outlet; or some index of local water quality indicators. The relationship between Y and X is denoted as

(5.1) $$y^n = f^n(X;Z),$$

for all $n = 1, 2, ...N$, where Z is set of factors that affect y^n but are not part of the conservation plan such as soil and land characteristics, crop rotations and other crop management practices, climate, etc. Potentially, Z represents a collection of all the land and climate characteristics for each field in each watershed.

One important note on (5.1) is that an environmental indicator , y^n , can be affected by conservation actions on fields within its own watershed as well as any watershed that drains into the watershed. One contribution of the paper is that the modeling framework employed realistically represents such interactions.

Denote T as the conservation possibility set that gives all feasible combinations of conservation plans and environmental outcomes. In other words, T is the set of all (X, Y) combinations that are technically feasible given the existing state of conservation technology, and subject to the physical constraints imposed by the environmental processes. The cost of a conservation plan is represented by a cost function, $c(X)$. In general, different conservation plans will result in different costs and different environmental outcomes. Thus, one obvious goal of watershed management is to achieve a desirable tradeoff of costs, $c(X)$, and benefits, Y . In addition, watershed stakeholders may value different environmental indicators differently. For example, a local watershed may have a goal of reducing its phosphorous loading in its lakes but does not feel the need to have its nitrate loading reduced, which may be a concern regionally. Thus, there can be tradeoffs among the different elements of Y .

These tradeoffs can be identified through the following multi-objective optimization problem:

(5.2)
$$\begin{aligned} \min \quad & [c(X),\ y^1, y^2, ...y^N] \\ s.t., \quad & (X, Y) \in T. \end{aligned}$$

The set of solutions to (5.2) consists of all conservation plans that are Pareto-optimal. A conservation plan X is Pareto-optimal if there is no $(X',Y') \in T$ such that $f^n(X') \leq f^n(X)$ and $c(X') \leq c(X)$, for all $n \in \{1,2,\ldots,N\}$, and such $m \in \{1,2,\ldots,N\}$, such that $f^m(X') < f^m(X)$ or $c(X') < c(X)$. In other words, the solutions to (2) together make up the efficiency possibility frontier given T and $c(\bullet)$. Since this frontier is conceptually very close to the production possibility frontier (PPF) in production economics, I will simply refer to it as the conservation PPF.

To illustrate the tradeoffs, suppose *N=2*. One can consider y^1 and y^2 as the nitrogen and phosphorus runoff at the watershed outlet, respectively. Alternatively, these indicators might be the local and regional targets for phosphorus. Then the conservation PPF based on problem (5.2) has three dimensions: $c(X)$, y^1, y^2. One way to interpret this PPF is that it represents the least cost necessary to achieve the two environmental outcomes y^1 and y^2. The subsequent analysis empirically identifies this conservation PPF for the study region. To gain a clear picture of the tradeoffs, one can also break down the three-dimensional PPF into different two-dimensional PPFs that are most often used in economic analysis. For example, one can derive a PPF for $c(X)$ and y^2, which is essentially a cost curve for y^2, while holding y^1 at a prefixed value. In practice, this can mean that the watershed planner intends to identify the tradeoffs between conservation costs and phosphorous loading while insuring the attainment of a nitrogen target, set to meet some ecological needs such as the mitigation of the Hypoxic zone in the Gulf of Mexico. Similarly, one can derive a two dimensional PPF for y^1 and y^2 while holding $c(X)$ at a prefixed value. This is an isocost curve, representing

all the efficient combinations of y^1 and y^2. This curve depicts the combinations of nitrogen and phosphorous loadings that are possible under a given budget.

The shape of the isocost curve, and thus the shape of the cost curve of y^2 for a given y^1, will critically depend on T, the conservation possibility set. In other words, they will depend on the functions $f^1(X)$ and $f^2(X)$. At one unlikely extreme, there may be a one-to-one correspondence between y^1 and y^2, e.g., $y^2 = f^2(X) = \alpha y^1 = \alpha f^1(X)$. In this case, the isocost curve for y^1 and y^2 degenerates to a single point, as shown in Figure 1(a). This happens if the impacts of the efficient allocation of conservation practices are proportional with respect to y^1 and y^2, and no other reallocation is efficient. At another unlikely extreme, all conservation practices that affect y^1 have no impact on y^2 and those that affect y^2 have no impact on y^1. A single practice that exhibits this property is the reduced application of nitrogen or phosphorous fertilizers. In that case, the isocost curve for y^1 and y^2 appears as in Figure 1(b). In particular, both ends of the curve touch the axes (which represent minimum achievable pollutant loadings). Essentially, the funding is split between the control of y^1 and y^2. The share of each pollutant control can range from zero to one hundred percent. More generally, most conservation practices have some impact on both pollutants, which implies that an efficient conservation plan will reduce both pollutants even though the degree of reduction may vary across the pollutants. Thus, the transformation curve often looks as illustrated in Figure 1(c), with some distances between both ends of the curve and the axes.

As a result, different forms of the isocost curves imply different levels of flexibility that watershed managers have in setting targets for different environmental outcomes. Figure 1(a) implies there is no flexibility at all—setting a target for y^1 is equivalent to setting a target for y^2. On the other hand, in a Figure 1(b), the targets are not linked at all which allows complete freedom in setting the targets. In the more realistic case, as shown in Figure 1(c), setting a target for one pollutant will have some implications for the other pollutant but there would be some flexibility for watershed planners. In practice, how much flexibility there is will depend on the characteristics of the watershed, the nature of the pollutants under consideration, and the practices that are included in the portfolio of pollution control.

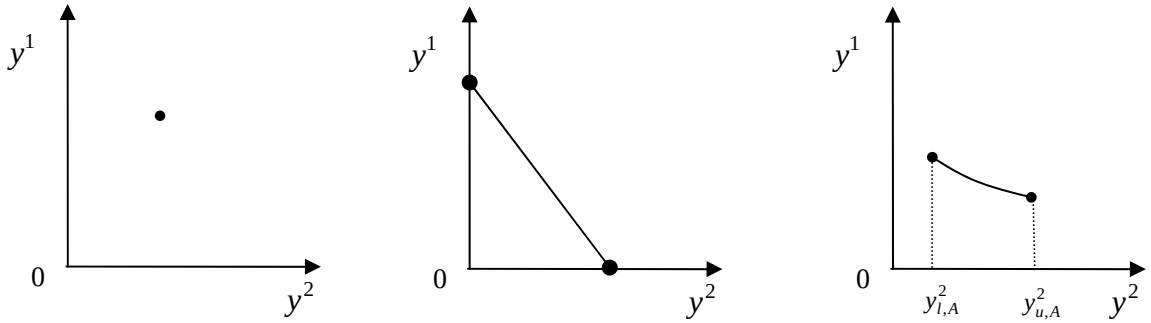

(a) One-to-one correspondence between y^2 and y^1

(b) Practices having separable impacts on y^2 and y^1

(c) The general case

Figure 1. An illustration of the possible shapes of an isocost curve

5.3. An Integrated Empirical Modeling Framework

To solve problem (5.2), one needs the knowledge of the relationship between water quality outcomes and conservation practices, as represented by equation (5.1). In economic analyses, biophysical relationships models are often expressed as a functional form which

gives the impression that one can apply standard mathematical optimization procedures. However, the relationship between water quality and conservation practices is very complex, and often determined by multiple processes. For example, to model the nitrogen loading at a watershed outlet, the whole life cycle of nitrogen, where mineralization, decomposition, and immobilization are important parts, has to be modeled in the watershed. In the empirical analysis, I use the Soil and Water Assessment Tool (SWAT) model. In SWAT, the nitrogen cycle is simulated using two inorganic forms and three organic forms. Figure 2 describes the process involved.

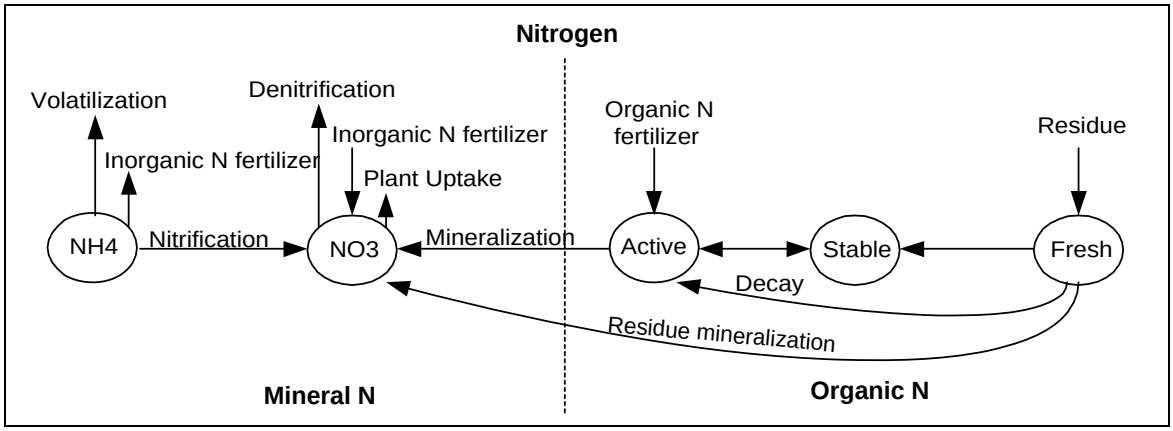

Figure 2. Nitrogen cycle as simulated in SWAT (adapted from SWAT Theoretical Document, Neitsch et al., 2005)

To most accurately represent the biophysical processes in a watershed, it is necessary to employ the full biophysical model rather than a set of more easily characterizable equations that proxy the model.

5.3.1. A Water Quality Model—The Soil and Water Assessment Tool

The SWAT model (Arnold et al., 1998; Arnold and Forher, 2005) is a conceptual, physically based, long-term, continuous watershed scale simulation model that also operates

on a daily time step. In SWAT, a watershed is divided into multiple subwatersheds, which are further subdivided into Hydrologic Response Units (HRU) that consist of homogeneous land use, management, and soil characteristics. Streamflow generation, sediment yield, and non-point-source loadings from each HRU are summed and the resulting loads are routed through channels, ponds, and/or reservoirs to the watershed outlet. Key components of SWAT include hydrology, plant growth, erosion, nutrient transport and transformation, pesticide transport, and management practices. Outputs provided by SWAT include streamflow and in-stream loading or concentration estimates of sediment, organic nitrogen, nitrate, organic phosphorous, soluble phosphorus, and pesticides. Previous applications of SWAT for streamflow and/or pollutant loadings have compared favorably with measured data for a variety of watershed scales (e.g., Arnold and Allen, 1996; Arnold et al., 1999, 2000; Santhi et al., 2001; Borah and Bera, 2004; Jayakrishnan et al., 2005; Gassman et al., 2007). Arnold et al. (2000) performed a stream flow validation study of the UMRB using input data based on the Hydrologic Unit Model for the United States modeling framework. The calibration and validation of SWAT for the UMRB region can be found in Gassman et al. (2006) and Jha et al. (2006).

5.3.2. Optimization Method—The Evolutionary Algorithm

Using SWAT directly in lieu of the function, $f^n(X;Z)$, in problem (5.2) poses practical solution challenges. One approach is to run the model for all all possible conservation plans and evaluate the cost and the pollution outcome of each combination. The Pareto frontier would then be the set of least cost combinations associated with each combination of pollution reductions. However, for any realistic watershed problem, this brute

force approach is infeasible. Specifically, given that there are I conservation practices possible for adoption on each field and there are $\sum_{j=1}^{J} K_j$ fields, this implies a total of $I^{(\sum_{j=1}^{J} K_j)}$ possible conservation plans to compare. In a watershed with hundreds of fields and several conservation practices, this comparison quickly becomes unwieldy. The combinatorial nature of the problem was recognized by Braden et al. (1989), and was one of the reasons for Khanna et al.'s (2003) decision to focus on a narrow band of land around streams.

Evolutionary algorithms provide a systematic way for searching through large search spaces. These algorithms mimic the process of biological evolution, which, in the words of Mitchell (1996), "in effect, is a method of searching for solutions among an enormous amount of possibilities." Researchers, beginning with Srivastava et al. (2002) and Veith et al. (2003) have used genetic algorithms (GA) in order to search for single cost-efficient watershed-level pollution reduction solutions. However, as discussed in the introduction, these papers examine small study areas and do not focus on the important issues of NPS pollution control considered in this study.

5.3.3. The Language and Logic of Evolutionary Algorithms

Beginning in 1950's and 1960's computer scientists came to a realization that the theory of biological evolution can be used as an optimization tool for engineering problems. Since the field of evolutionary computation owes its origins to observations of biological evolution, the terminology used has its analogs in biology, although, typically, the entities used to describe an optimization problem are much simpler than the real biological entities bearing the same name. A *genome* (or a *chromosome*) refers to a complete collection of

genes and fully describes an *individual* (a candidate solution in an optimization problem). A set of possible values that any gene can take is referred to as an *allele set*, or *alphabet.* Often, a genome representing a candidate solution is a one-dimensional array, or vector. A gene then is an element of this array and encodes a particular element of a candidate solution. A value of a gene comes from its allele set, also a vector. Analogous to haploid organisms in real biology, *offspring* is created from two parent individuals. During sexual reproduction, *recombination* (*crossover*) occurs: the offspring's genome consists of portions of each of the two parents' genomes. As in biological evolution, offspring are subject to *mutation:* a random substitution of a gene's value with a value from its allele set.

In this study, the following correspondence between the terminology of evolutionary algorithms and entities related to nonpoint source pollution is made. Table 1 provides the necessary terms:

Table 1. Terminology of evolutionary algorithms in relation to watershed optimization

Evolutionary computation term	Its interpretation in a nonpoint source pollution setting
Allele set	A set of mutually exclusive land use options and conservation practices
Individual (genome)	A distinct allocation of conservation practices and land use options in the watershed
Gene	Spatial unit of analysis (HRU)

In this application of evolutionary algorithms to spatial optimization, a genome is a vector of length *F*, where *F* is the number of spatial decision-making units. Each element of the vector (gene) is encoded with a value from the allele set *A*, and denotes a particular land use option.

As in biological evolution, individuals at every *generation* form *populations*, and are characterized by their *fitness*—a score which measures how well each individual is solving the optimization problem at hand (for example, a value of an objective function). Individuals possessing higher fitness scores are more likely to be selected for reproduction and therefore are more likely to pass along the characteristics associated with the candidate solutions they represent.

While there are many variations of evolutionary algorithms, most that can be called "genetic algorithms" have the following elements in common: populations of individual solutions, selection for reproduction according to fitness levels, crossover to produce new solutions (offspring), and random mutation of new offspring.

Given that in order to characterize the tradeoffs outlined above, a multiobjective optimization problem needs to be addressed, I turn to a class of evolutionary algorithms designed to solve multiobjective problems. Recent years have seen emergence of several multiobjective evolutionary algorithms. I use an algorithm called Strength Pareto Evolutionary Algorithm 2 (SPEA2), developed by Zitzler and Thiele (Zitzler, Laumanns, and Thiele, 2002).

The search process starts with a population of candidate solutions from which a new population is created by the process of selection, crossover, and mutation. The fitness score of each individual in the population is a function of how many other individuals in the population it dominates (in the sense of Pareto) and by how many individuals it is dominated by. The algorithm provides an approximate solution to problem (2) by preserving Pareto-nondominated individuals, by eliminating Pareto-dominated solutions, and by iteratively creating new candidate solutions and assessing how well they perform on the multiple

objectives outlined in (2). Furthermore, the algorithm takes into account the degree of "crowding" around an individual in order to preserve the diversity in the population and to explore a greater region of the objective space. Details of the fitness assignment in the algorithm are presented in Appendix D.

5.3.4. Integrating the Optimization Algorithm With the Water Quality Model

In this application, three major components were integrated to arrive at the final modeling framework. The first component is the logic and the fitness assignment method of a multiobjective evolutionary optimization algorithm, SPEA2. The second component is a publicly available C++ library of genetic algorithms, GALib, originally developed by Wall (1996), with the current version available online. The third component is the hydrologic model, the SWAT2005, coupled with a Windows-based database control system, i_SWAT (Campbell, 2006; Gassman et al., 2003). SPEA2 provides the fundamental multiobjective optimization logic, while GALib provides the basis that is needed to implement an evolutionary search algorithm. Finally, SWAT and i_SWAT provide a way to model the different conservation practices considered in this paper and model their watershed-level environmental impacts.

5.4. The Study Region and the Pollutants

The Upper Mississippi River Basin extends from the source of the Mississippi river at Lake Itasca in Minnesota to a point just north of Cairo, Illinois. The total drainage area is nearly 492,000 km^2, which lies primarily in parts of Minnesota, Wisconsin, Iowa, Illinois, and Missouri. Figure 3 contains a map of the Upper Mississippi River Basin and its position

in the central U.S. Cropland and pasture are the dominant land uses in the UMRB, which together are estimated to account for nearly 67 percent of the total area (NAS, 2000). Nutrient inputs (nitrogen and phosphorus) to fertilize the land are the primary sources of nonpoint source pollution in the UMRB stream system. These nutrients are also apparently the cause of a major oxygen-depleted hypoxic or "dead" zone in the Gulf of Mexico which has exceeded 20,000 km^2 (Rabalais et al., 2002). While the task force charged with assessing the causes of Gulf hypoxia in 2000 identified nitrogen (and, in particular, nitrate) contributions, as the primary nutrient loading causing the problem, more recent evidence suggests that both nitrate and phosphorous loads from the UMRB region (and elsewhere) are to blame (*Integrated Assessment,* 2000; e.g., Lohrentz et al., 1992, 1997, 1999; Ammerman et al., 2004; Sylvan et al., 2006). Recent evidence suggests that the UMRB is responsible for 43 percent of nitrate and for 26 percent of phosphorus loadings into the Gulf of Mexico (Aulenbach et al., 2007).

While nitrogen and phosphorous are believed to be the primary limiting nutrients contributing to the creation of the dead zone in the Gulf, they are also the culprits of substantial local water quality problems within many areas of the UMRB. While phosphorous is more often a target in Total Maximum Daily Load programs in the UMRB, there are also many water bodies listed as impaired due to high nitrogen concentrations. In short, water quality problems in the UMRB are substantial and multi-faceted. On the one hand, nutrients from the region negatively affect water quality in lakes and streams locally throughout the basin, negatively affecting recreation opportunities, wildlife viewing, and ecosystem functioning. On the other hand, these nutrients travel out of the watershed and

Figure 3. UMRB and the watershed outlet at Grafton (from Kling et al. (2006))

flow in to the Gulf of Mexico where they directly contribute to the large region devoid completely of life. No single regulatory authority has identified a standard or set of water quality standards for the many impacted lakes and streams in the region, but numerous Total Maximum Daily Load regulations, nutrient "criteria," and "targets" for nutrient reduction are in place or being developed by various state and federal agencies. Thus, the model described here representing a multitude of water quality targets at different spatial scales accurately describes the policy environment.

5.5. Algorithm Implementation and the Allele Set

There are a number of abatement activities that individual farmers can undertake to reduce nitrogen and phosphorous loadings from their fields. Various in-field conservation practices include conservation tillage (where residue from the previous year's crop is left on the ground to help reduce erosion), buffer strips, grassed waterways, as well as complete retirement of land from crop production in favor of other uses.[38] In addition, nitrogen and phosphorous loadings can be directly controlled by reducing the amount of application of nitrogen and phosphorous fertilizer to the crop. In this study, I consider several in-field conservation practices, a reduction in the quantity of nitrogen fertilizer applied, and retirement of land from crop production. With the exception of land retirement, all other practices are modeled in conjunction with the cropping system currently in place.[39]

Furthermore, some conservation practices are already a part of the baseline scenario. In this application, the conservation practices and cropping systems observed in the baseline are preserved, while allowing the algorithm to add other conservation practice options.

The attractiveness of this "baseline-aware" approach is clear. First, by preserving the crop rotations as observed in the data, an effort is made to realistically model the large agricultural landscape under study. Second, by not removing current conservation practices already in place, better policy relevance is achieved. It is, no doubt, interesting to "start from scratch", that is, to model the removal of all conservation practice from the landscape and let the algorithm allocate those in a cost-efficient manner, as it is likely that the historical allocation of practices is not efficient, given the water quality objectives being considered.

[38] The Conservation Reserve Program (CRP) is a very large, federally funded program that makes direct payments to farmers to remove their land from active production and instead plant trees or other perennial ground cover.

[39] The source of cropping systems and conservation practice coverage is the 1997 NRI Survey (Nusser and Goebel, 1997).

The prescriptions of the algorithm could then be used to gauge these inefficiencies. However, the historical investments in conservation practices are to some extent sunk costs, and to move forward to improve water quality one needs to heed the current state of the landscape. Further, given that improvements in water quality are of greatest policy interest, it is sensible that the worst situation, as far as water quality goes, is reserved for the status quo.

There is, however, an additional complication raised by preserving the baseline set of conservation practices. In executing the assignment of HRUs to a particular member of the allele set, a constraint which guaranteed that the new set of conservation practices is "no worse" than the baseline had to be added. This, in turn, necessitates imposing some form of ordering on conservation practices. For example, if an HRU is observed to contain a grassed waterway in the baseline, I constrained the algorithm to be able to replace it with a terrace, but not with contour farming. Thus, contour farming, grassed waterway, and terraces are implicitly ranked from 'weakest' to 'strongest'. Similarly, tillage practices are ranked by the amount of plant residue left on the field: conventional till, ridge till, mulch till, and no-till (CT, RT, MT, and NT, respectively). Also, if in the progression of the algorithm, a conservation practice is to be removed, extra care had to be taken to only revert as far back as the baseline set of conservation practices allows.

The following table presents the (unconstrained) allele set used in this study. As discussed above, for the HRUs which were observed to have the relevant conservation practice in the baseline, the allele set was constrained. Reduced fertilizer (RF) in the table above refers to a 20 percent reduction in nitrogen fertilizer application. The allele set is constructed to take into account the fact that many of the practices considered are not mutually exclusive and can be implemented jointly on any given field.

Table 2. Conservation options (allele set)

Allele number	Allele description
1	Conventional Till (CT)
2	Ridge Till (RT)
3	Mulch Till (MT)
4	No Till (NT)
5	CT+Contour
6	RT+Contour
7	MT+Contour
8	NT+Contour
9	CT+Grassed Waterway
10	RT+Grassed Waterway
11	MT+Grassed Waterway
12	NT+Grassed Waterway
13	CT+Terraced
14	RT+ Terraced
15	MT+Terraced
16	NT+Terraced
17	CT+RF
18	RT+RF
19	MT+RF
20	NT+RF
21	CT+Contour+RF
22	RT+Contour+RF
23	MT+Contour+RF
24	NT+Contour+RF
25	CT+Grassed Waterway+RF
26	RT+Grassed Waterway+RF
27	MT+Grassed Waterway+RF
28	NT+Grassed Waterway+RF
29	CT+Terraced+RF
30	RT+Terraced+RF
31	MT+Terraced+RF
32	NT+Terraced+RF
33	Land retirement

The practices considered are simulated using the SWAT model. In particular, land retirement is modeled by assigning a permanent grass cover to the HRU, fertilizer reductions are modeled by reducing nitrogen fertilizer applications (USDA-ERS) by 20 percent for all

crop rotations where nitrogen fertilizer is used, and the in-field practices (tillage, grassed waterways, contour farming, and terraces) are modeled by adjusting the SWAT model parameters in the manner suggested by Arabi et al. (2007) and Secchi et al. (2007).

To meaningfully capture a tradeoff between water quality objectives and total control costs, detailed information on the costs of all the options in the allele set is needed and was obtained from multiple sources. State-level costs of terraces, no-till, and contouring were gathered from the Natural Resource Conservation Service website[40]. The costs of grassed waterways were obtained from the CRP program office, and converted to a per acre protected, annualized basis using a 5 percent discount rate and a 20 year useful life term[41].

The costs of land retirement are proxied by the cash rental rates and the costs of nitrogen fertilizer reductions were developed using the yield curves inferred from Iowa State University Extension's N-Rate Calculator information for geographic zones and corn-soybean crop sequences for Iowa, Minnesota, Illinois, and Wisconsin. State-level data for fertilizer application allowed us to compute the implied reduction in corn yields. Predicted yield reduction, multiplied by the price of corn, served as an approximation to the cost of reducing nitrogen fertilizer application. Details on the computed cost of nitrogen fertilizer reduction are provided in the Appendix.

The algorithm was initialized with a population of 40 individuals. In order to efficiently exploit prior domain-specific knowledge, and in contrast to the earlier studies (e.g., Arabi et. al (2006), Bekele and Nicklow (2005)), the initial population was not created

[40] The cost of establishing a terrace had to be converted to an annualized, per acre, basis. To that end, a cost per foot reported by NRCS was multiplied by 166.7, as this many feet of a terrace can protect one acre of land (Kling et. al., 2005; Secchi et al., 2007). The resulting cost was annualized using a 5 percent rate of discount and a 25 year term representing the useful life of a terrace.

[41] It is assumed that 2 percent of a unit of land, appropriately converted to a grassed waterway, protects the entire unit of land (Kling et al., 2005).

completely at random. First, the initial population was seeded with an individual representing the baseline allocation of conservation practices, and an individual representing a scenario of all cropland in the UMRB being retired from production and placed under permanent grass cover (i.e., allele #33). These individuals represent the boundary points on the conservation PPF: the baseline individual results in the lowest cost, and highest nutrient loadings, while the "all cropland retired" individual results in the highest cost and lowest nutrient loadings. I further assist the algorithm in exploring the search space by seeding it with additional 32 individuals representing the uniform application of the alleles #1 through #32 onto the entire cropland in the watershed. The purpose (and the payoff) of such seeding is twofold: first, a good coverage of the objective space is achieved; and, second, the land use options which are immediately judged to be "good" help define the direction of the stochastic search and improve the algorithm's efficiency [42]. The rest of the initial population was generated by randomly assigning the cropland HRUs with one of the 33 alleles above (subject to the baseline constraint discussed above).[43] I expect good initial coverage of the objective space, thus assisting the evolutionary algorithm in exploring a wider range of the search space.

5.6. Empirical Analysis and Results

I apply the evolutionary algorithm to develop a conservation PPF which provides an approximate solution to the multiobjective optimization, using two distinct sets of objectives.

[42] For instance, seeding with every allele value proved to be a dramatic improvement over an algorithm which, in addition to defining the PPF boundaries by seeding the initial population with the baseline and allele #34 (retirement of all cropland), included an individual assigning all corn HRUs a 20 percent N fertilizer reduction (allele #17, "CT+RF"), and an individual assigning terracing, no-till, and fertilizer reductions (allele #32, "NT+Terraced+RF").

[43] An individual constructed in a way that strived to replicate as closely as possible, given the data limitations, the "Sound Conservation Practices" scenario of Kling et al. (2006) was also included, but was immediately dominated, and eliminated from subsequent generations.

The first set of results develops a PPF which relates to the regional water quality improvement objectives (motivated, perhaps, by the problem of hypoxia in the Gulf of Mexico). Specifically, the three objectives to be minimized are: 1) the cost of nonpoint source pollution control; 2) the mean annual nitrate loadings at the overall UMRB watershed outlet (Grafton, Illinois), and 3) the mean annual total phosphorus loadings at the UMRB outlet.

The second set of results is developed for objectives that incorporate both local water quality and Gulf hypoxia concerns. In particular, I wish to explore the set of conservation practices needed to reduce mean annual nitrate loadings by at least 30 percent in *each* of the subbasins in the UMRB (as represented by the 8-digit HUC watersheds).

The resulting frontiers for the two sets of objectives allow us to provide empirical answers to important policy questions. In particular, what is the nature of a tradeoff between the NPS control costs and NPS reductions? What are the costs of reducing nutrient loadings at the outlet for each of the nutrients separately, and jointly? Given a particular cost of control, what are the tradeoffs between nutrients? What practices should be used to control nitrates separately, phosphorus separately, and nitrates and phosphorus jointly? How do the answers change with a change in a spatial scale of nutrient reduction targets (i.e., when a subbasin-level targets for nitrates are employed)?

5.6.1. The Conservation PPF

The solution to a multiobjective optimization problem (2) is a three-dimensional (nitrates-phosphorus-cost) conservation PPF. A set of Pareto-nondominated individuals surviving after 463 generations (iterations of the evolutionary algorithm) provides an

approximation to the true frontier. Figures 4 and 5 provide two-dimensional projections and a three-dimensional visualization of the empirical frontier. The dashed lines in Figure 4 represent the baseline nitrates, P, and cost.

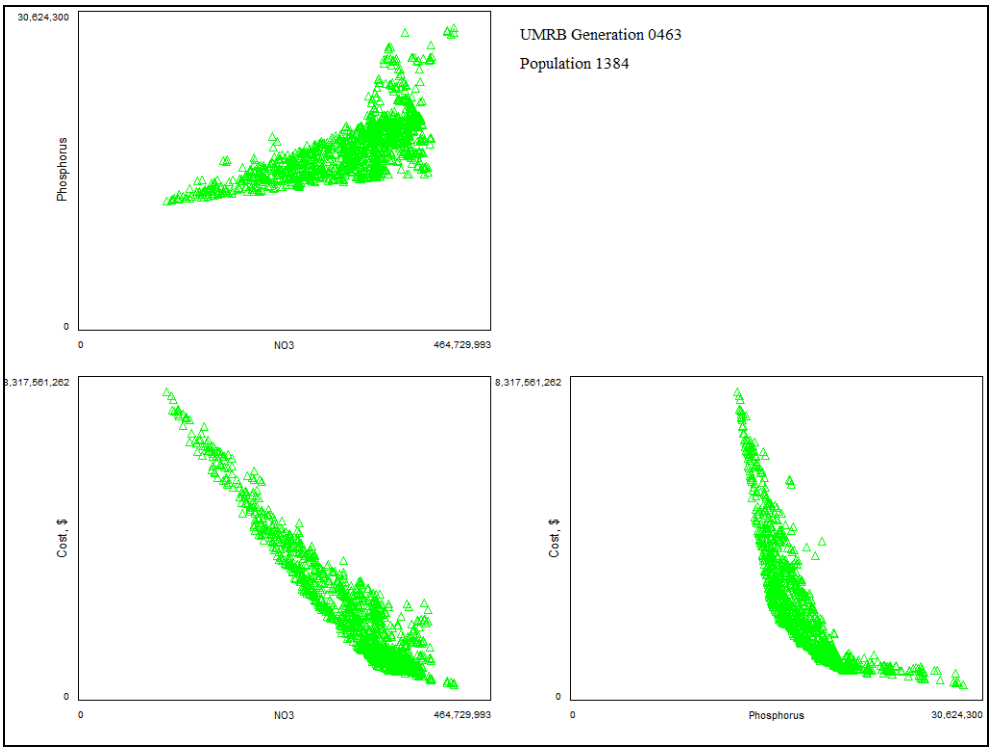

Figure 4. 2-dimensional projections of the empirical conservation PPF

Having access to the full conservation PPF provides empirical content to the conceptual discussion above and enables one to answer a wide array of relevant water quality policy questions. On one level, the PPF allows for a "look at the big picture": that is, quantification of various tradeoff schedules under different assumptions about the focus of water quality policy or the potential water quality improvement budget. In order to answer these kinds of questions, each individual on the PPF is treated as a data point characterized by outlet nitrate and phosphorus loadings, and control cost. The use of the frontier in this

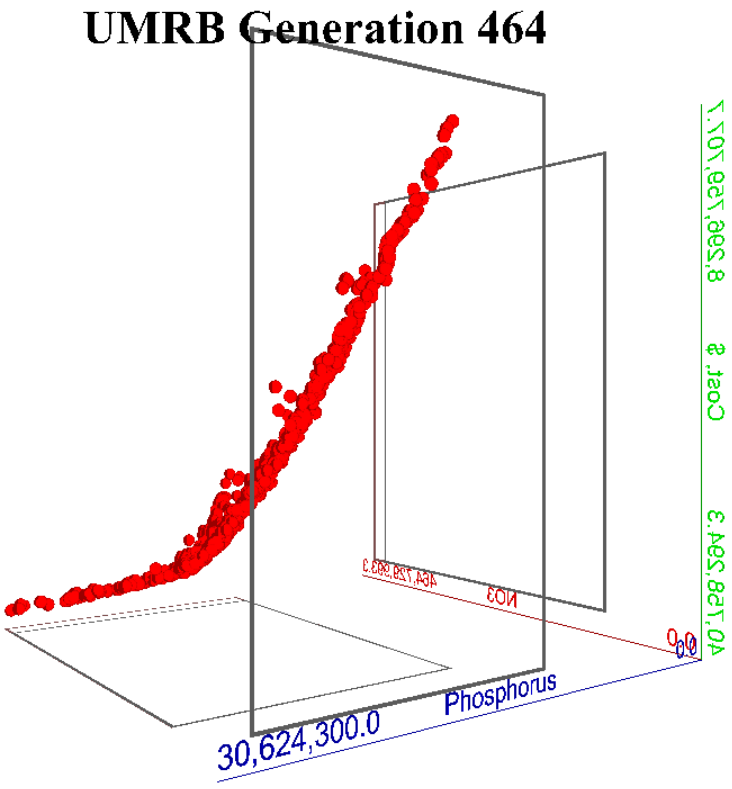

Figure 5. 3-dimensional vizualization of the empirical conservation PPF

fashion essentially answers a variety of "what?" questions: e.g., what is the cost of reducing nitrates by a given percentage, or what is the nature of the tradeoff between nutrients when an NPS pollution control budget is of particular magnitude?

However, the usefulness of the conservation PPF does not end there. By looking at the individuals comprising the frontier, one can look deeper and essentially ask the "how?" questions. Each one of the over 1300 non-dominated individuals in the frontier represents a unique mix of land use and conservation practices in the UMRB. A policymaker could then use the frontier in the following fashion: first, ask, what is the nature of the tradeoff between cost and a particular nutrient of interest? Then, using the public's preferences for water

quality, identify appropriate nutrient reduction targets. Then a policymaker can go back to the frontier, select an individual satisfying these water quality and cost criteria, and see which conservation practices are selected, and where they need to be implemented in the watershed in order to achieve the needed nutrient reductions.

The next section highlights the use of the PPF to answer the "what" questions on the nature of the tradeoffs. The section following selects a set of particular nutrient reduction targets and explores the "how" questions by breaking down the distribution of conservation practices which achieve the given water quality targets.

5.6.2. Tradeoffs of NPS Control Costs and Water Quality Benefits

This section illustrates the tradeoffs between nutrient reductions and control costs. These tradeoffs are captured by the total abatement cost curves which can be derived from the conservation PPF. Both Figures present nitrate loadings in terms of the percentage of baseline loadings (over 423,000 tons of nitrate-nitrogen) on the horizontal axis, and control costs in terms of the percentage of baseline cost (estimated to be just over $416 million per year), on the vertical axis.

Figure 6 contains cost curves for nitrate reductions under two different scenarios. Under one scenario, the cost curve is developed from the PPF in the absence of any constraint on phosphorus levels (as a lower envelope of the PPF in nitrate-cost space). Under an alternative scenario, a 30 percent concomitant reduction in phosphorus loadings is imposed as a constraint. As theory suggests, the constrained cost curve can be no lower than the unconstrained one, and that is indeed the case.

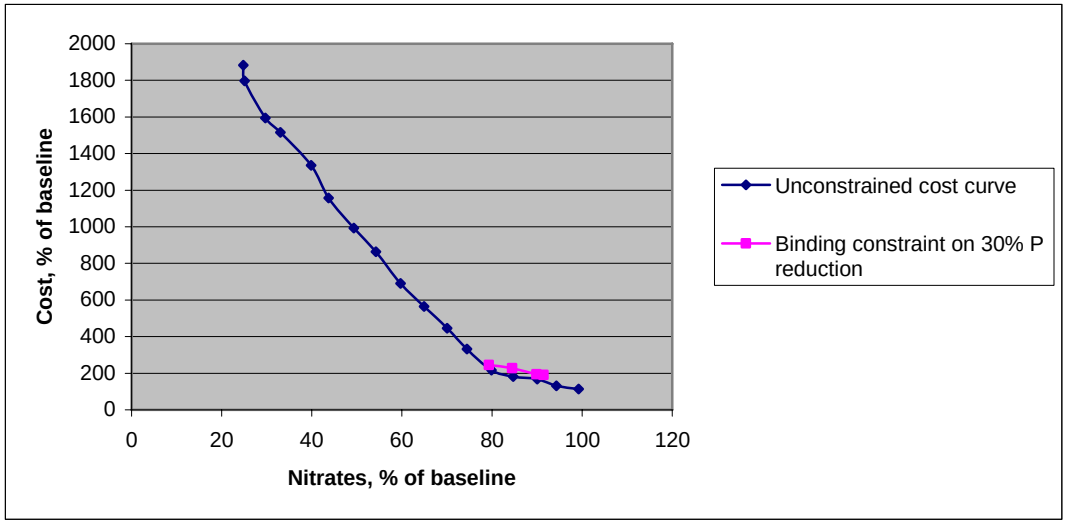

Figure 6. Cost-pollution tradeoff for nitrate loadings at the outlet

Figure 6 provides interesting insight on the interactions between conservation practices considered and the two nutrients. Note that while the unconstrained cost curve starts out at the baseline level of nitrate loadings, imposing a phosphorus constraint forces the curve to start at a level of nitrate loadings which is about 9 percent lower than the baseline. In other words, given the set of practices considered, once phosphorus loadings are reduced by 30 percent, an automatic reduction of about 9 percent in nitrate loadings follows. Further evidence of such interactions is revealed by the fact that the phosphorus constraint is only binding up to about a 20 percent reduction in nitrates. Greater reductions in nitrates lead to simultaneous reductions in phosphorus, suggesting complementarities in the set of practices used to achieve greater nitrate reductions. Also, as one can see from the Figure, the extra cost of achieving a 30 percent phosphorus target is relatively small. Over the range of nitrate reduction values where the phosphorus constraint is binding (from 9 to 20 percent reduction in nitrates), average extra cost is just over $168 million per year.

Interestingly, such complementarities are not evident in the case of modest phosphorus reduction targets. Figure 7 depicts an unconstrained phosphorus cost curve and a constrained phosphorus cost curve, subject to the 30 percent constraint on nitrate loadings. Baseline phosphorus loadings in the UMRB were estimated to be over 29,000 tons of total P per year. In this case, imposing a nitrate constraint automatically reduces phosphorus loadings by about 35 percent, and a nitrate constraint is binding up to a 40 percent reduction in phosphorus, and is not binding thereafter. Furthermore, in contrast to the case above, the average extra cost of achieving a nitrate target over the range where nitrate constraint is feasible and binding is estimated to be over $805 million per year.

These findings suggest an asymmetry between the impact of a set of practices used to achieve moderate nitrate reductions on phosphorus loadings and the impact of practices achieving moderate phosphorus reductions on nitrate loadings. In particular, for this watershed, a set of practices which achieves moderate nitrate reductions appears to be effective in controlling outlet phosphorus loadings, while the converse turns out to be false.[44] Thus, if water quality policy in the UMRB targets outlet nitrates, then a sizeable (30 percent) reduction in outlet phosphorus loadings come at no extra cost if the nitrate policy seeks reductions in excess of 20 percent, and come at a very moderate cost if the nitrate reduction targets fall between 9 and 20 percent. However, a policy seeking exclusively phosphorus loadings reductions at the outlet will not be effective in simultaneously controlling nitrates, unless an ambitious (in excess of 50 percent) phosphorus reduction target is specified.

[44] Indeed, examining the table of the consequences of uniform application of each of the alleles (subject to the "baseline-aware" constraints discussed above) reveals that only alleles containing terraces (#13, #14, and #15) are predicted to yield at least significant P reductions, and simultaneously provide moderate (greater than 20 percent) reduction in nitrates. Other sets of practices such as contouring or grassed waterways, while effective at controlling P loadings, were mostly ineffective in providing nitrates reductions in excess of 9 percent (without being combined with reduced nitrogen fertilizer applications).

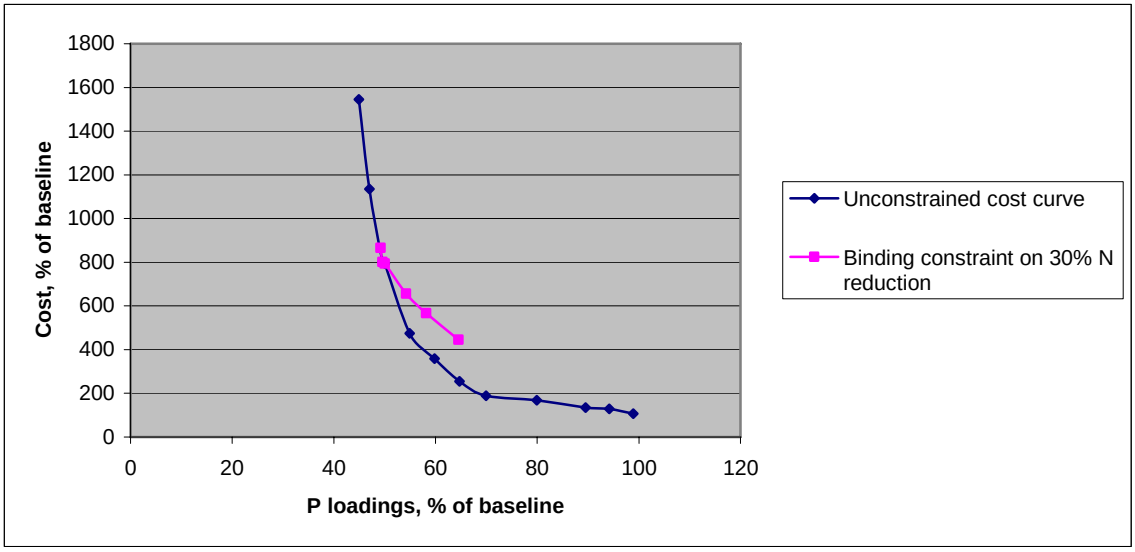

Figure 7. Cost-pollution tradeoff for Phosphorus loadings at the outlet

As the stringency of the nutrient control rises for nitrates (phosphorus), the constraint on phosphorus (nitrate) loadings becomes nonbinding. This is due to the complementarities in controlling both nutrients imbedded in the land retirement option. Once greater reliance on land retirement becomes necessary to further control nitrates (phosphorus), leading to simultaneous reductions in the other nutrient, the constraint on phosphorus (nitrates) becomes non-binding.

5.6.3. Tradeoffs Between Different Pollutants (Nitrates and P)

This section takes, literally, a different perspective on the nature of the tradeoffs implied by the conservation PPF. As highlighted in the theoretical discussion above, the tradeoff between different pollutants for a particular level of control costs can range from a curve spanning the entire range of possible nutrient values to just a single point, or anything

in between. Thus, theory alone provides fairly limited guidance as to what one should expect from a particular isocost curve.

The task of looking at the tradeoffs between nutrients is further complicated by the fact that, in order to properly explore such a tradeoff curve, all the points on the curve have to have identical control costs. This works well in theory, but, in the empirical application, a finite number of points define the PPF. Thus, potentially, only a few points may be located in a narrow band in a cost dimension to approximate such a tradeoff curve, and it is likely that one cannot identify distinct points along nitrate and phosphorus dimensions carrying identical control costs. These considerations make the empirical analysis of isocost curves somewhat limited[45].

Nonetheless, given these caveats, a set of tradeoffs depicted in Figure 9, drawn for successively higher levels of control costs, tells an interesting story. For the cost levels ranging from 200 to 500 percent of baseline cost, the empirical isocost curves span a wide range in the nutrient loadings space. Thus, a policymaker whose charge was to allocate a water quality improvement budget equal to 200 percent of baseline cost would be able to select from a fairly wide range of phosphorus pollution outcomes (roughly from 20 to 26 thousand tons), and a range of nitrate loadings ranging from 346 to 387 thousand tons. However, as the cost levels rise to 1000 percent, the dimensions of the empirical isocost curves decrease dramatically. This is consistent with the pattern observed in developing

[45] It should also be pointed out, that, given the diverse set of conservation practices being considered, I expect a dense set of individuals to occupy an isocost curve, as the tremendous number of possible reallocations of conservation practices implies that there is also a large number of possible allocations of conservation practices for a single level of cost. A full development of a (restricted) frontier in nitrate-phosphorus space could be undertaken using the methods employed in this study, and could serve as an interesting extension of this research. The current set of results demonstrate that such tradeoffs indeed exist, and that their dimensions and shape varies with the cost level and the practices used.

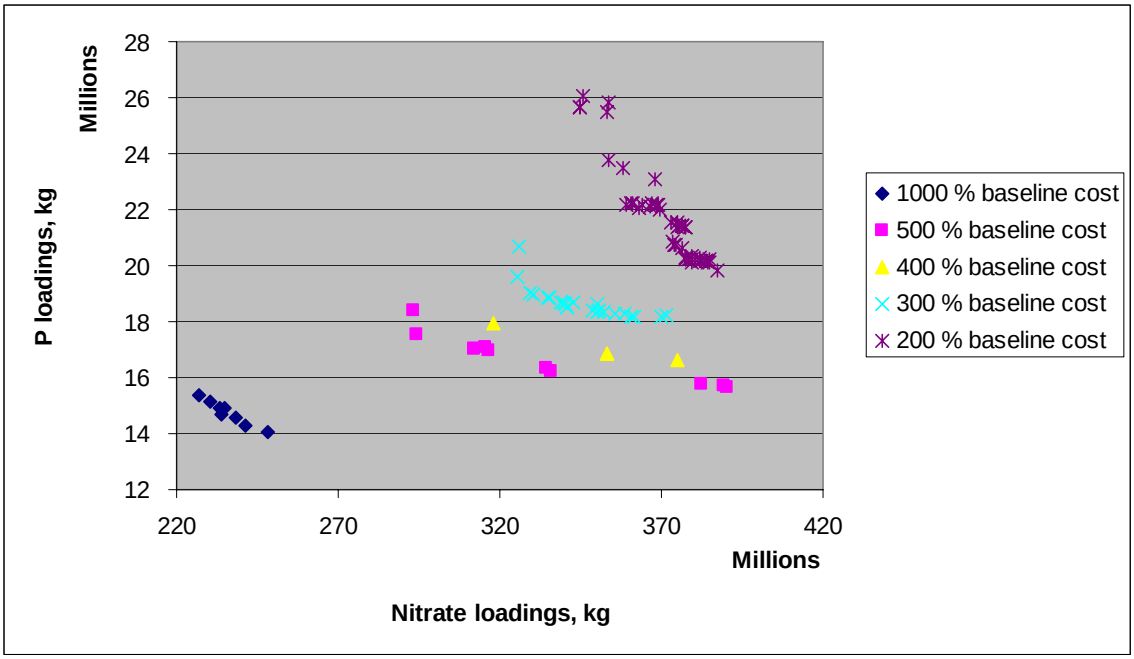

Figure 8. Tradeoffs between Nitrates and Phosphorus control

abatement cost curves for nutrients: as costs rise, use of land retirement becomes more widespread, which leads, eventually, to an essential collapse of the empirical isocost. As the size of the budget available for water quality improvements rises, an increased use of a practice which is effective at controlling both pollutants (land retirement) essentially leads to the elimination of the notion of tradeoff between the two nutrients.

The dimensions of the isocosts highlight the scope of the tradeoff, while the shape of the empirical isocost curves dictates the rate of the tradeoff. This marginal rate of substitution between nitrates and phosphorus changes depending on the size of the available pollution control budget.

5.6.4. Effects of Targeting Nutrients Separately or Jointly

The empirical frontier above consists of a large number of individuals, each representing a distinct way of placing conservation practices in the watershed. While the frontier itself summarizes the tradeoffs for a range of control costs and nutrient reductions, each individual on the empirical frontier contains information on the "look" of the watershed, that is, it is essentially a prescription for the application of conservation practices in the watershed. Potentially, a regulator makes use of the tradeoff information embedded in the frontier, and selects a set of appropriate nutrient reduction targets. A particular individual meeting these targets is then selected from the frontier, and it then specifies the quantity and the subbasin-level distribution of conservation practices in the watershed. Similarly to the development of unconstrained and constrained abatement cost curves presented in the section above, this section selects 30 percent as a target nutrient reduction.

A priori, one expects that whether nitrates and phosphorus at the outlet are targeted separately or jointly may have dramatic implications for which set of conservation practices should be used and where they should be located within the watershed. Further, this highlights the importance of careful planning of nutrient reduction goals. If a plan meant to control only nitrates (or phosphorus) is quite different from a plan controlling both pollutants, then implementing water quality policy in a piecemeal fashion (e.g., control nitrates first, then focus on phosphorus) may be socially costly and inefficient.

Careful empirical analysis is needed to assess the validity of these concerns. Next, the implications of targeting each nutrient for the allocation of conservation practices for a 30 percent reduction goal are analyzed.

First, Figure 9 below demonstrates how one identifies distinct individuals on the frontier, depending on the targeting strategy. Suppose a regulator wishes to reduce nitrate loadings by 30 percent. Such an individual (highlighted in red) is located at the intersection of the lower envelope of the frontier in nitrate-cost space and the line specifying the loadings target (dashed line). This individual lies on the unconstrained cost curve for nitrates identified above. Thus, by looking at the unconstrained nitrate abatement cost curve, it is clear that, as a result of reducing nitrates by 30 percent, phosphorus loadings are in fact reduced by more than 30 percent. However, focusing on phosphorus reductions alone (blue point) results in nitrate loadings much greater than the 30 percent reduction goal. Again, this is also evident from analyzing the empirical phosphorus abatement cost curve.

For the UMRB, striving for a 30 percent reduction in nitrates only also, as a by-product, (over)achieves a 30 percent phosphorus reduction goal. On the other hand, seeking to reduce phosphorus alone produces only slight reductions in nitrate loadings. Thus, for a 30 percent reductions target for the UMRB, 2 distinct individuals are identified from the empirical PPF. In general, of course, this does not have to be the case. Depending on the magnitude of the reduction target, the mix of conservation practices, and the nature of the watershed, one could also observe situations where three distinct scenarios are found (one for nitrate reductions, one for phosphorus reductions, and one for both), or where achieving a phosphorus reduction goal automatically implies the achievement of the nitrate goal, but achieving a nitrate goal does not imply the achievement of a phosphorus goal, or even the case where achievement of a target in one nutrient automatically implies the achievement of target reductions in the other[46].

[46] For example, in this watershed, if the target reductions are 20 percent for both nutrients, 3 distinct individuals are identified.

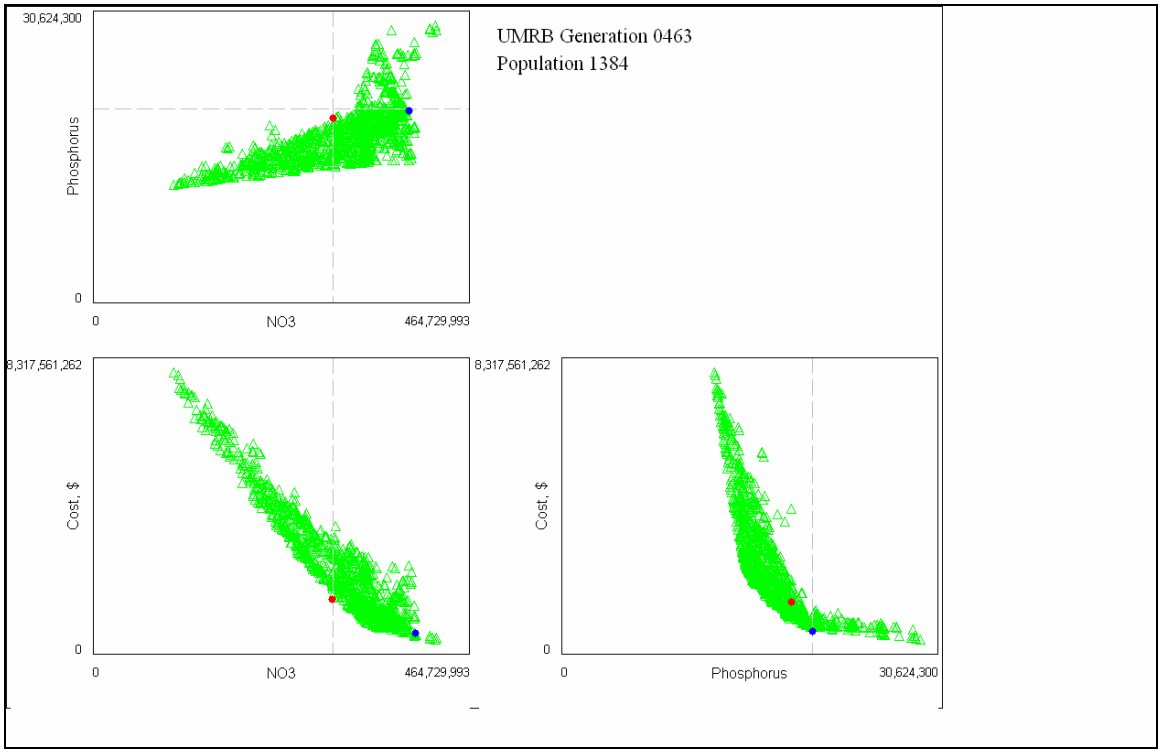

Figure 9. Graphical representation of targeting distinct nutrients

Each individual in the PPF is encoded with a unique identification number. An individual which achieves a 30 percent nitrate reduction goal and which is highlighted in red in the Figure above, is identified as individual #4715. An individual achieving the phosphorus target (highlighted in blue in the Figure above) is identified as individual #3821. Table 3 below lists the cost and pollution consequences for the 2 individuals:

Table 3. Consequences of targeting nutrients for a 30 percent reduction

Ind #	NO_3 loadings, tons/year	Total control cost, million $/year	Net control cost, million $/year	P loadings, tons/year	NO_3, % of baseline	Cost, % of baseline	P, % of baseline
4715 (red)	295,720	1,854	1,438	18,792	70	445.7	64.5
3821 (blue)	385,360	786	370	20,379	91.2	188.8	69.9

Individual #4715, achieving a 30 percent reduction in nitrates and almost a 36 percent reduction in phosphorus, is almost four times as costly as individual #3821, in terms of needed net control costs (total less baseline cost). Each of these individuals prescribes a distinct placement of conservation practices. *A priori*, I expect to see greater use of options containing nitrogen fertilizer reduction for individual #4715. Also, since this individual is also found to reduce phosphorus loadings, one expects to see practices which are effective at controlling phosphorus to also be selected.[47] That is, options containing terraces, grassed waterways, and contouring, as well as land retirement could be expected to have been selected for individual #4715. On the other hand, for the individual focusing on phosphorus (individual #3821), options containing nitrogen fertilizer reductions should not be selected, but, instead, a greater area of the watershed may be devoted to practices typically considered helpful in controlling erosion (and thus soil-bound phosphorus): terraces, conservation tillage, grassed waterways.

Land retirement is beneficial for both nitrate and phosphorus loadings, so no a priori ranking in its use between the two individuals is obvious. However, if "nutrient-specific" options are not sufficient to reach a 30 percent reduction, then some use of land retirement is expected. In particular, this could help explain some complementarities observed (i.e., that individual #4715 also reduces phosphorus by 36 percent, while targeting nitrates alone).

Empirical results confirm some of the expectations, while disproving others. Individual #4715 allocates most of the cropland to an option combining grassed waterways with nitrogen fertilizer reductions, to terraces combined with nitrogen fertilizer reductions, and to land retirement. Contouring proves to be a losing option, with none of the alleles

[47] The effects of uniform application of each of the alleles (subject to baseline constraints) are presented in Appendix D.

Table 4. Distribution of cropland between alleles for the 2 individuals

		Ind # 4715: 30% NO_3, 36% P reduction			Ind # 3821: 9% NO_3, 30% P reduction		
Allele number	**Allele description**	**area, km^2**	**percent of total area**	**Change from baseline, km^2**	**Area, km^2**	**percent of total area**	**Change from baseline, km^2**
1	Conventional Till (CT)	0	0	-78,071	0	0	-78,071
2	Ridge Till (RT)	0	0	-40,485	0	0	-40,485
3	Mulch Till (MT)	0	0	-78,144	0	0	-78,144
4	No Till (NT)	0	0	-35,413	0	0	-35,413
5	CT+Contour	0	0	-1,074	0	0	-1,074
6	RT+Contour	0	0	-52	0	0	-52
7	MT+Contour	0	0	-2,189	0	0	-2,189
8	NT+Contour	0	0	-576	0	0	-576
9	CT+Grassed Waterway	0	0	-2,299	76,154	31	73,855
10	RT+Grassed Waterway	0	0	-444	38,806	16	38,362
11	MT+Grassed Waterway	0	0	-4,087	78,376	31	74,289
12	NT+Grassed Waterway	0	0	-3,330	33,532	13	30,201
13	CT+Terraced	0	0	-75	75	0	0
14	RT+ Terraced	0	0	0	0	0	0
15	MT+Terraced	0	0	-2,875	2,875	1	0
16	NT+Terraced	0	0	-210	210	0	0
17	CT+RF	262	0	262	5,289	2	5,289
18	RT+RF	172	0	172	2,175	1	2,175
19	MT+RF	1,136	0	1,136	6,044	2	6,044
20	NT+RF	205	0	205	5,787	2	5,787
21	CT+Contour+RF	0	0	0	0	0	0
22	RT+Contour+RF	0	0	0	0	0	0
23	MT+Contour+RF	63	0	63	0	0	0
24	NT+Contour+RF	0	0	0	0	0	0
25	CT+Grassed Waterway+RF	77,296	31	77,296	0	0	0
26	RT+Grassed Waterway+RF	36,219	15	36,219	0	0	0
27	MT+Grassed Waterway+RF	73,007	29	73,007	0	0	0
28	NT+Grassed Waterway+RF	31029	12	31,029	0	0	0
29	CT+Terraced+RF	825	0	825	0	0	0
30	RT+Terraced+RF	1,429	1	1,429	0	0	0
31	MT+Terraced+RF	3,683	1	3,683	0	0	0
32	NT+Terraced+RF	1,035	0	1,035	0	0	0
33	Land retirement	22,962	9	22,962	0	0	0

containing contouring being included in the makeup of either individual. Terraces, despite their predicted effectiveness in reducing both nitrates and phosphorus (see Appendix), are present in a relatively small area. Application of grassed waterways is the main vehicle of achieving phosphorus reductions for individual #3821.

The columns in Table 4 which describe the change in land allocation relative to baseline indicate a major shift to grassed waterways for both individuals, as well as the addition of nitrogen fertilizer reductions for individual #4715.

Finally, and also somewhat unexpected, the use of land retirement is limited to individual #4715, with zero additional land retirement prescribed for phosphorus control. As land retirement is the most costly option, significant utilization of land retirement for the achievement of the 30 percent nitrate reduction goal is partially responsible for the large cost disparity between individuals #4715 and #3821.

5.6.5. Subbasin-level Distributions of Conservation Practices

This section describes in greater detail the geographic distribution of conservation practices which were selected to make up both individuals. The maps present additional conservation practices implemented on the landscape, relative to the baseline. In order to improve the readability of the maps, subbasin distributions of alleles other than “Land Retirement” are summed over the two main tillage types: “conventional tillage” (to include conventional till and ridge-till), and “conservation tillage” (to include mulch-till and no-till).

The first set of maps looks at the distribution of land retirement for individual #4715, as well as a map of land retirement costs used in implementing the algorithm. Retirement of additional 9 percent of the cropland in the UMRB from production is needed for the control

of nitrates, while no additional land retirement is a part of a solution which reduces phosphorus only (#3821).

Comparing the distribution of land retirement with the distribution of estimated costs of land retirement, it is clear that the algorithm does not allocate land to be retired from production based on cost considerations alone, but rather on the impact that the spatial placement of land retirement has on nutrient loadings at the outlet. In fact, expensive areas in Illinois (Illinois River Watershed) are to be retired from production. Interestingly, land retirement is prescribed in one single compact area of the UMRB. Allocation of land retirement to land in close proximity to the watershed outlet has important policy implications of targeting land retirement efforts for the reduction of nitrate export from the watershed.

The single most widely selected conservation practice for this particular set of nutrient reduction targets is grassed waterways (and grassed waterways with the addition of nitrogen fertilizer reductions for individual #4715).

In fact, grassed waterways is really the only conservation practice selected for individual #3821. The fact that some terraces appear to be a part of the individual is due to the nature of “baseline-aware” constraints imposed on the allele set. These constraints ensured that, if a conservation practice is present in the baseline data, the algorithm could not remove the conservation practice or step down to another, “weaker”, conservation practice. Given these constraints, for instance, if a cropland HRU was observed to be in mulch-till, with a terrace, then the algorithm could only change that particular HRU to no-till in the tillage dimension, add nitrogen fertilizer reductions, or retire the HRU from production. It would not be allowed, however, to apply grassed waterways if a terrace was already in place.

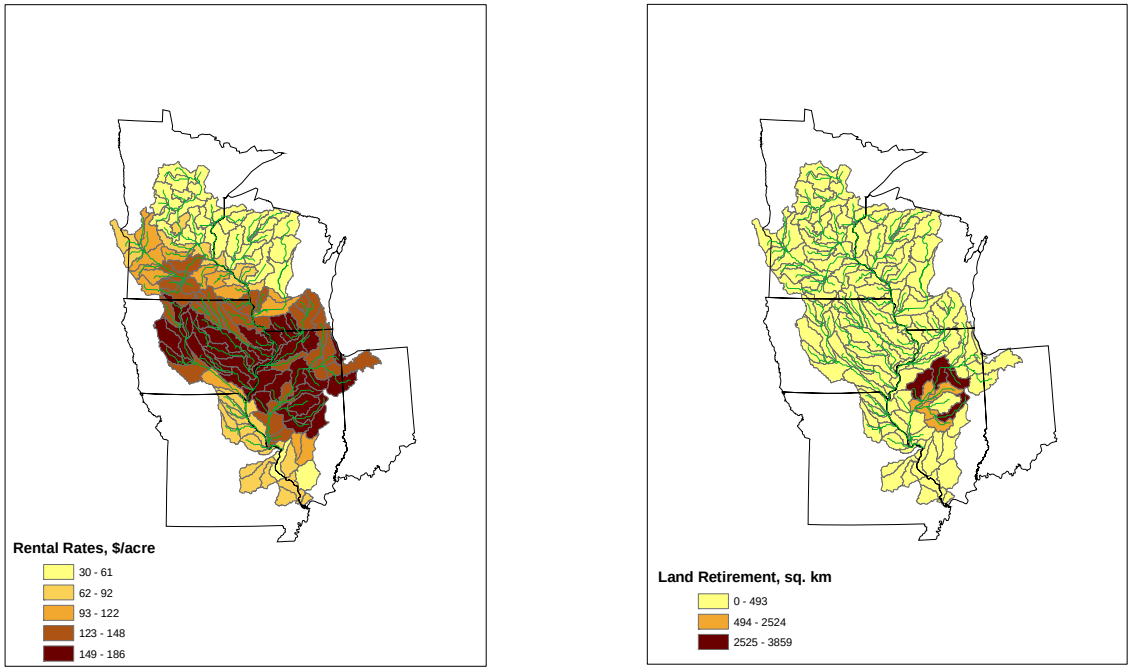

Figure 10. Cash rents and the distribution of land retirement, individual #4715

This explains the presence of terraced land as a part of makeup of individual #3821: the algorithm left the baseline terraced land as is.[48]

The two maps below present the distribution of grassed waterways in individual #3821. The map on the left presents grassed waterways interacted with "conventional"

[48] The presence of nitrogen fertilizer reduction alleles (#17-20) is observed as part of the makeup of individual 3821. This is counterintuitive, as nitrogen fertilizer reductions do very little to reduce outlet P (see Appendix). Mapping these alleles, it becomes apparent that the subbasins where these alleles are observed actually lie in Illinois, below the UMRB Grafton outlet. Thus, conservation practices in those subbasins do not affect nutrient loadings at Grafton, and, in the efficient solution, a zero-cost option should be selected for these subbasins. Fertilizer reductions are the cheapest conservation practice for Illinois but eventually, the algorithm should remove them from the subbasins which cannot help reduce loadings at Grafton. This again highlights the fact that the solutions produced by the algorithm are approximations to the truly efficient solutions.

tillage, while the map on the right presents grassed waterways combined with “conservation” tillage methods.

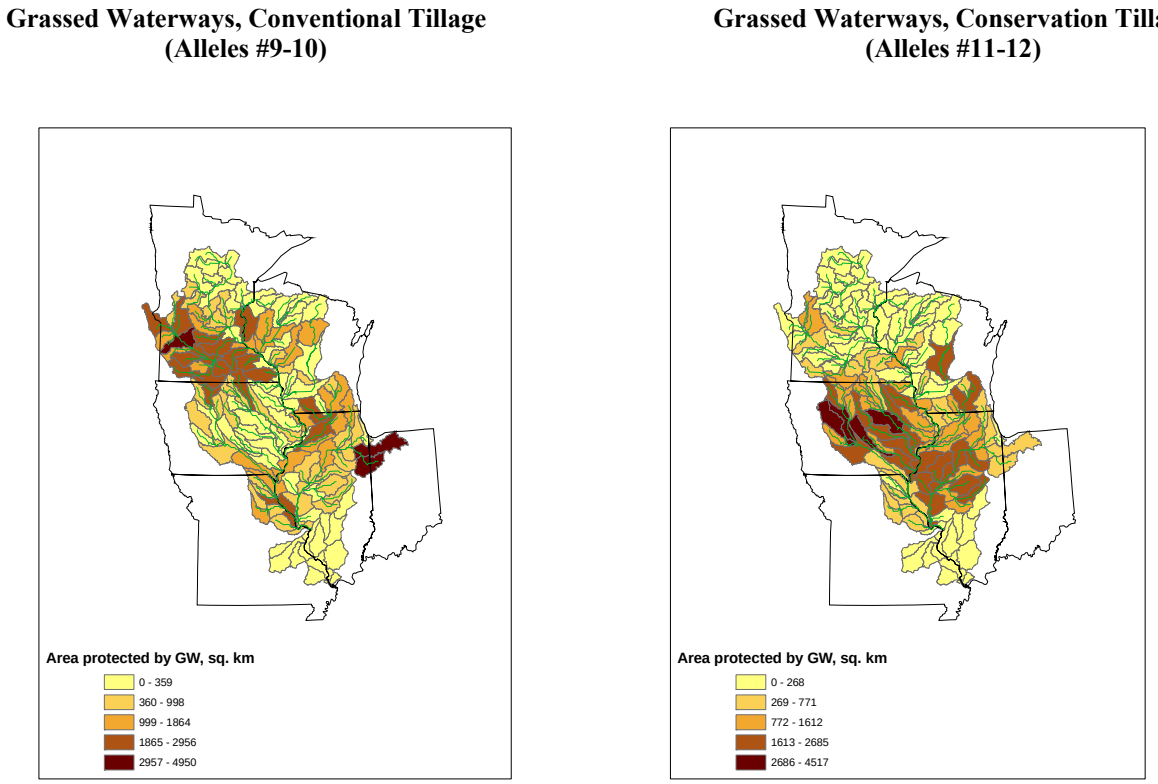

Figure 11. Distribution of grassed waterways, individual #3821

Grassed waterways combined with conventional tillage are predominant in the Minnesota, Northern Wisconsin, and Indiana portions of the UMRB, while grassed waterways with conservation tillage are selected by the algorithm for most of the Iowa and Illinois portions of the watershed. By overlaying the two maps it is clear that grassed waterways are prescribed for phosphorus control for the overwhelming majority of the subbasins in the UMRB.

For individual #4715, grassed waterways, in conjunction with nitrogen fertilizer reductions, are also prevalent. The distributions of grassed waterways, by tillage type, are presented below.

Grassed Waterways, Conventional Tillage, N fertilizer reduction (Alleles #25-26)

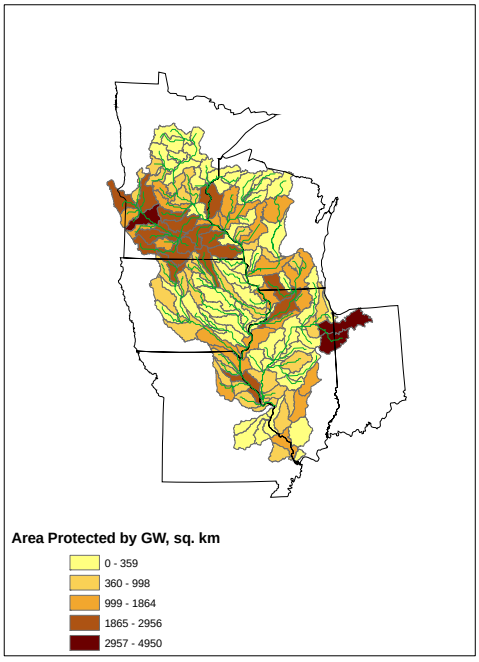

Grassed Waterways, Conservation Tillage, N fertilizer reduction (Alleles #27-28)

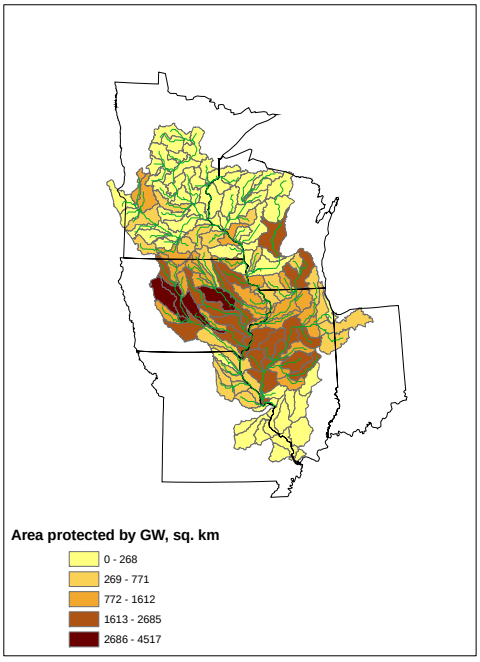

Figure 12. Distribution of grassed waterways, by tillage type, individual #4715

The distribution of grassed waterways across the two tillage types, ignoring the presence of fertilizer reductions is quite similar to the distribution within individual #3821.[49] This similarity, incidentally, has somewhat comforting policy implications. If the policy of

[49] In fact, given the nutrient reduction targets considered, protection of water quality by means of grassed waterways is recommended for most of the cropland HRUs in the UMRB for both individuals.

nutrient reductions in the UMRB proceeds sequentially, where phosphorus reduction strategy is implemented first, then, in order to achieve a nitrate target, no large-scale redistribution of grassed waterways would be required. Instead, adding fertilizer reductions 'on top of' existing grassed waterways, in conjunction with targeted land retirement, would consequently achieve the nitrate goal. Of course, if nitrate reduction is the goal, then phosphorus reductions follow immediately. This is an important finding, as nothing, in principle, guarantees that it should hold. The makeup of the two solutions could be quite distinct, which would then imply that choosing an initial nutrient reduction target is extremely important. However, for the UMRB, for the targets considered, it appears that if a policymaker gets the distribution of conservation practices right for one nutrient reduction goal, the other goal can subsequently be achieved with little to no (deadweight loss) spatial redistribution of conservation practices.

Finally, similarly to individual #3821, terraces present in the makeup of individual #4715 are also ones present in the baseline land use allocation. However, in contrast to #3821, nitrogen fertilizer reductions are added onto a large portion of terraced areas.

5.6.6. Implications of Selected Water Quality Targets

The analysis above was conducted under an objective of simultaneously reducing nitrate and phosphorus loadings at the outlet of the UMRB. Thus, in principle, the evolutionary algorithm only rewards those solutions which reduce nutrient loadings at the outlet subbasin, and does not directly seek reductions occurring in other subbasins in the watershed. This may have important implications for local water quality (subbasin-level

nutrient loadings). To illustrate, I again turn to individuals analyzed in the section above, and consider the spatial distribution of loadings of nitrates and phosphorus.

The first set of maps depicts the subbasin-level loadings of nitrates for individuals #4715 and #3821, expressed in terms of percentage of baseline loadings. The histogram below counts the number of subbasins where a particular loading reduction is observed.

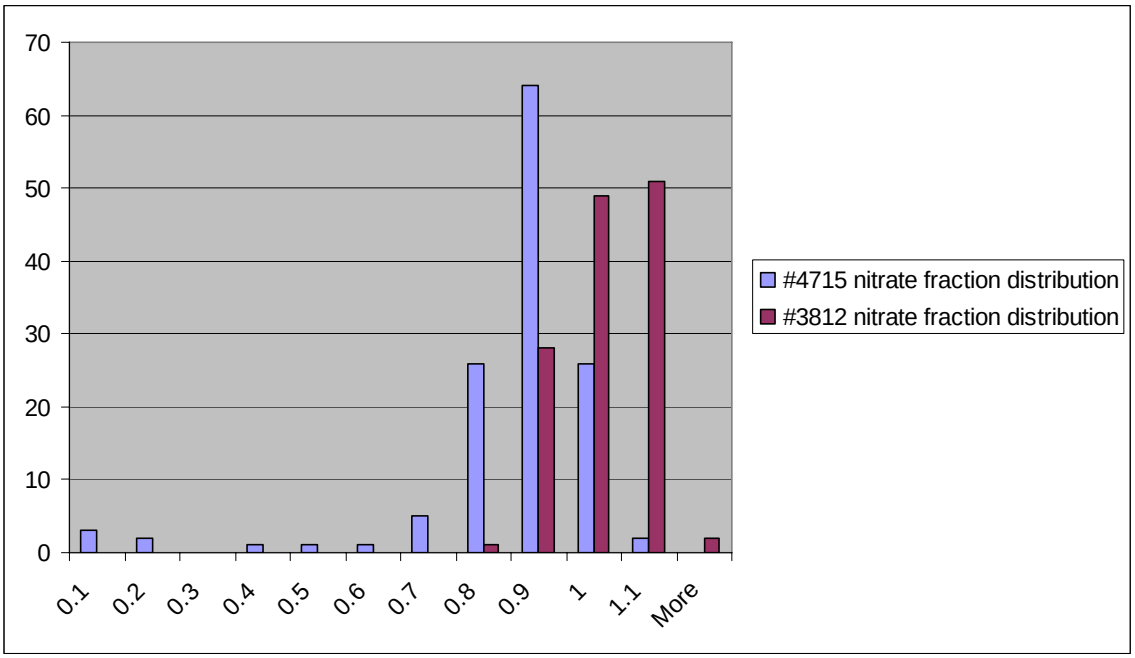

Figure 14. Histogram of subbasin nitrate loadings, by share of baseline loadings

As one can clearly see, setting a nutrient reduction goal in terms of reductions at the outlet of the watershed has profound implications for local water quality. When the goal is nitrate loading reductions at the outlet, the maps indicate that the algorithm allocates reductions very unequally, with a few subbasins where reductions are dramatic (over 90 percent), while many of the subbasins experience very modest nitrate loading reductions, if at

all. This is, of course, what one would expect the algorithm to do, given the location of the watershed outlet.

For individual #3821, about 20 subbasins out of 131 experience small reductions in nitrate loadings, with the remaining subbasins seeing no reductions at all or even an increase in nitrate loadings. Again, this is consistent with the nature of individual #3821, which is an individual which has been selected for its ability to reduce phosphorus alone, regardless of the consequence for nitrate loadings.

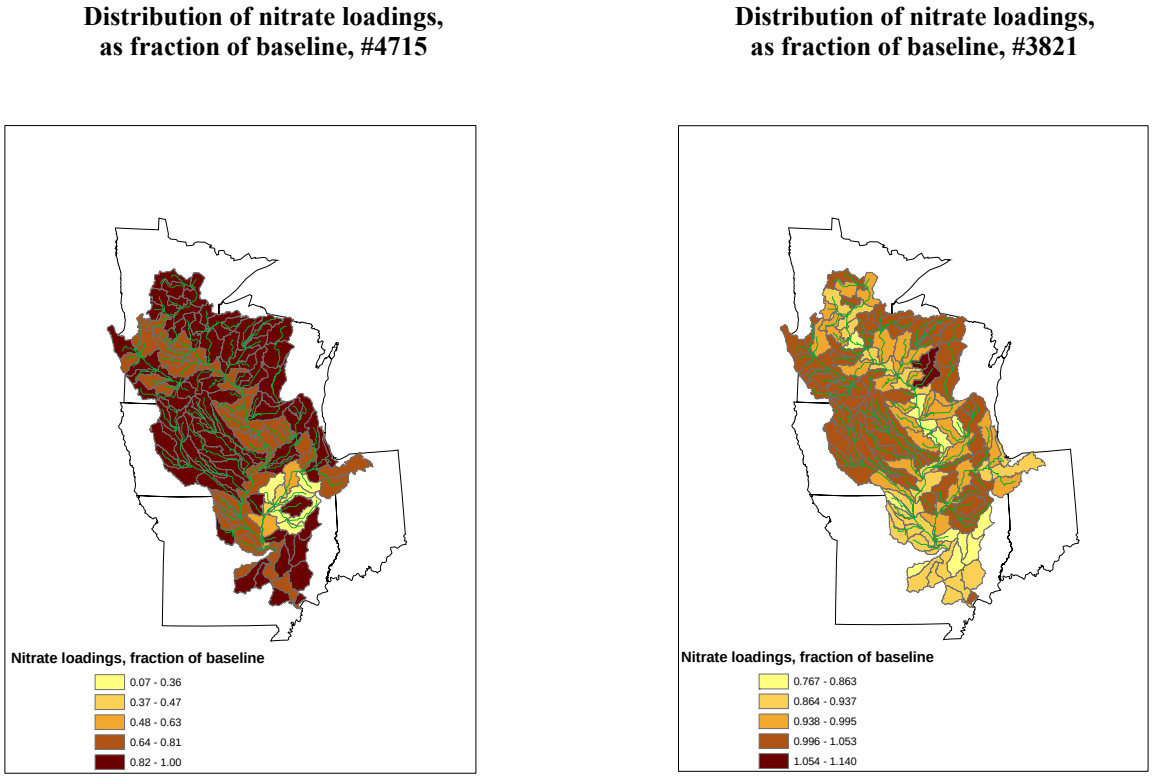

Figure 15. Subbasin nitrate loading distributions, individuals #4715 and #3821

It is also interesting to point out that some subbasins experiencing nitrate loading reductions follow the flow path of the Mississippi River (it is especially evident in

Minnesota), and of Illinois River. That is, the evolutionary algorithm allocates conservation practices to include nitrate loading reductions to the major waterways. Again, this is what one would expect the algorithm to do.

A different pattern is observed for subbasin-level phosphorus reductions. Maps below, as well as the histogram of subbasin loadings as a proportion of baseline loadings indicate that widespread application of grassed waterways (for both individuals), and land retirement (in the case of #4715) serves to produce a surprisingly uniform spatial distribution of sizeable phosphorus loading reductions.

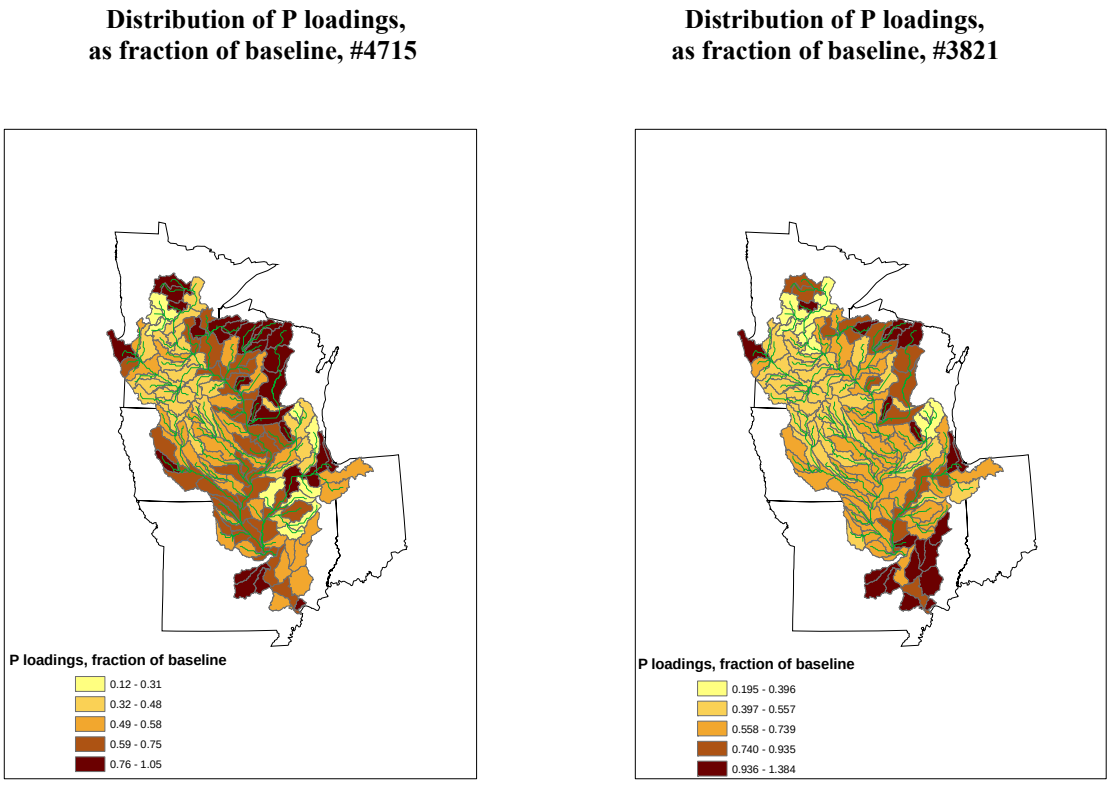

Figure 16. Subbasin phosphorus loading distributions, individuals #4715 and #3821

In particular, the mix of conservation practices describing individual #4715 produces a spatial pattern of reductions where only 16 subbasins do not experience phosphorus loading reductions. For individual #3812, loadings in 25 subbasins either do not decrease, or increase.

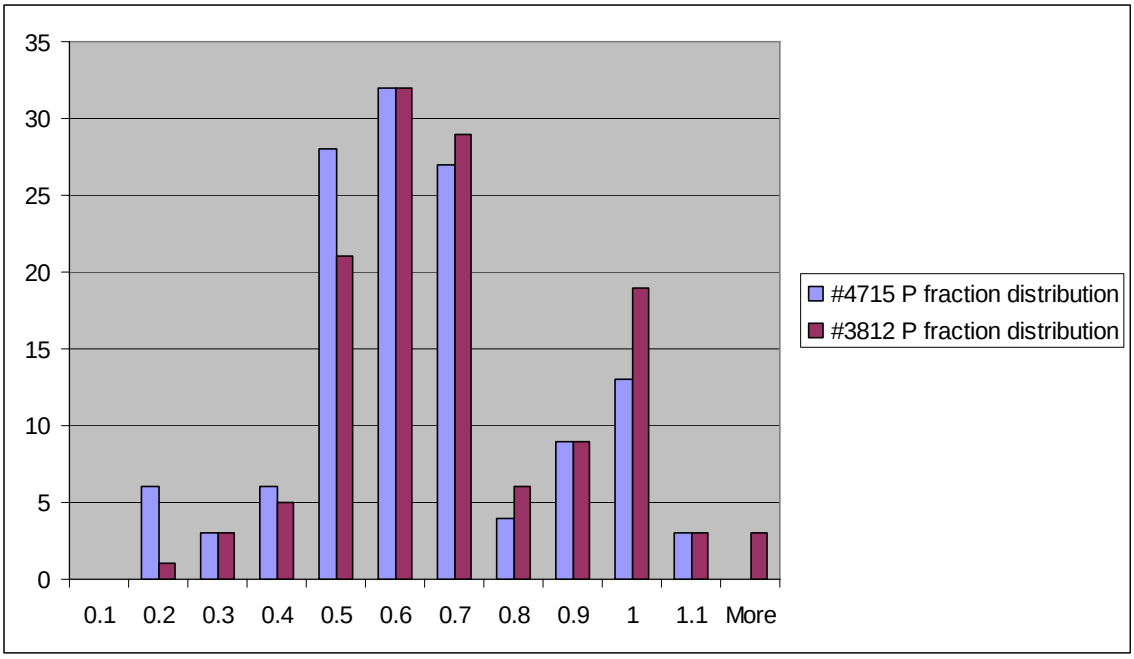

Figure 17. Histogram of subbasin phosphorus loadings, by share of baseline loadings

Thus, for the UMRB, the mix of conservation practices which efficiently reduces outlet phosphorus and nitrate loadings also produces large local water quality gains in terms of phosphorus loading reductions. Local nitrate loading reductions, on the other hand, are concentrated in a few select subbasins of the watershed.

One implication of these findings is that should a policy which strives to achieve outlet-level nitrate reductions for the UMRB be implemented, not only outlet-level phosphorus loadings are reduced automatically, but large and widespread improvements in

local P reductions can also be expected. Of course, many downstream loading reductions are inextricably linked to the introduction of conservation practices in the upstream subbasins.

5.7. Concluding Remarks

In this chapter, I examined the policy implications for efficient control of NPS pollution using a spatially explicit model of a large and critically important agricultural region: the Upper Mississippi River Basin in the central U.S. I derived the conservation production possibility frontier that explicitly incorporates the tradeoffs between pollution control costs and water quality benefits, between different pollutants, or between different control targets. To empirically estimate these tradeoffs, a modeling framework that (a) realistically incorporates the key attributes of NPS pollution and (b) is able to approximate the efficient solutions by optimally choosing the set of conservation practices for each spatial unit in the Basin was developed. The regional scale of the modeling framework facilitates the investigation of relevant policy analyses related to the growing "dead zone" in the Gulf of Mexico and the tradeoff between regional and local pollution reduction targets.

Several caveats should be mentioned. First, the enormity of the search spaces precludes one from characterizing the solutions obtained as truly efficient. However, I believe that the approximations found are quite relevant to policy analysis. Second, the results are indeed tied to the set of conservation practices and cost estimates. Although an effort was made to evaluate a wide variety of conservation practices discussed in water quality literature, inclusion of other possibly relevant practices (e.g., wetlands) may alter the results. This, however, is not so much a challenge to the modeling approach as an opportunity for further productive research.

Economists have long been able to point out that tradeoffs are ever-present in all of environmental policy, and in particular in nonpoint source pollution control. Tradeoffs are only meaningful when conservation policy options are efficient. Making such options explicit and thereby identifying numerous tradeoffs inherent in nonpoint source pollution control is the main contribution of this work.

5.8. References

Arabi, M., R. S. Govindaraju, and M. M. Hantush. 2006. Cost-effective allocation of watershed management practices using a genetic algorithm. *Water Resources Research* (42), W10429.

Arabi, M., J. Frankenberger, B. Engel, and J. Arnold. 2007. Representation of agricultural management practices with SWAT. *Hydrological Processes* (submitted).

Arnold, J.G., and P.M. Allen. 1996. Estimating hydrologic budgets for three Illinois watersheds. *Journal of Hydrology* 176: 57-77.

Arnold, J.G., and Fohrer, N. 2005. Current capabilities and research opportunities in applied watershed modeling. *Hydrological Processes* 19: 563-572.

Arnold, J.G., R. Srinivasan, R.S. Muttiah, and J.R. Williams. 1998. Large area hydrologic modeling and assessment part I: Model development. *Journal of American Water Resources Association* 34(1): 73-89.

Arnold, J.G., R.S. Muttiah, R. Srinivasan, and P.M. Allen. 2000. Regional estimation of base flow and groundwater recharge in the Upper Mississippi Basin. *Journal of Hydrology* 227: 21-40.

Arnold, J.G., R. Srinivasan, R.S. Muttiah, P.M. Allen, and C. Walker. 1999a. Continental scale simulation of the hydrologic balance. *Journal of American Water Resources Association* 35(5): 1037-1052.

Aulenbach, B.T., Buxton, H.T., Battaglin, W.A., and Coupe, R.H., 2007, Streamflow and nutrient fluxes of the Mississippi-Atchafalaya River Basin and subbasins for the period of record through 2005: U.S. Geological Survey Open-File Report 2007-1080. Available at: http://toxics.usgs.gov/pubs/of-2007-1080/index.html. Accessed August 1, 2007.

Bekele, E.G., and J.W. Nicklow. 2005. Multiobjective management of ecosystem services by integrative watershed modeling and evolutionary algorithms. *Water Resources Research, 41,* W10406, doi:10.1029/2005WR004090.

Borah, D.K., and M. Bera. 2004. Watershed-scale hydrologic and nonpoint-source pollution models: Review of applications. *Transactions of ASAE* 47(3): 789-803.

Braden, J.B., G.V. Johnson, A. Bouzaher, and D. Miltz. 1989. Optimal spatial management of agricultural pollution. *American Journal of Agricultural Economics* 61: 404–13.

Campbell, T. 2006. i_SWAT. Ames, Iowa: Center for Agricultural and Rural Development, Iowa State University. Available at: http://www.public.iastate.edu/~elvis/i_swat_main.html. Accessed May 6, 2006.

CENR, 2000, Integrated assessment of hypoxia in the northern Gulf of Mexico: National Science and Technology Council Committee on Environment and Natural Resources, Washington, DC. Available at: http://www.nos.noaa.gov/Products/pubs_hypox.html#fia. Accessed November 10, 2006.

Gassman, P.W., S. Secchi, M. Jha, and L. Kurkalova. 2006. Upper Mississippi river basin modeling system part 1: SWAT input data requirements and issues. In: Coastal Hydrology and Processes (ed. V.P. Singh and V.J. Xu). Water Resources Publications, Highlands Ranch, Colorado, pp. 103-116.

Gassman, P.W., M. Reyes, C.H. Green, and J.G. Arnold. 2007. The Soil and Water Assessment Tool: Historical development, applications, and future directions. *Transactions of ASABE*. (forthcoming).

Gassman, P.W., Campbell, T., Secchi, S., Jha, M., and Arnold, J.G., 2003. The i_SWAT software package: a tool for supporting SWAT watershed applications. In: SWAT2003: The 2nd International SWAT Conference, 1-4 July, Bari, Italy. Instituto di Ricerca sulle Acque, IRSACNR,Bari, Italy. pp. 66-69.

Jayakrishnan, R., R. Srinivasan, C. Santhi, and J.G. Arnold. 2005. Advances in the application of the SWAT model for water resources management. *Hydrologic Processes* 19(3): 749-762.

Jha, M., P.W. Gassman, S. Secchi, and J. Arnold. 2006. Upper Mississippi river basin modeling system part 2: baseline simulation results. In: Coastal Hydrology and Processes (ed. V.P. Singh and V.J. Xu). Water Resources Publications, Highlands Ranch, Colorado, pp. 117-126.

Jha, M., P.W. Gassman, S. Secchi, and J. Arnold. 2006. Upper Mississippi river basin modeling system part 2: baseline simulation results. In: Coastal Hydrology and Processes (ed. V.P. Singh and V.J. Xu). Water Resources Publications, Highlands Ranch, Colorado, pp. 117-126.

Khanna, M.,W. Yang, R. Farnsworth, and H. Onal. 2003. Cost effective targeting of CREP to improve water quality with endogenous sediment deposition coefficients. *American Journal of Agricultural Economics* 85: 538–53.

Kling, C.L., S. Rabotyagov, M. Jha, H. Feng, J. Parcel, P. Gassman, and T. Campbell. 2007. Conservation practices in Iowa: historical investments, water quality and gaps. Draft report. Center for Agricultural and Rural Development, Iowa State University, Ames, Iowa.

Kling, C. L., S. Secchi, M. Jha, H. Feng, and P.W. Gassman. 2006. Upper Mississippi river basin modeling system part 3: conservation practice scenario results. In: Coastal Hydrology and Processes (ed. V.P. Singh and V.J. Xu). Water Resources Publications, Highlands Ranch, Colorado, pp. 127-134.

Kling, C., S. Secchi, M. Jha, L. Kurkalova, H.F. Hennessy, and P.W. Gassman. 2005. Nonpoint source needs assessment for Iowa: The cost of improving Iowa's water quality. Final Report to the Iowa Department of Natural Resources. Center for Agricultural and Rural Development, Iowa State University, Ames, Iowa.

Kurkalova, L.A., Burkart, C., and Secchi, S., 2004. Cropland cash rental rates in the Upper Mississippi River Basin. 2004. Technical Report 04–TR 47. Center for Agricultural and RuralDevelopment, Iowa State University, Ames, Iowa. Available at: http://www.card.iastate.edu/publications/DBS/PDFFiles/04tr47.pdf. Accessed December 10, 2006.

Lohrenz, S.E., Fahnenstiel, G.L., Redalje, D.G., and Lang, G.A., 1992, Regulation and distribution of primary production in the northern Gulf of Mexico: In Program, N.C.O., Nutrient Enhanced Coastal Ocean Productivity, NECOP Workshop Proceedings, October 1991, Texas Sea Grant Publications, College Station, TX, p.95-104.

Lohrenz, S.E., Fahnenstiel, G.L., Redalje, D.G., Lang, G.A., Chen, X.G., and Dagg, M.J.,1997, Variations in primary production of northern Gulf of Mexico continental shelf waters linked to nutrient inputs from the Mississippi River: Marine Ecology-Progress Series, v. 155, p. 45-54.

Lohrenz, S.E., Fahnenstiel, G.L., Redalje, D.G., Lang, G.A., Dagg, M.J., Whitledge, T.E., and Dortch, Q., 1999b, Nutrients, irradiance, and mixing as factors regulating primary production in coastal waters impacted by the Mississippi River plume: Continental Shelf Research, v. 19, p. 1113-1141.

Lohrenz, S.E., Wiesenburg, D.A., Arnone, R.A., and Chen, X.G., 1999a, What controls primary production in the Gulf of Mexico?: In Sherman, K., et al., (eds.), The Gulf of Mexico Large Marine Ecosystem: Assessment, Sustainability and Management, Blackwell Science, Inc., Malden, MA, p. 151-170.

Mitchell, M. 1996. An introduction to genetic algorithms. Cambridge, Massachusetts: the MIT Press.

Montgomery, W.D. Markets in licenses and efficient pollution control programs. *Journal of Economic Theory* 1972; 5; 395-418.

NAS. 2000. The changing face of the UMR Basin; agriculture: Selected profiles of farming and farm practices. National Audubon Society, Upper Mississippi River Campaign, St. Paul, Minnesota. http://www.umbsn.org/news/documents/chg_face.pdf. Accessed November 5, 2006.

Neitsch, S.L., J.G. Arnold, J.R. Kiniry, R. Srinivasan, and J.R. Williams. 2005a. *Soil and Water Assessment Tool Theoretical Documentation*, version 2005. Temple, TX: Grassland, Soil and Water Research Laboratory, Agricultural Research Service.

Nusser, S. M., and J.J. Goebel. 1997. The national resources inventory: a long-term multisource monitoring programme. *Environmental and Ecological Statistics*. 4: 181-204.

Rabalais, N.N., Turner, R.E., and Scavia, D. 2002. Beyond science into policy: Gulf of Mexico hypoxia and the Mississippi River. *BioScience* 52(2): 129-141.

Ribaudo, M.O. 1986. Consideration of off-site impacts in targeting soil conservation programs. *Land Economics* 62: 402–11.

Ribaudo, M.O. 1989. Targeting the conservation reserve program to maximize water quality benefits. *Land Economics* 65: 320–32.

Santhi, C., J.G. Arnold, J.R. Williams, W.A. Dugas, R. Srinivasan, and L.M. Hauck. 2001a. Validation of the SWAT model on a large river basin with point and nonpoint sources. *Journal of American Water Resources Association* 37(5): 1169-1188.

Sawyer, J., E. Nafziger, G. Randall, L. Bundy, G. Rehm, B. Joern. 2006. Concepts and rational for regional nitrogen rate guidelines for corn. Iowa State University, Ames, Iowa. Available at: http://extension.agron.iastate.edu/soilfertility/nrate.aspx. Accessed April 10, 2006.

Seaber, P.R., F.P. Kapinos, and G.L. Knapp. 1987. Hydrologic Units Maps. U.S. Geological Survey, Water-Supply Paper 2294.

Secchi, S., P.W. Gassman, M. Jha, H.H. Feng, T. Campbell, and C.L. Kling. 2007. The cost of cleaner water: Assessing agricultural pollution reduction at the watershed scale. *Journal of Soil and Water Conservation.* 62(1): 10-21.

Secchi, S., M. Jha, L. A. Kurkalova, H. Feng, P.W. Gassman, C.L. Kling. 2005. The

designation of co-benefits and its implication for policy: water quality versus carbon sequestration in agricultural soils. CARD Working Paper 05-WP 389, Iowa State University, Ames, Iowa.

Shortle, J. S. and R. D. Horan. 2001. The Economics of Nonpoint Pollution Control. *Journal of Economic Surveys* 15(3): 255-289.

Srivastava, P., J.M. Hamlett, P.D. Robillard, and R.L. Day. 2002. Watershed optimization of best management practices using AnnAGNPS and a genetic algorithm. *Water Resources Research* 38(3): 1-14.

Sylvan, J.B., Dortch, Q., Nelson, D.M., Maier Brown, A.F., Morrison, W., and Ammerman, J.W. 2006. Phosphorus limits phytoplankton growth on the Louisiana shelf during the period of hypoxia formation. *Environmental Science and Technology*, 40 (24), 7548 - 7553.

United States Department of Agriculture, Economic Research Service. Fertilizer input data available at http://www.ers.usda.gov/Data/FertilizerUse. Accessed November 5, 2006.

United States Department of Agriculture, National Resource Conservation Service. Program cost data available at http://www.nrcs.usda.gov/PROGRAMS/EQIP/. Accessed November 5, 2006.

Veith, T.L., M.L. Wolfe, and C.D. Heatwole. 2003. Development of optimization procedure for cost-effective BMP placement. *Journal of the American Water Resources Association* 39(6): 1331-1343

Wall, M. 1996. GAlib: A C++ Library of Genetic Algorithm Components. Version 2.4.6. Available at: http://lancet.mit.edu/ga/. Accessed January 20, 2006.

Zitzler E., Laumanns M., and Thiele L. 2002. SPEA2: Improving the Strength Pareto Evolutionary Algorithm for Multiobjective Optimization. Evolutionary Methods for Design, Optimisation, and Control, CIMNE, Barcelona, Spain, pp. 95-100.

CHAPTER 6. GENERAL CONCLUSIONS

The four chapters above highlight the importance of both epistemic and aleatory uncertainty and suggest ways to handle some uncertainties inherent in contemporary environmental policy problems.

In the first chapter, I aim to characterize an optimal spatial allocation of land parcels to specific environmental practices explicitly dealing with uncertainty in both the benefits and program costs. The empirical application focuses on a heavily agricultural Iowa watershed, and atmospheric carbon sequestered by agricultural soils is used as a measure of environmental benefit. The results provide a magnitude of uncertainty discount for soil carbon offsets and the margin of safety necessary in the budget to ensure at the planning stage that the program's costs will not exceed the planned expenditures. Overall, the magnitudes of the uncertainty discount for soil carbon suggest that soil carbon sequestration in Iowa may be a viable option both for a regulator concerned with reducing greenhouse gas emissions and for an aggregator who considers consolidating land enrollment and selling carbon credits. Future research directions may include adding the time dimension to the problem, as well as addressing issues of contract design and compliance.

In the second chapter, the design of permit trading programs when the objective is to minimize the cost of achieving an *ex ante* pollution target; that is, one that is defined in expectation rather than an *ex post* deterministic value, is examined. I demonstrate that to minimize expected abatement costs regulators must use information on the joint distribution of firms' abatement costs, as well as the pollution delivery coefficients. As a result, the optimal trading ratio is a function of the delivery coefficient, as well as the moments of abatement costs, and the total permit allocation deviates from the pollution goal. These

findings differ from a typical permit market design, where no cost information is needed to achieve cost-efficiency, the trading ratio is set to the ratio of pollution delivery coefficients, and the permit allocation exactly equals the pollution goal. It is hoped that these findings may both contribute to a clearer understanding of the theoretical properties of a permit trading system with pollution targets specified in terms of averages, as well as serve to improve the design of real-world permit trading programs.

The third and the fourth chapters of the thesis build a simulation-optimization modeling framework for the analysis of efficient nonpoint source pollution reduction strategies. These essays integrate modern multi-objective optimization tools with a realistic water quality model to provide decision-makers with sets of cost-efficient pollution reduction solutions.

In the first application, I search for allocations of conservation practices that minimize the costs of achieving given water quality targets for all the major watersheds in the state of Iowa, a state greatly affected by nonpoint source pollution. The resulting set of tradeoffs is used to generate watershed-level nonpoint source pollution abatement curve. Availability of nonpoint source pollution abatement cost curves makes solving for a cost-minimizing way of reducing state-level nutrient loadings straightforward. In particular, watershed-level loading reduction allocations for a variety of state-level nutrient reduction goals are found. I also explore how the cost-minimizing solution changes as a result of imposing local water quality constraints.

Furthermore, watershed-level nutrient pollution reductions which minimize state-wide costs are translated into a specific mix and distribution of conservation practices which achieve these water quality goals. For the range of nutrient loading reductions considered,

grassed waterways (often implemented jointly with no-till and nitrogen fertilizer reductions) was the conservation practice selected most often. Terraces and targeted land retirement were also found to be a part of cost-minimizing solutions.

The results suggest that significant inefficiencies exist in the current suite of conservation practices in Iowa. This, in turn, signals an opportunity for reallocation of conservation practices in a way that could result in lower level of investment in conservation practices and in lower levels of nutrient pollution. For example, results indicate that a 20 percent reduction in state-level nitrate loading export, as well as a 30 percent reduction in watershed-level phosphorus loadings could be achieved at a cost which is lower than the baseline investment in conservation practices.

In the final chapter, I examine the policy implications for efficient control of nonpoint source pollution using a spatially explicit model of a large and critically important agricultural region: the Upper Mississippi River Basin in the central U.S. I derive the conservation production possibility frontier that explicitly incorporates the tradeoffs between pollution control costs and water quality benefits, between different pollutants, or between different control targets. To empirically estimate these tradeoffs, a modeling framework that (a) realistically incorporates the key attributes of NPS pollution and (b) is able to approximate the efficient solutions by optimally choosing the set of conservation practices for each spatial unit in the Basin was developed. The regional scale of the modeling framework facilitates the investigation of relevant policy analyses related to the growing "dead zone" in the Gulf of Mexico and the tradeoff between regional and local pollution reduction targets.

Future research potential of evolutionary algorithms in general, and of the coupled water quality model-evolutionary algorithm framework in particular, is enormous. Improvements in the water quality models and better availability of detailed spatial land use and conservation practices data can drastically increase the level of detail and realism of the obtained solutions. Considerations of additional or alternative environmental objectives (e.g., nutrient concentrations, or a specific quantile of the loadings distribution) may be in order to better address the nature of nutrient pollution. Increased computational capacity may allow for better characterizations of uncertainty imbedded in the input data and/or the water quality model parameters.

On a final note, I would like to mention that while research such as this one may be able to provide insights to policymakers on how to handle particular uncertainties and complexities which are endemic to most important environmental problems, the public should not accept the presence of uncertainties as an excuse for the lack of action. Academic research will likely never be able to resolve all the uncertainties associated with interactions of economic agents, social institutions, and the environment. Thus, when a pressing environmental issue (such as nonpoint source nutrient pollution) arises, a policy response ought not to wait for the "final answer" from the research community. Instead, policy and relevant research should co-exist in time, ideally with a positive feedback loop, where policy action stimulates research, and policy-relevant research has the power to influence policy discussions. I hope that this research contributes, to whatever extent, to improving the policy options for environmental protection.

APPENDIX A. APPENDIX TO CHAPTER 2

Proposition 1 (Paris and Easter, 1985). *If* $\mathbf{\Omega}$ *is a positive semi-definite matrix, the function* $\left(\mathbf{x}'\mathbf{\Omega}\mathbf{x}\right)^{1/2}$ *is convex.*

Proof. Let $\mathbf{w} = \lambda\mathbf{y} + (1-\lambda)\mathbf{z}$, where $\lambda \geq 0$ is a real scalar, and $\mathbf{y}$ and $\mathbf{z}$ are $N \times 1$ vectors. One then needs to show that $\left(\mathbf{w}'\mathbf{\Omega}\mathbf{w}\right)^{1/2} \leq \lambda\left(\mathbf{y}'\mathbf{\Omega}\mathbf{y}\right)^{1/2} + (1-\lambda)\left(\mathbf{z}'\mathbf{\Omega}\mathbf{z}\right)^{1/2}$. Invoking the Cauchy-Schwartz inequality, $\left(\mathbf{x}'\mathbf{\Omega}\mathbf{z}\right)^{2} \leq \left(\mathbf{x}'\mathbf{\Omega}\mathbf{x}\right)\left(\mathbf{z}'\mathbf{\Omega}\mathbf{z}\right)$, and since, by the definition of positive semi-definiteness, $\mathbf{x}'\mathbf{\Omega}\mathbf{x} \geq 0$ and $\mathbf{z}'\mathbf{\Omega}\mathbf{z} \geq 0$, obtain: $\left(\mathbf{x}'\mathbf{\Omega}\mathbf{z}\right) \leq \left(\mathbf{x}'\mathbf{\Omega}\mathbf{x}\right)^{1/2}\left(\mathbf{z}'\mathbf{\Omega}\mathbf{z}\right)^{1/2}$. Now,

$$
\begin{aligned}
(\mathbf{w}'\mathbf{\Omega}\mathbf{w}) &= \left[\lambda\mathbf{x} + (1-\lambda)\mathbf{z}\right]' \mathbf{\Omega}\left[\lambda\mathbf{x} + (1-\lambda)\mathbf{z}\right] \\
&= \lambda^2\mathbf{x}'\mathbf{\Omega}\mathbf{x} + 2\lambda(1-\lambda)\mathbf{x}'\mathbf{\Omega}\mathbf{z} + (1-\lambda)^2\mathbf{z}'\mathbf{\Omega}\mathbf{z} \\
&\leq \lambda^2\mathbf{x}'\mathbf{\Omega}\mathbf{x} + 2\lambda(1-\lambda)(\mathbf{x}'\mathbf{\Omega}\mathbf{x})^{1/2}(\mathbf{z}'\mathbf{\Omega}\mathbf{z})^{1/2} + (1-\lambda)^2\mathbf{z}'\mathbf{\Omega}\mathbf{z} \\
&= \left[\lambda(\mathbf{x}'\mathbf{\Omega}\mathbf{x})^{1/2} + (1-\lambda)(\mathbf{z}'\mathbf{\Omega}\mathbf{z})^{1/2}\right]^2
\end{aligned}
$$

Taking the square root on both sides, obtain the result, and letting $\boldsymbol{\delta} = \mathbf{x}$ and $\mathbf{\Sigma} = \mathbf{\Omega}$, it is clear that $\left(\boldsymbol{\delta}'\mathbf{\Sigma}\boldsymbol{\delta}\right)^{1/2}$ is convex.

APPENDIX B. APPENDIX TO CHAPTER 3

B.1. Proof of Equation (3.13)

Since the permit market constraint must hold for every level of firms' emissions, it also must hold for expected emissions levels, that is, $E[e_1^*] + tE[e_2^*] = \bar{P}^*_{permit}$. Taking the difference of this equation and the *ex ante* pollution constraint in (3.1), obtain

$$\bar{P}^*_{permit} - \bar{P}_{ante} = E[e_2^*]t^* - E[de_2^*] \tag{B.1}$$

Note that $E[de_2^*] = E[d]E[e_2^*] + Cov(d, e_2^*)$, $E[d] = \mu$, and $Cov(d, e_2^*) = \frac{Cov(d,\theta_2) - t^* Cov(d,\theta_1)}{2c}$. Rearranging equation (B.1) with these relationships, obtain (3.13).

B.2. More Details on $t^* < d$

First note that, if $\text{cov}(\theta_1, \theta_2) \le 0$, then clearly $t^* \ge d$ from (3.12). However, it is possible to have $t^* < d$, if $\text{cov}(\theta_1, \theta_2) > 0$ and large enough. The intuition is as follows. Equation (3.18) implies that the actual pollution level, compared to the *ex ante* target, depends on $(t-d)(t\theta_1 - \theta_2)$. If θ_1 is high when θ_2 tends to be low, then P_{actual} is high if $t - d > 0$. Since it is desirable to have a high pollution when marginal cost is high (i.e., θ_1 is high), it is optimal for $t^* - d > 0$. On the other hand, if θ_1 is high when θ_2 tends to be high, and if θ_2 tends to be so high that $(t\theta_1 - \theta_2) \le 0$, then P_{actual} will be relatively high only if $t - d \le 0$. In such a situation, $t^* - d \le 0$ is optimal. In the paper, most of our discussions focus on the case where $t^* - d > 0$. The other case can be analyzed similarly.

APPENDIX C. APPENDIX TO CHAPTER 4

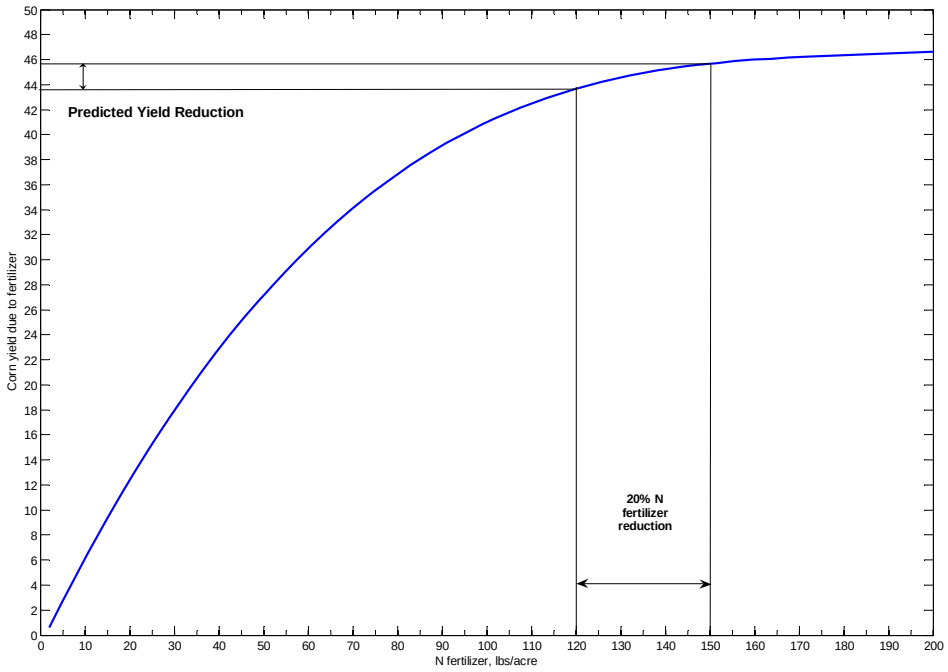

Figure 1C. Example of computation of corn yield reduction using a yield response curve (corn-soybean rotation)

Note: Polynomial response curve (N is fertilizer rate, lbs/acre):

$$yield = 2.099947\text{E-}09 \cdot N^4 + 6.122697\text{E-}06 \cdot N^3 - 0.003794412 \cdot N^2 + 0.734609417 \cdot N - 0.861475151$$

Table 1C. Fitted cost curve parameters

	Boyer	Des Moines	Floyd	Iowa	Little Sioux	Maquoketa
Intercept	18.8204	20.9101	18.3279	20.4981	17.5395	15.9875
N	-0.1284	-0.0015	-0.2808	**-0.0007**	**0.0041**	**-0.0169**
P	-0.1304	-0.0283	0.3302	0.0378	1.0507	2.2300
N^2	0.0022	1.31E-06	0.0109	**1.12E-06**	0.0003	**0.0177**
P^2	0.0252	0.0028	0.0447	0.0013	0.0229	6.8163
NP	-0.0207	-0.0003	-0.1008	-0.0003	-0.0258	-4.9884
R^2	*0.9394*	*0.9830*	*0.8719*	*0.7533*	*0.7170*	*0.6995*

Table 1C, continued

	Monona	Nishnabotna	Nodaway	Skunk	Turkey	Upper Iowa	Wapsipinicon
Intercept	18.2541	19.8098	17.9707	19.2702	18.2548	17.5869	19.3016
N	-0.4097	-0.0564	-0.2889	**-0.0010**	**0.0004**	-0.0324	-0.0164
P	0.8053	**-0.0012**	0.5255	0.0324	0.0479	0.6691	0.1135
N^2	0.0228	0.0004	0.0116	**1.31E-05**	**-0.0001**	**4.843E-05**	0.0001
P^2	0.0669	0.0011	**-0.0122**	0.0026	0.0067	-0.0558	0.0242
NP	-0.1832	-0.0014	-0.0537	-0.0023	-0.0063	-0.0902	-0.0068
R^2	*0.8132*	*0.7542*	*0.7789*	*0.7870*	*0.8495*	*0.9050*	*0.8212*

Nitrate and P loadings are scaled by dividing by 100,000.
Bold coefficients are not significant.

Table 2C. Reductions in nitrate loadings (relative to baseline) from a uniform application of each allele

Allele #	Allele Description	Boyer	Des Moines	Floyd	Iowa	Little Sioux	Maquoketa	Monona	Nishnabotna	Nodaway	Skunk	Turkey	Upper Iowa	Wapsipinicon
1	**Land retirement**	93	90	94	94	94	94	93	91	85	89	88	92	92
2	**CT**	-98	3	46	6	31	45	42	-2	-6	2	6	17	21
3	**CT RF**	1	17	56	19	40	57	53	7	3	13	15	2	33
4	**NT**	2	6	2	7	5	21	15	16	10	7	10	28	10
5	**NT RF**	19	22	18	22	19	35	31	30	24	20	23	19	25
6	**CT Terraced**	39	18	48	22	50	35	44	46	35	30	32	22	32
7	**CT Terraced RF**	52	34	60	36	60	49	58	57	46	44	44	37	45
8	**NT Terraced**	10	6	-5	9	10	16	9	22	14	5	15	-6	7
9	**NT Terraced RF**	27	22	12	24	26	32	27	37	29	20	30	13	23
10	**CT Contour**	13	9	45	13	38	39	40	19	7	12	12	14	24
11	**CT Contour RF**	25	24	57	27	48	52	54	30	17	26	23	28	37
12	**NT Contour**	2	2	-7	6	3	17	6	15	8	-2	5	-8	5
13	**NT Contour RF**	20	19	10	21	19	33	24	31	23	14	20	11	22
14	**CT GW**	28	17	53	20	46	44	52	30	21	30	25	29	33
15	**CT RF GW**	38	31	63	33	54	56	63	39	30	40	34	40	45
16	**NT GW**	14	9	5	10	12	22	20	24	18	14	19	6	13
17	**NT RF GW**	29	25	20	25	26	36	35	38	32	27	31	22	28

Table 3C. Reductions in phosphorus loadings (relative to baseline) from a uniform application of each allele

Allele #	Allele Description	Boyer	Des Moines	Floyd	Iowa	Little Sioux	Maquoketa	Monona	Nishnabotna	Nodaway	Skunk	Turkey	Upper Iowa	Wapsipinicon
1	**Land retirement**	81	86	87	86	87	90	74	78	77	84	82	86	86
2	**CT**	-129	-88	-27	-79	-17	-86	-53	-100	-91	-87	-79	-132	-101
3	**CT RF**	-86	-86	-25	-78	-14	-84	-48	-97	-87	-84	-77	21	-99
4	**NT**	31	42	54	38	42	37	26	37	34	44	21	-128	36
5	**NT RF**	33	43	54	39	44	37	27	38	36	45	23	24	38
6	**CT Terraced**	77	80	91	76	85	82	84	74	71	77	69	79	80
7	**CT Terraced RF**	78	80	91	76	86	83	85	75	71	77	69	79	81
8	**NT Terraced**	89	86	94	78	91	85	88	89	86	88	81	83	83
9	**NT Terraced RF**	89	87	94	78	91	86	89	89	87	89	82	85	85
10	**CT Contour**	-22	6	44	4	36	0	23	-25	-19	-6	-18	-25	-1
11	**CT Contour RF**	-19	7	45	5	38	1	26	-23	-17	-5	-16	-23	0
12	**NT Contour**	55	68	77	61	68	63	58	59	57	66	47	55	63
13	**NT Contour RF**	56	69	77	62	69	63	59	60	58	67	49	57	65
14	**CT GW**	-4	22	48	20	42	28	31	-10	-4	13	-7	6	18
15	**CT RF GW**	-2	23	49	21	43	29	34	-8	-2	15	-6	8	19
16	**NT GW**	61	69	78	62	70	67	61	63	62	69	51	59	65
17	**NT RF GW**	61	70	78	63	71	68	62	64	63	70	52	61	67

C.1. Incorporating Local Nutrient Reduction Targets

Given that the algorithm searching for efficient nitrate reductions at the watershed outlet produces a distribution of subbasin-level nitrate loadings where most of the subbasins do not experience nitrate loading reductions, it may be necessary to look for solutions which achieve local (subbasin-level) nitrate reduction goals. One then is facing a problem of incorporating (multiple) constraints into an evolutionary algorithm.

One way of incorporating multiple, subbasin-level, constraints into a multiobjective evolutionary algorithm is by means of a penalty function approach (Deb, 2001). For a particular individual X, a measure of overall constraint violation is computed, based on subbasin nutrient (e.g., nitrate) loadings implied by the allele makeup of X:

$\Omega(X) = \sum_{j=1}^{J} \max(0, N_j(X) - \beta N_j^{baseline})$, where $\beta \in (0,1]$ is the proportion of baseline loadings in each subbasin j to which nitrate loadings are to be reduced, and J is the total number of subbasins in the watershed. That is, a feasible solution $\hat{X}$ which satisfies all local nitrate constraints has an $\Omega(\hat{X})$ value of zero.

Then, each of the objectives in the multiobjective problem is augmented by scaled Ω to create new objectives $F^i(X) = f^i(X) + R_i \cdot \Omega(X)$, $i = 1,...,N$ (number of environmental objectives), and where R_i is chosen to appropriately scale Ω. The cost objective undergoes a similar transformation. For example, a set of objectives $(F^N, F^P, C) = (\Omega, f^P + R_P \cdot \Omega, c + R_c \cdot \Omega)$ sets up a problem the solution to which would be a Pareto-efficient frontier in the phosphorus-control cost space subject to the set of constraints on subbasin-level nitrate loadings.

What can one expect from a solution to the problem which incorporates local water quality targets? At first glance, one could expect that every subbasin's nutrient loadings would be reduced by the specified percentage. Upon more reflection, however, it definitely becomes possible that some subbasins may experience nutrient reductions greater than the required goal. One can conceive of a watershed where, in the upper reaches, required reductions are achieved exactly. There may be subbasins, however, which, due to the watershed's hydrology, benefit from reductions from several upstream subbasins at once (even if no abatement activity takes place in the subbasin in these particular subbasins). One can see then that, due simply to the hydrologic routing structure of the watershed, exact reductions in upstream subbasins could produce more than required reductions in the downstream subbasins.[50]

With these considerations in mind, I apply a two-dimensional version of the constraint-handling technique discussed above to the problem of reducing nitrates in every subbasin of the Des Moines River Watershed by 50 percent (that is, $\beta = 0.5$). That is, the two objectives in the multiobjective evolutionary algorithm become $(F^N, C) = (\Omega, c + R_c \cdot \Omega)$, where R_c is chosen to equal 1. The outcome of a two-dimensional problem is a two-dimensional frontier in (Ω, C) space, and the solutions satisfying the set of local nitrate reduction constraints are located on the $(0, C)$ axis.[51]

[50] This also relates to a standard feature of many traditional optimization problems, where imposing multiple constraints is likely to lead to some of the constraints being non-binding at the optimum.

[51] An alternative solution approach would be to abandon multiobjective evolutionary algorithms and to turn to a traditional, single-objective genetic algorithm. Framed in terms of fitness maximization, the fitness (s) of solutions satisfying the set of local nutrient constraints could be calculated as $s_i = C_{\max} - C_i$, where $C_{\max}$ is, for example, the highest cost observed at current generation, and C_i is the control cost for individual i. Solutions not satisfying the set of constraints could be assessed a fitness value of $s_i = C_{\max} - C_i - k \cdot \Omega_i$,

A two-dimensional version is chosen for two reasons. First, given the size of the search space, including an extra dimension (e.g., outlet P) in the problem could lead to a large number of individuals appearing which reduce P without attaining the nitrate standard, carry a higher control cost, but yet are non-dominated because of the P reductions. Second reason is more problem-specific. For an individual found to reduce outlet nitrates by 50 percent (individual #3610), subbasin-level nitrate reductions for several subbasins fall short of a 50 percent reduction achieved in the outlet subbasin (Table 4C):

Table 4C: Subbasin distribution of nutrient loadings for individual #3610 for the Des Moines River Watershed (focus on outlet nitrate reductions)

Subbasin	NO_3, tons/yr	P, tons/year	NO_3, % reduction	P, % reduction
1	1,369	83	37	58
2	4,589	182	34	51
3	6,297	141	22	66
4	21,243	688	31	44
5	5,435	181	32	24
6	5,234	236	70	63
7	422	52	90	82
8	29,388	1,001	46	55
9 (outlet)	35,012	1,034	50	59

Figure 1B presents the frontier from which an individual satisfying subbasin-level nitrate reductions can be found. Overall constraint violation, Ω, is depicted on the horizontal axis. Thus, an individual satisfying the set of local nitrate reduction constraints is located on the vertical axis. Individual #5335 was found in the portion of the frontier near the axis. As expected, the subbasin distribution of nitrate reductions is such that every subbasin, except

where Ω_i is the measure of overall constraint violation by individual i, computed in the manner discussed above, and $k > 0$ is a scaling factor.

subbasins 1, experience nitrate loading reductions of at least 50 percent, and subbasins 1 comes very close.

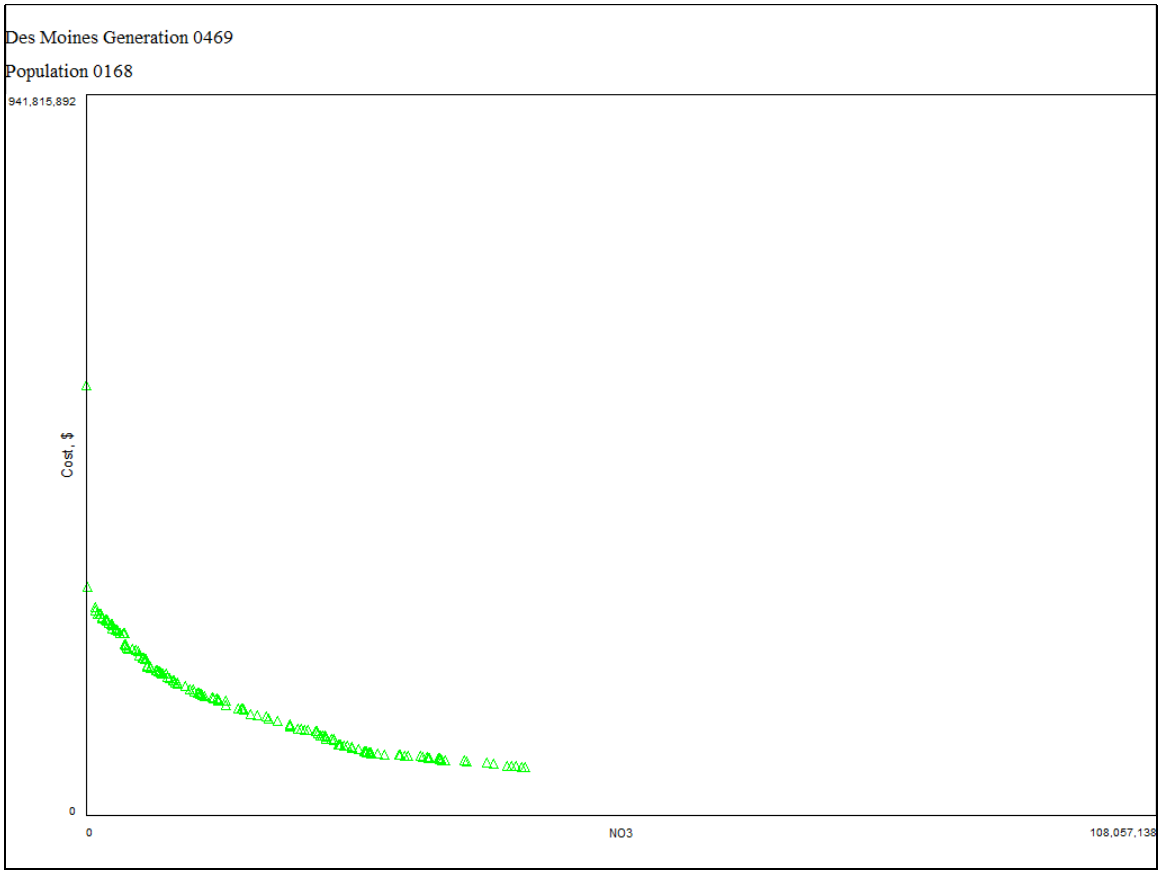

Figure 2C. Frontier incorporating 30 percent local nitrate reduction constraints, Des Moines River Watershed

Table 5C presents the subbasin distribution of nutrient loadings for individual #5335. While this individual achieves greater nitrate reductions on a subbasin level, subbasin-level P reductions are smaller in some subbasins, while they are larger in others.

The cost of individual #3610 was found to be about $295 million per year, while the cost of individual #5335 was found to be $299 million per year. Not surprisingly, enforcing

Table 5C. Subbasin distribution of nutrient loadings for individual #5335 for the Des Moines River Watershed (imposing local 50 percent nitrate reduction constraints)

Subbasin	NO_3, tons/yr	P, tons/year	NO_3, % reduction	P, % reduction
1	1,234	80	43	60
2	3,450	168	50	55
3	2,939	148	64	65
4	12,939	585	58	53
5	1,889	60	76	75
6	8,735	339	51	47
7	1,667	188	59	34
8	25,964	1,355	52	39
9 (outlet)	35,118	1,520	50	40

stricter standards for nitrates in all of the watershed subbasins results in a higher control cost.[52]

However, perhaps what is even more important than the cost difference is the potential difference in the set of conservation practices which would be required to achieve nitrate reductions in all the subbasins. This again highlights the connection of any "efficient" conservation placement to the set of environmental targets.

For this watershed, I find the following set of conservation practices which meet the local nitrate standard (distribution of total allele areas for individual #3610 are presented for comparison):

The differences in the algorithm's prescriptions are even more apparent in the map of subbasin-level distributions of the alleles for the two individuals.

[52] Individual #5335's P loadings are higher in some subbasins than those of #3610. If outlet-level P reductions are still the goal, the constrained version of the algorithm can be implemented in 3 dimensions (Ω, $P+R\Omega$, $C+R\Omega$), and an individual achieving same outlet P reductions as #3610 could be found. I expect such individual to be more costly than #5335.

Table 6C. Distribution of alleles for individuals #5335 and #3610

Allele Description	Individual #5335	Individual #3610
Land retirement	6,995	6,202
CT	226	16
CT RF	346	13
NT	334	65
NT RF	62	120
CT Terraced	49	26
CT Terraced RF	360	2,426
NT Terraced	19	0
NT Terraced RF	13	25
CT Contour	85	38
CT Contour RF	13	69
NT Contour	224	13
NT Contour RF	256	12
CT GW	27	2,309
CT RF GW	16,214	11,460
NT GW	39	12
NT RF GW	125	2,581

While individual #5335 employs land retirement to a somewhat larger extent, it is in the distribution of land retirement where the differences between the two individuals are most readily apparent. Relative to individual #3610, which falls short of the nitrate target in subbasins 1 through 5, and which does not allocate any land retirement to these subbasins, individual #5335 reduces nitrates in these subbasins by allocating land retirement to these subbasins. Interestingly, in subbasin 8, individual #5335 utilizes much less land retirement than individual #3610 does, while nitrate loadings in this subbasin are smaller for individual #5335 than for individual #3610. This observation, I believe, provides empirical support to the discussion above: that is, higher upland nitrate reductions achieved by the allele distribution of individual #5335 allows for scaling back the use of land retirement in subbasin 8, without sacrificing any nitrate reductions.

In addition to land retirement, grassed waterways (with and without nitrogen fertilizer

Individual #3610

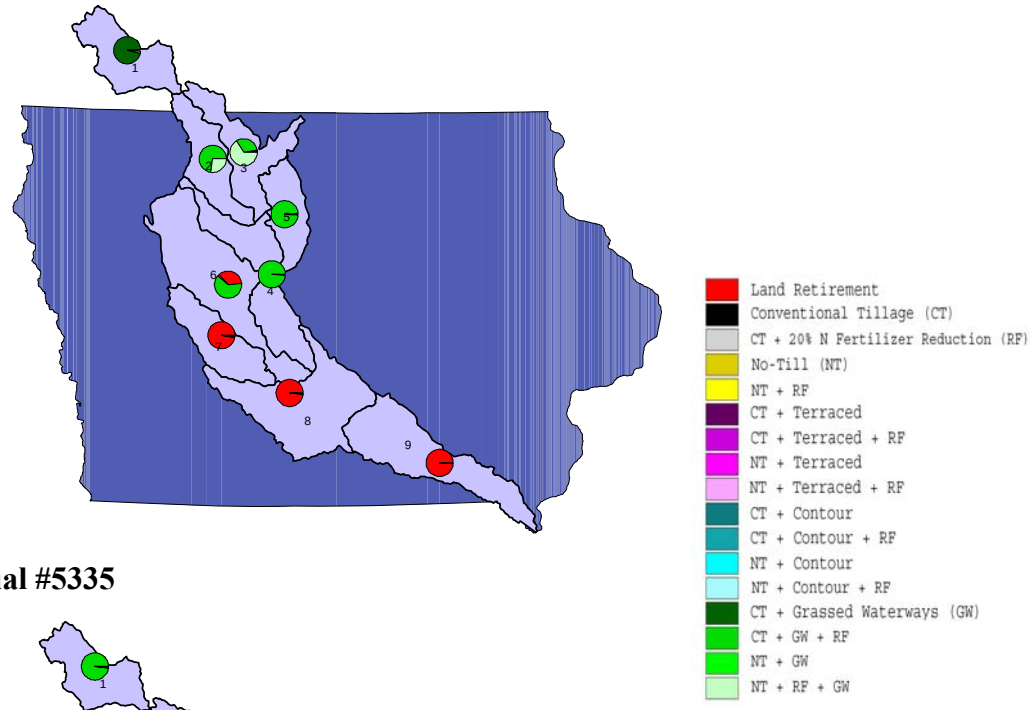

Individual #5335

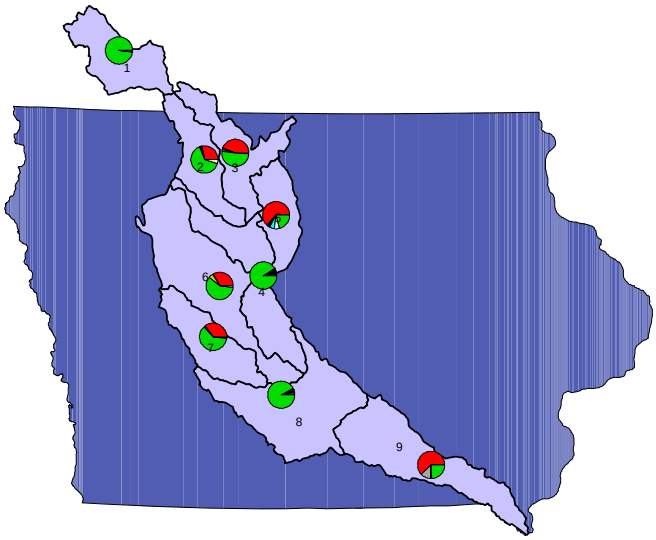

Figure 3C. Subbasin-level distribution of alleles for individuals #3610 and #5335

reductions) remain the preferred conservation practice option, which is consistent with the results reported above.

APPENDIX D. APPENDIX TO CHAPTER 5

Table 1D. Summary of cost estimates, by state

State name	Annualized cost of GW, per protected acre, $	Mean cash rental rate, $/acre	Cost of No-Till, $/acre	Annualized cost per terrace-protected acre, $
Illinois	7.4	133.9	22.2	22.0
Iowa	5.3	149.9	9.6	51.6
Minnesota	5.3	85.8	10.8	40.2
Missouri	3.9	79.6	12.9	13.7
Wisconsin	13.1	80.5	51.9	24.0

Table 2D. Estimates of cost of 20 percent nitrogen fertilizer application reduction

yield zone	State	N application, lb/acre	20% reduced	Corn-Corn Yield drag, bu	Cost, C-C, $/year	Corn-SB Yield drag, bu	Cost, C-S, $/year*
1	Illinois (North)	157.1	125.7	6.9	15.2	3.2	3.5
2	Illinois (Central)	157.1	125.7	5.8	12.8	5.4	5.9
2	Missouri(North)	153.4	122.8	7.1	15.6	3.4	3.7
3	Illinois(South)	157.1	125.7	6.4	14.1	4.9	5.4
3	Missouri (Central)	153.4	122.8	6.1	13.4	5.6	6.1
4	Iowa	125.3	100.2	8.1	17.9	3.1	3.5
5	Minnesota	114.1	91.3	3.0	6.7	2.5	2.8
6	Wisconsin	87.8	70.2	6.3	13.8	4.4	4.9

*Cost for the corn-soybean rotation is divided by 2 to get the annual cost.

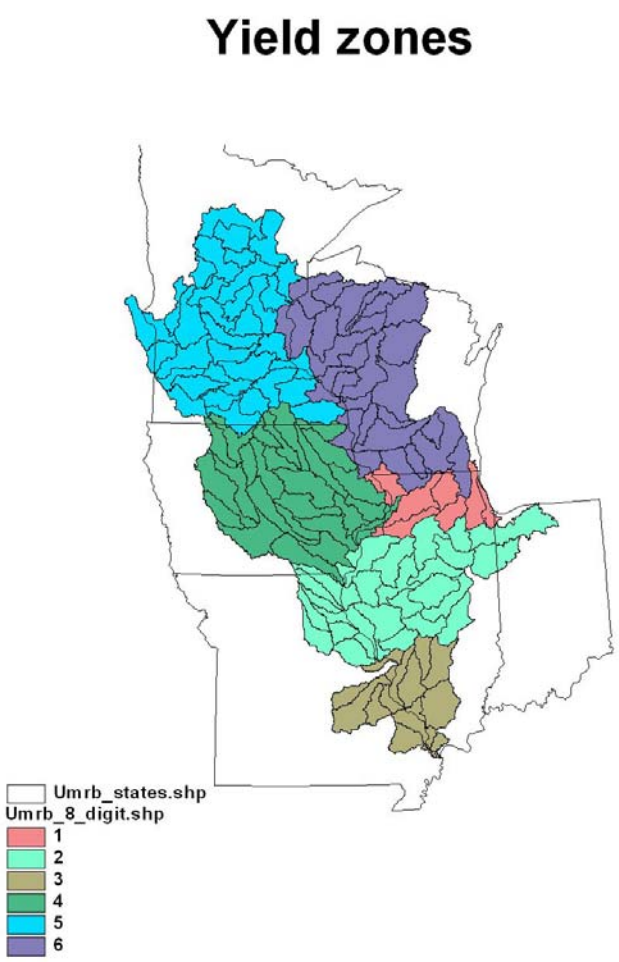

Figure 1D. Yield zones in the UMRB

D.1. SPEA2 Fitness Assignment

An individual $\mathbf{i}$ is assigned a strength value $S(\mathbf{i})$ which equals to the number of solutions it dominates:

(D.1) $$S(\mathbf{i}) = \left|\{\mathbf{j} \mid \mathbf{j} \in \mathbf{P}_t \cup \overline{\mathbf{P}}_t \wedge \mathbf{i} \succ \mathbf{j}\}\right|,$$

where $\bar{\mathbf{P}}_t$ is the original population at generation t, $\mathbf{P}_t$ is the temporary population created, $|\cdot|$ denotes the cardinality of a set, and $\succ$ corresponds to the Pareto dominance relation. On the basis of this definition of strength values, the raw fitness for individual $\mathbf{i}$ is calculated:

(D.2) $$R(\mathbf{i}) = \sum_{\mathbf{j} \in \mathbf{P}_t \cup \bar{\mathbf{P}}_t, \mathbf{j} \succ \mathbf{i}} S(\mathbf{j}).$$

Thus, the raw fitness of an individual is determined by the strength of the dominators (individuals that dominate $\mathbf{i}$). Then, the raw fitness value of $R(\mathbf{i}) = 0$ corresponds to a nondominated individual, while a high raw fitness value corresponds to an individual that is dominated by many other individuals (which in turn dominate other individuals). In light of this interpretation, fitness minimization used in the formulation of the algorithm makes intuitive sense. Figure 2 demonstrates the fitness assignment process and highlights the fact that individuals that are located in the "crowded" areas of the objective space get a higher raw fitness value, and therefore are less likely to be selected into a future generation. For instance, point F dominates points B, C, and A, and therefore gets a strength value of 3. Since point F is nondominated, its raw fitness is zero. Point D, on the other hand, dominates only A, and thus gets the strength value of one, but is dominated by point G, which itself dominates 3 points. Thus, point D gets the raw fitness value of 3. Point A is the "worst" point in the objective space, as it is associated with the highest cost and pollution levels. It itself does not dominate any other points, but is dominated by points F, G (with a strength value of 3), H (with a strength value of 2), D (with a strength value of 1), and E (with a strength value of 1). Therefore, the raw fitness value for point A is 3+3+2+1+1=10. Recalling that in this algorithm, individuals with the lower fitness scores are considered "more fit", it is clear that individual A is far less likely to survive into the next generation than, for example, point F.

Such assignment of raw fitness scores also takes into account the relative "isolatedness" of candidate solutions in the objective space. Conceptually, one would like the resulting Pareto-optimal frontier to span a large portion of the objective space. Therefore, candidate solutions on the interior of the frontier are somewhat less preferred than those close to the edges. In the figure, for example, while both points B and C are dominated, point C is dominated by both points F and G by virtue of its "interior" location in the objective space; whereas point B is dominated only by point F and not by point G: its pollution level is lower than that of G. As a result, point B has a raw fitness score of 3 as opposed to the score of 6 for C, and its "genetic makeup" is therefore less likely to be eliminated in the subsequent generations.

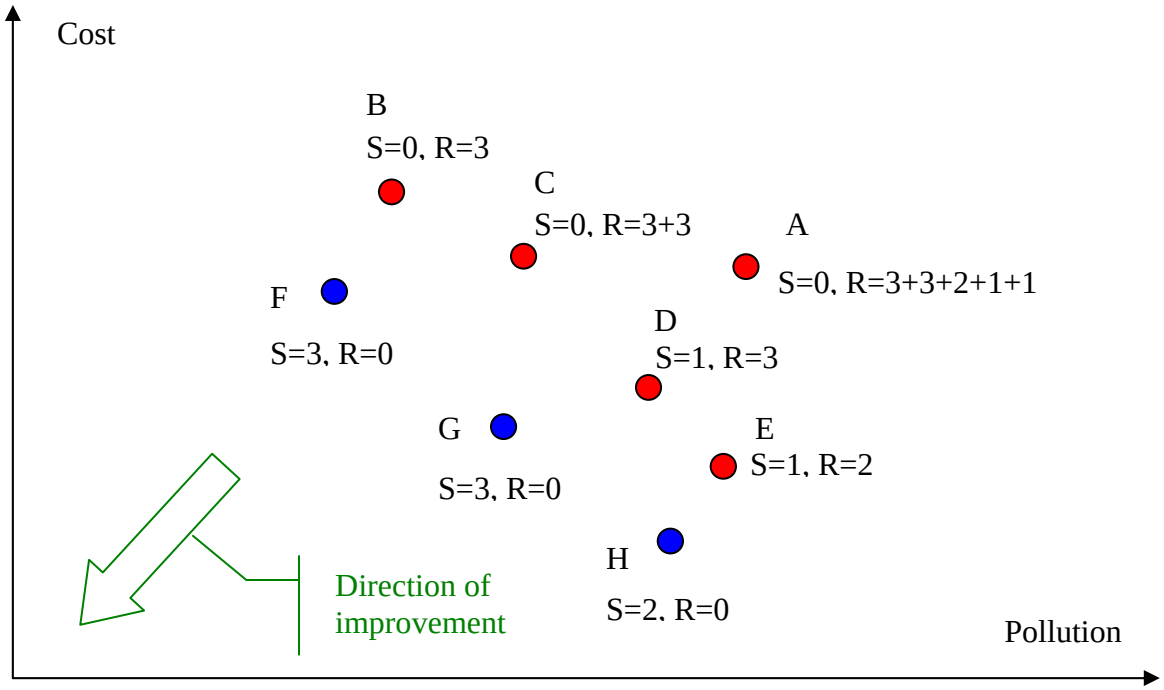

Figure 1B. Raw fitness assignment in SPEA2

Finally, while the raw fitness score assignment outlined above incorporates some information on the location of the solutions in the solution space, additional density information is also incorporated into the calculation of a fitness score. Density estimation technique is used to further differentiate between individuals that are located in the "crowded" areas of the objective space (less preferred) from those located in the relatively sparse areas of the objective space (more preferred). The density estimation technique used in SPEA2 is an adaptation of the k-th nearest neighbor method, where the density at any point is a decreasing function of the distance to the k-th nearest data point. For each individual $\mathbf{i}$, I calculate the distances (in objective space) to all the individuals in the population and the temporary population, and store them in a list. After sorting the list in an increasing order, the k-th element yields the distance, denoted as $\sigma_{\mathbf{i}}^{k}$. k is chosen to equal to the square root of the sum of the initial population size and the size of the temporary population ($\sqrt{40+12} \approx 7$). An additional measure of distance was incorporated into the algorithm in order to preserve diversity in the objective space. In each generation, the distance from a given individual to the center of the cube defined by the endpoints of the frontier was established. The purpose of this calculation is to further reward individuals who are located closer to the edges of the frontier, and thus prevent loss of diversity.

This distance is denoted as $\sigma_{\mathbf{i}}^{c}$. The density is computed as:

(D.3) $$D(\mathbf{i}) = \frac{1}{\sigma_{\mathbf{i}}^{k} + 0.25\sigma_{\mathbf{i}}^{c} + 2},$$

where 2 is added to the denominator to ensure that the value of the density is greater than zero and less than one. Given the raw fitness score and the estimated density, the fitness of an

Table 1B. Nutrient loading consequences from a uniform application of each of the alleles (subject to baseline constraints)

Allele #	Allele Description	NO_3, tons/year	P, tons/year	Cost, thousand $/year	N, % baseline	P, % baseline	Cost, % baseline
1	Conventional Till (CT)	422,740	29,139	416,031	100	100	100
2	Ridge Till (RT)	424,480	29,166	416,031	100	100	100
3	Mulch Till (MT)	411,680	25,747	704,559	97	88	169
4	No Till (NT)	429,340	22,359	1,173,998	102	77	282
5	CT+Contour	417,960	21,636	1,024,211	99	74	246
6	RT+Contour	420,400	21,720	1,024,211	99	75	246
7	MT+Contour	415,380	19,975	1,312,739	98	69	316
8	NT+Contour	442,600	18,848	1,782,178	105	65	428
9	CT+Grassed Waterway	386,440	20,292	793,859	91	70	191
10	RT+Grassed Waterway	388,940	20,424	793,859	92	70	191
11	MT+Grassed Waterway	385,840	19,210	1,082,387	91	66	260
12	NT+Grassed Waterway	414,860	18,913	1,551,826	98	65	373
13	CT+Terraced	389,780	15,013	2,507,686	92	52	603
14	RT+ Terraced	391,880	15,158	2,507,686	93	52	603
15	MT+Terraced	394,260	15,031	2,796,214	93	52	672
16	NT+Terraced	428,780	16,215	3,265,653	101	56	785
17	CT+RF	368,200	28,613	1,056,221	87	98	254
18	RT+RF	369,480	28,632	1,056,221	87	98	254
19	MT+RF	355,760	25,250	1,344,749	84	87	323
20	NT+RF	369,720	21,755	1,814,188	87	75	436
21	CT+Contour+RF	359,660	21,264	1,664,401	85	73	400
22	RT+Contour+RF	361,400	21,338	1,664,401	85	73	400
23	MT+Contour+RF	355,380	19,615	1,952,929	84	67	469
24	NT+Contour+RF	378,320	18,370	2,422,368	89	63	582
25	CT+Grassed Waterway+RF	333,060	19,932	1,434,049	79	68	345
26	RT+Grassed Waterway+RF	334,980	20,053	1,434,049	79	69	345
27	MT+Grassed Waterway+RF	330,780	18,836	1,722,577	78	65	414
28	NT+Grassed Waterway+RF	355,940	18,375	2,192,016	84	63	527
29	CT+Terraced+RF	331,980	14,783	3,147,876	79	51	757
30	RT+Terraced+RF	333,680	14,919	3,147,876	79	51	757
31	MT+Terraced+RF	335,040	14,778	3,436,404	79	51	826
32	NT+Terraced+RF	365,380	15,791	3,905,843	86	54	939
33	Land retirement	100,060	12,457	7,921,487	24	43	1,904

individual $\mathbf{i}$ is calculated as:

(D.4) $$F(\mathbf{i}) = R(\mathbf{i}) + D(\mathbf{i}).$$

In order to preserve the logic of the original GA library which was set up for fitness score maximization, I use K-fitness score as the actual fitness score used by the program, where K=100000.

ACKNOWLEDGEMENTS

I would like to thank my thesis committee members for their guidance and support throughout my graduate education and the thesis writing process. First, I would like to express my gratitude to my major professor, Dr. Catherine Kling. Her continued support and encouragement were, as far as I am concerned, the factors which contributed most to the completion of my degree. I am especially grateful for the support Dr. Kling gave me not as an economist, but as a friend. With the exception of Dr. Opsomer, I have had the privilege of learning from most of my committee members: Dr. Kling, Dr. Herriges, Dr. Kilkenny, and Dr. Zhao in a classroom. Despite their diverse teaching styles, they each share a passion for their subject, which, combined with their insistence on excellence, greatly enhanced my student experience. A special thanks goes to Dr. Maureen Kilkenny for being my major professor in the master's program, for her wise guidance then and continued support thereafter. Additional thanks are due to Todd Campbell and Dr. Hongli Feng. Todd's vast expertise in programming and all things computers in general has been a tremendous help in completing this research. Discussions of environmental problems, ranging from carbon sequestration to water quality with Dr. Feng have yielded numerous invaluable insights. Finally, U.S. Environmental Protection Agency's Science to Achieve Results Graduate Fellowship provided important support for my graduate study. I also thank Dr. Dale Manty, my project officer, for his encouragement throughout my fellowship term.